

ERRATA

Abstract

- p. ix, l. 7 -“...low-complexity multiuser detectors...” should be read as “...low-complexity multiuser detector...”
- p. x, l. 20 -“...Guassian...” should be replaced by “...Gaussian...”

Chapter 1

- p. 3, l. 12 -“...1960’s...” should be replaced by “...1980’s...”. It should also be noted that Qualcomm was the first company to actually produce a system [87]. Previously, only military systems had been developed.
- p. 6, l. 12 The squared minimum Euclidean distance is defined as
$$d_{min}^2 = \min_k d_{i,k}^2, k = 1, \dots, K,$$
where $d_{i,k}^2$ is given by (3.34) and (3.35) for synchronous and asynchronous systems respectively.

Chapter 2

- p.10, l. 9 -“third generation spread spectrum systems” should be replaced by “third generation mobile and personal communications systems”.
- p. 10, l. 14 -“IS-54” should be replaced by “IS-136”.
- p. 11, l. 1 - Remark: It should be noted that virtually all cellular radio standards call for the use of sectored antennas. CDMA does not gain capacity because of this, rather it gains through the use of voice activity detection and the soft degradation as the interference levels increase.
- p. 11, l. 18 and p. 12, l. 7 - Include references [87] and [88] after “... shown in Fig. ...”.
- p. 13, Section 2.4 - Design Methodology and Implications
It should be noted that one advantage of long spreading codes is that they avoid a number of synchronisation problems, particularly in coherent systems. Long codes have the advantage that they do not exhibit short term periodicities that can cause spurious locking of the phase locked loops used for carrier and timing recovery.
- p. 20 - Following equation (2.11), $R_i(m)$ should be replaced by $R_i(0)$.
- p. 20 - $R_i(0)^{k,k'}$ should be replaced by $R_i(m)^{k,k'}$.
- p. 22, Section 2.7.1 -
Solution to the near far problem - Note that multiuser detection (MUD) only provides resistance to the near far problem in any practical context, although in theory it solves it.
Increased capacity - Note that MUD increases the available channel capacity. It merely allows for better use of the available capacity.

- p. 25-26, 1. 6 - Note that the decorrelating detector causes noise enhancement only if $\mathcal{R}_{k,k}^{-1} > 1$. The structure of this detector is analogous to zero forcing equalisation. This detector completely eliminates MAI if \mathcal{R} is invertible.

Chapter 3

- p. 34, 1. 6 - "...followed" should be replaced by "...reproduced".
- p. 35 - $p(c_k)$ is the probability that the encoder chooses the path c_k to send.
- p. 37 - Remark: When we calculate a distance spectrum line with d_i^2 , we need to find all error events of different lengths L , that share this distance, d_i^2 . The lengths normally have a large range. Note that it is not possible to compute the infinite set of all distances, hence we propose to truncate the computation of the spectrum after a sufficiently large L . As a rule of thumb we have used the cut off threshold to be $T = 2.5$ times the squared minimum distance.
- p.37 - The partial distance spectrum can be defined as the set of all pairs $\{d_i^2, A_{d_i^2}\}$, where $d_i^2 \leq T d_{min,i}^2$, T is the cut off threshold.
- p. 46 1. 4 - The sentence "Any finite .. irregular" should be deleted. Note that in general to obtain the complete distance spectrum requires an exhaustive search. This is due to the irregularity of the finite state machine structure of a multiuser system.
- p.47 1. 3 - The following reference should be included.
[Benedetto] Benedetto S, Mondin M, Montorsi G, "Performance evaluation of trellis-coded modulation schemes", *Proceedings of the IEEE*, vol.82, no.6, June 1994, pp.833-55.
The sentence "The synchronous algorithm can thus be written as follows:" should be replaced by "Knowing the distances and multiplicities, the algorithm in [Benedetto] has been modified to allow the partial distance spectrum to be computed for the multiuser case."
- p.47, 1. 26 - The words "(say 31)" should be removed. Historically, a processing gain of 31 is not considered large in spread spectrum signalling. Note that IS-95, which is a narrow band spread spectrum system has a processing gain of approximately 128.
- p.48 - In fig. 3.7 $\varepsilon_1, \varepsilon_2$ and ε_3 should be replaced by $\varepsilon_{i,1}, \varepsilon_{i,2}$ and $\varepsilon_{i,3}$ respectively.
- p.50 - In fig. 3.8 $\varepsilon_1, \varepsilon_2$ and ε_3 should be replaced by $\varepsilon_{i+1,1}, \varepsilon_{i+1,2}$ and $\varepsilon_{i,3}$ respectively.
- p.51 1. 3 - $\bar{P}'(e)$ should be replaced by $P'(e)$.
- p.51 1. 4 - The words "normalised error" should read as "normalised squared estimation error probability". W' should also be replaced by \bar{W}' .
- p.51, 3.7.1 no. 5 - "normalised variance" should read as "normalised standard deviation".
- p.52 1. 9 - Replace "(SNR)" by " $(SNR = \frac{E_b}{N_0})$ ". In the remainder of the thesis SNR is also defined as $\frac{E_b}{N_0}$.

- p.54 last line - Remark: In general there is no guarantee that the fading processes of all users on the down link are identical. In fact in reality this is hardly the case. In accordance with the previous statements, the last line should be deleted or justified for only hypothetical cases.
- p.55, Condition 2 - $\{\varepsilon' < \varepsilon, \varepsilon'' < \varepsilon\}$ is satisfied if $|\varepsilon'_j(i)| \leq |\varepsilon_j(i)|$ for all $j = 1, \dots, K$ and $i = -M, \dots, M$.
- p.61, - Fig 3.18 should be labelled as follows, x-axis - User index, k , y-axis - User index, k and z-axis - Average Variance of MAI.
- Remark - The complexity of the distance spectrum calculations has been reported separately in the following two references.
 - 1) Schlegel C and Wei L, "A simple way to compute the minimum distance in multiuser CDMA systems", *IEEE Transactions on Communications*, vol.45, no.5, May 1997, pp.532-5.
 - 2) Jana R and Wei L, "Performance bounds for optimum coded multiuser DS-CDMA systems", in. Proc. of *IEEE International Conference on Communications Systems*, Singapore, Nov. 1996.

Chapter 4

- p. 65, l. 3 - This reference should be included. "Boudreau GD, Falconer DD, Mahmoud SA. A comparison of trellis coded versus convolutionally coded spread-spectrum multiple-access systems *IEEE Journal on Selected Areas in Communications*, vol.8, no.4, pp.628-40, May 1990."
- Throughout the majority of chapter 4 the author has dealt only with convolutional codes. Towards the end of the chapter, numerical results are presented on the complexity of the tree search for rate 2/3 Ungerboeck 8-PSK trellis codes.
- p. 71, Eqn. (4.18) - Γ is the total number of output symbols in the multiuser joint trellis.
 - p. 71, l. 2 - $D(E) = \varepsilon^T \mathcal{R}_m^{m+L} \varepsilon$ is the distance matrix, where $\varepsilon = \{\varepsilon_1, \varepsilon_2, \dots, \varepsilon_K\}$ represents the error vector for all users and \mathcal{R}_m^{m+L} is the correlation matrix given by (4.19).
 - p.83 - The numerator in the second term in equation (4.67) should read as $\mathbf{c}_i^H \mathbf{A}_i \mathbf{c}_i$.
 - Part I - Remark: In this thesis, an information theoretic approach for the capacity of multiuser systems has not been pursued. For the benefit of the reader, two references are included namely,
 - 1) S.V. Hanly and D.N.Tse, "Multi-access, fading channels: Part II: Delay limited capacities," *IEEE Transactions on Information Theory*, vol. 44, No. 7, pp. 2816-2831, Nov. 1998.
 - 2) S.V. Hanly, "Capacity and power control on spread spectrum macrodiversity radio networks," *IEEE Transactions on Communications*, Vol. 44, No. 2, pp. 247-256, Feb. 1996.

Chapter 5

- p. 95, l. 10 - The sentence “Diffraction...impenetrable body.” should read as “Diffraction occurs when the radio path between the transmitter and receiver is obstructed by a surface that has sharp irregularities (edges). The secondary waves resulting from the obstructing surface are present throughout the space and even behind the obstacle, giving rise to a bending of waves around the obstacle, even when a line-of-sight path does not exist between transmitter and receiver, (see page 78, [91]).”
- p. 96 last line - Remark: It should be noted that WSSUS is a special case arising from more general definitions of Bello’s work, [14].
- p. 98 section 5.5 - Replace $f_{c(\tau,t)c^*(t',\tau')}(t, t', \tau, \tau')$ by $p_{c(\tau,t)c^*(t',\tau')}(t, t', \tau, \tau')$.
- p. 102 section 5.9 - The sentence “Physically, (5.4) represents a ...” should be changed to “Physically, (5.4) may be modelled as a densely tapped transversal filter.”
- p. 105 - Remark: It should be noted that the model of [120] and Jake’s model correspond to isotropic scattering in the vicinity of the receive antenna of the mobile terminal. In general this model will not apply at a base station.
- p. 111, 113 - The captions of figures 5.12 and 5.14 should be interchanged.
- p. 116 - It should be noted that the Viterbi algorithm may be effectively applied whenever a recursively additive metric can be defined. This is in fact the motivation for using the log-likelihood in receiver and decoder design. In the more general context of dynamic programming many other metrics are possible.

Chapter 6

- p. 122 - Remark: The RAKE receiver used in CDMA systems utilizes the large bandwidth of spread spectrum signalling waveforms to achieve multipath diversity. The conventional RAKE receiver is optimal for slow fading frequency selective scenarios, and is implicitly based on a time-invariant channel model. In fact, practical implementations rely on slow fading to obtain accurate channel estimates by averaging over several symbols. Indeed, the errors incurred in channel estimation are primarily responsible for the performance degradation of the RAKE receiver under fast fading. The fast fading channel is an inherently time-varying system. Figure 6.1 shows a multiuser RAKE receiver that employs *joint time – frequency representations* (TFRs) of the time-varying mobile wireless channel. In the absence of MAI, corresponding to the single user case, the optimal receiver for each user is the TF RAKE receiver with maximal-ratio-combining (MRC), which coherently combines the different multipath-Doppler shifted signal. Note that MRC requires the knowledge of the channel coefficients H_k , which may be estimated through a pilot transmission. The optimal multiuser detector essentially augments the single user receiver by suppressing MAI. The multiuser separation is followed by a whitening operation to decorrelate the noise in the estimates. Finally, MRC is applied to the different multipath-Doppler components of each user.
- p.132 - Remark: An approximation to the error performance is produced and that this approximation is asymptotically an upper bound when all possible error events are included.

- p.134 - Equation (6.43), the first factor to be differentiated should be $(\zeta - p_i)^{n_i}$.
- p.136 - The second paragraph should refer to figure 6.6.

Chapter 7

- p. 145 - 146 - Remark: For the sake of clarity it was shown that the $E\{y_m | \tilde{\mathbf{B}}, \mathcal{Y}_{m-1}\}$ is the minimum mean squared error estimate of y_m . This result is also shown in [81]. It is sufficient to assert this well known result. Similarly, we assert that (7.19) is the Innovations process (see reference [81]). A brief note on innovations sequence is provided for the benefit of the reader. Suppose $\{y_m\}$ is a sequence of Gaussian vectors.

Define $\tilde{y}_m = \frac{y_m - E\{y_m | \mathcal{Y}_{m-1}\}}{\sigma^2}$. Then $\{\tilde{y}_m\}$ is an innovations sequence.

- 1) $\{\tilde{y}_m\}$ is a linear combination of y_0, y_1, \dots, y_m
- 2) By the orthogonality principle, $\{\tilde{y}_m\}$ is orthogonal to y_0, y_1, \dots, y_m and all linear combinations of these variables.

Conditions 1) and 2) imply $E\{\tilde{y}_m \tilde{y}_n'\} = 0, m \neq n$. Furthermore, \tilde{y}_m is independent of $\tilde{y}_n, m \neq n$.

If $\{y_m\}$ is NOT a Gaussian sequence, then $E\{y_m | \tilde{\mathbf{B}}, \mathcal{Y}_{m-1}\}$ is constructed as the best non-linear prediction. In general $E\{\tilde{y}_m \tilde{y}_n'\} = 0$ and $\{\tilde{y}_m\}$ is an independent Gaussian sequence (see [Kailath]).

[Kailath] T. Kailath, "The innovations approach to detection and estimation theory", *Proceedings of the IEEE*, vol. 58, no. 5, May 1970.

- p. 150 - Remark: The algorithm in section 7.3 is closely related to the work of Hart and Taylor [49]. However, it also investigates the effect of multiple access interference (MAI) in a CDMA environment. Furthermore, ideas on the decomposition of (Cholesky factorisation) $\mathcal{R}_{\nu\nu}^{-1}$ were explored.
- p. 158 - The horizontal axis of figure (7.7) should be labelled as "Number of Users".

Performance Evaluation Of Single User and Multiuser CDMA Systems

Rittwik Jana

B.E. (Hon I), The University of Adelaide

A thesis submitted for the degree of
Doctor of Philosophy at
The Australian National University



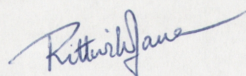
May 1999

To my parents, Sukumar and Rina for their love and support.
To my wife and sister, Jaya and Sanjukta for their inspiration and love.

© Rittwik Jana

Typeset in Palatino by T_EX and L^AT_EX 2_ε.

Except where otherwise indicated, this thesis is my own original work.



Rittwik Jana

19 May 1999

UNIVERSITY OF
MANNING
MANNING, N.S.W.

Contents

Acknowledgments	viii
Abstract	ix
List of Publications	x
List of Figures	xii
List of Acronyms	xvii
Notation	xix
1 Introduction	1
1.1 Research Account	5
1.2 Thesis Contributions	8
2 Introduction to CDMA Multiuser Detection	10
2.1 Direct Sequence Spread Spectrum	10
2.2 CDMA Forward Link	11
2.3 CDMA Reverse Link	12
2.4 Design Methodology and Implications	13
2.5 Basic DS-CDMA System Model	14
2.5.1 Synchronous AWGN CDMA Channel Model	17
2.5.2 Asynchronous AWGN CDMA Channel Model	19
2.6 Interference Rejection	21

2.7	The Multiuser Detection Problem	21
2.7.1	Advantages of Multiuser Detection	22
2.7.2	Disadvantages of Multiuser Detection	23
2.8	Optimum Multiuser Detection	23
2.9	Suboptimal Receivers	24
2.9.1	Linear Complexity Receivers	25
2.10	Nonlinear Receivers	26
2.11	Adaptive Multiuser Detection	28
2.12	Summary	30
3	Performance Evaluation of Optimum Multiuser DS-CDMA Systems	32
3.1	Introduction	32
3.2	Bit Error Probability Bounds	33
3.3	Bit Error Probability Bounds for Multiuser DS-CDMA	38
3.4	System Model	41
3.5	Procedure to Compute The Near Ideal Noise Whitening Filter	45
3.6	The Partial Distance Spectrum Calculation	46
3.6.1	Synchronous Case	46
3.6.2	Asynchronous	47
3.7	Average BEP for Random Codes	50
3.7.1	Procedure to estimate the BEP	51
3.8	Numerical Results	52
3.9	Summary	57
4	Performance Evaluation of Trellis Coded Multiuser CDMA	63
4.1	Introduction	64

4.2	System Model	67
4.3	Normalised Minimum Squared Euclidean Distance	70
4.4	Properties of $d_{min,i}^2$ for Coded Multiuser CDMA	74
4.4.1	Upper Bound on Squared Minimum Euclidean Distance	74
4.4.2	Effect of \mathcal{R} on d_{min}^2	78
4.4.3	Asymptotic efficiency for coded CDMA	82
4.5	Numerical Results	85
4.6	Summary	88
5	The Transmitter, Multipath Channel and Receiver	91
5.1	Introduction	92
5.2	The Transmitter	92
5.3	Radio Propagation and Mother Nature	94
5.4	Channel - Linear Time Varying Filter	96
5.5	Channel - Random Time Varying Filter	98
5.6	Complex Gaussian Distributions	98
5.7	Wide Sense Stationary Uncorrelated Scattering (WSSUS)	100
5.8	Delay Spread and Doppler Spread	100
5.9	Discrete Delay and Discrete Time Channel Modelling	102
5.10	Simulating the Channel	104
5.11	The Time and Frequency Selective Channel	106
5.12	The Time Selective Channel	107
5.13	The Frequency Selective Channel	108
5.14	The Receiver Front End	109
5.15	Received Signal Model	111
5.16	Detection Criteria	114

5.17	Multiuser Detection in Multipath Fading Channels	117
5.18	MLSE Receiver Analysis	118
5.19	Summary	119
6	Optimum Multiuser Detection for Known Time Varying, Frequency Selective Rayleigh Channels	120
6.1	Introduction	121
6.2	MUKCIR Receiver Derivation	123
6.2.1	White Noise	126
6.2.2	The Time Invariant Frequency Selective Channel	127
6.2.3	The Time Selective Frequency Flat Channel	128
6.2.4	The Time Invariant Frequency Flat Channel	129
6.3	Receiver Operation	130
6.4	Receiver Analysis	130
6.5	Numerical Results	134
6.6	Summary	138
7	Predictor Based Multiuser Detection for Time Varying, Frequency Selective Rayleigh Channels	140
7.1	Introduction	141
7.2	MUKCA Receiver Derivation	143
7.3	SUKCA Receiver Derivation	148
7.3.1	The SUKCIR Receiver Derivation	150
7.4	Receiver Operation	151
7.5	Receiver Analysis	151
7.6	Numerical Results	154
7.7	Summary	156

8	Conclusion	160
8.1	Achievements	160
8.2	Future Research	162
A	A Suboptimal Multiuser CDMA Receiver Using Sequential Decoding	164
A.1	Introduction	164
A.2	Metric Functions for Sequential Detection	165
A.3	Numerical Results	169
A.4	Conclusion	169
A.5	Appendix	169
B	Change Detection in Teletraffic Models	173
B.1	Abstract	173
B.2	Introduction	173
B.3	Signal Models	175
B.3.1	Markov Modulated Poisson Process (MMPP)	175
B.3.2	Long Memory Processes	176
B.3.2.1	Fractional ARIMA	176
B.4	On-Line Change Detection	178
B.4.1	MMPP	179
B.4.2	Gaussian FARIMA	179
B.4.2.1	Gaussian FARIMA(0, d , 0)	180
B.4.2.2	Gaussian FARIMA(1, d , 0) and FARIMA(0, d , 1)	181
B.5	Simulation	182
	Bibliography	190

Amendments required by Examiners inside front cover

Acknowledgements

While I was a research student at the Australian National University I was fortunate to have Dr. Lei Wei, Dr. Brian D. Hart and Dr. Rodney A. Kennedy as my supervisors.

My initial education in the area of multiuser communications was under the perceptive direction of Dr. Lei Wei, Dr. Christian Schlegel and Dr. Lars Rasmussen. Lei has helped and guided me towards the completion of this thesis with much helpful criticisms and many valuable suggestions. His family and friends have been most supportive during the “not so good” times and I am deeply indebted.

Dr. Brian D. Hart (and his little red pen) has spent many hours discussing the details of the CDMA channel with me. His support and encouragement has made a significant difference to the state of my mind and I cherish our continuing friendship. For this, and for the way in which his enthusiasm has inspired and encouraged me, I express my sincerest gratitude. Cheerio mate!

Dr. Rodney Kennedy deserves many thanks for his guidance and insight. I thank him especially for the scholarship and the financial help he provided. Rod is still somewhat of a mentor to me and I regard his suggestions/criticisms very highly.

Many thanks to the wine connoisseur Dr. Subhrakanti Dey with whom I have spent many hours talking about everything from CDMA to life in general. To date I still wonder why our discussions get vague towards the end of the bottle!! Here's to you mate! Salut!

I am most thankful to my family, the most caring people in this world. They have been behind me through thick and thin and it is not possible to thank them enough for their continuous encouragement and support. Special thanks to my wife Jaya, for all her support and care. Thanks petal. By now I am convinced she knows how Trellis Coded Modulation works!!

The support that I have received from the CRC for Robust Systems in the form of a scholarship and various professional development programs is gratefully acknowledged also. Last but not least I thank all the staff and students especially Ms. Maria Davern, Mr. Deva Borah and Dr. Predrag Rapajic in the Telecommunications Engineering Group who have been extremely supportive through their friendship and stimulating discussions. My colleagues at the Defence Science and Technology Organisation deserve a special mention. Doing a full-time job and studying part-time is very demanding and I am grateful to each and everyone who has supported me through this phase of my life.

Abstract

The work in this thesis addresses a variety of issues relating to single user and multiuser detection schemes in the context of broadband wireless communications.

These studies present a simple and effective technique to evaluate the performance of Direct Sequence - Code Division Multiple Access systems using multiuser detectors over additive white Gaussian noise channels and mobile fading channels; the development of optimum multiuser receiver architectures to combat the fading channel's time variation and frequency selectivity; and the design of a low-complexity multiuser detectors to achieve near optimum performance.

Spread spectrum communication is a well known technique which has found enormous utility in mobile communication systems. In a cellular environment where there are a large number of users simultaneously active, it is an extremely difficult task to characterise the performance of such a system. Much work has been done in the recent past and is still underway to develop computationally attractive algorithms to evaluate such complex systems. In the first part of the thesis we utilise analytic or semi-analytic methods to evaluate the system performance over AWGN and fading channels through the computation of some key parameters:

- Squared minimum Euclidean distance d_{min}^2 ,
- Number of nearest neighbours,
- Partial distance spectrum,
- Bit error probability (BEP) bounds.

Though this technique relies on already published contributions such as the union bound and other statistical tools like importance sampling, we recognize its importance and usefulness in many system environments. With the use of this method it is now possible to obtain upper and lower bounds on the BEP for an uncoded multiuser CDMA system in complex channels and high system load.

The use of error control coding and the addition of redundant bits allows for the detection and/or correction of errors. Accordingly, we show how to evaluate a Trellis-Coded Modulated (TCM) multiuser CDMA system. In particular, three properties of the squared minimum Euclidean distance, d_{min}^2 measure are studied. The significance of this parameter stems from the fact that it determines the asymptotic performance of the system.

The author derives an upper bound on d_{min}^2 for a multiuser system using error control coding, studies how d_{min}^2 is affected by non-orthogonal spreading sequences and shows the relationship between d_{min}^2 in coded and uncoded synchronous multiuser systems for certain special cases.

In the second half of the thesis, we focus on the development of more sophisticated receivers to combat the harsh nature of the wireless environment. In particular, the wireless channel is modelled as a time varying, frequency selective Rayleigh fading channel. Four receivers are proposed namely the 1) Multiuser Known Channel Impulse Response Receiver (MUKCIR), 2) Multiuser Known Channel Autocovariance Receiver (MUKCA), 3) Single User Known Channel Impulse Response Receiver (SUKCIR) and 4) Single User Known Channel Autocovariance Receiver (SUKCA). The MUKCIR receiver assumes perfect knowledge of the channel impulse response. The MUKCA receiver however, relies on the channel's second order statistics only. Simulations and analysis show that both the optimal receivers are capable of exploiting joint Doppler and delay spreads to achieve substantial gains. Due to the overwhelming exponential complexity of the optimal receivers, two linear complexity receivers are also proposed. Both receivers provide a useful tradeoff between *a priori* information, performance and complexity.

Although suboptimal multiuser detection has not been the major focus of this thesis, we present a novel multiuser receiver that uses a sequential decoding algorithm. The reduced complexity receiver metric is derived using a Gaussian approximation technique. It has a performance comparable to the optimal receiver for a high system load.

List of Publications

1. Lei Wei and Rittwik Jana, "Performance Bounds for Optimum Multiuser DS-CDMA Systems," *IEEE Transactions on Communications*, accepted for publication, in Press.
2. Rittwik Jana, Brian D. Hart and Ben D. Benison, "Optimal multiuser and single user detection for time varying frequency selective CDMA channel," submitted to *IEEE Journal of Selected Areas on Communications*, May '99.
3. Rittwik Jana and Subhrakanti Dey, "Change detection for teletraffic data," submitted to *IEEE Transactions on Signal Processing*, February '99.
4. Rittwik Jana, Lars K. Rasmussen and Lei Wei, "Upper Bounds on the minimum Euclidean distance for Coded Multiuser CDMA," in *Proc. of IEE 2nd Bi-annual mobile communications conference*, South Australia, April '95.
5. Rittwik Jana and Lei Wei, "Robust multiuser CDMA receiver using sequential detector," in *Proc. of IEE International Symposium on Signal Processing and its Applications*, Brisbane, August '96.
6. Rittwik Jana and Lei Wei, "Properties on minimum Euclidean distance for Coded Multiuser CDMA systems," in *Proc. of IEEE International Symposium on Spread Spectrum and its Applications*, Mainz, Germany, September '96.
7. Rittwik Jana and Lei Wei, "Performance bounds for optimum multisuser DS-CDMA systems," in *Proc. of IEEE Personal Indoor Mobile Radio Communications Conference (PIMRC)*, Taiwan, October 96.
8. Rittwik Jana and Lei Wei, "Performance bounds for optimum coded multiuser DS-CDMA systems," in *Proc. of IEEE International Conference on Communications Systems*, Singapore, November 96.
9. Brian D. Hart and Rittwik Jana, "Optimal Multiuser Detection of Bandlimited DS-CDMA signals, distorted by Time-Varying Frequency Selective Multipath Channels," in *Proc. of IEEE Vehicular Technology Conference*, Canada, May '98.
10. Rittwik Jana, Brian D. Hart and Ben D. Benison, "Optimal multiuser and single user detection for time varying frequency selective CDMA channel," submitted to *IEEE Globecom '99 Conference*, Brazil, Jan. '99.
11. Rittwik Jana and Subhrakanti Dey, "Change detection for teletraffic data", submitted to *Conference of Decision and Control (CDC)*, Phoenix, Feb' 99.

12. Rittwik Jana, "Multiuser DS-CDMA Case Studies," *Technical Report*, Telecom Australia/Mobile Communications Research Centre, University of South Australia, May '94.
13. Rittwik Jana, "Minimum Euclidean Distance of multiuser coded CDMA," *Technical Report*, Telecom Australia/Mobile Communications Research Centre, University of South Australia, Aug. '94.

The following papers are not related to this thesis, however, they were also produced during the thesis.

1. Richard Taylor and Rittwik Jana, "An analysis of transmission and storage gains from sliding checksum methods," submitted to *IEEE Transactions of Knowledge and Data Engineering*, Jan. '99.
2. T. Andrew Au , W. D. Blair and Rittwik Jana, "Exploiting CORBA in a military tactical environment," submitted to *Journal of Battlefield Technology*, April '99.
3. P.D. Coddington, K.A. Hawick, K.E. Kerry, J.A. Matthews, A.J. Silis, D.L. Webb, P.J. Whitbread, C.G. Irving, M.W. Grigg, R. Jana and K. Tang, "Implementation of a Geospatial Digital Library using Java and CORBA," in *Proc. of Tools Pacific*, Melbourne '98.
4. M.W. Grigg, P.J. Whitbread, C.G. Irving, A.K. Lui, R. Jana, "Component based architecture for a distributed imagery library system," accepted for *Sixth International Conference on Distributed Multimedia Systems (DMS-99)*, Japan, July '99.
5. William. D. Blair and Rittwik Jana, "A Transmission Availability Forecast Service for Internet Protocol Networks," accepted for *IEEE International Conference on Networks (ICON'99)*, Brisbane, September '99.
6. Richard Taylor and Rittwik Jana, "Checksum Testing of Remote Synchronisation Tool," *Defence Science and Technology Organisation technical report*, DSTO-TR-0627, March '98.
7. Richard Taylor and Rittwik Jana, "An analysis of transmission and storage gains from sliding checksum methods," *Defence Science and Technology Organisation technical report*, DSTO-TR-0743, November '98.
8. William. D. Blair and Rittwik Jana, "A Transmission Availability Forecast Service for Internet Protocol Networks," *Defence Science and Technology Organisation technical report*, DSTO-RR-0146, April '99.
9. William. D. Blair and Rittwik Jana, "Voice Services Options for the Battlespace (Land) Communications System," *Defence Science and Technology Organisation technical report*, in preparation.

List of Figures

2.1	IS-95 CDMA forward link	12
2.2	IS-95 CDMA reverse link	13
2.3	DS-CDMA System Model	16
2.4	Conventional DS-CDMA Detector	19
2.5	Interference rejection (IR) techniques for wireless digital communications [61]	22
2.6	Optimum multiuser detector	25
2.7	Organisational chart for multiuser interference rejection in DS-CDMA [61]	26
2.8	Adaptive "single-user" receiver	29
3.1	Correct path and an error path in a trellis of length L	34
3.2	Correct path and an error path in a trellis of length L	35
3.3	Distance Spectrum and Bound Computation	37
3.4	State Diagram and Error Events for a 3-user Synchronous system	39
3.5	State Diagram and Error Events for a 3-user Asynchronous system	40
3.6	Baseband equivalent model of a multiuser CDMA system	44
3.7	Distance computation for a synchronous tree	48
3.8	Distance computation for an asynchronous tree	50
3.9	Comparison of union bounds for different thresholds T , synchronous CDMA with binary random spreading codes of length 31, $I = 31$	52
3.10	Synchronous system partial distance spectrum	53
3.11	Asynchronous system partial distance spectrum	53

3.12	Synchronous system - Average upper and lower bounds for a 31-user DS-CDMA system with binary random spreading codes, $N=31$	58
3.13	Asynchronous system -Average upper and lower bounds for a 31-user DS-CDMA system with binary random spreading codes, $N=31$	58
3.14	BEP bounds as a function of the number of users I for $E_b/N_0 = 7\text{dB}$ with binary random signature waveforms of length 31.	59
3.15	BEP versus the number of users for slow Rayleigh fading channel, $E_b/N_0 = 34\text{dB}$, cosine pulse shaping	59
3.16	Comparison of Verdú and Forney bound	60
3.17	Mean of \mathcal{F} for synchronous systems, Mean MAI = 0.1491	60
3.18	Variance of \mathcal{F} for synchronous systems, average variance of MAI for 10000 sets = 0.0225	61
3.19	Mean of \mathcal{F} for asynchronous systems	61
3.20	Variance of \mathcal{F} for asynchronous systems	62
4.1	Multistage DFE multiuser equalisation followed by Soft Viterbi algorithm	65
4.2	Baseband equivalent model for coded CDMA and SU receiver	66
4.3	Baseband equivalent model for coded CDMA	69
4.4	Equivalent discrete model of the system	70
4.5	Trellis diagram and arbitrary mapping format of a 4 state and a 2 state code	72
4.6	Linear processing filter \mathcal{D} before spreading	78
4.7	$\lambda_{\min}(\mathcal{R}_m^{m+L})$ and $\lambda_{\max}(\mathcal{R}_m^{m+L})$ as a function of L for the best and worst cases	86
4.8	$\lambda_{\max}(\mathbf{H}_{i,L})$ as a function of L for the best and worst cases	87
4.9	Lower bounds and exact values of η_i for 100 sets of \mathcal{R}	88
4.10	Number of paths kept vs time interval	89
5.1	Multiuser CDMA communication system	92
5.2	Chip waveforms in time domain, $\chi = 0.3$ for cosine and root raised cosine	94
5.3	Chip waveforms in frequency domain	95

5.4	The Mobile communications environment	96
5.5	Typical delay power profile, $\tau_F =$ first arrival delay, $\tau_{rms} =$ rms delay, $L_\tau T_s = \tau_L - \tau_F$ maximum excess delay, $\tau_L =$ final arrival delay	101
5.6	Channel impulse response represented as a tapped delay line	103
5.7	Polar plot of a fading process generated by filtering complex white noise by the truncated and windowed impulse response of (5.37). This process evolves smoothly.	106
5.8	Logarithmic plot of fading amplitude vs time	107
5.9	Plot of channel tap phase (radians) vs time. Large phase shifts occur dur- ing deep fades	108
5.10	Power spectral density of a sample windowed and truncated fading process	109
5.11	Plot of the amplitude of the time and frequency selective channel's ampli- tude transfer function as a function of time and frequency	110
5.12	Plot of the amplitude of the time selective channel's transfer function as a function of time and frequency	111
5.13	Tapped delay line model of frequency selective channel	112
5.14	Plot of the amplitude of the frequency selective channel's transfer function as a function of time and frequency	113
5.15	A basic receiver front end	114
6.1	Time-frequency RAKE receiver	122
6.2	MUKCIR receiver block diagram	130
6.3	BER-SNR curves for different union bounds: all one symbol error events; and all one and two symbol error events	135
6.4	BER-SNR curves for root raised cosine chip pulse shaping with varying excess bandwidth, χ for 1 user	136
6.5	BER-SNR curves for root raised cosine chip pulse shaping truncated to different lengths	137
6.6	BER-SNR curves of the MUKCIR receiver for a fast time varying frequency selective channel where $f_D T_s = 0.1$, $L_\tau T_s = 0.5 T_s$, $r = 2$, $N = 5$, $P = 2$. . .	138

6.7	Effect on the MUKCIR receiver's BER of varying the number of independent paths, P , $K = 1$, $L_\tau T_s = 0.5T_s$, $f_D T_s = 0.01$	139
6.8	Effect on the MUKCIR receiver's BER of varying the Doppler and delay spreads, $r=2$, $N=4$, $P=2$	139
7.1	Different detector realisations	142
7.2	Branch metric computation	152
7.3	BER-SNR curves of the MUKCA receiver for a fast time varying frequency selective channel where $f_D T_s = 0.1$, $L_\tau T_s = 0.5T_s$, $r = 2$, $N = 5$, $P = 2$	156
7.4	Effect on the MUKCA receiver's BER of varying the number of independent paths, P , where $r = 2$, $N = 4$, $L_\tau T_s = 0.5T_s$, $f_D T_s = 0.01$	157
7.5	Effect on the MUKCA receiver's BER for varying delay spreads, where $f_D T_s = 0.01$ and $P = 2$	157
7.6	Effect on the MUKCA receiver's BER for varying Doppler spreads, where $L_\tau T_s = 0.5T_s$, $P = 2$	158
7.7	Effect of the single user and MUKCA receiver's BER for varying the number of users, where $L_\tau T_s = 0.5T_s$, $f_D T_s = 0.01$, $SNR = 25dB$	158
7.8	Effect of the MUKCA receiver's BER for different predictor lengths, W , where $K = 2$	159
A.1	Exact pdf of $p_0(y_i)$ for 10 users	171
A.2	Pdf of the approximation error for 10 users	171
A.3	BER-SNR curves for 10 users	172
B.1	Change detection for a MMPP process	184
B.2	Delay in detection for a MMPP process, Plot of Average delay-Threshold	184
B.3	Change detection for ARIMA(0, d , 0) process, $d_H = 0.1$ ($t = 0..999$), $d_K = 0.3$ ($t = 1000..1999$) and $d_H = 0.1$ ($t = 2000..2999$)	185
B.4	Change detection for ARIMA(1, d , 0) process, $d_H = 0.1$, $\phi = 0.2$ ($t = 0..999$); $d_K = 0.3$, $\phi = 0.4$ ($t = 1000..1999$); $d_H = 0.1$, $\phi = 0.2$ ($t = 2000..2999$)	185
B.5	Change detection for ARIMA(0, d , 1) process, $d_H = 0.1$, $\theta = 0.2$ ($t = 0..999$); $d_K = 0.3$, $\theta = 0.4$ ($t = 1000..1999$); $d_H = 0.1$, $\theta = 0.2$ ($t = 2000..2999$)	186

B.6	Delay in detection for ARIMA(0, d , 0) process, $d_H = 0.1$, ($t = 0..999$); $d_K = 0.3$, $\theta = 0.4$ ($t = 1000..1999$); $d_H = 0.1$, $\theta = 0.2$ ($t = 2000..2999$)	186
B.7	Change detection for ARIMA(0, d , 0) process, Tested $dK = 0.20$, Actual $dK = 0.3$	187
B.8	Change detection for ARIMA(0, d , 0) process, Tested $dK = 0.25$, Actual $dK = 0.3$	187
B.9	Change detection for ARIMA(0, d , 0) process, Tested $dK = 0.3$, Actual $dK = 0.3$	188
B.10	Change detection for ARIMA(0, d , 0) process, Tested $dK = 0.35$, Actual $dK = 0.3$	188
B.11	Change detection for ARIMA(0, d , 0) process, Tested $dK = 0.40$, Actual $dK = 0.3$	189

List of Acronyms

<i>Term</i>	<i>Definitions</i>
ARMA	Autoregressive Moving Average
AWGN	Additive White Gaussian Noise
B-CDMA	Broadband Code Division Multiple Access
BEP	Bit Error Probability
BPSK	Binary Phase Shift Keying
bps	Bits per second
CIR	Channel Impulse Response
CDMA	Code Division Multiple Access
dB	Decibel
DC	Decorrelator
DDFD	Decorrelating Decision Feedback Detector
DFE	Decision Feedback Equaliser
DPD	Differential Phase Detection
DS	Direct Sequence
FARIMA	Fractional Autoregressive Integrated Moving Average
FH	Frequency Hopping
FDMA	Frequency Division Multiple Access
FSM	Finite State Machine
GA	Gaussian Approximation
GQF	Gaussian Quadratic Function
GSM	Global System for Mobile
iid	Independent and identically distributed
ISI	Intersymbol Interference
IS-95	Interim Standard 95
KCA	Known Channel Autocovariance
KCIR	Known Channel Impulse Response
LOS	Line Of Sight
LNA	Low noise amplifier
MAI	Multiple access interference
MAPSD	Maximum <i>A Posteriori</i> Sequence Detector
MF	Matched Filter
MLSD	Maximum Likelihood Sequence Detector
MMPP	Markov modulated Poisson process
MU	Multiuser
MUKCIR	Multiuser Known Channel Impulse Response

MUKCA	Multuser Known Channel Autocovariance
NWMF	Noise Whitening Matched Filter
OCIS	Optimal Conditional Importance Sampling
pdf	Probability density function
PSD	Power Spectral Densities
QAM	Quadrature Amplitude Modulation
QPSK	Quadrature Phase Shift Keying
rms	Root mean square
RNF	Root Nyquist Filter
SNR	signal to noise ratio
SSMA	Spread Spectrum Multiple Access
SU	Single User
SUKCIR	Single User Known Channel Impulse Response
SUKCA	Single User Known Channel Autocovariance
TDMA	Time Division Multiple Access
US	Uncorrelated Scattering
VA	Viterbi Algorithm
WSSUS	Wide Sense Stationary Uncorrelated Scattering

Notation

<i>Variable</i>	<i>Meaning</i>
$b_{i,k}$	information bit for i th symbol and k th user
$\mathbf{b}_{i,k}$	hypothesised bit for i th symbol and k th user
\mathbf{b}	vector containing transmitted symbols for all users, all symbol intervals, Part I
\mathbf{B}	matrix containing transmitted symbols for all users, all symbol intervals, Part II
$\tilde{\mathbf{B}}$	matrix containing hypothesised symbols for all users all symbol intervals, Part II
$c_k(t, \tau)$	channel impulse response for k th user
$C_\zeta(\zeta)$	characteristic function of pdf, $p(\kappa)(\kappa)$, Part II
d^2	squared Euclidean distance
d_{min}^2	minimum squared Euclidean distance
\mathcal{D}	set of all possible squared Euclidean distances
\mathcal{E}_k	error event of user k
$\underline{\mathcal{E}}$	set of all error events
E_k	k th user's energy scale factor
f_D	Doppler frequency
$f_{i,i',k,k'}$	ISI term in sequence metric between symbols and users, Part II
\mathcal{F}	Cholesky factor of correlation matrix \mathcal{R}
Γ_i	path metric in trellis for symbol i
\mathbf{G}	kernel of a Gaussian quadratic function, Part II
\mathbf{g}	column vector composed of \mathbf{h} and \mathbf{n} to define κ , Part II
$h(t)$	signature convolved with channel sequence
I	total transmission interval, Part II
\mathbf{I}	identity matrix
K	number of users
κ	total number of input bits in error control code for all users, Part I
κ	Gaussian quadratic function
χ	excess bandwidth
L	length of an error event, Part I
L	intersymbol interference length, Part II
L_h	length of received pulse, Part II
L_s	signature waveform length, Part II
L_τ	maximum delay spread, Part II
$\lambda_{min}(\cdot)$	minimum eigenvalue of (\cdot)
$\lambda_{max}(\cdot)$	maximum eigenvalue of (\cdot)
λ_i	branch metric in trellis for symbol i
M	number of elements in transmit alphabet

$m_{i,k}$	matched filter term in sequence metric for i th symbol and k th user, Part II
N	chips per spreading sequence
N_0	noise power spectral density
$n(t)$	AWGN process
Ω	total transmission interval, Part I
η_k	asymptotic efficiency of user k
P	number of multipaths, Part II
$p(\cdot)$	pdf of (\cdot)
p_i	poles of a characteristic function, Part II
$q_{k,m}$	output symbol for k th user and m th branch in trellis, Part I
\mathcal{R}	correlation matrix of spreading codes
R	error control code rate
$r(t)$	received waveform, Part I
r	fractional chip sampling rate, Part II
$r'(t)$	matched filter output
$s_k(t)$	spreading code of k th user
σ_i	state of trellis for symbol i , Part II
$\sigma_m^2(\mathbf{B})$	variance of prediction error, Part II
T	distance computation cut off threshold
T_c	chip waveform duration
T_s	symbol duration
θ_k	carrier phase of k th user
$w(\mathcal{E})$	Hamming weight of error event \mathcal{E}
$w_{m,l}$	l th coefficient for the ML predictor y_m
\mathcal{W}	$K \times K$ diagonal matrix of user energies, Part I
W	predictor filter length, Part II
\mathbf{y}	whitened matched filter output vector, Part I
\mathbf{y}	received waveform vector, Part II
y_m	m th sample of received waveform vector \mathbf{y} , Part II
\mathcal{Y}_{m-1}	all received samples up to symbol interval $m - 1$
Y	total number of data bearing received samples, Part II
ζ_k	time delay of k -th user for asynchronous CDMA
$z_{i,k}$	matched filter noise output for i th symbol and k th user

Functions

$Q(x)$	complementary error function
$[a, b]$	an inclusive integer range between a and b
(a, b)	an exclusive integer range between a and b
$(a, b]$	integer range from a to and including b
$[a, b)$	integer range from and including a to b
$a \in A$	a is in A
\mathbf{X}^{-1}	inverse of matrix \mathbf{X}
\mathbf{X}^T	transpose of matrix \mathbf{X}
\mathbf{X}^H	Hermitian of matrix \mathbf{X}
x^*	complex conjugate of x

$\text{Re}\{.\}$	Real part of $\{.\}$
$\text{Im}\{.\}$	Imaginary part of $\{.\}$
$\text{diag}(\cdot)$	diagonal of a square matrix
$\text{eig}\{.\}$	eigenvalue of $\{.\}$

The author has tried not to reuse variables. However, in certain circumstances it proved necessary to improve the readability of the thesis. The annotations “Part I/Part II” indicate where the variables are used.

Introduction

Mobile communications has had a significant impact on today's society. The various forms of wireless communications - mobile telephones, cordless phones and radio pagers - continue to experience growth, showing a large increase in the number of users.

On one level the mobile communication system appears as several independent users transmitting to a single base station. Due to the uncoordinated nature of the users' transmissions, the uplink (mobiles to base station) is more difficult to manage than the downlink (base station to mobiles). This is because the downlink is effectively synchronized since it comes from one source.

In wireless communication the precious transfer medium (commonly known as the channel) can be visualized as a region of the time frequency plane. For example a particular user may transmit at a particular time t with a particular frequency f . Space may also be used as another dimension, where directional antennae may be required. The way in which the users utilise the channel resource is determined by the accessing scheme used in the communications system.

Conventional multiple access schemes simply partition the time frequency plane into K slices, one for each user. The users then employ their own particular slice for communication, and the receiver examines the corresponding portion of the time frequency plane for the signal transmitted by the user. Signalling in such a way implies that the users transmit over orthogonal channels where there is no interference from one user's channel to another's. In Time-Division-Multiple-Access the partitioning is in time, so that each user utilises the entire frequency spectrum available but at different times. In Frequency-Division-Multiple-Access the partitioning is in frequency, and the users trans-

mit data at the same time but in different frequency slots. The advantages of each scheme over the other have been thoroughly debated and the best of the two probably depends on implementation issues such as complexity, protocols, bandwidth and power limitations [54][63]. The most popular digital standard for multiple access communications in Europe and Australia is the Global System for Mobile Communications (GSM) which is based on TDMA [91][54].

Spread-Spectrum-Multiple-Access (SSMA) is a well known technique which has also found numerous applications in cellular communications [54][127]. Each user employs the entire channel resource to transmit a particular symbol. Specifically, the users transmit at the same time using the same bandwidth. Consequently the channels over which the users communicate to the receiver are not necessarily orthogonal to one another and co-channel (multiuser) interference results [135]. Co-channel interference also arises in FDMA and TDMA, but between users that occupy different cells [62]. That is why frequency planning is so important in GSM. Detection of data transmitted using the SSMA scheme may seem hopeless. An analogy which indicates that this is not so is our ability to discern different musical instruments in an orchestral piece of music. SSMA works via knowledge of the waveform that makes each user (instrument) unique. So although each user transmits at the same time using the same bandwidth the actual waveforms or chip sequences (pitch/timbre) are sufficiently different to allow the receiver (ear) to determine the data (notes) that each user transmits.

SSMA gained popularity initially in the 1960's for military reasons. The waveforms used for transmission were constructed to appear as noise. The original motivation was both to conceal transmission and to combat intentional jamming [112].

In spread-spectrum technology a modulated waveform is modulated (spread) a second time in such a way as to generate an expanded bandwidth or wideband signal. In such a system, each user's signal is identified by its unique spreading waveform. Some applications and potential advantages of spread spectrum systems include [85]:

- Improved interference rejection,
- Low-density power spectra for signal hiding,
- Increased capacity and spectral efficiency,

-
- Antijam capability,
 - Secure communications

To the naive observer, the spread spectrum signal looks like noise. It is true however, that the same noise-like signal will appear over and over on the channel allowing covert reception. Spread spectrum systems come in many flavours. The most commonly used techniques are the following

- Direct-sequence (DS) CDMA
- Frequency hopping (FH) CDMA
- Carrier sense multiple access (CSMA) spread spectrum (for wireline communications)
- Hybrid spread spectrum methods

Several companies made substantial investments in SSMA in the early 1960's, Qualcomm being the first [87][88]. Control over the waveform transmitted by a particular user can be achieved using spreading codes and a chip waveform. The resulting access scheme is termed Direct Sequence SSMA or simply DS-Code Division Multiple Access (DS-CDMA). Another commonly employed SS modulation technique is Frequency Hopping Multiple Access (FH). The FH subsystem produces a spreading effect by pseudo randomly hopping the radio frequency (RF) carrier frequency over the available RF frequencies [91][86]. This thesis will focus on DS-CDMA systems only.

In a cellular system, a number of mobiles communicate with one base station. Each mobile is concerned only with its own signal while the base station must detect all signals. Thus, the mobile has the knowledge of only its own chip sequence while the base station has information of all the chip sequences. As the handset complexity must be minimal (where size, weight and cost are critical), and because a CDMA system could potentially have a large number of users (a few hundreds in practice), multiuser detection can only be feasibly realised at the base station.

CDMA systems with single-user detection suffer two major drawbacks: the near-far problem and a limited network capacity due to multiple access interference. The con-

ventional receiver demodulates each signal using the corresponding single-user detector (matched filter followed by a threshold decision device) thereby treating the multiple access interference as white Gaussian noise, or equivalently, ignoring the cross-correlations between the modulating signals of different users [127]. Since the matched filter contains a component which is linear in the amplitude of each of the interfering user, the strongest user often severely interferes with the other users. This effect can very often swamp the desired user's signal strength. Consequently, the anti jamming capability of the weakest user is severely tested and its BER degrades substantially. This imbalance in the received powers is referred to as the near-far problem. Thus in order to maintain an acceptable BER for all users, the DS-CDMA system requires strict power control for each user. Even with perfect power control the interference limits the number of users to only 10% of the maximum capacity [87]. It is not surprising that reliable performance from the conventional detector has been possible only for low bandwidth efficiencies [24]. The capacity is calculated for Gaussian (thermal) noise only, but single user receivers treat interference as noise also. Thus even when the noise is removed, there is still MAI and thus there are still errors. The system is therefore interference limited.

These drawbacks of single-user detection have initiated recent interest into more sophisticated receiver structures such as joint multiuser detection, in which the multiuser interference is treated as part of the information rather than noise. The study of the optimum demodulator by Verdú [121][122][124] shows that while significantly superior performance over the conventional detector is possible, it requires a marked increase in computational complexity which is exponential in the number of users. Thus when the number of users is large the optimum detector becomes too expensive to implement. Therefore, detectors are sought which can closely approximate the performance of the optimum receiver, yet whose complexity is more comparable to the complexity of the conventional single user receiver. In this thesis we will study both optimum and sub-optimum receivers. In particular, multiuser receivers are designed that are optimum for the time varying frequency selective Rayleigh fading channel.

1.1 Research Account

This thesis is organised in two parts. Part I investigates performance evaluation techniques for both uncoded and coded multiuser DS-CDMA systems in Gaussian and slow fading channels. Part II is devoted to the study of receiver designs for multiuser DS-CDMA systems in the presence of time varying frequency selective Rayleigh fading channels.

Chapter 2 provides the necessary background information on spread spectrum systems. A specific CDMA communication system model (IS-95) is discussed in some detail which helps us to identify some of the design methodologies and implications. A basic DS-CDMA system model is constructed which will be augmented as the need arises from chapter to chapter. Finally, a comprehensive literature survey is provided on CDMA and multiuser detection in particular. It is beyond the scope of this thesis to cover all the background of DS-CDMA; however, the reader will quickly establish a strong CDMA foundation and thus appreciate some of the potential enhancements currently being proposed.

Chapter 3 focuses on the performance evaluation of DS-CDMA systems over Gaussian and slow Rayleigh fading channels. The performance evaluation of CDMA systems is a complicated task, even on Gaussian channels [91]. The optimal multiuser detector is not only too complicated to implement but accurate analysis of its error performance is even more complicated, having a complexity of $O(3^K)$ [124]. Most of the work to date has focussed on the concept of asymptotic efficiency. The asymptotic efficiency indicates that the logarithm of the error probability goes to zero with the same *slope* as the single user bit error rate. In this chapter a simple and efficient method is proposed and investigated to evaluate the bit error performance for synchronous and asynchronous multiuser DS-CDMA systems. A generalisation of the work in [102] is used to compute upper and lower bounds on the bit error probability of optimal multiuser detection without error control coding. A 31 user system using random binary signature sequences of length 31 is modelled. Recently, Monte-Carlo simulations with Importance Sampling (IS) techniques have been proposed and studied [104][78][79][139]. Importance sampling biases (scaling/shifting) the noise distribution such that more samples are taken from the important regions. In this chapter we use an optimal conditional importance sampling

(OCIS) method developed by Wei [139] to obtain performance bounds. Specifically, upper and lower bounds on the bit error probability for a specific spreading sequence set were computed and then averaged over a few thousand sets of spreading codes using OCIS techniques. It is also shown that this technique can be readily applied to a time invariant frequency flat Rayleigh fading channel.

Chapter 4 considers the problem of multiuser detection with error control coding. Often in an attempt to improve performance, error control coding is used on each of the users' transmitted data sequences. Two important questions were answered for coded multiuser systems, namely: 1) is it worthwhile studying coded multiuser systems, and if so 2) by how much does the performance of coded CDMA degrade with multiuser interference compared to that of a system with no multiuser interference? In particular, two properties of the minimum squared Euclidean distance d_{min}^2 were studied. The distance measure is an important criterion to characterise the performance of a coded system. First, an upper bound on d_{min}^2 is derived. It will be shown that the multiuser upper bound is identical to the single user upper bound. This confirms the intuitive idea that the multiuser system performance (in terms of BER) cannot be better than a system with one user, hence the reason for comparing multiuser receivers' performances to the single user bound. Second, we study the effect of non-orthogonal spreading on d_{min}^2 . As a result, the concept of asymptotic efficiency for the uncoded case shown by Lupas and Verdu [66] is extended for the coded case. We show ways to calculate the asymptotic efficiency for an infinite dimension spreading code cross-correlation matrix. Last but not least, we show that for the special case of a convolutionally coded synchronous multiuser system, d_{min}^2 is no less than the product of the free distance of the error control code and the minimum Euclidean distance of the corresponding uncoded system.

Chapter 5 investigates the modelling aspects of the wireless propagation environment and introduces the theories and practices of receiver design. The physics of radio propagation is reviewed and a discrete delay, time varying frequency selective channel model suitable for digital simulation is described. The receiver has the job of deciding which symbol sequence was originally transmitted based on all the information it has. We review the maximum likelihood (ML) and the maximum *a posteriori* (MAP) criteria of optimality applied to data symbols and sequences. This chapter introduces the reader to the concepts and notations adopted throughout Part II of the thesis.

Chapter 6 discusses the problem of optimum multiuser detection in a time varying frequency selective Rayleigh fading channel. Due to scatterers and mobility, the received signal contains the sum of delayed and dynamically distorted replicas. This results in amplitude and phase distortion as a function of time (time variation) and frequency (frequency selectivity). Accordingly, a multiuser maximum likelihood sequence detector is developed for linearly modulated signals sent over a time varying frequency selective Rayleigh fading channel. The receiver assumes perfect knowledge of the channel's impulse response, hence its name - the Multiuser Known Channel Impulse Response Receiver (MUKCIR). Simulations and analysis show that the receiver is capable of exploiting joint Doppler and delay spreads to achieve substantial gains. The optimal receiver's complexity is however, exponential in the number of users and as a consequence we propose (in chapter 7) a possible realisation of a linear complexity receiver using techniques learnt in Chapter 7.

Chapter 7 designs, simulates and analyses another multiuser maximum likelihood sequence detector for the time varying frequency selective Rayleigh fading channel. Unlike the MUKCIR developed in chapter 6, this receiver avoids the unrealistic assumption of perfect knowledge of the channel impulse response. Instead it relies on the channel's second order statistics only. The receiver uses predictors to estimate the received signal and forms a weighted Euclidean distance between the predicted and the received samples. Once again results show that it is capable of exploiting the implicit Doppler and delay diversity of fast fading frequency selective channels. The operation of the receiver and the prediction process are described to give the reader an intuitive feeling. Due to the overwhelming exponential complexity of the optimal receiver, a linear complexity receiver is proposed and simulated. The receivers of chapter 6 and 7 provide a useful tradeoff between *a priori* information, performance and complexity.

Chapter 8 contains concluding remarks and some possible directions for future work.

Appendix A derives and simulates a suboptimal multiuser detector that uses a sequential decoding algorithm. This is an application of a depth first search algorithm to multiuser interference suppression using an improved metric function that has a performance comparable to the optimal receiver's metric. This reduced complexity receiver metric is derived using a Gaussian approximation technique.

Appendix B is provided as supplementary reading material. During the thesis, the author and his colleague, (Dr. Subhrakanti Dey, Department of Systems Engineering, Australian National University) also researched the design and implementation of change detection algorithms for various teletraffic models. In particular, we devise likelihood based ratio tests to detect distributional changes in common teletraffic models such as the Markov modulated Poisson process (MMPP), and processes exhibiting long range dependency like the family of Gaussian fractional ARIMA processes. As a continuation of this work, we are currently investigating the feasibility of these techniques to detect the change in user population in a dynamic CDMA system.

1.2 Thesis Contributions

We now list the technical contributions made in this thesis.

- Performance evaluation techniques using Monte-Carlo simulations and importance sampling methods for both the synchronous and asynchronous uncoded CDMA system.
- Upper and lower bounds on the bit error probability of optimal multiuser detection for a synchronous and asynchronous 31 user CDMA system using different chip pulse shapes.
- Properties of the “squared minimum Euclidean distance” measure for a multiuser CDMA system using error control coding. The upper bound on the squared minimum Euclidean distance was derived. Upper and lower bounds were derived for the ratio of minimum distance between a non-orthogonal and an orthogonal system (ie. asymptotic efficiency).
- The design, analysis and simulation of the multiuser known channel impulse response receiver for a time varying frequency selective Rayleigh fading channel.
- The design, analysis and simulation of a “predictor based” multiuser receiver for a time varying frequency selective Rayleigh fading channel. The design and simulation of a linear complexity single user receiver.

- The design and simulation of a suboptimal receiver with an improved metric function using a Gaussian approximation technique.

Introduction to CDMA Multiuser Detection

Overview: This chapter will provide the necessary background information on spread spectrum systems, and the DS-CDMA system in particular. The fundamental concepts of multiuser and single user detection will be introduced. A simple system model of DS-CDMA will then be presented to familiarize the reader with the notations and assumptions used later in the thesis. Finally, a literature review highlights the state-of-the-art research on this topic.

2.1 Direct Sequence Spread Spectrum

Spread spectrum multiple access communication, known commercially as CDMA, is a driving technology behind the rapidly advancing personal communications industry. Several third generation spread spectrum systems such as direct sequence (DS) and frequency-hopped (FH) have all been standardised. However, these lead to different air interfaces and thus are not interoperable with each other.

CDMA is a modulation and multiple access scheme based on spread spectrum communications. Proponents of the CDMA technology cite several potential advantages over the traditional FDMA AMPS and TDMA IS-54 approaches [38][133]. The CDMA system, pioneered by Qualcomm Incorporated of San Diego, was standardised and is known as the IS-95 standard of the Electronics Industries Association (EIA IS-95). Statistics show that voice activity in a full duplex two-way conversation is about 40%. It is difficult to exploit voice activity in a TDMA or FDMA based system because of the time delays

associated with reassigning channel resources in speech pauses. However, in a CDMA system this can be handled very easily by reducing the transmission rate in the absence of speech, thereby reducing interference to other users, which finally translates to an increase in system capacity. Another direct advantage to CDMA system designers is that special frequency reuse plans are not necessary. This is because each user is distinguished from other users by virtue of a unique signature code. Hence, reducing co-channel interference by frequency reuse is no longer required. Nonetheless, there are other sources of interference. Since all users share the same frequency bandwidth, every user is interfering with every other user. This has direct implications in the proper design of power control algorithms. The current standard uses both open loop and closed loop power control techniques to optimise system performance. In addition to reducing multiple access interference (MAI), the base station also uses three sectored antennas (each covers 120° of the azimuth).

This thesis will concentrate only on direct sequence systems. We start with a brief description of the forward (base station to mobile station) and reverse link (mobile to base station) of a typical DS-CDMA system.

2.2 CDMA Forward Link

The forward link utilises a combination of frequency division, pseudorandom code division and orthogonal signal multiple access techniques. This is shown in Fig. 2.1.

The underlying maximum data rate of the forward link is 9600 bits/sec. The speech coder detects speech activity and changes the data rate to a lower value during quiet intervals. The bit stream is partitioned in blocks then convolutionally encoded by a rate $\frac{1}{2}$ code with constraint length 9. This 19.2 kbits/sec data output stream is then interleaved over a 20 msec interval for burst error protection in a fast fading channel. The interleaved data is multiplied by a long code, which serves as a privacy mask. The privacy mask is used as a first level security mechanism. The data is next spread using orthogonal Walsh codes of length 64, resulting in a data rate of 1.228 Mchips/sec. This is then separated into I and Q streams, each of which is modified by a unique short code of length 32768. Finally, the information is transmitted as filtered quadrature phase shift keying (QPSK) modulation. Note that different signals transmitted from a given base station can be

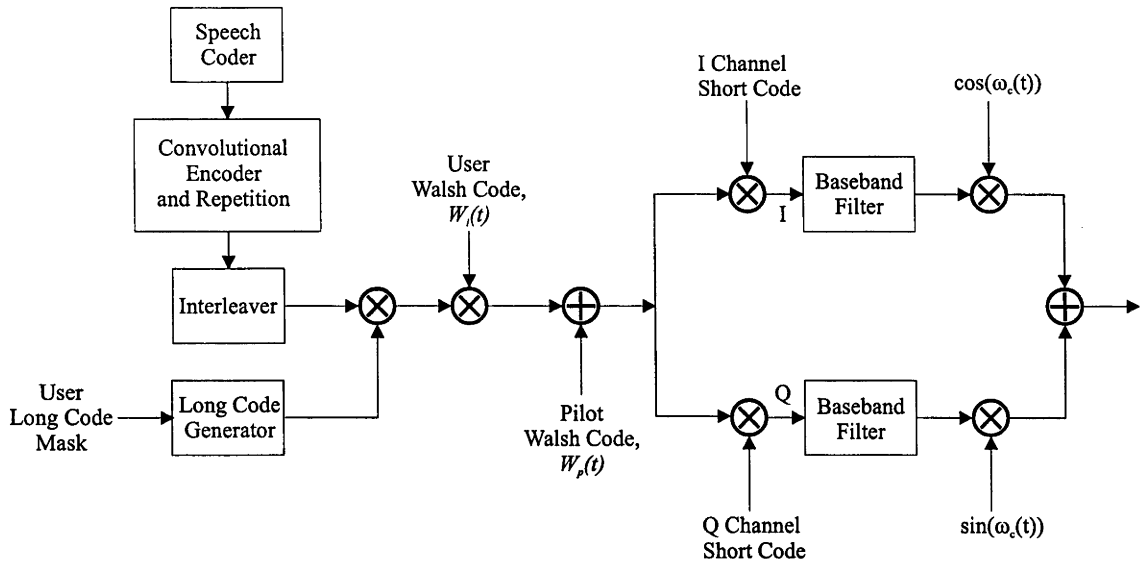


Figure 2.1: IS-95 CDMA forward link

distinguished at the mobile receiver by the choice of orthogonal Walsh code. In this way the CDMA modulator can establish 64 channels on the same carrier frequency on the forward link. Pilot information is transmitted at a relatively higher power level to allow the carrier phase to be tracked to permit coherent demodulation of the data bearing signals. The mobile receiver uses a number of correlators for demodulating the data bearing signals from the base station.

2.3 CDMA Reverse Link

The reverse link is shown in Fig. 2.2. The data rate of the reverse link is also 9600 bits/sec. The information stream is partitioned once again into 20 msec blocks followed by convolutional encoding by a 1/3 code with constraint length 9. This provides a coded bit rate up to 28.8 kbits/sec which is then interleaved. Code words of 6 bits each are formed. The code words select one of the 64 different orthogonal codes for transmission. In this case the Walsh code is determined by the information being transmitted (a way of achieving 64-ary modulation). The chip rate at the output of the Walsh modulator is 307.2 kchips/sec which is further spread to 1.228 Mchips/sec using the mobile-specific long code. The data stream is once again split into I and Q streams where it is multiplied by the same short code pair as that used for the forward link. The resulting spread spectrum

signal is then carried over the air interface with a filtered offset-QPSK modulation. The signals from the multiple transmitting users are distinguished at the base station by their use of the very long $2^{42} - 1$ pseudo-noise (PN) sequence. Each user has a unique time offset. At the base station, the received signal is processed by non coherent RAKE receivers

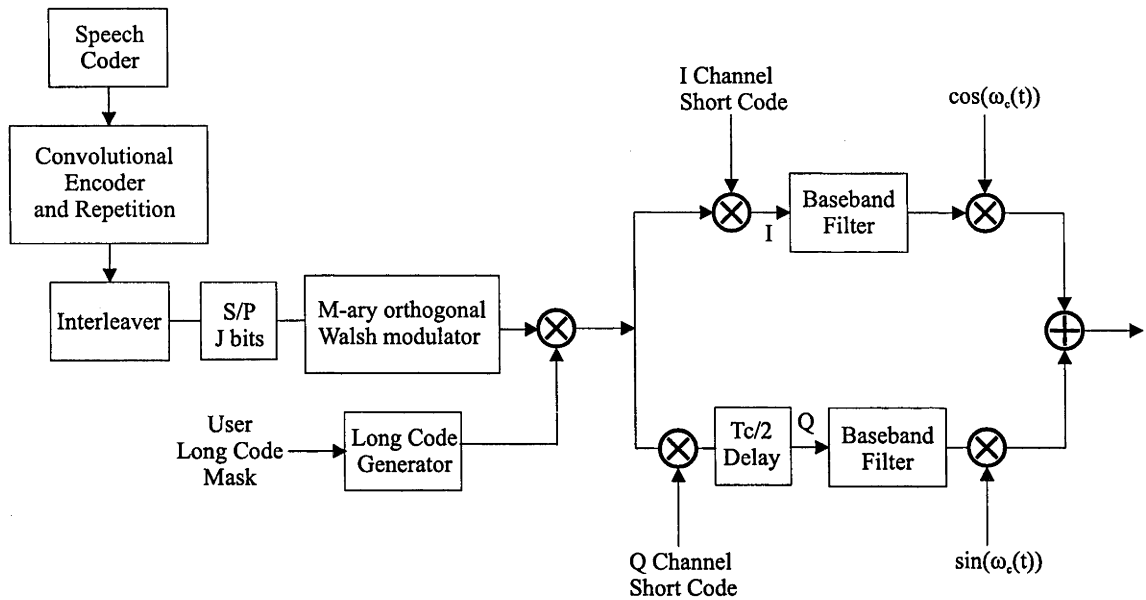


Figure 2.2: IS-95 CDMA reverse link

since there is no provision for pilot information. The P strongest paths are ordered and combined via a bank of delay filters.

2.4 Design Methodology and Implications

Let us now consider some CDMA design methodologies. There are basically two philosophies [119] which favour different lengths of pseudo-noise (PN) sequences used as spreading codes:

- Long Codes - the PN sequence's period is much longer than the symbol period.
- Short Codes - the PN sequence's period is exactly one symbol period

This thesis will only consider short codes although it can be generalised to long codes. In Part I, we will concentrate on the performance evaluation of uncoded and coded

CDMA systems using random codes. We do not select spreading codes with particularly good auto-correlation and cross-correlation properties to suppress MAI. In fact, it has been shown that the use of random codes incurs no penalty in the sum capacity asymptotically as the number of users increase [45][44]. In Part II, we will investigate the performance of two multiuser detectors for the time-varying, frequency-selective Rayleigh channel. The spreading sequences will once again be chosen randomly and are constrained to one symbol interval. However, there is some amount of signature overlapping due to the use of root raised cosine chip pulse shaping. The use of short codes facilitates the design of multiuser receiver structures.

As discussed in the previous sections, the IS-95 CDMA standard adopts the long code philosophy. At the heart of this approach is the fundamental claim that the MAI appears as wideband AWGN [132]. As the number of users increase the contribution from the interfering users (assuming each have equal received power) can be approximated by a Gaussian random variable [119]. This claim is a misconception as pointed out by Verdú on many occasions and is the underlying reason for the near far problem of CDMA. In the common situation where all of the signals arriving at the receiver are of different signal strengths, the stronger signals tend to swamp the weak signals. Because of this, an accurate power control mechanism is required in the IS-95 reverse link to limit fluctuations in the received signal's power to within a fraction of a dB.

Single user detection is often tied to the concept of Matched Filtering. In this case the received signal is correlated with the spreading sequence and the correlator's output is generally followed by a decision device. When there is only one user (ie. no MAI) this detection scheme is optimal. However, in the multiuser scenario it is only optimal if the delays are known perfectly and the signature sequences of all users are orthogonal (ie. no MAI) [127]. To reiterate, the Gaussian approximation disregards the rich structure of the MAI, thereby losing valuable information that could have been used to make more accurate decisions.

2.5 Basic DS-CDMA System Model

In this section a basic system model will be described. This basic model will be augmented in each chapter to allow new parameters to be incorporated as the need arises.

The model consists of a data source, a transmitter, a channel, a receiver and a data sink. The source data is usually source encoded to reduce the amount of redundancy (data compression), then channel encoded to allow a limited number of transmission errors to be corrected. The encoded signals are then mapped to a signal constellation (eg. BPSK, QPSK). The i th transmitted symbol (a constellation point in the signal space) of the k th user is denoted by $b_{i,k}$. The signature sequence for the i th time interval and k th user is $s_{i,k}(t)$. In a spread spectrum system, the number of chips per symbol period, N , is known as the processing gain. It determines the signal's resistance to jamming or multiple interferers [127]. It is defined as the ratio of the symbol duration to the chip duration as

$$N = T_s/T_c \quad (2.1)$$

For a reverse link it is appropriate to model each user as transmitting independently. This asynchronism amongst users can also be characterised by a delay ζ_k . The delay is fractionally chip aligned. In the basic model, each chip uses rectangular pulse shaping. In the later chapters we will relax this to incorporate raised cosine and root raised cosine pulse shaping.

Radio propagation is usually characterised by three partially separable effects known as path loss, shadowing and multipath fading. Path loss characterises the reduction in the received power level, $P(r)$ with distance r . It generally follows an inverse power law in the distance between the transmitter and the receiver, as

$$P(r) = P(r_0) \left(\frac{r_0}{r}\right)^n, n \sim 2, \dots, 4 \quad (2.2)$$

Shadowing is caused by terrain features in the propagation environment. It imposes large scale variations on the path loss formula. Typically a log-normal distribution has been best found to fit the experimental data in an urban area. In our work, we can ignore path loss and shadowing, as these large scale attenuations are compensated by power control. Only multipath affects the system performance and receiver design. The multipath model will be described in detail in Part II (chapter 5). For now, it suffices to know that due to the cluttered environment, the signal transmitted from the base station reflects,

diffracts and is scattered off trees, buildings, hills and other obstacles before arriving at the receiver. These travel different distances, so they arrive with different carrier phases and add as a complex sum. In the “time invariant frequency flat” case, where all the paths have similar lengths and the mobile terminal is moving slowly, the channel is characterised by a single complex gain, c_k when there are many paths. It is Rician distributed if there is a line of sight (LOS) component and Rayleigh distributed otherwise. Thus the total received signal can be modelled as the sum of each user’s transmitted signal multiplied by this complex gain (see Fig. 2.3), as

$$r(t) = A(t, \mathbf{b}) + n(t) \tag{2.3}$$

where

$$A(t, \mathbf{b}) = \sum_{k=1}^K \sum_{i=0}^{\Omega-1} \sqrt{E_{i,k}} b_{i,k} c_k s_k(t - iT_s - \zeta_k) \tag{2.4}$$

$\sqrt{E_{i,k}}$ is the gain for power control in the i th interval for the k th user. This model is typical of a reverse link where each user has their own independent delays.

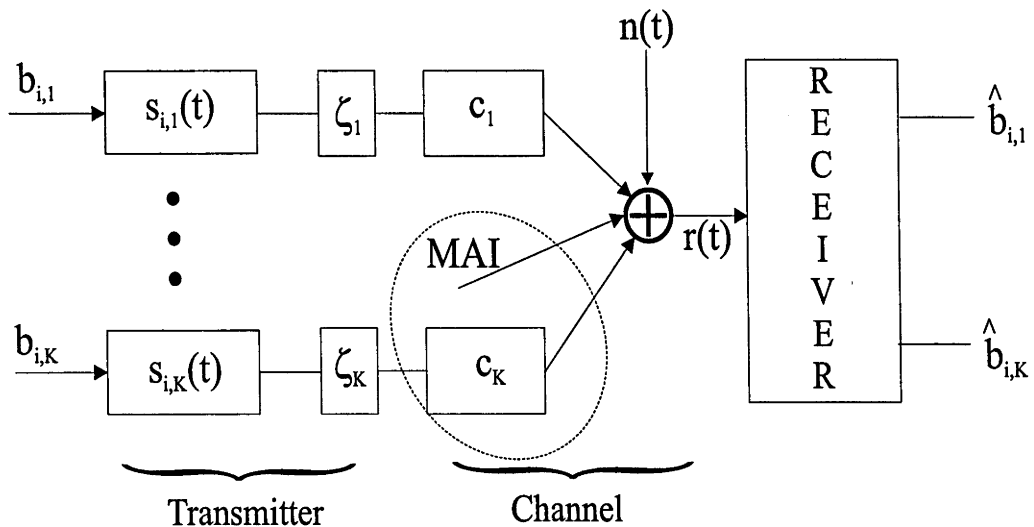


Figure 2.3: DS-CDMA System Model

At the receiver there are three options in order to obtain a set of sufficient statistics

about the received signal. The continuous time waveform can either be sampled at the Nyquist rate $1/T_r = r/T_c$, the chip rate $1/T_c$, or the symbol rate $1/T_s$. For the chip matched filtering case, a front end filter matched to the chip waveform is used. For an AWGN or frequency flat, time invariant channel the received waveform is passed through a filter matched to the set of preassigned signature waveforms and sampled at the symbol rate. It is the output of these filters that is important and has been used in various ways to cancel MAI to produce a reliable decision. We discuss some of these methods in a later section.

2.5.1 Synchronous AWGN CDMA Channel Model

In this section we assume all transmitters are synchronised to the same time origin (ie. a synchronous model) and that the channel exhibits no multipath. K users transmit their respective symbols $b_{i,k}$ where i denotes the symbol interval $i \in \{0, \dots, \Omega - 1\}$. The spreading code used by user k at symbol interval i consists of N chips and is stored in the vector $\mathbf{s}_{k,i}$. By arranging the K spreading codes at time i in a matrix \mathbf{S}_i , the energies, $\sqrt{E_{i,k}}$ of all users in a matrix \mathbf{W}_i , the data bits in a vector \mathbf{b}_i and the noise samples in a vector \mathbf{n}_i , the received signal samples \mathbf{r}_i over the i th symbol period can be written as

$$\mathbf{r}_i = \mathbf{S}_i \mathbf{W}_i \mathbf{b}_i + \mathbf{n}_i \quad (2.5)$$

where

$$\begin{aligned} \mathbf{S}_i &= (\mathbf{s}_{1,i}, \dots, \mathbf{s}_{K,i}) \in \{-1, 1\}^{N,K} \\ \mathbf{W}_i &= \text{diag}(\sqrt{E_{i,1}}, \dots, \sqrt{E_{i,K}}) \in \mathbb{R}^{K,K} \\ \mathbf{b}_i &= (b_{i,1}, \dots, b_{i,K})^T \in \{-1, 1\}^K \\ \mathbf{n}_i &= (n_{i,1}, \dots, n_{i,N})^T \in \mathbb{R}^N \end{aligned}$$

Hence, for the entire transmitting interval $i = \{0, \dots, \Omega\}$

$$\begin{aligned} \mathbf{S} &= \text{diag}(\mathbf{S}_0, \dots, \mathbf{S}_{\Omega-1}) \in \{-1, 1\}^{\Omega N, \Omega K} \\ \mathbf{W} &= \text{diag}(\mathbf{W}_0, \dots, \mathbf{W}_{\Omega-1}) \in \mathbb{R}^{\Omega K, \Omega K} \\ \mathbf{b} &= (\mathbf{b}_0^T, \dots, \mathbf{b}_{\Omega-1}^T)^T \in \{-1, 1\}^{\Omega K} \\ \mathbf{n} &= (\mathbf{n}_0^T, \dots, \mathbf{n}_{\Omega-1}^T)^T \in \mathbb{R}^{\Omega N} \end{aligned}$$

so that the entire output of the channel is simply

$$\mathbf{r} = \mathbf{S}\mathbf{W}\mathbf{b} + \mathbf{n} \in \mathbb{R}^{\Omega N} \tag{2.6}$$

The received waveform is matched to the set of signature waveforms used for transmission. The MF output can thus be written as

$$\begin{aligned} \mathbf{r}' &= \mathbf{S}^T \mathbf{r} \\ &= \mathbf{S}^T \mathbf{S}\mathbf{W}\mathbf{b} + \mathbf{S}^T \mathbf{n} \\ &= \mathcal{R}\mathbf{W}\mathbf{b} + \mathbf{S}^T \mathbf{n} \end{aligned} \tag{2.7}$$

where \mathcal{R} is the non-negative definite correlation matrix

$$\begin{aligned} \mathcal{R} &= \mathbf{S}^T \mathbf{S} \in \mathbb{R}^{\Omega K, \Omega K} \\ &= \begin{bmatrix} \mathbf{R}_0(0) & \underline{0} & \dots & \dots & \underline{0} \\ \underline{0} & \mathbf{R}_1(0) & \dots & \dots & \underline{0} \\ \underline{0} & \underline{0} & \mathbf{R}_2(0) & \dots & \underline{0} \\ \vdots & \vdots & \vdots & \ddots & \vdots \\ \underline{0} & \underline{0} & \underline{0} & \dots & \mathbf{R}_{\Omega-3}(0) & \underline{0} \\ \underline{0} & \underline{0} & \underline{0} & \dots & \underline{0} & \mathbf{R}_{\Omega-2}(0) & \underline{0} \\ \underline{0} & \underline{0} & \underline{0} & \dots & \underline{0} & \underline{0} & \mathbf{R}_{\Omega-1}(0) \end{bmatrix} \end{aligned} \tag{2.8}$$

and

$$\mathbf{R}_i(0) = \mathbf{S}_i^T \mathbf{S}_i \tag{2.9}$$

The MF receiver is a direct application of a single user system to the multiuser case. The second term in (2.7) represents the white noise being coloured, with autocorrelation matrix $N_0\mathcal{R}$.

If the MF output is now passed through a thresholding function, such as $\text{sgn}(\cdot)$ a conventional detector is realised. It treats all other transmissions as noise. The structure of this receiver is shown in Fig. 2.4.

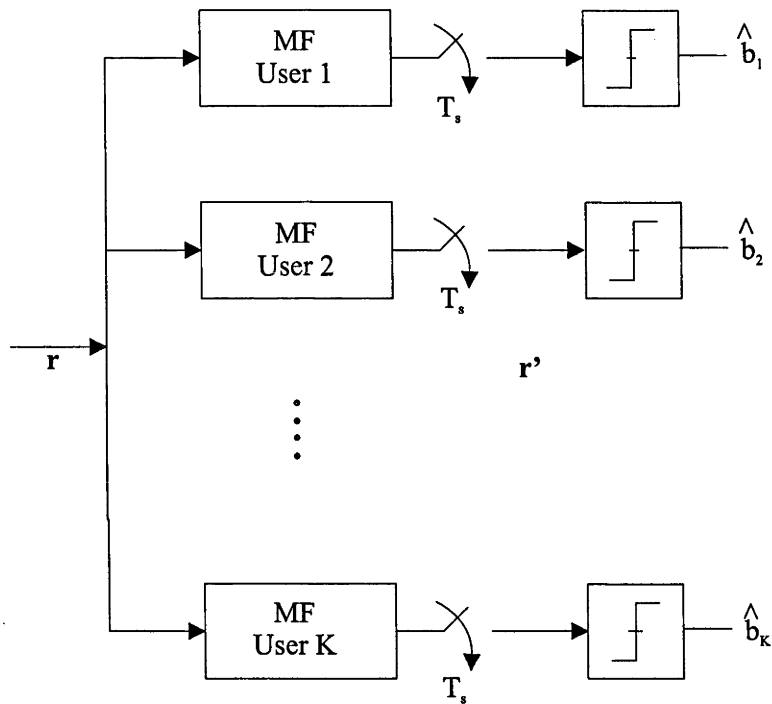


Figure 2.4: Conventional DS-CDMA Detector

2.5.2 Asynchronous AWGN CDMA Channel Model

Asynchronism between users can also be handled in a similar way. The received signal after a bank of MFs can be expressed in a linear algebraic form as

$$r' = \mathcal{R}Wb + S^T n \tag{2.10}$$

where the correlation matrix \mathcal{R} is now block tri-diagonal since the spreading codes that arrive more than a symbol apart do not overlap. It equals

$$\mathcal{R} = \begin{bmatrix} \mathbf{R}_0(0) & \mathbf{R}_1^T(1) & \underline{0} & \cdots & \underline{0} \\ \mathbf{R}_1(1) & \mathbf{R}_1(0) & \mathbf{R}_2^T(1) & \cdots & \underline{0} \\ \underline{0} & \mathbf{R}_2(1) & \mathbf{R}_2(0) & \cdots & \underline{0} \\ & & & \ddots & \vdots \\ \vdots & \vdots & \vdots & & \mathbf{R}_{\Omega-3}(0) & \mathbf{R}_{\Omega-2}^T(1) & \underline{0} \\ \underline{0} & \underline{0} & \underline{0} & \cdots & \mathbf{R}_{\Omega-2}(1) & \mathbf{R}_{\Omega-2}(0) & \mathbf{R}_{\Omega-1}^T(1) \\ & & & & \underline{0} & \mathbf{R}_{\Omega-1}(1) & \mathbf{R}_{\Omega-1}(0) \end{bmatrix} \quad (2.11)$$

where

$$\mathbf{R}_i(m) \in \mathbb{R}^{K,K}, 0 \leq i \leq \Omega - 1 \text{ is symmetric, and}$$

$$\mathbf{R}_i(1) \in \mathbb{R}^{K,K}, 1 \leq i \leq \Omega - 2 \text{ is strictly upper triangular}$$

The (k, k') th element of $\mathbf{R}_i(m)$ describes the energy collected by the k th user's matched filter at symbol interval i due to the transmission by user k' in the symbol interval $i - m$. Since $\mathbf{R}_{i-1}(-1) \equiv \mathbf{R}_i^T(1)$, $\mathbf{R}_i(-1)$ has been replaced by $\mathbf{R}_{i+1}^T(1)$ in (2.11). $\mathbf{R}_i(m)$ equals

$$\begin{aligned} \mathbf{R}_i(0)^{k,k'} &= \mathbf{s}_j^{T,k,i} \mathbf{s}_j^{k',i-m}, \\ k, l &\in \{1, \dots, K\} \\ i &\in \{0, \Omega - 1\} \\ m &\in \{-1, 0, 1\} \end{aligned}$$

In the asynchronous case it is possible to transform the problem into an equivalent synchronous case. In the one shot approach, where each symbol interval is considered separately, bit overlapping between users can be regarded as separate transmissions by fictitious users [123]. Take, for example, a 2 user case where bit 0 of user 1 occupying the interval $[0, T]$ overlaps with bit -1 of user 2 over the interval $[0, \zeta_2]$ and also bit 0 of user 2 over the interval $[\zeta_2, T]$. This problem can be decomposed into a 3-user synchronous channel. At the heart of this approach is the partitioning of the signature waveform of user 2 to its left and right components. The one shot detector has lower complexity than the asynchronous detector at the expense of some performance degradation.

2.6 Interference Rejection

As more users transmit over the top of one another the increased sharing of spectrum naturally translates into a higher likelihood of users interfering with one another. Interference rejection (IR) techniques allow more users to be supported within the available spectrum as compared to a system lacking IR techniques. Moreover, as more than one technology usually exists at any time, as older technologies are superseded by newer ones, hybrid networks are inevitable. For example, an IS-95 CDMA system overlaid with AMPS results in AMPS-to-IS-95 and IS-95-to-AMPS interference on adjacent cells. Another example is broadband CDMA (B-CDMA) suggested by Schilling et al. [98]. It co-exists with the current cellular services yet provides additional capacity to the network. B-CDMA causes interference to existing services yet must be robust to their interference, such as high powered narrowband interference from TV and FM radio stations. In satellite systems, geostationary satellites can interfere with each other as well as with LEO satellites. In all these situations, interference rejection techniques may be applied to null out unwanted distortions and considerably improve the quality of service. An organisational chart of the many interference cancellation techniques to date can be found in Fig. 2.5

In this thesis we will be mainly concerned with wideband interference. An example of wideband interference is multiple access interference (MAI). A comprehensive literature survey on multiuser detection can be found in many references [32, 61, 74, 127]. We highlight some of the key contributions here.

2.7 The Multiuser Detection Problem

Multiuser detection is the study of strategies to demodulate the digital information sent simultaneously by several transmitters who share a common channel. As is well known the conventional single user detector minimises the probability of error in a single user channel (in the absence of interfering users). However, this scheme is no longer optimal when there are several users. In fact, it is necessary to obtain information about all users so that they can be demodulated *jointly* to produce a more accurate decision. This problem of joint demodulation and decoding is the multiuser detection problem.

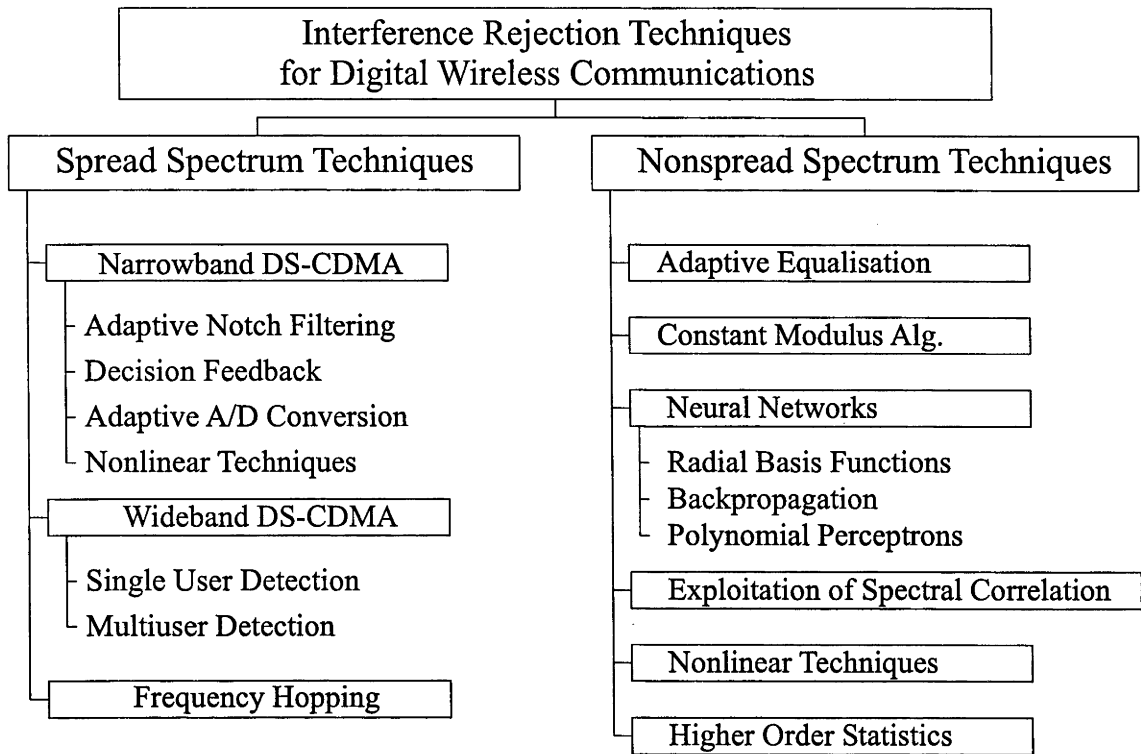


Figure 2.5: Interference rejection (IR) techniques for wireless digital communications [61]

2.7.1 Advantages of Multiuser Detection

Solution to the Near Far problem - Correlation receivers are susceptible to the near far problem when multiple access signals are received with different signal powers. Before the emergence of multiuser detection, success in this area has been very limited and the only remedies were fast and accurate power control and the design of signals with even more stringent crosscorrelation properties. The solution to the near far problem has been advertised as the main achievement of multiuser detection.

Increased capacity - Greater channel capacity can be achieved by using interference rejection techniques like multiuser detection to mitigate MAI. The reduction in interference power transforms into either an increase in system capacity or a reduction in the mobile's average transmit power. Compared to the conventional single user detector, it has been reported that multiuser detector doubles or triples channel capacity [61].

2.7.2 Disadvantages of Multiuser Detection

Too complicated - The optimal multiuser receiver is hopelessly too complex to be implemented. As a result, several sub-optimal receivers have been proposed to approximate it. Sophisticated signal processing techniques such as the use of adaptive equalisation, neural networks and other nonlinear approaches still require a heavy computational load. As digital signal processing capabilities improve these schemes are starting to show more promise.

Incomplete Analytical Performance Results - BER analyses of the numerous multiuser techniques are beginning to become more complete. However, there is still scope for further analysis to include their impact on the overall system capacity, so that their contributions may be fully appreciated.

Increased need for estimation - In a practical multiuser system there is an increased need for parameter estimation. There are more system unknowns (eg. signature sequences of all users, timing synchronisation parameters for all users), but the observation space is of the same order.

2.8 Optimum Multiuser Detection

A Maximum Likelihood (ML) multiuser sequence detector selects the most likely transmitted sequence according to

$$\hat{\mathbf{b}}_{ML} = \arg \max_{\mathbf{b} \in \{-1,+1\}^{\Omega K}} p(\mathbf{r}|\mathbf{b}) \quad (2.12)$$

Verdú [122] proposed this receiver in 1986 and it is generally known as the optimum receiver. The likelihood function that needs to be maximised can be written as

$$\begin{aligned}
\hat{\mathbf{b}}_{ML} &= \arg \max_{\mathbf{b} \in \{-1,+1\}^{\Omega K}} p(\mathbf{r}|\mathbf{b}) \\
&= \arg \max_{\mathbf{b} \in \{-1,+1\}^{\Omega K}} \frac{1}{\det(2\pi\mathbf{R}_{nn})} \exp \left[-\frac{1}{2}(\mathbf{r} - \mathbf{S}\mathbf{W}\mathbf{b})^H \mathbf{R}_{nn}^{-1} (\mathbf{r} - \mathbf{S}\mathbf{W}\mathbf{b}) \right] \\
&= \arg \min_{\mathbf{b} \in \{-1,+1\}^{\Omega K}} (\mathbf{r} - \mathbf{S}\mathbf{W}\mathbf{b})^H \mathbf{R}_{nn}^{-1} (\mathbf{r} - \mathbf{S}\mathbf{W}\mathbf{b}) \\
&= \arg \min_{\mathbf{b} \in \{-1,+1\}^{\Omega K}} |\mathbf{r} - \mathbf{S}\mathbf{W}\mathbf{b}|^2 \text{ in white noise,} \\
&= \arg \min_{\mathbf{b} \in \{-1,+1\}^{\Omega K}} \mathbf{r}^H \mathbf{r} - 2\mathbf{b}^H \mathbf{W}\mathbf{S}^H \mathbf{r} + \mathbf{b}^H \mathbf{W}\mathbf{S}^H \mathbf{S}\mathbf{W}\mathbf{b} \\
&= \arg \min_{\mathbf{b} \in \{-1,+1\}^{\Omega K}} -2\mathbf{b}^H \mathbf{W}\mathbf{S}^H \mathbf{r} + \mathbf{b}^H \mathbf{W}\mathbf{S}^H \mathbf{S}\mathbf{W}\mathbf{b}
\end{aligned} \tag{2.13}$$

assuming the white Gaussian noise with autocorrelation matrix equal to

$$\mathbf{R}_{nn} \triangleq \frac{1}{2} \mathbf{E}\{\mathbf{nn}^T\} = N_0 \mathbf{I} \tag{2.14}$$

$\mathbf{r}' = \mathbf{S}^H \mathbf{r}$ in (2.13) can be viewed as a bank of MF followed by a Viterbi algorithm (VA) instead of a hard decision device as is the case for a conventional single user detector (see Fig. 2.6). The VA has an exponential complexity in the number of users. In the K user case, there are 2^K possible realisations of \mathbf{b} and no algorithm exists that can solve (2.13) via a number of steps that is polynomial in the number of users [123]. It has been shown in [124] that the MLSD algorithm belongs to the class of longstanding combinatorial problems such as the travelling salesman problem which are NP-hard.

2.9 Suboptimal Receivers

Although the optimum detector achieves important performance gains over the conventional single user detector, the price for this is its exponential complexity in the number of users. This has triggered the search for low-complexity multiuser detectors that exhibit good performance and are also near far resistant. An organisational chart in Fig. 2.7 shows the various techniques used to combat MAI from a DS-CDMA perspective.

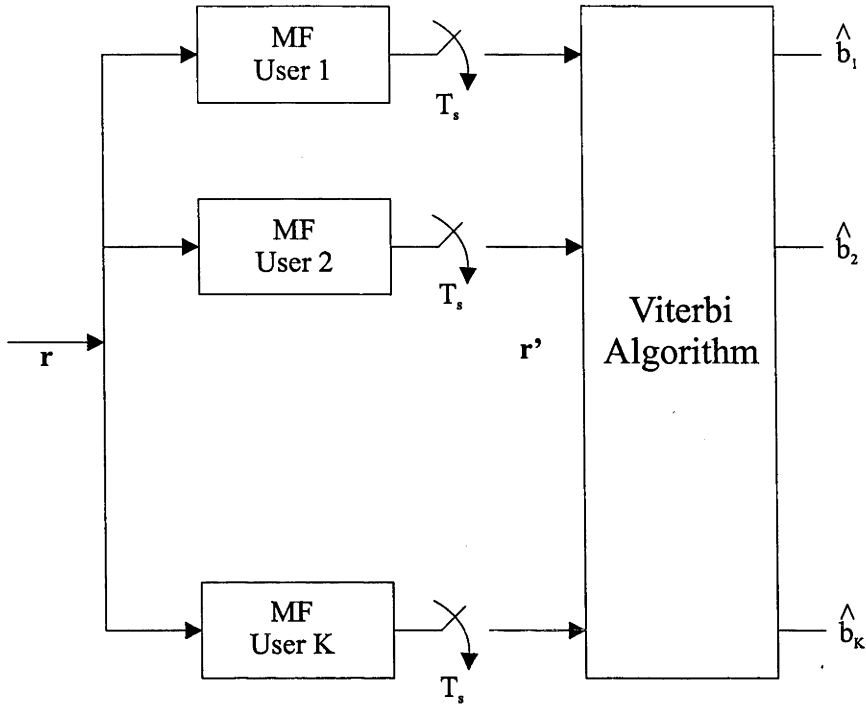


Figure 2.6: Optimum multiuser detector

2.9.1 Linear Complexity Receivers

In the context of multiuser detection, a linear complexity receiver is one whose complexity is linear in the number of users. In general, a linear transformation of the MF outputs is produced to pass soft information onto a subsequent stage of the detection process [31][114][138][146].

Decorrelating detector - This receiver multiplies the MF outputs in (2.7) by the inverse cross-correlation matrix \mathcal{R}^{-1} . Note that the decorrelating detector completely eliminates MAI. However, the power of the noise is $N_0(\mathcal{R}^{-1})$ which is greater than the noise power at the output of the MF. The bit error rate for the k th user of the decorrelator is given by

$$P_k = Q\left(\sqrt{\frac{E_k}{N_0 \mathcal{R}_{k,k}^{-1}}}\right) \tag{2.15}$$

where $\mathcal{R}_{k,k}^{-1}$ is the (k, k) th element of the matrix \mathcal{R}^{-1} . Observe that the decorrelating detector requires a matrix inversion which is not particularly suitable for a large number

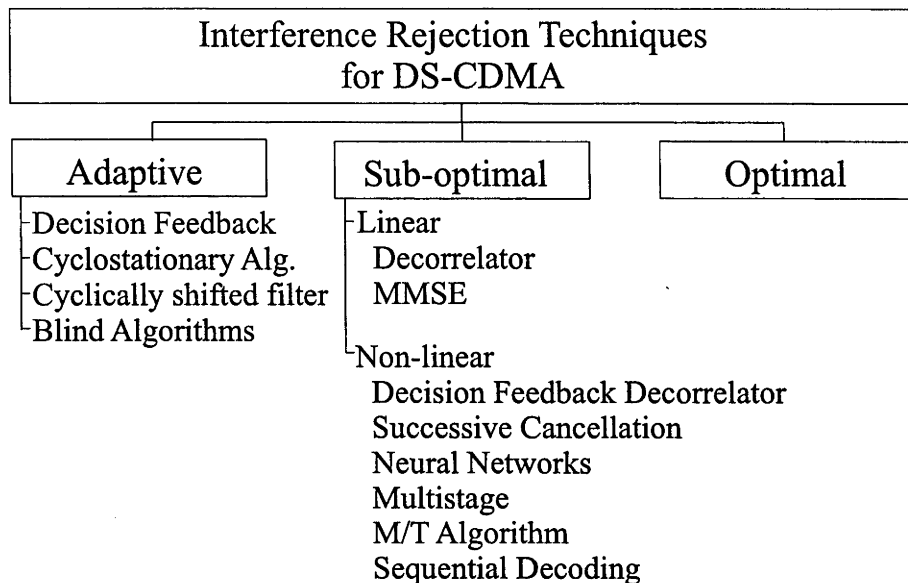


Figure 2.7: Organisational chart for multiuser interference rejection in DS-CDMA [61]

of users. On the other hand, the decorrelating receiver provides the same degree of near far resistance as the optimum multiuser receiver and is substantially easier to compute. Furthermore, it does not require knowledge of the powers of the interfering users.

MMSE - The linear minimum mean squared error (MMSE) detector replaces the inverse cross-correlation matrix \mathcal{R}^{-1} by $[\mathcal{R} + N_0\mathbf{W}^{-2}]^{-1}$ such that noise enhancement is balanced against MAI. The MMSE detector can outperform a decorrelating detector when the desired user is strong and all the interferers are very weak. Essentially this receiver is a multidimensional version in its output of the MMSE linear equaliser for the single-user ISI channel [32]. Unlike the decorrelator it does not require the assumption of linear independence for all signature waveforms. It is an appealing solution due to its relative ease in an adaptive implementation. Its performance is similar to the decorrelator in the absence of background noise but approaches the conventional single user detector in the presence of significant MAI.

2.10 Nonlinear Receivers

Nonlinear receiver structures can be mainly classified into four categories:

-
- Multistage Detectors
 - Decision Feedback Detectors
 - Successive Interference Cancellers
 - Neural Networks

In general these receivers detect the stronger users first and these are then cancelled from the signal so that weaker users may be detected. Problems of error propagation and long delays are inevitable, but these receivers promise to be practical and efficient solutions to the near far problem.

Multistage detection techniques involve repetitive detection/cancellation steps. All users are detected in the first stage and then used in the next stage to cancel interference present in the signal of the desired user. Due to delay and complexity constraints it is desirable to limit the number of stages to two. To obtain more reliable estimates, the decorrelator is often chosen as the first stage. Two important design questions arise [32]:

- How should the initial stage be chosen?
- How should the subsequent processing stages be chosen?

Successive Interference Cancellers cancel the strongest signal before detection of the other signals because it has the most negative effect. Subtracting off the strongest remaining signal at each step assumes accurate estimation and ordering of the received user amplitudes. Hence, the process must operate fast enough so as not to introduce large decision delays. Viterbi has concluded that the complexity and the processing delay make the application of this scheme questionable [134]. A parallel successive interference cancellation method was recently proposed whereby all of the users' signals are subtracted simultaneously from all other users [84]. This scheme outperforms the successive scheme when all users are received with equal strength. Both schemes outperform the conventional detector. Decision feedback detectors are another class of receivers that use feedforward and feedback filters to cancel MAI [29][31].

Neural networks have only been recently used for CDMA applications. Multiuser detection using a backpropagation neural net was proposed by Aazhang to approximate the

MLSD receiver [1]. These algorithms can simultaneously account for non-linearity in decision boundaries between signal states, non-stationarity and non-Gaussian interference. A radial basis function neural network was used by Mitra to perform multiuser detection and has shown near-optimal performance in realistic communication environments [73].

2.11 Adaptive Multiuser Detection

Adaptive detection is required for practical time varying channels. The receivers are continually being optimised as the channel conditions or the user environment changes.

MMSE - The minimum mean squared error (MMSE) solution has been used on a number of occasions [68][69]. The channel output is first passed through a filter matched to the chip waveform and then sampled at the chip rate. This MMSE detector computes filter coefficients, $w(i)$, adaptively based on minimising the mean squared error for each user as

$$\mathbf{w}_{i+1} = \mathbf{w}_i - \mu \epsilon(i) \mathbf{r}_i \quad (2.16)$$

where μ is the step size. This is the Least Mean Squares (LMS) algorithm. To increase the acquisition speed of the LMS algorithm, other faster algorithms like the Recursive Least Squares (RLS) have been used [69].

Rapajic et al. proposed a "single-user" asynchronous receiver where the receiver is trained by a known training sequence in the start up phase before actual data transmission [89]. This receiver is termed "single-user" since only one user's spreading code and delay is known and utilised by the receiver. A fractionally spaced LMS filter is adapted instead of the standard MF with fixed coefficients. Simulation results have verified a substantial improvement in BER when compared to the conventional single user detector. This is shown in Fig. 2.8. Lately in [90] Rapajic also investigated an adaptive transmitter-receiver pair such that the transmitter signatures are adjusted according to a MSE criterion during data transmission. Systems employing such a scheme in the presence of MAI can achieve the matched filter bound as they can eliminate interference.

Cyclostationary algorithms have been applied successfully to interference rejection in

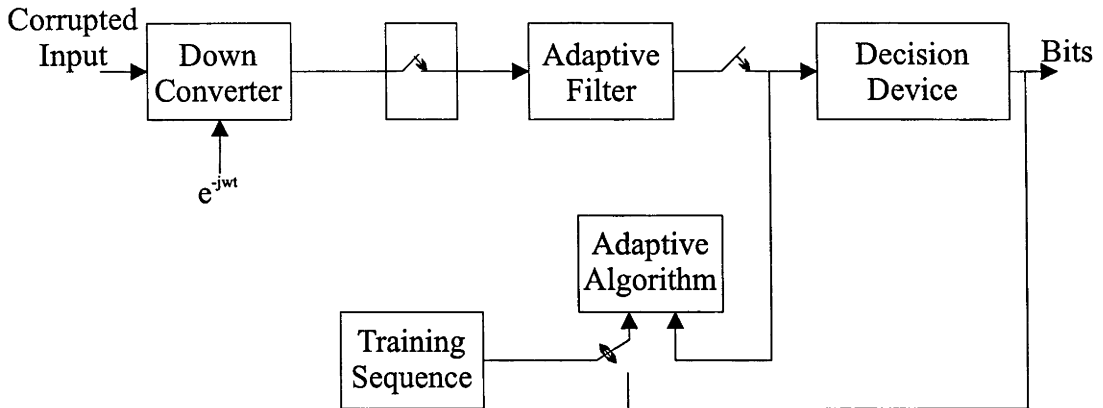


Figure 2.8: Adaptive “single-user” receiver

DS-CDMA [2]. Cyclostationary CDMA signals have periodic statistical properties that exist at the chip rate. By exploiting spectral diversity in CDMA networks, a more stable and robust system is realised. Aue and Reed also show how spectral correlation can be exploited by an adaptive filter [10].

Blind detection algorithms are also of interest in their own right since they enable receivers to asynchronously acquire a transmission at any time. Adaptive multiuser detectors generally solve this problem by using a training phase to initialise filter coefficients and system parameters and thus prepare themselves for future data transmissions. However, this training sequence is wasteful in terms of capacity, and in a multiuser environment training is required for all users. In a fading channel retraining is needed after a user experiences a deep fade. Detection before the next training sequence is therefore unreliable. Blind detection removes this dependence since the receiver can recover automatically. Such receivers can be classified into three main categories, namely [70]:

1. The receiver knows the timing and spreading waveform of the desired user.
2. The receiver knows only the spreading waveform of the desired user.
3. The receiver does not know any information about the desired user, other than the fact that the desired user signal is digitally modulated at a given symbol rate.

Honig [52] proposed a blind linear complexity near-far resistant receiver of category (1), namely the constrained minimum output energy, (CMOE) receiver. The strategy is to

minimise the output error, which is equivalent to minimising the MSE. It has global convergence due to the convexity of the cost function. Category (2) receivers are usually subspace based blind receivers. Recently, subspace based representations of multiuser detectors have been considered in [136]. If the signal and noise subspaces can be estimated, the problem reduces to one of finding the best fit among different hypothesized propagation channels with the estimated subspaces. One example is the MUSIC algorithm which minimises the projection of the hypothesised signal vectors onto the estimated noise subspace. Category (3) would be classified as blind equalisation for a system with one user and blind source separation for multiple users. This class of receivers use higher order statistics (HOS) to separate digitally modulated sources.

The Constant Modulus Algorithm (CMA) has recently been applied to this area. For constant modulus signals (eg. frequency shift keying (FSK), phase shift keying (PSK)) the CMA works by adapting a filter to restore the signal's constant envelope thereby rejecting interference and suppressing the channel's distortions. It is attractive due to its relatively low complexity and faster local convergence rate. However, the cost function does not distinguish between the desired user and interfering symbols, which leads to a number of local minima. To this end many variations of the modified CMA have been studied, namely linearly constrained CMA and anchored CMA [72][59].

The application of blind adaptive algorithms to the suppression of multiuser interference is a continuing area of research that promises to provide substantial performance gains over conventional reception, yet with very low complexity.

2.12 Summary

This chapter provided an overview of spread spectrum communications, in particular code-division-multiple-access. An overview of the IS-95 CDMA standard was given to highlight the current standards and design methodologies. A basic direct sequence CDMA system model has been introduced although further elaborations will be incorporated. Finally, a survey of the various techniques used for interference rejection has been presented with special attention to wideband interference (MAI).

PART 1

Performance evaluation techniques of uncoded and coded multiuser DS-CDMA systems in Gaussian and slow Rayleigh fading channels

OVERVIEW: We investigate methods to compute accurate bit error probability bounds for an uncoded multiuser CDMA system accommodating a large number of users. These bounds are useful since they provide a theoretical benchmark to compare other practical receiver designs. In the later half of this section we study parameters and algorithms to evaluate a multiuser CDMA system using error control coding.

Performance Evaluation of Optimum Multiuser DS-CDMA Systems

Overview: The exact bit error rate (BER) performance of a CDMA system with a large number of users is difficult to compute analytically. An efficient method is proposed to compute accurate BER bounds for various system configurations. This simple yet powerful method relies on well known bounding techniques and can provide theoretical benchmarks for comparison with other receiver designs.

3.1 Introduction

Recently joint multiuser detection, in which the multiuser interference is treated as part of the information, rather than noise, has attracted much attention. The seminal work of Verdú has shown that significant performance improvement and optimum near far resistance over the conventional detector can be achieved by a maximum likelihood multiuser detector [121] [122]. The substantial improvements however, are obtained at the expense of a dramatic increase in computational complexity. This complexity grows exponentially with the number of users. Thus, as the number of users increases, the optimum detector becomes infeasible. It is therefore necessary to use a “near” optimum, low complexity detector for CDMA systems which accommodates a large number of users.

Since then many low complexity multiuser detectors have been proposed. Lupas and Verdú considered a linear complexity multiuser detector in [66][67]. The linear multiuser detector achieves optimum near-far resistance but cannot provide “close” to optimum performance. A multistage technique was proposed by Varanasi and Aazhang [114][115],

and Duel-Hallen suggested the decorrelating decision feedback detector (DDFD) [29]. Due to error propagation, the multistage multiuser detector and the DDFD achieve “near” optimum performance only when the interfering users are significantly stronger than the user under consideration (ie. the weakest user benefits the most).

Many other suboptimum detectors have been proposed in the last decade and have claimed to be “near” optimum. The question is how near is “near”? Does there exist a benchmark to compare all variants of receiver designs and performances? To date a reliable performance measure like the bit error rate or the asymptotic efficiency is not known for a large number of users, except for the single user bound which is a simple performance lower bound. This makes it hard to compare objectively the performances claimed by the numerous suboptimum multiuser detectors.

This chapter will first provide background information on multiuser error events. This will then provide the basis to compute bit error probability bounds, in particular an exact lower bound and a tight upper bound for a multiuser DS-CDMA system corrupted by additive white Gaussian noise or a time-invariant frequency flat Rayleigh fading channel.

It will be shown that on Gaussian channels, the upper bound converges to the lower bound at moderate to large signal to noise ratios. However, on fading channels the upper bound does not converge and hence, only a lower bound is obtained. From numerical simulations, it will be shown that (a) the bit error probability (BEP) of a 31 user CDMA system with binary random spreading codes of length 31 is only 2 to 4 times higher than the BEP of the single user system, (b) the number of users that can be accommodated in an asynchronous CDMA system is larger than the processing gain and (c) the optimum multiuser detection outperforms linear detection (eg. the decorrelating detector) by about 2.8 to 5.7 dB.

3.2 Bit Error Probability Bounds

The information data bits are usually passed through an encoder (finite-state machine, FSM) before they are modulated and transmitted over the wireless channel. The transitions of the FSM are determined by the input data sequence. We also know that the optimum decoder is a copy of this FSM, which attempts to retrace the path (ie., the state

sequence) taken by the encoder. The decoder will make an error if the path it follows does not match with the one taken by the encoder. The data is decoded progressively, as the algorithm traverses through a trellis. An important measure of interest is the bit error probability associated with such a decoder.

An analytic technique to evaluate bounds on the error probability was presented in [35] and [101] and this will be followed here. An error event occurs when the decoded path differs from a correct path. An instance of an error event is shown in Figure 3.1. The decoder makes an incorrect estimate by following the incorrect path $e_{i,j}$ at time j and remerges with the correct path, c_k at time $j + L$. The overall probability of error can be computed by summing each individual constituent error probability. To do this an exhaustive trellis search has to be performed which is extremely inefficient.

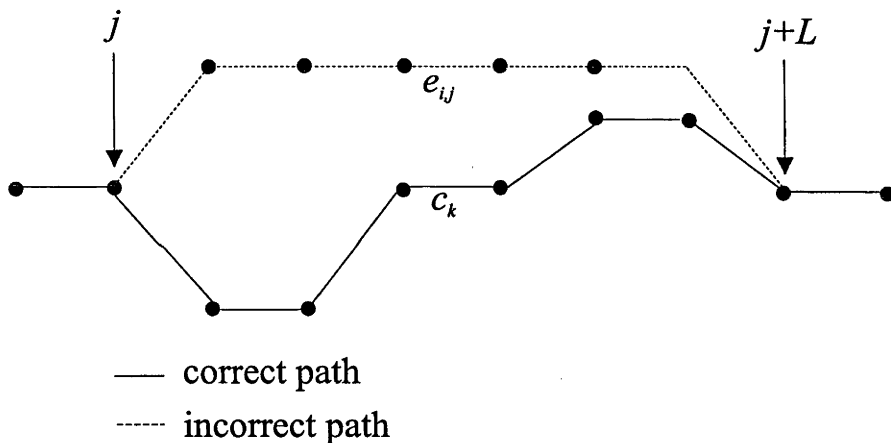
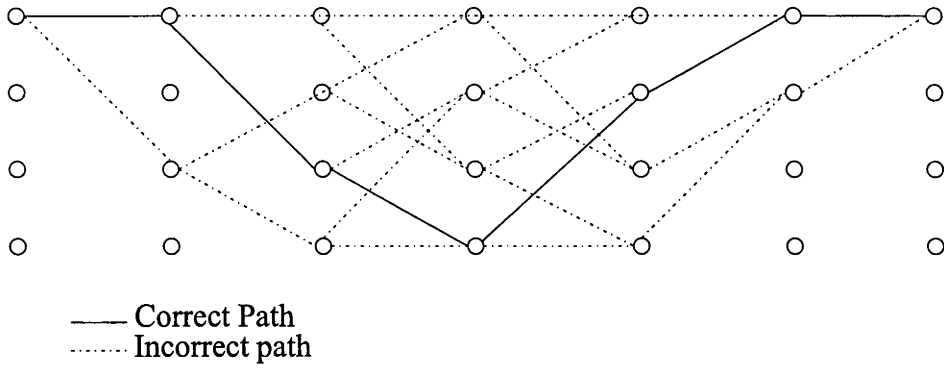


Figure 3.1: Correct path and an error path in a trellis of length L

For simplicity and conciseness we adopt notations and methodologies from [101]. The figure below shows an example of a correct path (solid) and all possible incorrect paths (dashed). Without loss of generality, we assume that the error events originate at the zero state and terminate at the zero state.

The probability of sequence error from the transmitted sequence c_k , P , is the probability that any incorrect path is chosen, ie. the probability of the union of individual errors


 Figure 3.2: Correct path and an error path in a trellis of length L
 $e_{i,j}$,

$$P(c_k) = Pr \left(\bigcup_j \bigcup_i e_{i,j} \mid c_k \right) \quad (3.1)$$

where $e_{i,j}$ denotes the divergence of the i -th error path from the correct path c_k at time interval j . By averaging over all possible correct paths we obtain

$$P = \sum_{c_k} p(c_k) Pr \left(\bigcup_j \bigcup_i e_{i,j} \mid c_k \right) \quad (3.2)$$

where $p(c_k)$ is the probability of choosing the correct path c_k . The union bound states that the probability of the union of events is not greater than the sum of their individual probabilities,

$$Pr \left(e_{i,1} \cup e_{i,2} \cup e_{i,3} \cdots \mid c_k \right) \leq \sum_j Pr(e_{i,j} \mid c_k) \quad (3.3)$$

Using the above statement (3.2) can be simplified as

$$P \leq \sum_{c_k} p(c_k) \sum_j Pr \left(\bigcup_i e_{i,j} \mid c_k \right) \quad (3.4)$$

(3.4) calculates the probability of any error at any time j . Since an infinite trellis looks identical at every time unit it is possible to eliminate the sum over j in (3.4) to obtain the

error probability per time unit

$$P \leq \sum_{c_k} p(c_k) Pr \left(\bigcup_i e_i | c_k \right) \quad (3.5)$$

where e_i is the event that an error starts at an arbitrary but fixed time unit. Applying the union bound again over i , the probability of error is upper bounded by

$$P \leq \sum_{c_k} p(c_k) \sum_{e_i} Pr(e_i | c_k) \quad (3.6)$$

$Pr(e_i | c_k)$ is usually a binary hypothesis test and is written as

$$Pr(e_i | c_k) = Q \left(\sqrt{d_{k,i}^2 \frac{RE_b}{2N_0}} \right) \quad (3.7)$$

where R is the code rate in bits/symbol, N_0 is the one-sided noise power spectral density, E_b is the energy per bit and $d_{k,i}^2$ is the squared Euclidean distance between the signals on the error path e_i and the correct path c_k . $Q(\cdot)$ is defined as

$$Q(x) = \frac{1}{\sqrt{2\pi}} \int_x^\infty \exp(-y^2/2) dy \quad (3.8)$$

The upper bound on the P can now be written as

$$P \leq \sum_{c_k} p(c_k) \sum_{e_i | c_k} Q \left(\sqrt{d_{k,i}^2 \frac{RE_b}{2N_0}} \right) \quad (3.9)$$

$$= \sum_{i, d_i^2 \in \mathcal{D}} A_{d_i^2} Q \left(\sqrt{d_i^2 \frac{RE_b}{2N_0}} \right) \quad (3.10)$$

where \mathcal{D} is the set of all possible squared Euclidean distances d_i^2 ; $A_{d_i^2}$, the average multiplicity is the average number of times d_i^2 occurs. The average bit error probability can also be simply obtained by finding the average number of bit errors on the error paths, $B_{d_i^2}$ with distance d_i^2 . This bit error probability bound - also known as the Forney bound

[35] can be further elaborated to

$$P \leq \sum_{i, d_i^2 \in \mathcal{D}} Q \left(\sqrt{d_i^2 \frac{RE_b}{2N_0}} \right) \sum_{e_i \in \mathcal{E}_d} 2^{-w(e_i)} w(e_i) \quad (3.11)$$

where the set \mathcal{E}_d contains all error events with a squared Euclidean distance d_i^2 , and $w(e_i)$ is the Hamming weight of the error event e_i .

It is sufficient to realise at this stage that by computing the distance spectrum - the set of pairs $\{d_i^2, A_{d_i^2}\}$, the upper bound on the true probability of error can be determined. Similarly, a lower bound can also be obtained when \mathcal{D} contains error events of minimum squared Euclidean distances only. The upper bound, being a union of all possible error events, tends to be loose. The tightness of the bounds relates to how closely the lower and upper bounds agree and the asymptotic behaviour refers to the bounds at high signal to noise ratios.

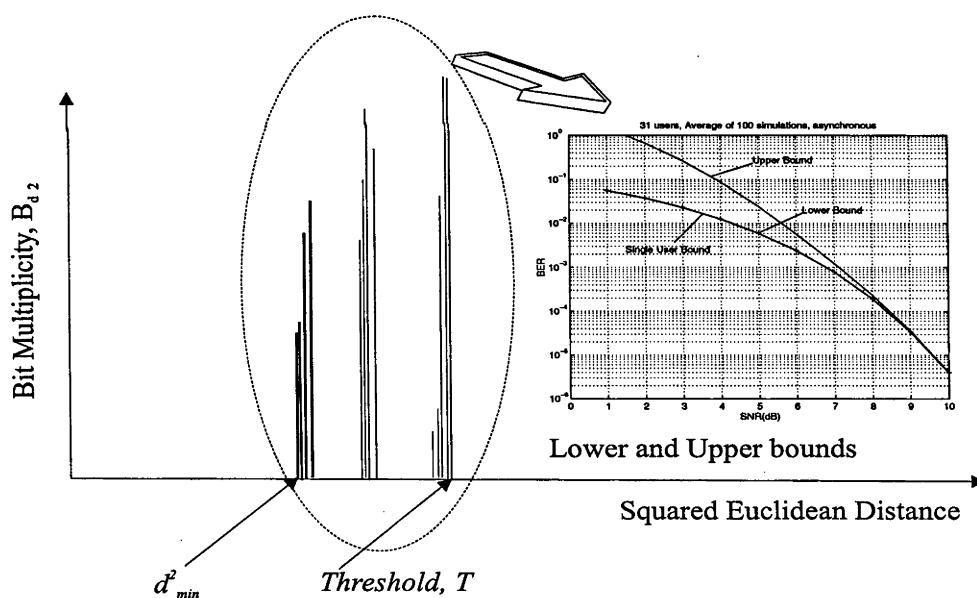


Figure 3.3: Distance Spectrum and Bound Computation

Figure 3.3 captures the essential idea of bound computation. The distance spectrum is precomputed for a particular channel realisation (ie. one \mathbf{R} matrix). Note that it is not possible to compute the infinite set of all pairs $\{d_i^2, A_{d_i^2}\}$, in the distance spectrum. The probability of very long error events is negligible; consequently, the set can be truncated

using a threshold, T . The larger T gets, the more computationally intensive it becomes to compute the *partial distance spectrum*. However, the truncated upper bound and the true upper bound agree much more closely. Tighter upper bounds have been suggested by Verdú [125]. These bounds are calculated based on a special set of error sequences - *indecomposable* error sequences. They are carefully constructed such that all error sequences in this set are orthogonal to each other and every possible error sequence can be reconstructed by a linear combination of elements in this minimal set. The Verdú bound can thus be written as

$$P \leq \sum_{i, d_i^2 \in \mathcal{D}} Q \left(\sqrt{d_i^2 \frac{RE_b}{2N_0}} \right) \sum_{e_i \in \mathcal{F}_d} 2^{-w(e_i)} w(e_i) \quad (3.12)$$

where \mathcal{F}_d denotes the set of indecomposable error sequences. The special properties that define the method of decomposability can be found in [122].

3.3 Bit Error Probability Bounds for Multiuser DS-CDMA

It is a difficult task to determine analytically the exact bit error probability of multiuser DS-CDMA systems. Most of the research to date has focussed on the concept of asymptotic efficiency, η_k defined in [121] as

$$\eta_k = \sup \left\{ 0 \leq r \leq 1; \lim_{\sigma \rightarrow 0} P_k(\sigma) / Q \left\{ \frac{\sqrt{rE_k}}{\sigma} \right\} < \infty \right\} \quad (3.13)$$

P_k and E_k are the bit error probability and the energy per bit for the k th user respectively; and σ^2 is the variance of the additive white Gaussian noise. The asymptotic efficiency indicates that the logarithm of the error probability goes to zero with the same *slope* as the single user bit error rate with energy $\eta_k E_k$. It was proved in [122][124] that the computation complexity of the asymptotic efficiency is an NP-hard combinatorial optimisation problem. Known bounding techniques similar to ideas presented in section 3.2 will be used to estimate the bit error probability of optimum multiuser detection for both synchronous and asynchronous systems on Gaussian and time-invariant frequency flat fading channels. We demonstrate that the computation of the minimum distance (and hence the asymptotic efficiency) of optimum multiuser detection, albeit NP-hard in general, can be performed in almost all cases.

Both synchronous and asynchronous systems can be modelled as finite state machines. This is shown in Fig. 3.4 In the synchronous situation all transmissions can be mapped

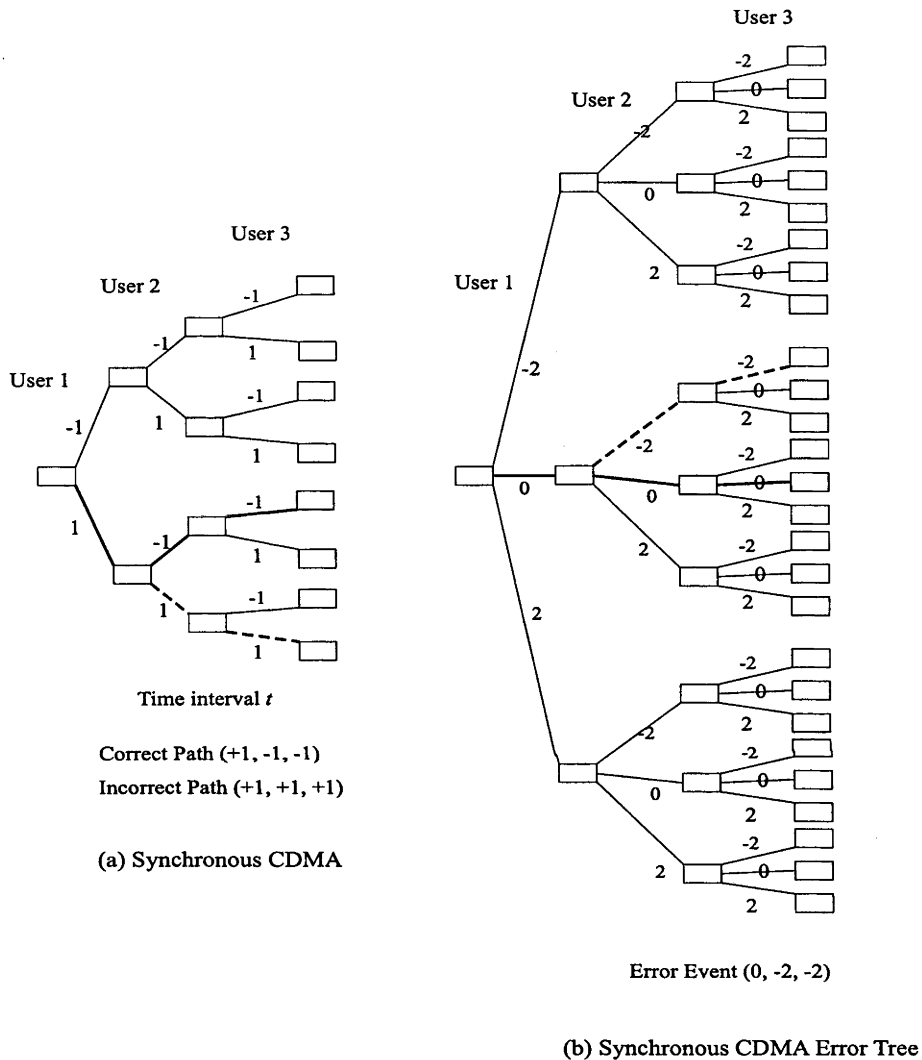


Figure 3.4: State Diagram and Error Events for a 3-user Synchronous system

to a particular path along a binary tree. Each level of the tree is partitioned with respect to a user. For simplicity we assume that the users are using antipodal signalling. The correct path is shown in bold and the incorrect decoded path is shown in dashed lines. User 1 is not in error, but user 2 and 3 are. An error tree can be used to convey the same information, where each error event maps to a particular path along the error tree. The error tree grows very quickly and has 3^K paths for a binary uncoded synchronous system, where K is the number of active users. In this case there is no ISI or delay spread, so each symbol does not overlap with later ones.

For asynchronous CDMA systems, an error event \mathcal{E} is defined in the traditional way such that it starts when the error state sequence differs from the correct state sequence and ends when the two sequences merge again for the first time. This is a generalisation of the standard intersymbol interference trellis to the MU arrangement. The distance measure has to be calculated based on errors made by users in previous symbols as well as their influence in the current time interval. Fig. 3.5 shows the state transitions and the remergence of the error events (bold lines) for an asynchronous system. Note that a valid error event occurs when all users have merged back with the correct sequences.

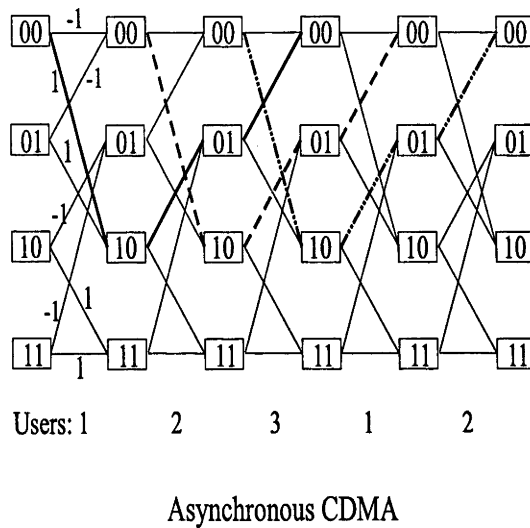


Figure 3.5: State Diagram and Error Events for a 3-user Asynchronous system

Some notations have to be introduced at this stage to describe multiuser error events and its associated BEP. Let $A_c(t)$ and $A_e(t)$ be the noiseless received waveforms associated with the correct and errored sequences of \mathcal{E} respectively. The normalised squared Euclidean distance of \mathcal{E} , $d^2(\mathcal{E})$, is then defined as $\| A_c(t) - A_e(t) \|^2 / 4E_b$ where $\| x(t) \|^2 = \int_{-\infty}^{\infty} x^2(t)dt$. We also assume that the bit energy of all users are the same, i.e. $E_1 = E_2 = \dots E_k = E_b$. Let $w(\mathcal{E})$ be the Hamming distance between two bit sequences associated with \mathcal{E} , \mathcal{D} be the set of all possible distances, $\underline{\mathcal{E}}_{d,k}$ be the subset of error events for user k for which $d(\mathcal{E}) = d$ and $\underline{\mathcal{E}}_{d_{min}}$ be the subset of error events in for which $d(\mathcal{E}) = d_{min}$, which is the minimum normalised Euclidean distance. The average bit error probability (averaged over all users) for a given spreading code set S_i can then

be bounded by a lower bound and an upper bound [35] respectively

$$P(e|\mathbf{S}_i) \geq A_{d_{min}^2} Q \left(\sqrt{\frac{2E_b d_{min}^2}{N_0}} \right) \quad (3.14)$$

$$P(e|\mathbf{S}_i) \leq \sum_{d \in \mathcal{D}} A_{d^2} Q \left(\sqrt{\frac{2E_b d^2}{N_0}} \right) \quad (3.15)$$

where

$$A_d^2 = \frac{1}{K} \sum_{k=1}^K \sum_{\mathcal{E} \in \mathcal{E}_{d,k}} 2^{-w(\mathcal{E})} w(\mathcal{E}),$$

K is the total number of users and $A_{d_{min}^2}^2$ is the probability that the transmitted sequence is such that one of its congruent error sequences in which at least one error occurs and has the minimum possible distance, d_{min} . $w(\mathcal{E})$ is the Hamming weight of \mathcal{E} . We assume that random spreading codes are used. Our interest is in the average BEP over different spreading code sets. There are mainly two motivations for using random codes. First, random signature waveforms are often used in practice, since proper design of codes with very low crosscorrelation is not a simple task. Second, the performance of a system with random codes can always be regarded as an upper bound on the BEP of a system with a “good” set of spreading codes. The BEP is thus computed by averaging $P(e|\mathbf{S}_i)$ over a few hundred or thousand sets of spreading codes, determined by a normalised standard deviation $\varepsilon^\#$. The basis for this is a technique called Optimal Conditional Importance Sampling [139] (see section 3.7). Importance sampling techniques biases the noise distribution such that more samples are taken from the important regions.

3.4 System Model

Consider a general asynchronous DS-CDMA system and a set of unity energy preassigned periodic signature waveforms, $s_k(t)$ $k = 1, 2, \dots, K$ of duration T_s . The input

signal to the receiver is

$$r(t) = A(t, \mathbf{b}) + n(t) \quad (3.16)$$

where

$$A(t, \mathbf{b}) = \sum_{k=1}^K \sum_{i=-M}^M b_{i,k} s_k(t - iT_s - \zeta_k) c_k \exp(j\theta_k), \quad (3.17)$$

M is a positive integer which can be infinite, $b_{i,k}$ is the transmitted signal of the k th user at the time interval $(iT_s, iT_s + T_s]$, ζ_k is the random transmission delay, which is assumed to be uniformly distributed over $(0, T_s]$ for asynchronous systems and zero for synchronous systems, and $n(t)$ is white complex Gaussian noise with double sided power spectral density N_0 where $N_0 = 2\sigma^2$.

For additive white Gaussian noise channels, $c_k = \delta$. For slow time-invariant Rayleigh fading channels, c_k is a single complex gain. It is also assumed that $\zeta_1 \leq \zeta_2 \leq \dots \leq \zeta_K$, and that the receiver has perfect knowledge of the carrier phase θ_k , the time delay ζ_k , and the bit energy of the received signal.

The sampled output of a bank of matched filters is (similar to [67])

$$\mathbf{r}' = \mathcal{R}\mathcal{W}\mathbf{b} + \mathbf{z}, \quad (3.18)$$

where

$$\mathbf{r}' = [\mathbf{r}'_{-M}, \dots, \mathbf{r}'_M] = [r'_{-M,1}, r'_{-M,2}, \dots, r'_{-M,K}, \dots, r'_{M,1}, \dots, r'_{M,K}]^T, \quad (3.19)$$

$$\mathbf{b} = [\mathbf{b}_{-M}, \dots, \mathbf{b}_M] = [b_{-M,1}, b_{-M,2}, \dots, b_{-M,K}, \dots, b_{M,1}, \dots, b_{M,K}]^T, \quad (3.20)$$

$$\mathbf{z} = [\mathbf{z}_{-M}, \dots, \mathbf{z}_M] = [z_{-M,1}, z_{-M,2}, \dots, z_{-M,K}, \dots, z_{M,1}, \dots, z_{M,K}]^T, \quad (3.21)$$

$$\mathcal{R} = \begin{bmatrix} \mathbf{R}_1(0) & \mathbf{R}_1(-1) & \cdot & \cdot & \mathbf{R}_1(-\Omega) \\ \mathbf{R}_2(1) & \mathbf{R}_2(0) & \cdot & \cdot & \mathbf{R}_1(-\Omega + 1) \\ \cdot & \cdot & \cdot & \cdot & \cdot \\ \cdot & \cdot & \cdot & \cdot & \cdot \\ \mathbf{R}_\Omega(\Omega) & \cdot & \cdot & \mathbf{R}_\Omega(1) & \mathbf{R}_\Omega(0) \end{bmatrix} \quad (3.22)$$

$$\mathcal{W} = \sqrt{E_b} \mathbf{I}_{\bar{K}}, \quad (3.23)$$

$\Omega = 2M + 1$, $\mathbf{I}_{\bar{K}}$ is a $\bar{K} \times \bar{K}$ identity matrix, $\bar{K} = \Omega K$, the superscript T denotes matrix transpose, \mathbf{z}_i is the matched filter output noise vector with the $K \times K$ autocorrelation matrix given by

$$E[\mathbf{z}_i \mathbf{z}_m^T] = \frac{1}{2} N_0 \mathbf{R}_i(i - m), \quad (3.24)$$

where the (k, q) -th element of $\mathbf{R}_i(i - m)$ is

$$R_i^{kq}(i - m) = \int_{-\infty}^{\infty} s_k(t - \zeta_k) s_q(t + (i - m)T_s - \zeta_q) dt \exp(j2\pi(\theta_k - \theta_q)) \quad (3.25)$$

In (3.22), for a large processing gain (say 31), we only need to consider inter-chip interference (ICI) from two symbol durations (ie. minimum 31 chips at each side or $\mathbf{R}_i(k) = \mathbf{0}$ for $|k| > 2$). If the processing gain is very small (say 8), then in (3.22) we have to consider ICI from more symbol durations for root Nyquist (root raised cosine) pulses. If time limited pulses such as rectangular or cosine pulses are used $\mathbf{R}(2) = \mathbf{R}(-2) = \mathbf{0}$. For synchronous systems, $\mathbf{R}(2) = \mathbf{R}(1) = \mathbf{R}(-2) = \mathbf{R}(-1) = \mathbf{0}$. It is easy to show that $\mathbf{R}^H(2) = \mathbf{R}^H(-2)$, $\mathbf{R}^H(1) = \mathbf{R}^H(-1)$ and $\mathbf{R}^H(0) = \mathbf{R}(0)$, where the notation $(.)^H$ denotes Hermitian transpose. In a later section, we will evaluate upper and lower bounds for asynchronous DS-SS-CDMA systems using different chip pulse shapes, namely rectangular, cosine and root raised cosine.

From the above arguments, the correlation matrix \mathcal{R} is symmetric. It is also assumed that the matrix \mathcal{R} is positive definite. This condition has been well justified by Lupas and Verdú (see linear independence assumption in [67]). Since \mathcal{R} is positive definite and symmetric, it is possible to find a unique lower triangular, non-singular matrix \mathcal{F} such that $\mathcal{R} = \mathcal{F}^T \mathcal{F}$ (Cholesky decomposition, [40]). Thus the matrix \mathcal{F} has the following structure:

$$\mathcal{F} = \begin{bmatrix} \mathbf{F}_1(0) & \mathbf{0} & \cdot & \cdot & \mathbf{0} \\ \mathbf{F}_2(1) & \mathbf{F}_2(0) & \cdot & \cdot & \mathbf{0} \\ \mathbf{F}_3(2) & \mathbf{F}_3(1) & \mathbf{F}_3(0) & \cdot & \mathbf{0} \\ \cdot & \cdot & \cdot & \cdot & \cdot \\ \mathbf{0} & \cdot & \mathbf{F}_\Omega(2) & \mathbf{F}_\Omega(1) & \mathbf{F}_\Omega(0) \end{bmatrix} \quad (3.26)$$

It has been shown by Wei et al. [140] that by applying a post-processor filter, namely the whitening filter to the output of the matched filter, the performance is greatly enhanced when dealing with sub-optimum detectors. In particular, the M- and the T- algorithm (reduced tree search algorithms) detectors based on whitened filter outputs can achieve “near” optimum performance at a very low complexity compared to the optimum detector. If the whitening filter $(\mathcal{F}^T)^{-1}$ is applied to the sampled output of the MF, the whitened MF output vector stored in \mathbf{y} is

$$\mathbf{y} = \mathcal{F}\mathbf{W}\mathbf{b} + \mathbf{n} \tag{3.27}$$

where

$$\mathbf{y} = [y_{-M}, \dots, y_M] = [y_{-M,1}, y_{-M,2}, \dots, y_{-M,K}, \dots, y_{M,1}, \dots, y_{M,K}]^T, \tag{3.28}$$

and $\mathbf{n} = [n_{-M}, \dots, n_M] = [n_{-M,1}, n_{-M,2}, \dots, n_{-M,K}, \dots, n_{M,1}, \dots, n_{M,K}]^T$, is a white Gaussian noise vector with autocorrelation matrix, $R(\mathbf{n}) = \frac{N_0}{2} \mathbf{I}_{\bar{K}}$.

Fig. 3.6 shows the system diagram of a typical multiuser CDMA system using a whitening MF.

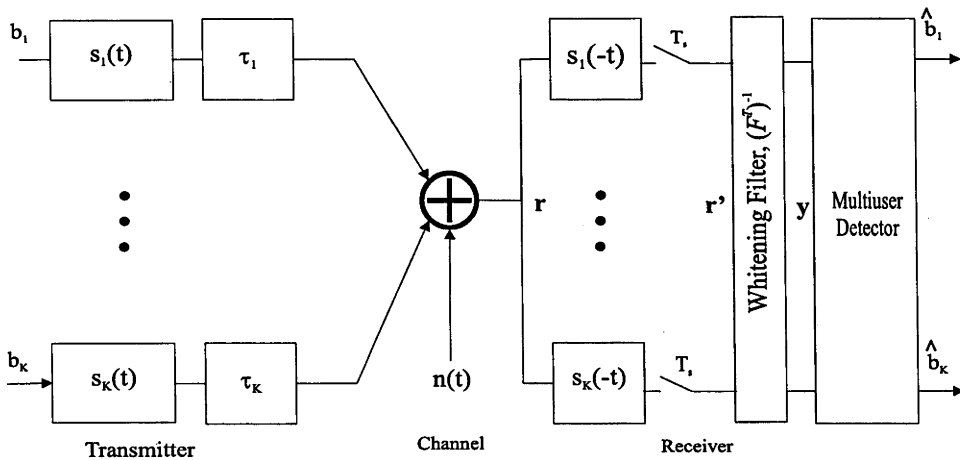


Figure 3.6: Baseband equivalent model of a multiuser CDMA system

In a practical system the whitening filter is related to time varying system parameters. Time variations such as the arrival and departure of users, random signature waveforms and multipath effects make it necessary to derive the whitening filter after each system change. It is obvious that the matched filter detector complexity is far less than a detector

based on a whitened matched filter. To derive the whitening filter by Cholesky decomposition requires $K^3/3$ multiplications. Compared to the decorrelator detector which requires $K^3/2$ multiplications to obtain the inverse of \mathcal{R} [29], it is seen as a rather attractive solution.

It is important to realise that to obtain an ideal whitening filter, the correlation matrix \mathcal{R} has to be factorised. As the size of the matrix grow large (ie. $\Omega \rightarrow \infty$), the Cholesky decomposition becomes impractical. The ideal whitening filter is also an infinite impulse response filter. As a more realistic option, Wei [140] proposed a finite impulse response filter which is a more viable real-time option as $\Omega \rightarrow \infty$. In any case, for the relevance of the work here it is assumed that \mathcal{R} can be factorised and that there exists a unique lower triangular non-singular matrix \mathcal{F} .

3.5 Procedure to Compute The Near Ideal Noise Whitening Filter

For asynchronous systems the average BEP is computed using cosine and root Nyquist chip pulse shaping. In [140] a method was shown to derive a near ideal noise whitening filter for time limited pulses. For root Nyquist filtering, $\mathbf{F}(l)$ can be determined by the following procedures:

Step1 :

Find $\mathbf{F}_M(0)$. { Cholesky Decomposition $\mathbf{F}_M^T(0)\mathbf{F}_M(0) = \mathbf{R}_M(0)$ }

Set $\mathbf{F}_{M+1}(1) = \mathbf{F}_{M+1}(2) = 0$

Step2 :

Loop $i=M, \dots, 1$

$$\mathbf{F}_i(1) = (\mathbf{F}_i^T(0))^{-1} [\mathbf{R}_i(1) - \mathbf{F}_{i+1}^T(1)\mathbf{F}_{i+1}(2)]$$

$$\mathbf{F}_i(2) = \mathbf{F}_i^T(0)^{-1}\mathbf{R}_i(2)$$

$$\mathbf{F}_{i-1}^T(0)\mathbf{F}_{i-1}(0) = \mathbf{R}_{i-1}(0) - \mathbf{F}_i^T(1)\mathbf{F}_i(1) - \mathbf{F}_{i+1}^T(2)\mathbf{F}_{i+1}(2)$$

Step3 :

$$\mathbf{F}(l) = \mathbf{F}_1(l), l = 0, 1, 2.$$

Thus for a reasonably large M (say 10), one can obtain $\mathbf{F}(l)$.

3.6 The Partial Distance Spectrum Calculation

In this section we present a method to compute the partial distance spectra for both synchronous and asynchronous systems. The distance spectrum can only be computed by an exhaustive tree search, as a consequence of the irregularity of multiuser systems. Any finite state machine can be classified as regular, quasi-regular or irregular. If the system is regular or quasi-regular, then one can obtain the distance spectrum by considering just one path as the correct path. However, if it is irregular then it is not possible to truncate or prune the exhaustive tree search during computation of the distance spectra.

3.6.1 Synchronous Case

The decision rule for the optimum synchronous multiuser detector is to select the symbol vector $\hat{\mathbf{b}}$ which minimises the Euclidean metric

$$\hat{\mathbf{b}} \in \arg \min_{\mathbf{b} \in \{-1,+1\}^K} \|\mathbf{y} - \mathcal{F}\mathcal{W}\mathbf{b}\|^2 = \arg \min_{\mathbf{b} \in \{-1,+1\}^K} \sum_{k=1}^K \lambda_{i,k} \quad (3.29)$$

where

$$\lambda_{i,k} = \left(y_{i,k} - \sum_{k'=1}^k \mathbf{F}_i^{(k,k')}(0) E_{k'} b_{i,k'} \right)^2 \quad (3.30)$$

is the k -th user metric function based on the whitened filter outputs and $\mathbf{F}_i^{(k,k')}(0)$ denote the (k, k') -th element of the lower triangular matrix $\mathbf{F}(0)$ at a time interval i . The squared minimum Euclidean distance for time i and user k is therefore

$$d_{min}^2 = \min_{\mathbf{b}, \hat{\mathbf{b}} \in \{-1,+1\}^K} \|\mathcal{F}\mathcal{W}\hat{\mathbf{b}} - \mathcal{F}\mathcal{W}\mathbf{b}\|^2 \quad (3.31)$$

$$= \min_{\mathcal{E}_i \in \{-2,0,2\}^K, \mathcal{E}_{i,k} \neq 0} \|\mathcal{F}\mathcal{W}\mathcal{E}_i\|^2 \quad (3.32)$$

$$= \min_{\mathcal{E}_i \in \{-2,0,2\}^K, \mathcal{E}_{i,k} \neq 0} \sum_{k=1}^K d_{i,k}^2 \quad (3.33)$$

$$d_{i,k}^2 = \left(\sum_{k'=1}^k \mathbf{F}_i^{(k,k')}(0) E_{k'} \mathcal{E}_{i,k'} \right)^2 \quad (3.34)$$

where the error event $\underline{\mathcal{E}}_i$ is a vector consisting of the individual errors of each user, (ie. $\underline{\mathcal{E}}_i = [\mathcal{E}_{i,1}, \mathcal{E}_{i,2}, \dots, \mathcal{E}_{i,K}]$) during a particular time interval i .

The synchronous algorithm can thus be written as follows:

1. Start at root node, for user number $k = 1$.
2. Compute distance, $d_{i,k}^2$ and accumulate in D_i^2
3. Store error path Hamming weight.
4. Drop paths from future extension with $D_i^2 \geq$ threshold, T .
5. Increment k to the next user;
6. If $k = K$ stop and compute bit multiplicity, probability of error else go to 2).

The computation of the minimum distance is straightforward, since a threshold T of twice the single user distance will ensure discarding most of the paths in the tree search. In general, the number of branches searched by the above algorithm is significantly smaller than the full tree. This is shown in Fig. 3.7.

3.6.2 Asynchronous

We proceed along similar lines to that described above and compute a partial distance spectrum for asynchronous systems. The error vector now comprises of elements from the current and previous symbol intervals. The algorithm is broken up into two phases. The first phase (startup phase for symbol interval i) extends branches in the same fashion as the synchronous case, (ie. the incremental distance $d_{i,k}^2$ is calculated using only $F_i(0)$). It is assumed that there are no users in error before the startup time interval. The distance metric is given as in (3.34). The cumulative distance is always carried along with the paths. At any time interval, paths with distances greater than the threshold, T are eliminated. This is done in a recursive manner. From the second time interval and beyond the contribution to the overall distance is not only from users within the current symbol but also from users in the previous symbols intervals.

For large processing gains (say 31) it is only necessary to consider inter-chip interference (ICI) from the previous two symbol intervals. For time limited chip pulse shapes

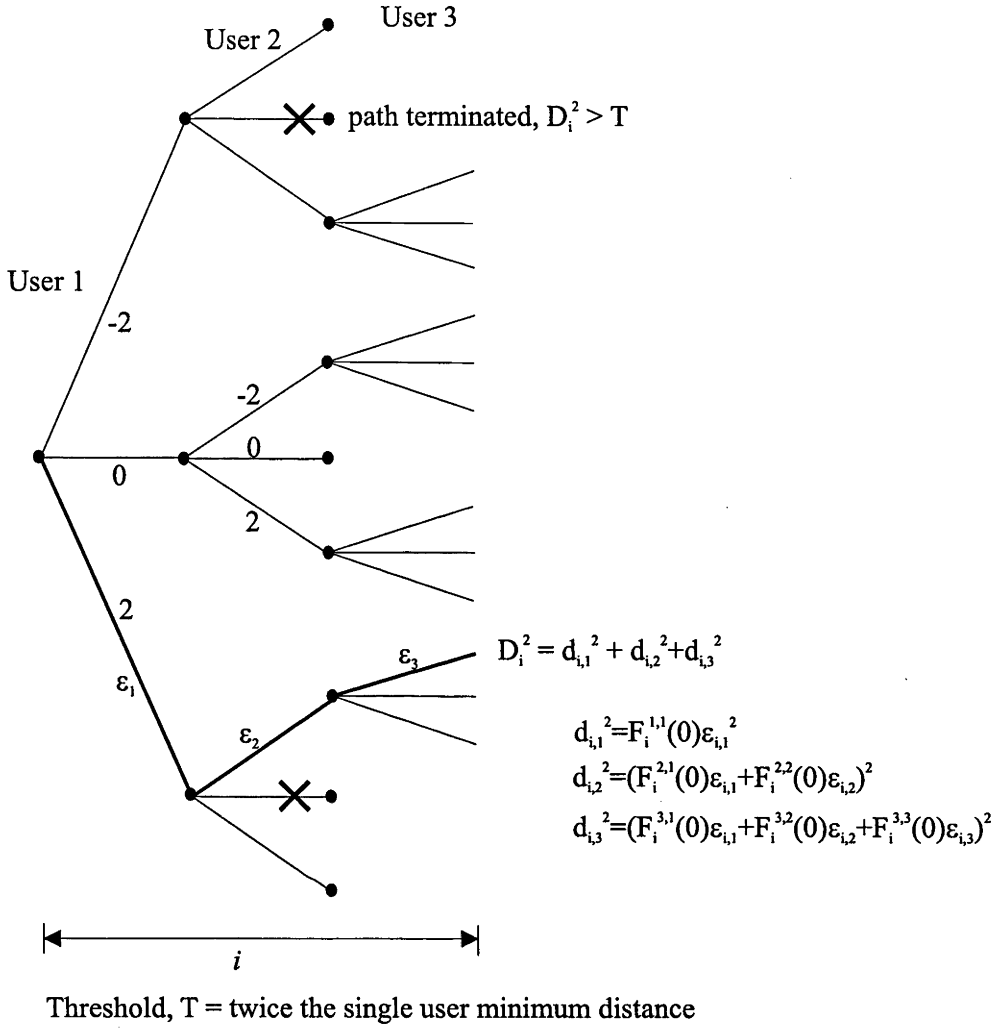


Figure 3.7: Distance computation for a synchronous tree

such as cosine or rectangular, the incremental distance $d_{i,k}^2$ is written as

$$d_{i,k}^2 = \left(\sum_{k'=1}^k F_i^{(k,k')}(0) E_{k'} \mathcal{E}_{i,k'} + \sum_{k'=k+1}^K F_i^{(k,k')}(1) E_{k'} \mathcal{E}_{i-1,k'} \right)^2 \quad (3.35)$$

For root Nyquist chip pulse shaping (where the interference is from the previous 2 symbol periods), the generic incremental distance beyond the startup phase is given by

$$d_{i,k}^2 = \left(\sum_{k'=1}^k F_i^{(k,k')}(0) E_{k'} \mathcal{E}_{i,k'} + \sum_{k'=1}^K F_i^{(k,k')}(1) E_{k'} \mathcal{E}_{i-1,k'} + \sum_{k'=k+1}^K F_i^{(k,k')}(2) E_{k'} \mathcal{E}_{i-2,k'} \right)^2$$

A successful error event in the asynchronous situation occurs when all K users have merged back with the correct sequence. The terminating conditions are

- 1) All users have merged back with the correct sequence for a particular error event, or
- 2) The cumulative distance $D_{i,k}^2$ has grown beyond the threshold, or
- 3) The tree has been completely searched.

Until these terminating criteria are met, paths need to be extended indefinitely. Note that the deletion of paths was strictly based on the property that the incremental distance can only be positive. If however, the distance computation was based on the MF output [121], paths with $D_{i,k}^2$ can not be dropped since a future branch may arise in a negative distance increment. For each valid error event its associated squared Euclidean distance and the bit multiplicity are recorded. The general asynchronous algorithm (cosine chip pulse shaping) can be written as follows:

1. Initialise threshold, T ; Set user index $k = 1$;
2. Synchronous start-up phase. Construct error tree as per synchronous case for initial symbol interval.
3. Compute incremental distance $d_{i,k}^2$ and accumulate in D_i^2 according to 3.34.
4. Retain path information (ie. Hamming weight and accumulated distance so far) with $D_i^2 \leq T$ for future extensions.
5. If $k = K$, increment time interval to $i + 1$.
6. Compute incremental distance $d_{i+1,k}^2$ according to 3.35 and accumulate.
7. Check if any of the terminating criteria is met else go to 6.
8. For all successful paths (accumulated distance less than T after termination), compute bit multiplicity and BER.

The following diagram (Fig. 3.8) helps to illustrate the operation of the algorithm. For the sake of clarity, in a 3 user system, if the incremental distance metric $d_{i+1,k}^2$ is being calculated at time interval $i + 1$ and $k = 2$, contributions from user 1 and 2 are calculated with the use of $\mathcal{F}_{i+1}(0)$ while user 3 is computed using $\mathcal{F}_{i+1}(1)$.

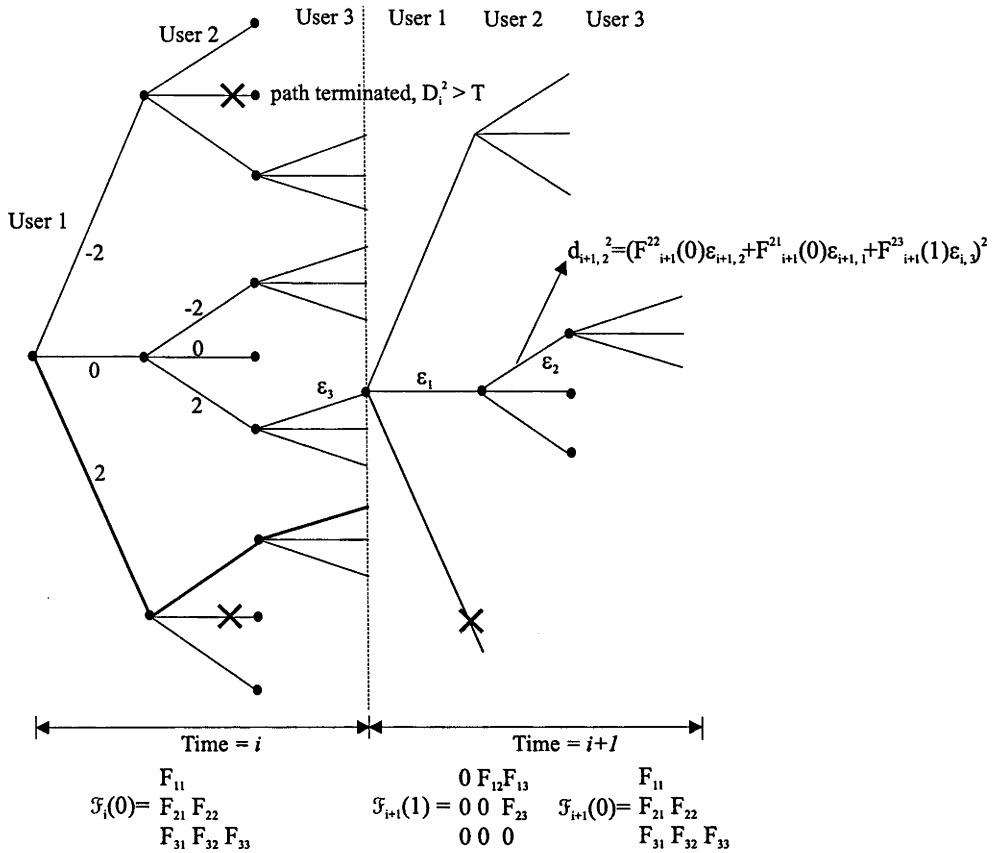


Figure 3.8: Distance computation for an asynchronous tree

3.7 Average BEP for Random Codes

A technique called Optimal Conditional Importance Sampling [139] has been applied to estimate the average BEP. From the preceding sections, it is possible to calculate the conditional error probability, $P(e|\mathbf{S})$ given a particular correlation matrix, where \mathbf{S} is a sample matrix from the density $p_{\mathbf{S}}(\mathbf{S})$. Applying the total probability theorem, we have

$$P(e) = \int_{\mathbb{R}(\mathbf{S})} P(e|\mathbf{S})p_{\mathbf{S}}(\mathbf{S})d\mathbf{S} \tag{3.36}$$

where $\mathbb{R}(\mathbf{S})$ is the space spanned by the set of randomly selected spreading codes. For a small number of matrices one can compute the exact value of $P(e)$. However, for a large set this becomes practically impossible. An approximation technique well suited for this can be found in Appendix 1 of [139] where it is shown that one can estimate $P(e)$ by its

unbiased estimator $P'(e)$, where

$$P'(e) = \frac{1}{\Xi} \sum_{i=1}^{\Xi} P(e|\mathbf{S}_i) \quad (3.37)$$

Ξ is the number of simulation trials and \mathbf{S}_i are independent realisations of \mathbf{S} which are generated according to the pdf of \mathbf{S} , $p_{\mathbf{S}}(\mathbf{S})$. Since $\bar{P}'(e) = P(e)$, the estimator of the error probability in (3.37) is unbiased and its normalised error, \bar{W}' is given by

$$\bar{W}' = \int_{\mathbb{R}(\mathbf{S})} P^2(e|\mathbf{S}) p_{\mathbf{S}}(\mathbf{S}) d\mathbf{S} \quad (3.38)$$

However, the evaluation of (3.38) has the same complexity as (3.36), thus we can estimate it also using an unbiased estimator, given by

$$\epsilon^{\#} = \sqrt{\frac{\bar{W}^{\#} - P'(e)^2}{\Xi P'(e)^2}} \quad (3.39)$$

$$\bar{W}^{\#} = \frac{1}{\Xi} \sum_{k=1}^{\Xi} P^2(e|\mathbf{S}_i), \quad (3.40)$$

The normalised standard deviation, $\epsilon^{\#}$, indicates the number of simulation trials required for a reliable estimate of the probability of error. The approach of (3.40) is similar to that used to estimate γ and γ^* in [78] and [79].

3.7.1 Procedure to estimate the BEP

The procedure followed to estimate the BEP is outlined below,

1. Generate a set of random spreading codes, time delays, ζ_i and carrier phases, θ_i .
2. Compute $\mathbf{R}(l)$ based on (3.25)
3. Compute $\mathbf{F}(l)$ based on the algorithm in section 3.5
4. Find a partial distance spectrum using the method in section (3.6.2).
5. Compute $P(e|\mathbf{S}_i)$ based on (3.15) and then the estimated normalised variance, $\epsilon^{\#}$ to monitor the accuracy of the estimator. If $\epsilon^{\#}$ is too large (say $> 5\%$), go back to

step 1 and run more simulations.

3.8 Numerical Results

In this section we use the above algorithm to evaluate performance bounds for asynchronous CDMA with binary random signature waveforms of length 31. For asynchronous systems we use both cosine and root Nyquist pulse shaping, while the results for synchronous CDMA apply for all pulse shapes since there is no interference between chips for each user. $T = 2.5$ times the minimum distance of the single user system and $\epsilon^\# < 5\%$ for all simulation results.

The effect of the threshold T , can be seen in Fig.3.9. At low signal to noise ratios (SNR) the union bound is loose and truncation is not valid, however, at moderate to high SNR the bound is both valid and effective since error events with minimum distance only contribute at large. Therefore, as a rule of thumb we can compute an approximate upper bound by selecting T to be 2.5 times d_{min} of a single user system.

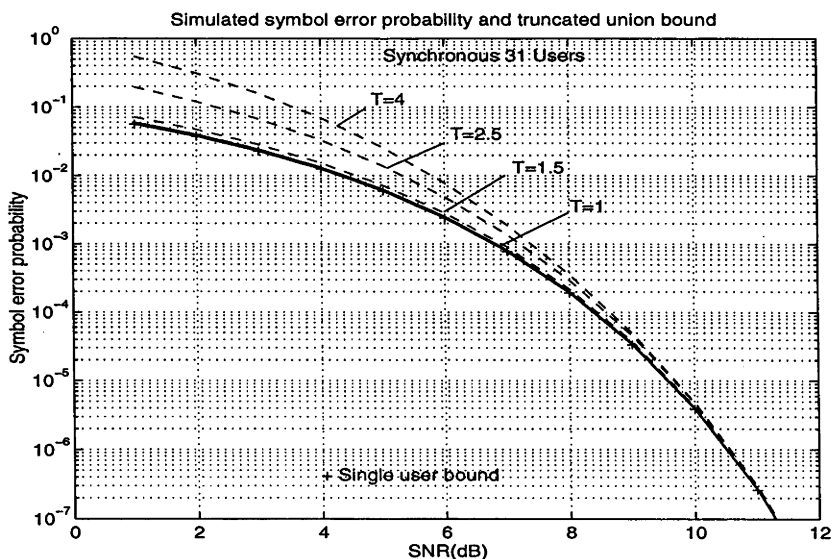


Figure 3.9: Comparison of union bounds for different thresholds T , synchronous CDMA with binary random spreading codes of length 31, $I = 31$.

Figs. 3.10 and 3.11 show the partial distance spectra of synchronous and asynchronous systems for the worst case of 100 simulations. For synchronous systems the distances

have only a few possible values, while for asynchronous the distance spectrum is much denser and many of the distances are concentrated about 2 and 4.

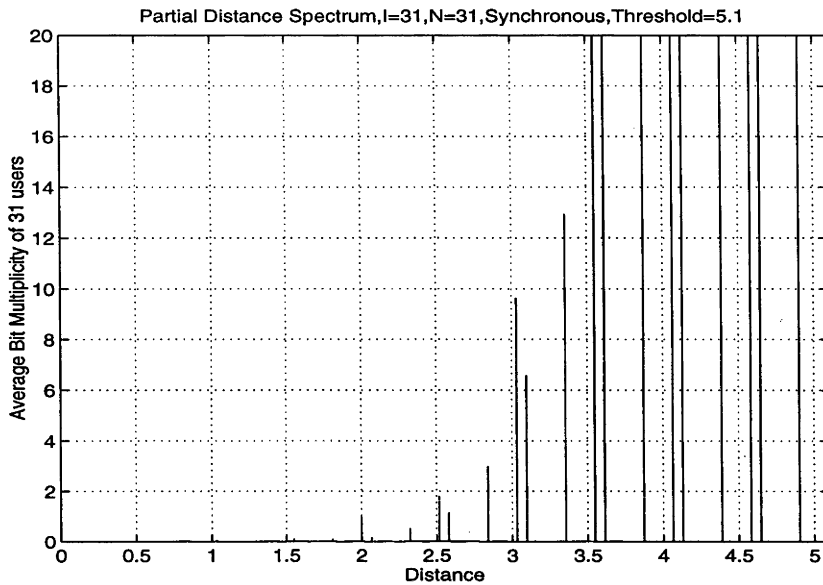


Figure 3.10: Synchronous system partial distance spectrum

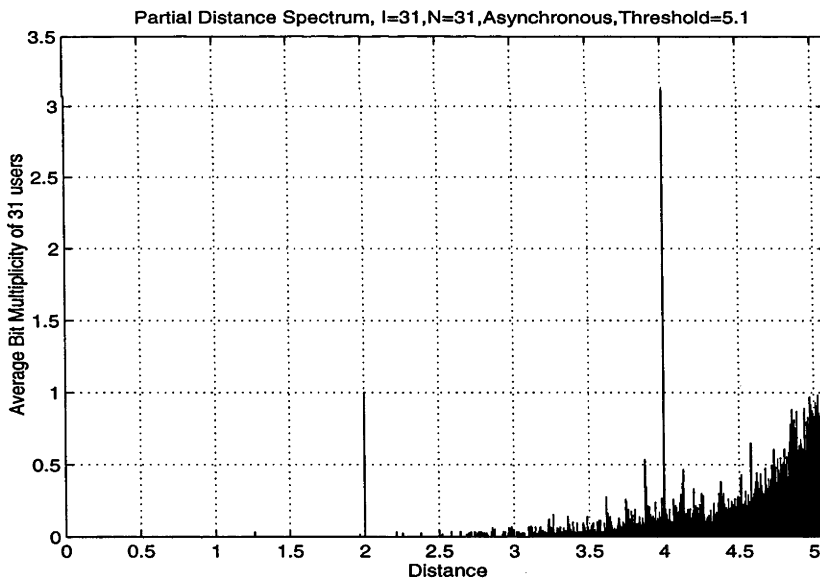


Figure 3.11: Asynchronous system partial distance spectrum

Figs. 3.12 and 3.13 show the upper and lower bounds on the BER as a function of E_b/N_0 for CDMA systems with 31 users and a spreading length of 31, using cosine pulse shaping. Over thousand sets of binary random spreading code were generated. It can be seen that the lower and upper bounds are asymptotically tight at high signal to noise

ratios.

Fig. 3.14 shows the average BEP as a function of the number of users, I , for $E_b/N_0 = 7\text{dB}$. Clearly the lower and upper bounds are very tight. It is seen that as the number of users increases the optimum BEP increases slightly for both synchronous and asynchronous systems. The BEP for $I=30$ is about twice that of the single user case which agrees with the simulation results in [138] and [140]. The BEP of the decorrelator detector is estimated by

$$P(e) = \frac{1}{K\Omega} \sum_{k=1}^{\Omega} \sum_{i=1}^K Q \left(\frac{\sqrt{w_i/(\mathcal{R}^{-1}(\mathbf{S}_i))^{ii}}}{\sigma} \right). \quad (3.41)$$

In the asynchronous scenario, a system with root Nyquist chip pulse shaping has a performance slightly worse than one with a cosine pulse. There are three interesting phenomena. (a) The maximum number of users that can be accommodated in asynchronous systems is larger than the processing gain without catastrophically increasing the BEP. However, the number of users that can be accommodated in synchronous systems is limited to the processing gain [138], (b) The optimum asynchronous system has a much lower BEP than the synchronous case. This can be explained by investigating the statistical properties (namely mean and variance) of $\mathbf{F}^{i,i}(0)$, where $\mathbf{F}^{i,i}(0)$ indicates the diagonal element of $\mathbf{F}(0)$. The value of $\mathbf{F}^{i,i}(0)$ indicates how much energy is present in the signal domain of the i th user. The higher the correlation between the users the lower the value of $\mathbf{F}^{i,i}(0)$, generally leading to a poorer system performance. Typically the values of $\mathbf{F}^{i,i}(0)$ in synchronous systems are smaller than in asynchronous systems. In summary, asynchronism decreases the correlation between spreading codes, which explains why asynchronous systems outperform synchronous ones. (c) For $E_b/N_0 = 7\text{dB}$, the optimum detector significantly outperforms the linear detector by about 2.8 to 5.7 dB (20 to 31 users) for asynchronous systems with cosine pulse shaping.

In a typical cellular system both forward and reverse channels experience Rayleigh fading. For time-invariant frequency flat fading channels, we have obtained similar bounds on the BEP for optimal detection. However, the upper bound does not converge for the fading channel, hence we can only estimate the BEP of the system using the lower bound. For the down-link, the fading processes of all users are identical, thus the Q-function in

(pp. 717, [86] ie. bit error rate over a flat Rayleigh fading channel) is simply replaced by,

$$P(d) = \frac{1}{2} \left(1 - \sqrt{\frac{d_{min}^2 E_b}{N_0 + E_b d_{min}^2}} \right) \quad (3.42)$$

In (3.42), we assume that the channel parameters do not change over the error event with the minimum distance. For the up-link, the fading process of each user is independent and has a Rayleigh distribution. We will estimate the bit error probability by computing the lower bound on $P(e|S_i)$ in (3.14) for a given set of spreading codes and fading parameters. In Fig. 3.15, the BEP as a function of the number of users is plotted for a time-invariant frequency flat Rayleigh fading channel and cosine pulse shaping. It shows that the BEP for 31 users is almost the same as the single user bound which is supported by the simulation results in [137]. For the down-link, the error rate is slightly higher than that for up-link. Up to 150,000 sets of binary random spreading codes were tried to ensure $\varepsilon^\# < 5\%$.

Fig. 3.16 compares the tightness of the upper bounds for a 5 user asynchronous system, with random binary spreading codes of length 31 using the Forney bound and Verdú's theory of indecomposable error events. An error sequence $\mathcal{E} \in \underline{\mathcal{E}}$ is *decomposable* into $\mathcal{E}' \in \underline{\mathcal{E}}$ and $\mathcal{E}'' \in \underline{\mathcal{E}}$ if

1. $\mathcal{E} = \mathcal{E}' + \mathcal{E}''$
2. $\mathcal{E}' < \mathcal{E}, \mathcal{E}'' < \mathcal{E}$
3. $\langle S(\mathcal{E}'), S(\mathcal{E}'') \rangle \geq 0$

where the final condition is the inner product of the multiuser signal modulated by the error sequences \mathcal{E}' and \mathcal{E}'' ,

$$\langle S(\mathcal{E}'), S(\mathcal{E}'') \rangle = \sum_{i=-M}^M \sum_{k'=1}^K \sum_{i=i'-1}^{i'+1} \sum_{k=1}^K \mathcal{E}'_{k'}(i') \mathcal{E}''_k(i) \int_{-\infty}^{\infty} s_{k'}(t - i'T_s - \zeta_{k'}) s_k(t - i'T_s - \zeta_k)$$

The procedures followed to determine decomposability of error events are outlined below:

1. Find all error events in $\underline{\mathcal{E}}$

2. Create a set Σ of all possible combinations of error events. The conditions for constructing such a set are (a) there is no element in the combination set which is larger than 2 or smaller than -2, (b) there is no cancellation at any position in set Σ . For example, consider a 2 user system using BPSK. Let the set of all error events be $\underline{\mathcal{E}} = [\mathcal{E}_1 \mathcal{E}_2] = (0, 2), (2, 0), (0, -2), (-2, 0), (2, -2), (2, 2)$. Set $\Sigma = (2, 2), (-2, 2), (2, -2), (-2, -2)$. The combined error event of $(2, 0)$ and $(2, -2)$ is $(4, -2)$. This is discarded since one of its element is larger than 2. Similarly, $(2, 0)$ is discarded due to the cancellation of the first element in $(2, 0)$ and $(-2, 2)$.
3. Check if set Σ has any identical error events, \mathcal{E} in the original set $\underline{\mathcal{E}}$. If it does then that error event \mathcal{E} can be decomposed into the constituent error events \mathcal{E}' and \mathcal{E}'' .
4. Using \mathcal{E}' and \mathcal{E}'' check decomposability criteria.
5. If all conditions are satisfied then delete \mathcal{E} from original set.

For a 31 user system, we need to examine approximately $1.75e8$ combined error events, which is too computationally intensive. We will however calculate the Verdú upper bound for a 5 user system and show its tightness relative to the Forney bound (see Fig. 3.16).

In Fig. 3.17 and 3.18 the mean and variance of multiuser interference for synchronous CDMA systems is shown. It is seen that the mean of diagonal terms of \mathcal{F} increases and the variance decreases as the user index, i increases. The diagonal element is well above the interference except for the first few users. For synchronous systems, we define the sample mean as

$$\bar{\mathbf{F}}^{j,k}(0) = \frac{1}{\Xi} \sum_{i=1}^{\Xi} | \mathbf{F}_i^{j,k}(0) | \quad (3.43)$$

Figs. 3.19 and 3.20 show the mean and the variance of an asynchronous system using cosine chip pulse shaping (ie. \mathcal{F} has components $\mathbf{F}(0)$ and $\mathbf{F}(1)$ only) plotted against a delay index k . To explain, the user delay index k , is analogous to a finite impulse response filter tap. The figures illustrate that (a) the diagonal element (tap 1) contains about 80% of the total energy and the remaining energy spread across the interfering 30 users(taps) as a result of the non-orthogonal signature sequences, (b) the average in-

interference energy of each tap is lower than in the synchronous situation. The statistical properties of \mathcal{F} were obtained by averaging over 10000 sets of binary random spreading codes of length 31. In summary, as the number of users increases the the interfering energy is shared or distributed among users and previous symbols. The impact of this is a marginal improvement in the BER performance for asynchronous systems. Compared to corresponding synchronous systems, the interfering energy of each tap is lower while the energy in the diagonal element is much higher. This also gives us some explanations why many low complexity detectors can provide near optimum performance.

3.9 Summary

This chapter has used the union bounding technique to evaluate the optimal performance of synchronous and asynchronous multiuser DS-CDMA systems. An algorithm has been presented to compute bounds on the BEP of CDMA systems. The truncated upper bound was calculated by considering distances up to a threshold, T . It was found that the upper and lower bounds on Gaussian channels converge when the error probability is less than 10^{-4} . Numerical results and simulations show that the optimal performance of asynchronous systems is better than synchronous systems. Another observation is the graceful degradation in the bit error probability for optimum multiuser detection as the number of users in the system exceed the processing gain. This is in contrast to the performance of CDMA systems employing single user detection. The BEP of asynchronous systems with 31 users and binary random spreading codes of length 31 is very close to the BEP of the single user bound. The optimum detector outperforms the linear detector by about 2.8 to 5.7 dB. Finally a lower bound was obtained for slow frequency flat Rayleigh fading channels. This bound was very close to the single user bound.

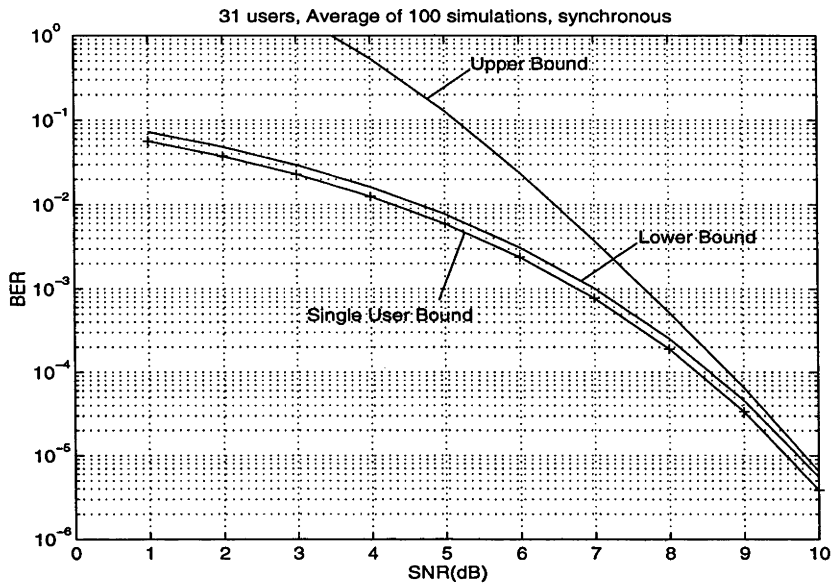


Figure 3.12: Synchronous system - Average upper and lower bounds for a 31-user DS-CDMA system with binary random spreading codes, $N=31$

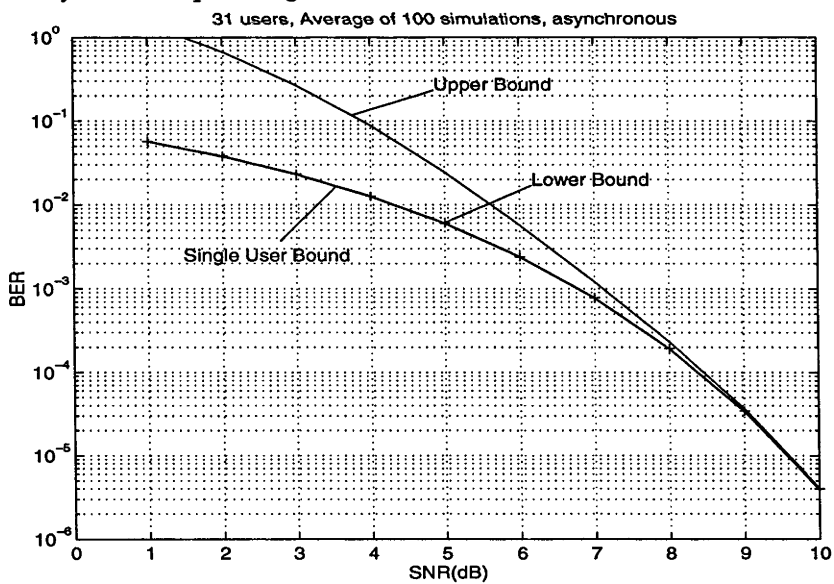


Figure 3.13: Asynchronous system - Average upper and lower bounds for a 31-user DS-CDMA system with binary random spreading codes, $N=31$

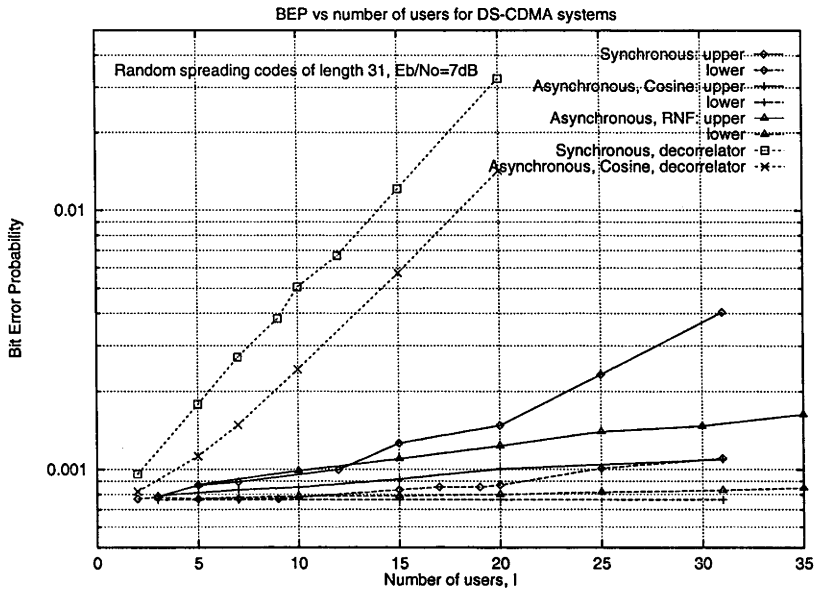


Figure 3.14: BEP bounds as a function of the number of users I for $E_b/N_0 = 7\text{dB}$ with binary random signature waveforms of length 31.

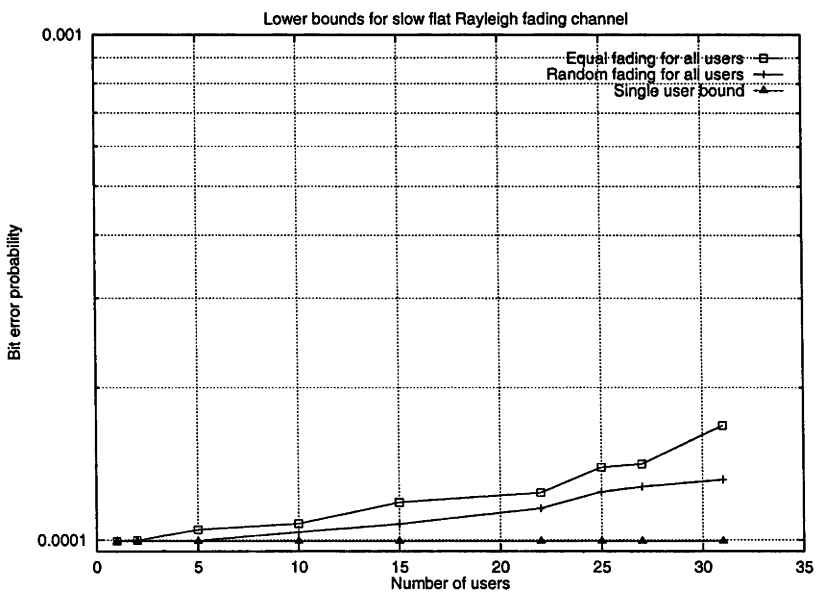


Figure 3.15: BEP versus the number of users for slow Rayleigh fading channel, $E_b/N_0 = 34\text{dB}$, cosine pulse shaping

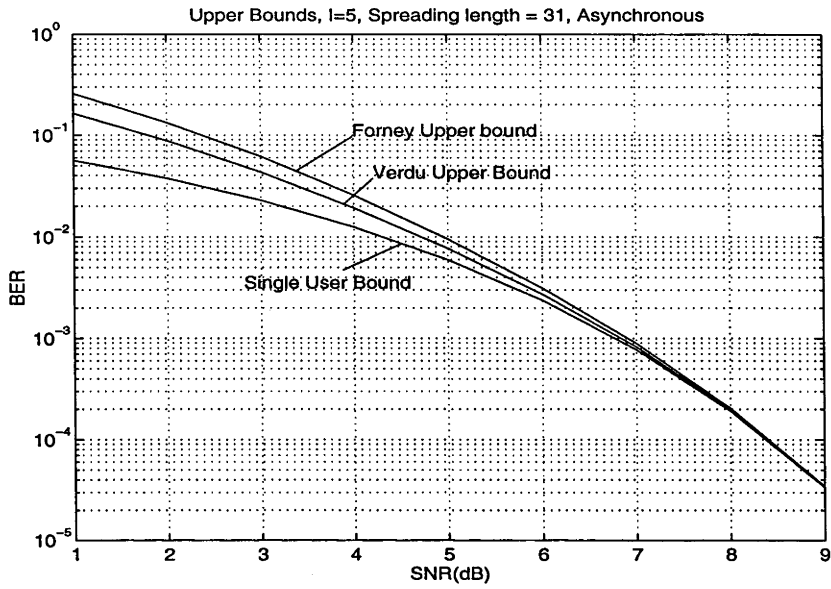


Figure 3.16: Comparison of Verdú and Forney bound

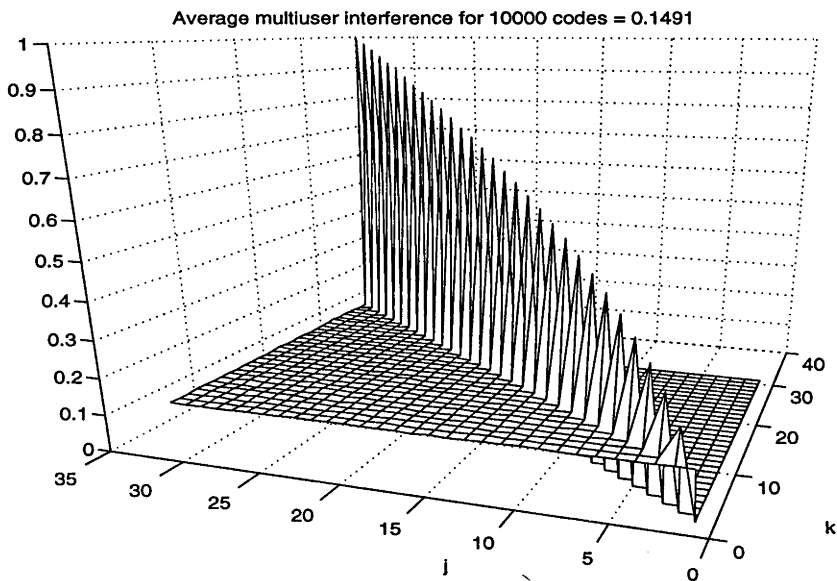


Figure 3.17: Mean of \mathcal{F} for synchronous systems, Mean MAI = 0.1491

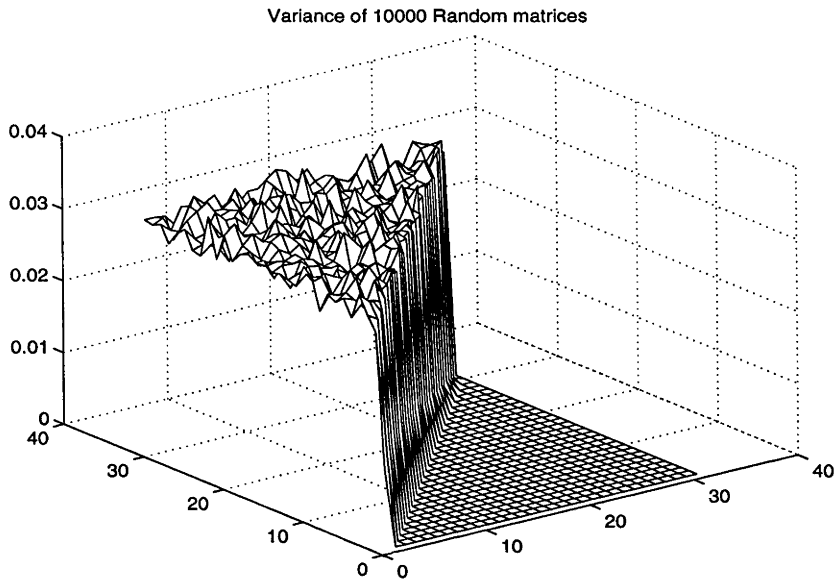


Figure 3.18: Variance of \mathcal{F} for synchronous systems, average variance of MAI for 10000 sets = 0.0225

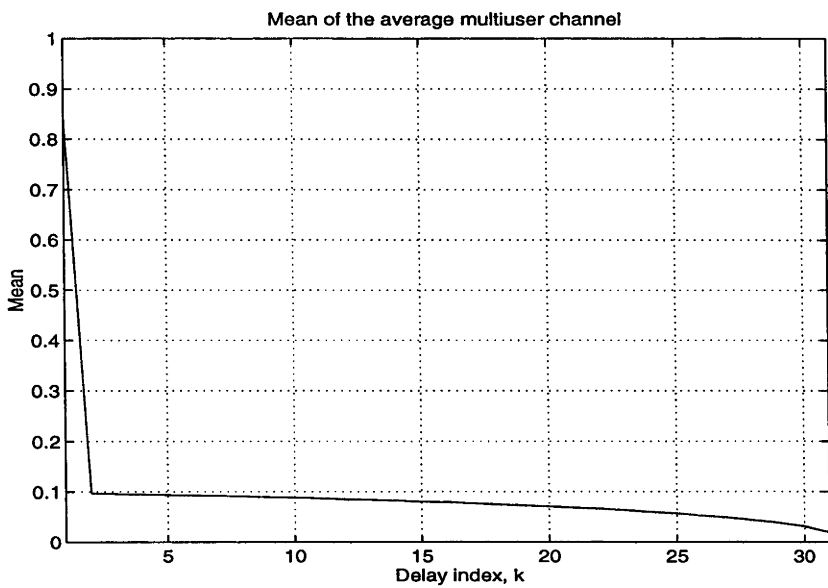


Figure 3.19: Mean of \mathcal{F} for asynchronous systems

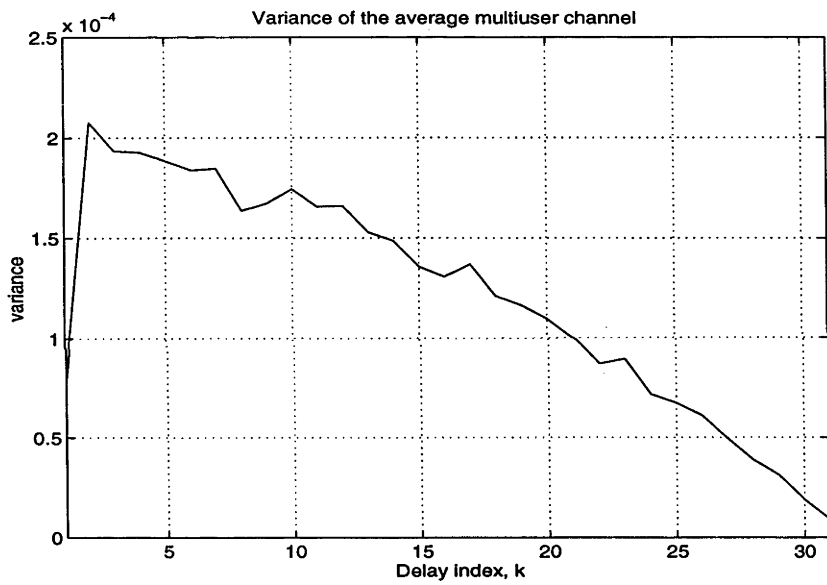


Figure 3.20: Variance of \mathcal{F} for asynchronous systems

Performance Evaluation of Trellis Coded Multiuser CDMA

Overview: This chapter shows how to evaluate a Trellis-Coded Modulated (TCM) multiuser CDMA system. It describes the parameters and algorithms used to evaluate their performances. The performance of trellis codes, like that of block codes, depends on a suitably defined minimum distance property of the code. In particular, we study three properties of the minimum squared Euclidean distance, (d_{min}^2) namely (a) an upper bound on d_{min}^2 , (b) the effect of non-orthogonal spreading on d_{min}^2 and (c) the relationship between d_{min}^2 in coded and uncoded synchronous multiuser systems. We prove that if all users use trellis codes with the same memory length and the same number of input bits but different signal mapping sets, the upper bound on the normalised minimum squared Euclidean distance for a multiuser CDMA system with non-orthogonal spreading is identical to that of a system with one user. The results indicate that the coded multiuser system may be able to recover the minimum distance loss of an uncoded multiuser system due to non-orthogonal spreading (if there is such a loss). As a result, we derive and study upper and lower bounds on the ratio of d_{min}^2 between a system with non-orthogonal and orthogonal spreading. Finally, we show that the minimum squared Euclidean distance for a convolutional coded synchronous multiuser system is no less than the product of the free distance and the minimum Euclidean distance for a corresponding uncoded synchronous multiuser system.

4.1 Introduction

In a CDMA system, several users transmit information simultaneously and independently over a common channel using preassigned signature waveforms. If the signature waveforms are orthogonal, the conventional single-user detector (sampled matched filter followed by a threshold decision device) provides optimum demodulation. However, in practice, such as in the mobile radio environment, non-orthogonal, but low correlation, signature waveforms are often used. The problem of the design of strictly orthogonal codes for a large number of users (relative to the processing gain) is known to be a difficult problem for the synchronous case; the practical reality of asynchronous transmission renders this pursuit almost futile. Hence, nonorthogonal spreading waveforms with low crosscorrelation properties such as pseudo random sequences are employed in practice [39][77][95][43]. In a CDMA system with non-orthogonal waveforms conventional single-user detection suffers two main drawbacks. First, it requires strict control of the transmitter power of each user, which in most cases is difficult to achieve and second, as the number of users approaches the processing gain, the conventional detector performs poorly. These drawbacks are caused by the fact that the conventional detector treats multiuser interference as noise rather than exploiting the rich multiuser correlation structure to achieve interference cancellation.

There has been a large amount of interest recently in the design of multiuser receivers for CDMA systems. Most of this work has focussed on uncoded links (ie. without the use of error control coding) [121][31][114][89][4]. These receivers treat all signals as information bearing and decode all users jointly. The significant "value add" that multiuser detectors promise is enhanced spectral utilization and a reduced need for precise power control. The substantial improvements however, are obtained at the expense of a dramatic increase in complexity. The complexity grows exponentially with the number of users. Thus when the number of users is large the optimum detector [121] becomes infeasible. As a consequence, much effort has been directed towards sub-optimal receiver structures for both Gaussian and fading channels [114][115][100][89][8][69].

Combining forward error-control (FEC) coding with CDMA is a relatively new approach that has been studied only recently [37][50][42][7][100][56][5]. Error control codes are necessary for reliable performance of cellular systems. When convolutional codes

are employed by all users, the optimal sequence detector is more complex than the optimal detector for the uncoded case (since there is additional memory associated with each user due to error control coding). Once again, research efforts have been directed to the design of numerous sub-optimal methods. Some of the key contributions in the area of multiuser detectors for encoded data are discussed below.

A successive cancellation technique using a class of orthogonal convolutional codes was applied to CDMA systems [131]. The author showed that the use of very low rate codes is an ideal choice for CDMA since it is able to support a composite data rate to bandwidth ratio of greater than 1 bits/sec/Hz (ie. an improvement over traditional multiple access schemes like TDMA and FDMA). When used by a large number of users in the presence of white Gaussian background noise, these special codes achieved an aggregate data rate approaching the Shannon capacity of Gaussian noise channels.

Reference [37] discussed multistage detection for convolutionally encoded signals. Two approaches were taken, (a) a partition trellis based receiver, in which equalisation and decoding were done separately (see Fig. 4.1) and (b) an optimum sequence estimator, where the decoded symbols of the interferers were used to cancel the multiple access interference from the desired user's signal. It was realised that the exponential dependence of the time-complexity-per-bit (TCB) on the number of users rendered the optimal decoder prohibitive for a realistic system. Nevertheless, the optimal receiver is important since it represents a benchmark that can be used to compare the performances of suboptimal schemes.

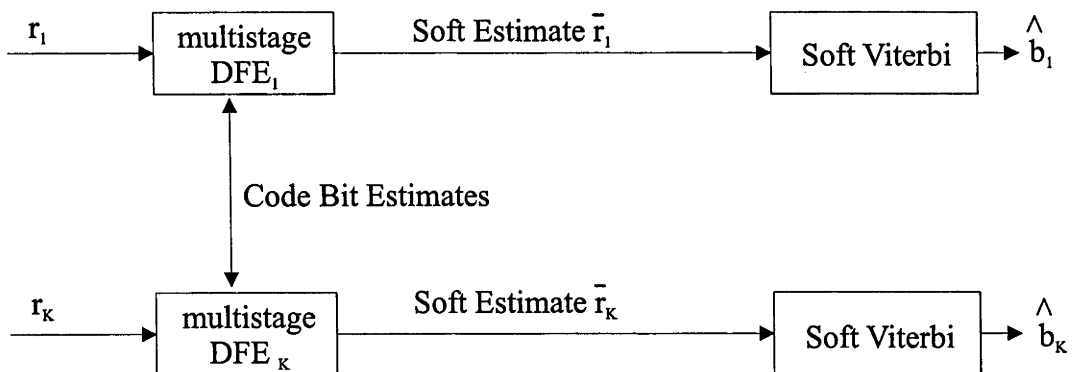


Figure 4.1: Multistage DFE multiuser equalisation followed by Soft Viterbi algorithm

A novel scheme was proposed by [100] which used single user trellis decoding rather than optimal joint decoding in an attempt to reduce complexity (see Fig.4.2). The single user decoders take a soft metric from a multiuser device that is responsible for decoupling the multiuser channel into single user channels. This is another example where the multiuser equalisation is done prior to the decoding operation. In the case where the near orthogonal Gold codes were employed the loss from single user performance was minimal however in the random code channel, the loss was several dB. The random code channel appears to be a more harsh environment than the Gold code synchronous channel. In any case the design of this decoupling receiver is important since it will form the basis of any future implementation of a practical system.

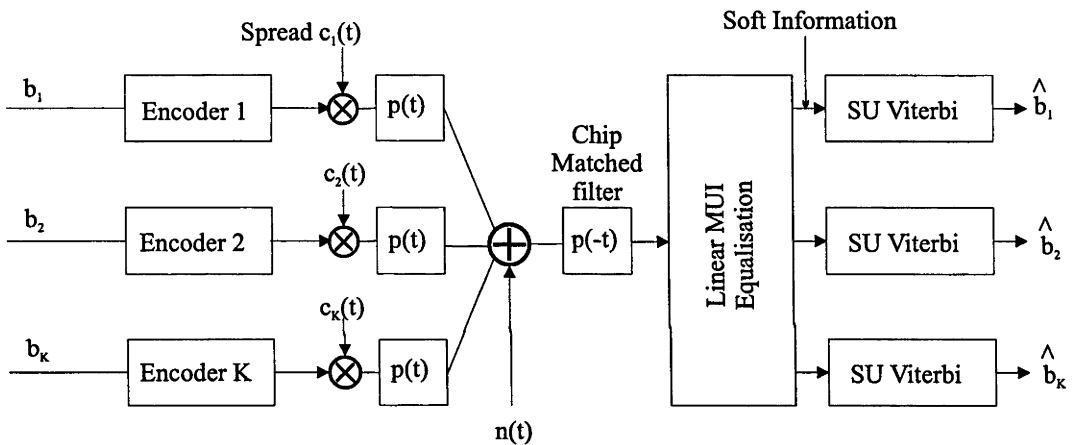


Figure 4.2: Baseband equivalent model for coded CDMA and SU receiver

Most of the research to date has focussed on the design of multiuser receiver structures with error control coding. The performance evaluation of these receivers can be studied by computing the “minimum distance” measure. This “measure” is directly related to the bit error performance and will ultimately enlighten us on how to design more robust CDMA systems, ie. combating multiuser interference by using error control codes to enhance performance. In this chapter we will not design sub-optimal receivers but rather investigate properties of the squared Euclidean distance, d_{min}^2 for coded multiuser systems. The asymptotic performance for the optimal multiuser detector is determined by d_{min}^2 . We are interested in the question: Is there any loss in the upper bound of d_{min}^2 due to a non-orthogonal or non-singular spreading waveform set? Based on a natural extension of Calderbank et al. [22] we will derive upper bounds on d_{min}^2 for coded CDMA

systems given any trellis code. It will characterise the behaviour of such systems. If the upper bound on d_{min}^2 for a coded multiuser system is significantly worse than that of a single user system, it may not even be worthwhile studying coded multiuser systems. We show that the multiuser minimum squared Euclidean distance is upper bounded by single user systems. The effect of non-orthogonal spreading on d_{min}^2 is studied next. This effort extends the work of Lupas and Verdú [66] for uncoded system to a coded system. In particular, upper and lower bounds are derived on the ratio between d_{min}^2 in systems with non-orthogonal and orthogonal spreading. Last but not least, we show that it is possible to compute d_{min}^2 for the coded multiuser case provided we know the minimum Euclidean distance for the corresponding uncoded case.

4.2 System Model

Consider a general asynchronous DS-SS system and a set of unity energy preassigned periodic signature waveforms, $s_i(t)$ $i = 1, 2, \dots, K$ of duration T_s . We assume that

- the i -th user uses a trellis code with k_i input bits, n_i output bits and memory length of ν_i bits
- the input and output bits of different users are independent
- the input k_i bits are represented as a 2^{k_i} -ary symbol, $b_{m,i}$
- the output n_i bits are mapped into the 2^{n_i} -ary two dimensional symbol $x_{m,i}$ (ie., QPSK or QAM mapping) where m is the symbol interval

The input signal to the receiver is

$$r(t) = A(t, \mathbf{b}) + n(t) \quad (4.1)$$

where

$$A(t, \mathbf{b}) = \sum_{i=1}^K \sum_{m=-M}^M \exp(j\theta_i) x_{m,i} s_i(t - mT_s - \zeta_i), \quad (4.2)$$

M is a positive integer which can be infinite, θ_i is the carrier phase, ζ_i is the random transmission delay, which is assumed to be uniformly distributed over $(0, T_s]$ for asynchronous systems and zero for synchronous systems, and $n(t)$ is white complex Gaussian noise with double sided power spectral density N_0 where $N_0 = 2\sigma^2$. We also assume that $\zeta_1 \leq \zeta_2 \leq \dots \leq \zeta_K$, and that the receiver has perfect knowledge of the carrier phase θ_i , the time delay ζ_i . This model closely follows that of section 3.4.

$x_{m,i}$ is the transmitted signal of the i th user at the time interval $(mT_s, mT_s + T_s]$. It is a function of the most recent symbol ($b_{m,i}$) and previous ν_i symbols ($b_{m-1,i}, \dots, b_{m-\nu_i,i}$) of user i , the mapping function being represented by $\sigma(\cdot)$. Thus

$$x_{m,i} = \sigma(b_{m,i}, b_{m-1,i}, \dots, b_{m-\nu_i,i}). \quad (4.3)$$

For the multiuser case the output symbol vector \mathbf{x}_m can be represented in a similar form to (4.3) as,

$$\mathbf{x}_m = [x_{m,1}, \dots, x_{m,K}] = \sigma'(b_{m,1}, \dots, b_{m-\nu_1,1}, \dots, b_{m,K}, \dots, b_{m-\nu_K,K}) \quad (4.4)$$

The multiuser joint trellis represents a trellis code with $\kappa = k_1 + k_2 + \dots + k_K$ inputs and a constraint length of $V = \nu_1 + \nu_2 + \dots + \nu_K$ bits. Using a notation similar to Lupas and Verdú [67], we obtain sufficient statistic at the output of the matched filter bank,

$$\mathbf{r}' = \mathcal{R}\mathbf{X} + \mathbf{z}, \quad (4.5)$$

where $r_{m,i}$ is the sampled output of the matched filter for the m -th bit of the i -th user and

$$\mathbf{r}' = [\dots, r'_{m,1}, r'_{m,2}, \dots, r'_{m,K}, \dots]^T, \quad (4.6)$$

$$\mathbf{X} = [\dots, \mathbf{x}_{m-1}, \mathbf{x}_m, \mathbf{x}_{m+1}, \dots]^T \quad (4.7)$$

$$\mathbf{z} = [\dots, z_{m,1}, z_{m,2}, \dots, z_{m,K}, \dots]^T \quad (4.8)$$

and the symmetric correlation matrix \mathcal{R} is

$$\mathcal{R} = \begin{bmatrix} \cdot & \cdot & \cdot & \cdot & \cdot & \cdot \\ \cdot & \mathbf{R}(1) & \mathbf{R}(0) & \mathbf{R}(-1) & \mathbf{0} & \cdot \\ \cdot & \mathbf{0} & \mathbf{R}(1) & \mathbf{R}(0) & \mathbf{R}(-1) & \cdot \\ \cdot & \cdot & \cdot & \cdot & \cdot & \cdot \end{bmatrix} \quad (4.9)$$

The baseband model of the receiver is shown in (4.3).

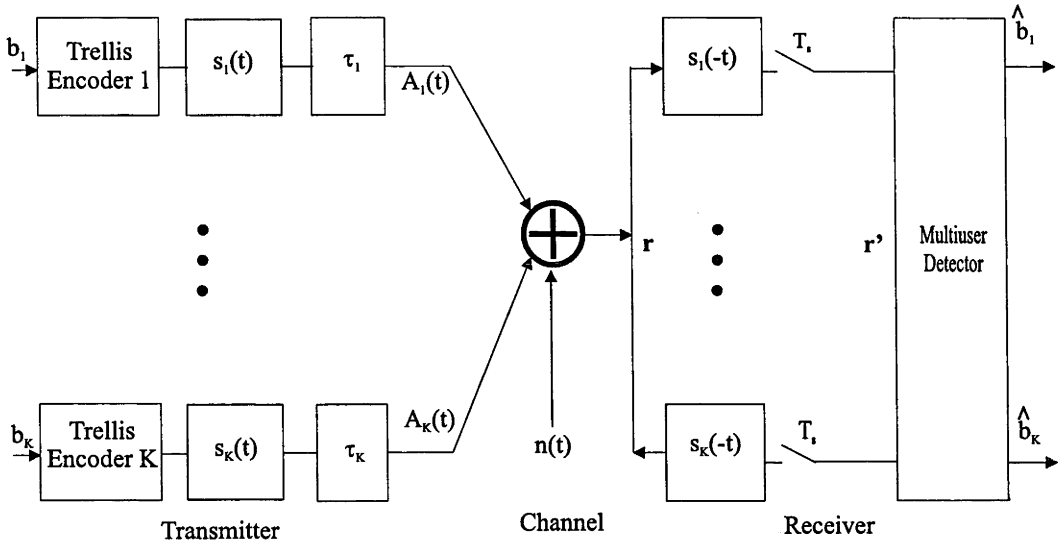


Figure 4.3: Baseband equivalent model for coded CDMA

As in chapter 3, it is assumed that the matrix \mathcal{R} is positive definite. This condition has been well justified by Lupas and Verdú (see linear independence assumption in [67]). Since \mathcal{R} is positive definite and symmetric, it is possible to find a unique lower triangular, non-singular matrix \mathcal{F} such that $\mathcal{R} = \mathcal{F}^T \mathcal{F}$ (Cholesky decomposition, [40]). Thus the matrix \mathcal{F} has the following structure:

$$\mathcal{F} = \begin{bmatrix} \cdot & \cdot & \cdot & \cdot & \cdot & \cdot \\ \cdot & \mathbf{F}(1) & \mathbf{F}(0) & \mathbf{0} & \mathbf{0} & \cdot \\ \cdot & \mathbf{0} & \mathbf{F}(1) & \mathbf{F}(0) & \mathbf{0} & \cdot \\ \cdot & \cdot & \cdot & \cdot & \cdot & \cdot \end{bmatrix} \quad (4.10)$$

where $\mathbf{F}(0)$ is a $K \times K$ lower triangular matrix with a non-zero diagonal (ie. $\mathbf{F}^{m,l}(0) = 0$ if $l > m$ and $\mathbf{F}(1)$ is an upper right triangular matrix with a zero diagonal (ie. $\mathbf{F}^{m,l}(1) = 0$ if $l \geq m$). Thus, if the whitening filter $(\mathcal{F}^T)^{-1}$ is applied to the sampled output of the

matched filter, the output vector is

$$\mathbf{y} = \mathcal{F}\mathbf{X} + \mathbf{n} \tag{4.11}$$

where

$$\mathbf{y} = [\cdots, y_{m,1}, y_{m,2}, \cdots, y_{m,K}, \cdots]^T \tag{4.12}$$

and \mathbf{n} is a white complex Gaussian noise vector with autocorrelation matrix $R(\mathbf{n}) = \frac{1}{2}N_0\mathbf{I}$. where \mathbf{I} is an identity matrix. Similar to the work of Forney [35], we adopt an equivalent discrete model of the multiuser system illustrated in Figure (4.4).

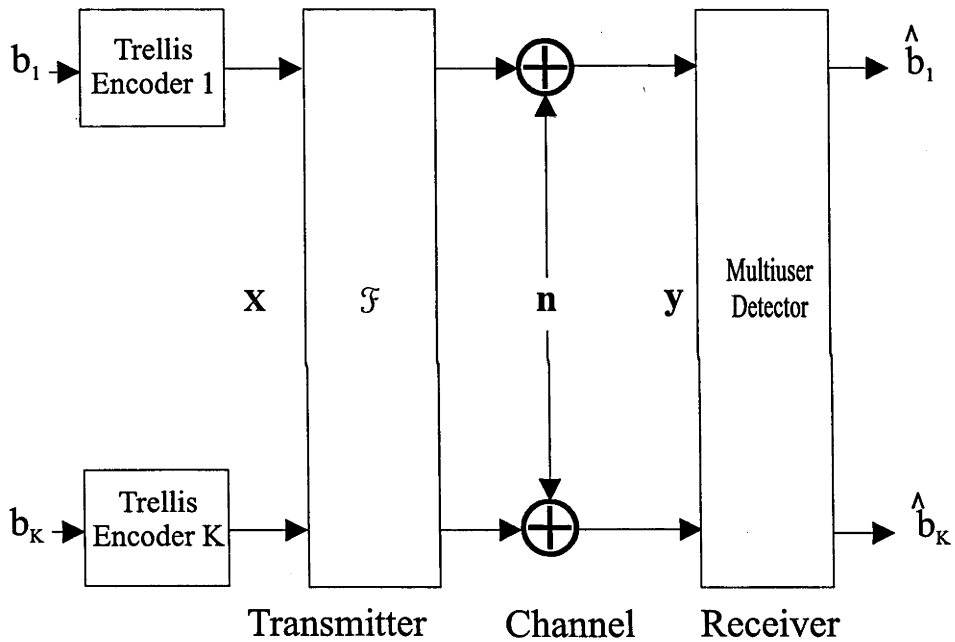


Figure 4.4: Equivalent discrete model of the system

4.3 Normalised Minimum Squared Euclidean Distance

In this section we will use matrix notation to define a multiuser error event and its associated distance measure. Let an error event E of length L last from time m to time $m + L$, ie. the decoder having decided $\hat{\mathbf{X}} = (\hat{x}_{m+1}, \cdots, \hat{x}_{m+L})$ instead of the correct sequence

$\mathbf{X} = (\mathbf{x}_{m+1}, \dots, \mathbf{x}_{m+L})$. The squared Euclidean distance $d^2(E)$ is

$$d^2(E) = \|\mathcal{F}(\mathbf{X} - \hat{\mathbf{X}})\|^2 \quad (4.13)$$

$$= \mathbf{Q}^H \mathcal{E}^T \mathcal{R}_m^{m+L} \mathcal{E} \mathbf{Q} \quad (4.14)$$

$$= \mathbf{Q}^H \mathbf{D}(E) \mathbf{Q} \quad (4.15)$$

where $\mathbf{D}(E)$ is a symmetric, positive, semi-definite matrix which is called the distance matrix,

$$\mathbf{Q}^T = [\mathbf{Q}_1^T, \dots, \mathbf{Q}_K^T] \quad (4.16)$$

$$= [q_{1,0}, \dots, q_{1,\Gamma_1-1}, \dots, q_{K,0}, \dots, q_{K,\Gamma_K-1}] \quad (4.17)$$

is a vector comprising of all possible output symbols, Γ

$$\Gamma = \sum_{i=1}^K \Gamma_i = \sum_{i=1}^K 2^{\nu_i+k_i} \quad (4.18)$$

\mathcal{E} is a $\Gamma \times KL$ matrix such that $\mathbf{X} - \hat{\mathbf{X}} = \mathcal{E} \mathbf{Q}$ where $\mathcal{E} = [\mathcal{E}_1, \mathcal{E}_2, \dots, \mathcal{E}_K]$.

\mathcal{R}_m^{m+L} is a $KL \times KL$ correlation matrix given by,

$$\mathcal{R}_m^{m+L} = \begin{bmatrix} \mathbf{R}(0) & \mathbf{R}(-1) & \mathbf{0} & \mathbf{0} & \mathbf{0} & \dots & \mathbf{0} \\ \mathbf{R}(1) & \mathbf{R}(0) & \mathbf{R}(-1) & \mathbf{0} & \cdot & \cdot & \cdot \\ \mathbf{0} & \cdot & \cdot & \cdot & \cdot & \cdot & \cdot \\ \vdots & \cdot & \cdot & \cdot & \cdot & \cdot & \cdot \\ \cdot & \cdot & \cdot & \cdot & \mathbf{R}(1) & \mathbf{R}(0) & \mathbf{R}(-1) \\ \mathbf{0} & \dots & \mathbf{0} & \mathbf{0} & \mathbf{0} & \mathbf{R}(1) & \mathbf{R}(0) \end{bmatrix} \quad (4.19)$$

For a code with k input bits and a memory length of ν bits, there are a total of $2^{\nu+k}$ unique branches in its trellis. If each branch is mapped onto a symbol q , the maximum number of symbols is $2^{\nu+k}$. Let us look at the following example to illustrate the above concepts.

Example 1: Consider a two user system with a 4 and 2 state trellis code with mapping illustrated by Fig. 4.5.

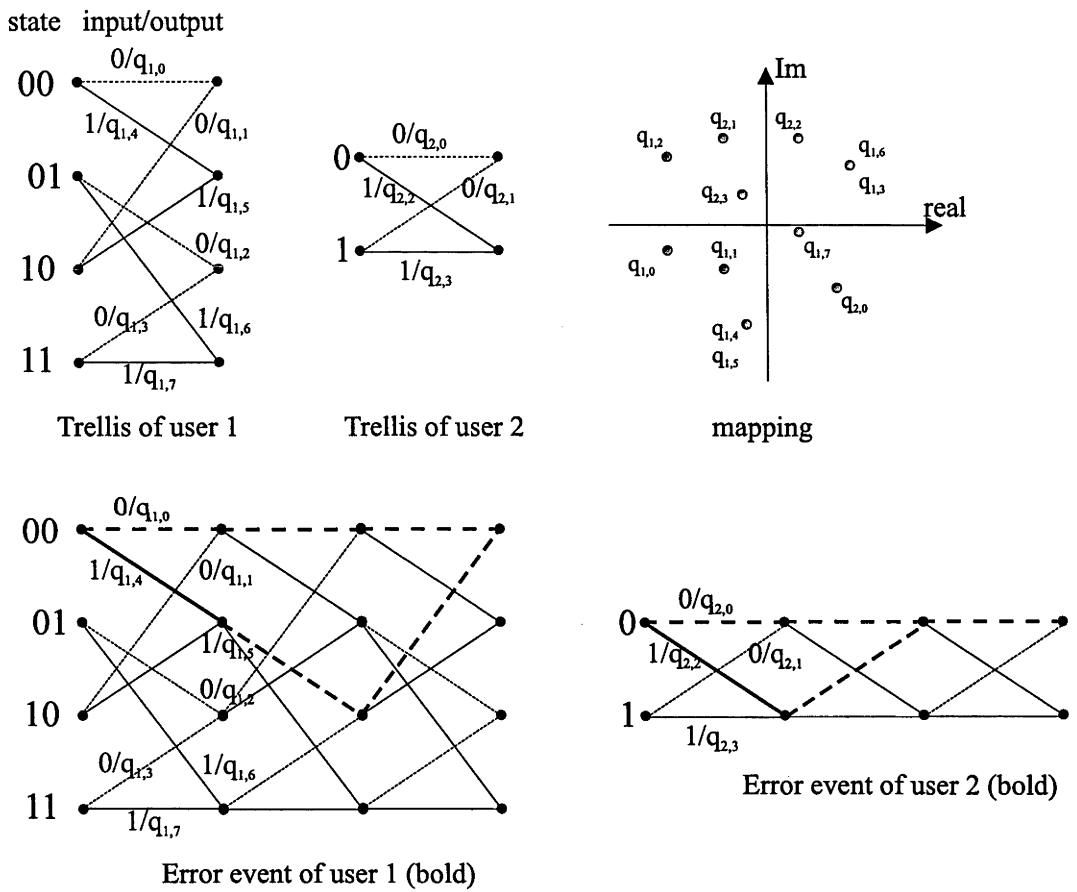


Figure 4.5: Trellis diagram and arbitrary mapping format of a 4 state and a 2 state code

The normalised squared Euclidean distance of error event

$$E = \{\mathbf{X}, \hat{\mathbf{X}}\} = \{(q_{1,0}, q_{2,0}, q_{1,0}, q_{2,0}, q_{1,0}, q_{2,0}), (q_{1,4}, q_{2,2}, q_{1,2}, q_{2,1}, q_{1,1}, q_{2,0})\}$$

is

$$d^2(E) = \mathbf{Q}^H \boldsymbol{\varepsilon}^T \mathcal{R}_0^3 \boldsymbol{\varepsilon} \mathbf{Q} \quad (4.20)$$

where

$$\mathbf{Q} = \begin{bmatrix} Q_1 \\ Q_2 \end{bmatrix} \quad (4.21)$$

$$= [q_{1,0}, \dots, q_{1,7}, q_{2,0}, \dots, q_{2,3}]^T \quad (4.22)$$

$$\boldsymbol{\varepsilon} = [\boldsymbol{\varepsilon}_1 \boldsymbol{\varepsilon}_2] \quad (4.23)$$

$$= \begin{bmatrix} 1 & 0 & 0 & 0 & -1 & 0 & 0 & 0 & | & 0 & 0 & 0 & 0 \\ 0 & 0 & 0 & 0 & 0 & 0 & 0 & 0 & | & 1 & 0 & -1 & 0 \\ 1 & 0 & -1 & 0 & 0 & 0 & 0 & 0 & | & 0 & 0 & 0 & 0 \\ 0 & 0 & 0 & 0 & 0 & 0 & 0 & 0 & | & 1 & 0 & -1 & 0 \\ 1 & -1 & 0 & 0 & 0 & 0 & 0 & 0 & | & 0 & 0 & 0 & 0 \\ 0 & 0 & 0 & 0 & 0 & 0 & 0 & 0 & | & 0 & 0 & 0 & 0 \end{bmatrix} \quad (4.24)$$

$$\mathcal{R}_0^3 = \begin{bmatrix} R_{11}(0) & R_{12}(0) & 0 & 0 & 0 & 0 \\ R_{12}(0) & R_{22}(0) & R_{21}(1) & 0 & 0 & 0 \\ 0 & R_{21}(1) & R_{11}(0) & R_{12}(0) & 0 & 0 \\ 0 & 0 & R_{12}(0) & R_{22}(0) & R_{21}(1) & 0 \\ 0 & 0 & 0 & R_{21}(1) & R_{11}(0) & R_{12}(0) \\ 0 & 0 & 0 & 0 & R_{12}(0) & R_{22}(0) \end{bmatrix} \quad (4.25)$$

The *minimum* Euclidean distance of user i can now be given as

$$d_{min,i}^2 = \min_{E \in \mathcal{Z}_i} \mathbf{Q}^H \boldsymbol{\varepsilon}^T \mathcal{R}_0^L \boldsymbol{\varepsilon} \mathbf{Q} \quad (4.26)$$

where \mathcal{Z}_i is the set of all finite-length error sequences with $\boldsymbol{\varepsilon}_i \neq \mathbf{0}$ (ie. the i th user must be in error).

Let $\mathcal{Z} = \{\mathcal{Z}_i : i = 1, \dots, K\}$ and P be the average power, ie.,

$$P = \frac{1}{2^{\kappa+V}} \sum_{i=1}^K \sum_{m=0}^{2^{k_i+\nu_i}} q_{i,m}^2 = \frac{1}{2^{\kappa+V}} Q^H Q \quad (4.27)$$

4.4 Properties of $d_{min,i}^2$ for Coded Multiuser CDMA

In this section we will investigate two properties of $d_{min,i}^2$. Specifically we will derive an upper bound for the multiuser squared minimum Euclidean distance and secondly we will investigate the effect of non-orthogonal spreading on $d_{min,i}^2$.

4.4.1 Upper Bound on Squared Minimum Euclidean Distance

We are concerned with the transmission of digital data using trellis codes to gain immunity over standard uncoded methods. Let us consider the upper bound of the normalised squared minimum Euclidean distance d_{min}^2 of a coded multiuser CDMA system for any given non-orthogonal and non-singular spreading waveform set and any trellis code mapping format. That is

$$d_{min}^2/P = \max_Q \frac{\min_i d_{min,i}^2}{P} = \max_Q \min_{E \in \mathcal{Z}} \frac{Q^H D(E) Q}{P}. \quad (4.28)$$

Upper bounds for d_{min}^2 in a single-user scenario using trellis codes have been well studied by coding theorists. We generalise the results of Calderbank et al. [22] to a multiuser environment. In this section we are interested in the question, is there any loss in the upper bound on d_{min}^2 due to a non-orthogonal and non-singular spreading waveform set? It is easy to verify that the upper bound is the same as those for the single-user case by selectively choosing an orthogonal spreading code set. This is not very informative, so we choose to study the upper bound without constraining ourselves to a specific set or sets of spreading codes, rather the ensemble over all spreading codes and all trellis code mapping formats. It is thus important to realise that should the upper bound for the case $\mathcal{R} \neq \mathbf{I}$ be significantly worse than the single-user upper bound, the coded multiuser system may not be useful in practice and therefore not worthwhile studying at all. Let us

familiarise ourselves with some of the results in [22]. First, an upper bound on d_{min}^2 for a trellis code with constraint length, ν and k input bits is

$$d_{min}^2/P \leq 4\left(1 + \frac{\nu}{k}\right) \quad (4.29)$$

if k divides ν , and second, Lemma 3 of [22] states that the total number of times $m_i(x(a))$, a branch with symbol $x(a)$ occurs in section i of the error events of set S , is given by

$$m_i(x(a)) = \frac{2 |S|}{2^{k+\nu}} \quad (4.30)$$

In the following two lemmas it is proved that the two properties hold for $\mathcal{R} \neq \mathbf{I}$.

Lemma 4.1 *The i -th diagonal entry of the distance matrix $D(E)$ is equal to the total number of times the branch with symbol q_i appears in an error event of length L .*

Proof: For a given error event, the i -th diagonal entry of $D(E)$,

$$D(E)^{ii} = e_i^T \mathcal{R}_0^L e_i \quad (4.31)$$

where e_i is the i -th column vector of \mathcal{E} . Since e_i consists only of $-1, 0, +1$,

$$D(E)^{ii} = n_{e_i} (\mathcal{R}_0^L e_i) \quad (4.32)$$

where n_{e_i} denotes the number of non-zero elements of vector e_i . Since $(\mathcal{R}_0^L)^{ii} = 1$, $D(E)^{ii} = n_{e_i}$. ■

For the above example we have $D(E)^{11} = 3R^{11}(0) = 3$

Lemma 4.2 *All row sums of $D(E)$ are zero.*

Proof: It is true since all row sums of \mathcal{E} are zero. ■

Proposition 4.1 *If all users use trellis codes with the same memory length and the same number of input bits but different signal mapping sets (ie. $\nu_i = \nu, k_i = k, i = 1, \dots, K$)*

and k divides ν , then the normalised squared minimum Euclidean distance d_{min}^2 for a trellis coded multiuser CDMA system with $\mathcal{R} \neq \mathbf{I}$ satisfies

$$d_{min}^2/P \leq 4\left(1 + \frac{\nu}{k}\right) \quad (4.33)$$

which is identical to the single-user case of (4.29).

Intuitively for $\mathcal{R} = \mathbf{I}$, this amounts to computing the upper bound for a multiuser joint trellis code with a total constraint length of $K\nu$ and input bits of Kk .

Proof:

$$d_{min}^2/P = \max_Q \min_{E \in \mathcal{Z}} \frac{Q^H D(E) Q}{P} \quad (4.34)$$

$$= 2^{\kappa+V} \max_Q \min_{E \in \mathcal{Z}} \frac{Q^H D(E) Q}{Q^H Q} \quad (4.35)$$

Let S be an arbitrary set of error events and S^L be the set of all error events of minimal length L where $L = (\nu + k)/k$. Since the minimum distance is upper bounded by the average,

$$d_{min}^2/P \leq \frac{2^{\kappa+V}}{|S^L|} \max_Q \frac{Q^H \left(\sum_{E \in S^L} D(E)\right) Q}{Q^H Q} \quad (4.36)$$

Let $D_L = \sum_{E \in S^L} D(E)$, we then have

$$d_{min}^2/P \leq \frac{2^{\kappa+V}}{|S^L|} \max_Q \frac{Q^H D_L Q}{Q^H Q} \quad (4.37)$$

$$= \frac{2^{\kappa+V}}{|S^L|} \lambda_{max}(D_L) \quad (4.38)$$

where $\lambda_{max}(\cdot)$ denote the largest eigenvalue of matrix (\cdot) . According to the Gershgorin circle theorem [40], the distance between the eigenvalue and diagonal element is always less than or equal to the row sum of the off diagonal elements. From lemma 4.2, (ie.

$\lambda - diagonal \leq diagonal$).

$$\lambda_{max}(D_L) \leq 2(diagonal) = 2 \left(\frac{2L |S^L|}{2^{\kappa+V}} \right) \quad (4.39)$$

Thus for a minimum length $L = (\nu + k)/k$,

$$d_{min}^2/P \leq 4L \quad (4.40)$$

$$= 4\left(1 + \frac{\nu}{k}\right) \quad (4.41)$$

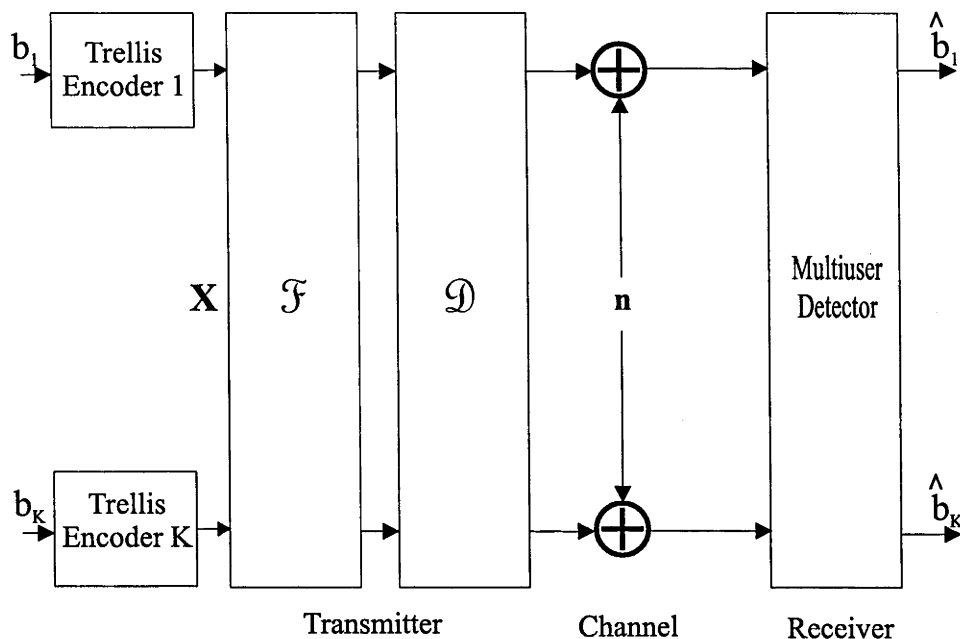
■

Proposition (4.1) indicates that the correlation matrix does not affect the *upper bound* of the normalised squared minimum Euclidean distance. This suggests that one may be able to find an error control code that can cancel the influence of the correlation matrix. Hence, the trellis coded multiuser system may be able to recover the minimum distance loss of the uncoded multiuser system due to the correlation matrix (if there is such a loss).

It is worth mentioning that if we introduce a linear processing filter \mathcal{D} before spreading (see Fig. 4.6), such that $\mathcal{D} = \mathcal{F}^{-1}$, then the correlation between users due to non-orthogonal spreading codes can be eliminated. Therefore, if there is a code that can achieve the above upper bound for the single-user system (*ie.* $\mathcal{R} = \mathbf{I}$), then by proper design of a multiuser joint trellis code (trellis code and filter \mathcal{F}^{-1}), the above upper bound for the multiuser CDMA system can also be achieved. This spreading process can be viewed as a joint encoding scheme (*ie.* to incorporate the effect of a decorrelating filter along with the trellis code). However, this will violate the assumption that all users are encoded independently. But of course, for all practical purposes, the transmitter generally does not know how to construct this filter, which motivates us to investigate the next topic - the loss in minimum distance due to the effect of \mathcal{R} .

Proposition 4.2 *If the error control code is catastrophic or the correlation matrix \mathcal{R} singular, then the coded multiuser system is not feasible*

Proof: An encoder with generator matrix $G(D)$ is catastrophic if there exists a $u(D)$ such that $H_w(u(D)) = \infty$ and $H_w(u(D)G(D)) < \infty$, where $H_w(\cdot)$ denote the Hamming


 Figure 4.6: Linear processing filter \mathcal{D} before spreading

distance of the sequence. Such an encoder will imply that a finite number of errors in the received sequence can cause an infinite number of errors in the data sequence $u(D)$. ■

4.4.2 Effect of \mathcal{R} on d_{min}^2

It is easy to show that if the filter \mathcal{D} is used in the system, the minimum squared Euclidean distance of user i is given by

$$d_{min,i}^2 = \min_{E \in \mathcal{Z}_i} Q^H \mathcal{E}^T \mathcal{D}^T \mathcal{R} \mathcal{D} \mathcal{E} Q \quad (4.42)$$

In this section we study the effect of \mathcal{R} by evaluating the ratio of the squared minimum distance of user i between the system with \mathcal{R} and a system with orthogonal spreading codes $\mathcal{R} = \mathbf{I}$,

$$\eta_i = \frac{\min_{E \in \mathcal{Z}_i} Q^H \mathcal{E}^T \mathcal{D}^T \mathcal{R} \mathcal{D} \mathcal{E} Q}{\min_{E \in \mathcal{Z}_i} Q^H \mathcal{E}^T \mathcal{D}^T \mathcal{D} \mathcal{E} Q} = \frac{\min_{E \in \mathcal{Z}_i} \epsilon^H \mathcal{R} \epsilon}{\min_{E \in \mathcal{Z}_i} \epsilon^H \epsilon} \quad (4.43)$$

where $\epsilon = \mathcal{DE}Q$ for a given error event E . The following lemma is important for further analysis.

Lemma 4.3 (a)

$$\lambda_{min}(\mathcal{R}_m^{m+L+1}) \leq \lambda_{min}(\mathcal{R}_m^{m+L}) \quad (4.44)$$

$$\lambda_{max}(\mathcal{R}_m^{m+L+1}) \geq \lambda_{max}(\mathcal{R}_m^{m+L}) \quad (4.45)$$

(b) If \mathcal{R} is positive definite, $\lambda_{min}(\mathcal{R}_m^{m+L})$ and $\lambda_{max}(\mathcal{R}_m^{m+L})$ for $L = 1, 2, \dots, \infty$ form two convergent series.

Proof: If a matrix A is Hermitian, the Rayleigh coefficient $\frac{x^H Ax}{x^H x}$ is bounded by $\lambda_{min}(A)$ and $\lambda_{max}(A)$ [40].

$$\lambda_{min}(A) \leq \frac{x^H Ax}{x^H x} \leq \lambda_{max}(A) \quad (4.46)$$

(a) can be illustrated by the following arguments. Let \mathcal{R}_m^{m+10} be of the form

$$\mathcal{R}_m^{m+10} = \begin{bmatrix} \mathbf{R}(0)_{1,1} & \mathbf{R}(-1)_{1,2} & \mathbf{0} & \mathbf{0} & \mathbf{0} & \dots & \mathbf{0} \\ \mathbf{R}(1)_{2,1} & \mathbf{R}(0)_{2,2} & \mathbf{R}(1)_{2,3} & \mathbf{0} & \cdot & \cdot & \cdot \\ \mathbf{0} & \cdot & \cdot & \cdot & \cdot & \cdot & \cdot \\ \cdot & \cdot & \cdot & \cdot & \cdot & \cdot & \cdot \\ \cdot & \cdot & \cdot & \cdot & \cdot & \cdot & \mathbf{0} \\ \cdot & \cdot & \cdot & \cdot & \mathbf{R}(1)_{9,8} & \mathbf{R}(0)_{9,9} & \mathbf{R}(1)_{9,10} \\ \mathbf{0} & \dots & \mathbf{0} & \mathbf{0} & \mathbf{0} & \mathbf{R}(1) & \mathbf{R}(0)_{10,10} \end{bmatrix}$$

and \mathcal{R}_m^{m+30} be of the form

$$\mathcal{R}_m^{m+30} = \begin{bmatrix} \mathbf{R}(0)_{1,1} & \mathbf{R}(-1)_{1,2} & \mathbf{0} & \mathbf{0} & \mathbf{0} & \dots & \mathbf{0} \\ \mathbf{R}(1)_{2,1} & \mathbf{R}(0)_{2,2} & \mathbf{R}(1)_{2,3} & \mathbf{0} & \cdot & \cdot & \cdot \\ \mathbf{0} & \cdot & \cdot & \cdot & \cdot & \cdot & \cdot \\ \cdot & \cdot & \cdot & \cdot & \cdot & \cdot & \cdot \\ \cdot & \cdot & \cdot & \cdot & \cdot & \cdot & \mathbf{0} \\ \cdot & \cdot & \cdot & \cdot & \mathbf{R}(1)_{29,28} & \mathbf{R}(0)_{29,29} & \mathbf{R}(1)_{29,30} \\ \mathbf{0} & \dots & \mathbf{0} & \mathbf{0} & \mathbf{0} & \mathbf{R}(1) & \mathbf{R}(0)_{30,30} \end{bmatrix}$$

where \mathcal{R}_m^{m+30} can be written as

$$\mathcal{R}_m^{m+30} = \begin{pmatrix} \mathcal{R}_m^{m+10} & Y \\ Y^H & Z \end{pmatrix} \quad (4.47)$$

where $\lambda_{min}(\mathcal{R}_m^{m+30})$ is the minimum eigenvalue of the correlation matrix \mathcal{R}_m^{m+30} and equals

$$\lambda_{min}(\mathcal{R}_m^{m+30}) = \min_{x \neq 0} \frac{x^H \mathcal{R}_m^{m+30} x}{x^H x} = \min_{x \neq 0, x^H x = 1} x^H \mathcal{R}_m^{m+30} x \quad (4.48)$$

Rewrite $x = \begin{pmatrix} y_{10} \\ \tilde{y} \end{pmatrix}$. Now (4.48) can be written as

$$\lambda_{min}(\mathcal{R}_m^{m+30}) = \min_{x^H x = 1} (y_{10} \ \tilde{y}) \begin{pmatrix} \mathcal{R}_m^{m+10} & Y \\ Y^H & Z \end{pmatrix} \begin{pmatrix} y_{10} \\ \tilde{y} \end{pmatrix} \quad (4.49)$$

$$\leq \min_{x^H x = 1, \tilde{y} = 0} (y_{10} \ \tilde{y}) \begin{pmatrix} \mathcal{R}_m^{m+10} & Y \\ Y^H & Z \end{pmatrix} \begin{pmatrix} y_{10} \\ \tilde{y} \end{pmatrix} \quad (4.50)$$

From eqn.(4.50)

$$\lambda_{min}(\mathcal{R}_m^{m+30}) \leq \min_{y_{10}^H y_{10} = 1} y_{10}^H \mathcal{R}_m^{m+10} y_{10} = \lambda_{min}(\mathcal{R}_m^{m+10}) \quad (4.51)$$

As $n \rightarrow \infty$ the eigenvalues of \mathcal{R}_m^{m+n} get smaller. The same analysis applies for the maximum eigenvalues.

(b) Since $\lambda_{min}(\mathcal{R}_m^{m+L})$ decreases monotonically and is lower bounded by 0 and $\lambda_{max}(\mathcal{R}_m^{m+L})$ increases monotonically and upper bounded by ∞ ($< \infty$), $\lambda_{min}(\mathcal{R}_m^{m+L})$ and $\lambda_{max}(\mathcal{R}_m^{m+L})$ form two convergent series. ■

We now state the following proposition about the upper and lower bound of the ratio, η_i .

Proposition 4.3 For any trellis code and filter \mathcal{D} used in the system, the ratio η_i is bounded by

$$\lambda_{min}(\mathcal{R}) \leq \eta_i \leq \lambda_{max}(\mathcal{R}), \quad i = 1, \dots, K. \quad (4.52)$$

Proof: Let ϵ_1 and ϵ_2 be two vectors of length L_1 and L_2 (ie. elements of both ϵ_1 and ϵ_2 are zero outside $(m, m + L_j]$) to satisfy

$$\epsilon_1 = \arg \min_{E \in \mathcal{Z}_i} \epsilon^H \mathcal{R} \epsilon \quad (4.53)$$

$$\epsilon_2 = \arg \min_{E \in \mathcal{Z}_i} \epsilon^H \epsilon \quad (4.54)$$

$$\frac{\epsilon_1^H \mathcal{R}_m^{m+L_1} \epsilon_1}{\epsilon_1^H \epsilon_1} = \frac{\epsilon_1^H \mathcal{R} \epsilon_1}{\epsilon_1^H \epsilon_1} \leq \eta_i = \frac{\min_{E \in \mathcal{Z}_i} \epsilon^H \mathcal{R} \epsilon}{\min_{E \in \mathcal{Z}_i} \epsilon^H \epsilon} \leq \frac{\epsilon_2^H \mathcal{R} \epsilon_2}{\epsilon_2^H \epsilon_2} = \frac{\epsilon_2^H \mathcal{R}_m^{m+L_2} \epsilon_2}{\epsilon_2^H \epsilon_2} \quad (4.55)$$

Since

$$\lambda_{min}(\mathcal{R}_m^{m+L}) \leq \frac{\epsilon^H \mathcal{R}_m^{m+L} \epsilon}{\epsilon^H \epsilon} \leq \lambda_{max}(\mathcal{R}_m^{m+L}) \quad (4.56)$$

we have

$$\lambda_{min}(\mathcal{R}_m^{m+L_1}) \leq \eta_i = \frac{\min_{E \in \mathcal{Z}_i} \epsilon^H \mathcal{R} \epsilon}{\min_{E \in \mathcal{Z}_i} \epsilon^H \epsilon} \leq \lambda_{max}(\mathcal{R}_m^{m+L_2}) \quad (4.57)$$

According to lemma 4.3, we have

$$\lambda_{min}(\mathcal{R}) \leq \lambda_{min}(\mathcal{R}_m^{m+L_1}) \leq \eta_i \leq \lambda_{max}(\mathcal{R}_m^{m+L_2}) \leq \lambda_{max}(\mathcal{R}) \quad (4.58)$$

■

The above proposition shows that for a given \mathcal{R} , regardless of the kind of linear filter and trellis code used, the minimum distance ratio is bounded by the minimum and maximum eigenvalues of \mathcal{R} . For specific linear filters we can obtain tighter bounds.

Lemma 4.4 (a) If $\mathcal{D} = \mathbf{I}$, then $\eta_i \leq 1$.

(b) If $\mathcal{D} = \mathcal{F}^{-1}$, then $\eta_i \geq 1$

Proof: (a) If $\mathcal{D} = \mathbf{I}$, the minimisation of the denominator in eqn. (4.43) (ie. $\min_{E \in \mathcal{Z}_i} \epsilon^H \epsilon$) can be realised by an error event (say ϵ') which only user i has error (ie. $\mathcal{E}_i \neq \mathbf{0}$) and all others do not have error (ie. $\mathcal{E}_j = \mathbf{0}$ for $j = 1, \dots, i-1, i+1, \dots, K$). We then have

$$\min_{E \in \mathcal{Z}_i} \epsilon^H \mathcal{R}_m^{m+L} \epsilon \leq \epsilon'^H \mathcal{R} \epsilon' = \epsilon'^H \epsilon' \quad (4.59)$$

(b) If $\mathcal{D} = \mathcal{F}^{-1}$, then $\eta_i = \frac{\min_{E \in \mathcal{Z}_i} Q^H \mathcal{E}^T \mathcal{E} Q}{\min_{E \in \mathcal{Z}_i} Q^H \mathcal{E}^T \mathcal{R}^{-1} \mathcal{E} Q}$ and we can prove (b) similarly ■

For uncoded binary systems and $\mathcal{D} = \mathbf{I}$ part (a) of the lemma 4.4 was shown by Verdú and η_i is equivalent to the concept of asymptotic efficiency of user i given by (9) in [122]. For an infinite dimensional matrix \mathcal{R} , it is difficult to compute the exact value of the minimum and maximum eigenvalues. However, according to lemma 4.3 it is possible to estimate the above bounds.

4.4.3 Asymptotic efficiency for coded CDMA

If $\mathcal{D} = \mathbf{I}$, an analysis similar to [66] can be carried out to obtain a tighter lower bound for η_i . Let us reorder the matrix \mathcal{R} as

$$\underline{R} = \begin{bmatrix} \mathbf{A}_i & \mathbf{a}_i \\ \mathbf{a}_i^T & \mathbf{I} \end{bmatrix} \quad (4.60)$$

where \mathbf{A}_i is obtained from \mathcal{R} by deleting all rows and columns related to the i -th user and \mathbf{a}_i is comprised of the columns related to the i -th user with the entries of the i -th user removed. Let

$$\begin{bmatrix} \mathbf{A}_i & \mathbf{a}_i \\ \mathbf{a}_i^T & \mathbf{I} \end{bmatrix}^{-1} = \begin{bmatrix} \mathbf{G}_i & \mathbf{g}_i \\ \mathbf{g}_i^T & \mathbf{H}_i \end{bmatrix} \quad (4.61)$$

For example 1, $i = 1$ and $L = 3$ we have,

$$\underline{R} = \begin{bmatrix} R_{22}(0) & 0 & 0 & | & R_{12}(0) & R_{21}(1) & 0 \\ 0 & R_{22}(0) & 0 & | & 0 & R_{12}(0) & R_{21}(1) \\ 0 & 0 & R_{22}(0) & | & 0 & 0 & R_{12}(0) \\ - & - & - & - & - & - & - \\ R_{12}(0) & 0 & 0 & | & R_{11}(0) & 0 & 0 \\ R_{21}(1) & R_{12}(0) & 0 & | & 0 & R_{11}(0) & 0 \\ 0 & R_{21}(1) & R_{12}(0) & | & 0 & 0 & R_{11}(0) \end{bmatrix} \quad (4.62)$$

Proposition 4.4 If $\mathcal{D} = \mathbf{I}$, then

$$\eta_i \geq \frac{1}{\lambda_{max}(\mathbf{H}_i)} \quad (4.63)$$

where \mathbf{H}_i can be contracted by partitioning \mathcal{R} into \underline{R} and taking its inverse. As a special case for synchronous CDMA, $\eta_i \geq \frac{1}{((\mathbf{R}(0))^{-1})^n}$ which is the same as (2.13) of [66].

Proof: If $\mathcal{D} = \mathbf{I}$, then

$$\min_{E \in \mathcal{Z}_i} \epsilon^H \epsilon = \min_{E \in \mathcal{Z}_i} (\mathcal{E}_i Q_i)^H \mathcal{E}_i Q_i. \quad (4.64)$$

Since $\epsilon^H \mathcal{R} \epsilon$, $(\mathcal{E}_i Q_i)^H \mathcal{E}_i Q_i$ and $\frac{\epsilon^H \mathcal{R} \epsilon}{(\mathcal{E}_i Q_i)^H \mathcal{E}_i Q_i}$ are positive for $E \in \mathcal{Z}_i$,

$$\eta_i = \frac{\min_{E \in \mathcal{Z}_i} \epsilon^H \mathcal{R} \epsilon}{\min_{E \in \mathcal{Z}_i} \epsilon^H \epsilon} \geq \min_{E \in \mathcal{Z}_i} \frac{\epsilon^H \mathcal{R} \epsilon}{(\mathcal{E}_i Q_i)^H \mathcal{E}_i Q_i} \quad (4.65)$$

Let $\mathbf{e}_i = \mathcal{E}_i Q_i$ and $\mathbf{c}_i = [\mathbf{e}_i^T, \dots, \mathbf{e}_{i-1}^T, \mathbf{e}_{i+1}^T, \dots, \mathbf{e}_K^T]^T$. We then obtain

$$\min_{E \in \mathcal{Z}_i} \frac{\epsilon^H \mathcal{R} \epsilon}{(\mathcal{E}_i Q_i)^H \mathcal{E}_i Q_i} = \min_{E \in \mathcal{Z}_i} \frac{\begin{bmatrix} \mathbf{c}_i^H & \mathbf{e}_i^H \end{bmatrix} \begin{bmatrix} \mathbf{A}_i & \mathbf{a}_i \\ \mathbf{a}_i^T & \mathbf{I} \end{bmatrix} \begin{bmatrix} \mathbf{c}_i \\ \mathbf{e}_i \end{bmatrix}}{\mathbf{e}_i^H \mathbf{e}_i} \quad (4.66)$$

$$= \min_{E \in \mathcal{Z}_i} \left(1 + \frac{\mathbf{c}_i \mathbf{A}_i \mathbf{c}_i}{\mathbf{e}_i^H \mathbf{e}_i} + \frac{\mathbf{c}_i^H \mathbf{a}_i \mathbf{e}_i + \mathbf{e}_i^H \mathbf{a}_i^T \mathbf{c}_i}{\mathbf{e}_i^H \mathbf{e}_i} \right) \quad (4.67)$$

where the minimum of this is achieved by any element \mathbf{c}_i such that

$$\mathbf{A}_i \mathbf{c}_i^H = -\mathbf{a}_i \mathbf{e}_i \quad (4.68)$$

Since \mathcal{R} is positive definite, so is \mathbf{A}_i . Thus substituting $\mathbf{c}_i = -\mathbf{A}_i^{-1} \mathbf{a}_i \mathbf{e}_i$ in (4.67), we have

$$\min_{E \in \mathcal{Z}_i} \frac{\epsilon^H \mathcal{R} \epsilon}{(\mathcal{E}_i Q_i)^H \mathcal{E}_i Q_i} = \min_{E \in \mathcal{Z}_i} \left(1 - \frac{\mathbf{c}_i^H \mathbf{A}_i \mathbf{c}_i}{\mathbf{e}_i^H \mathbf{e}_i} \right) = \min_{E \in \mathcal{Z}_i} \left(1 - \frac{\mathbf{e}_i^H \mathbf{a}_i^T \mathbf{A}_i^{-1} \mathbf{a}_i \mathbf{e}_i}{\mathbf{e}_i^H \mathbf{e}_i} \right) \quad (4.69)$$

Then simplifying the above expression we obtain

$$\min_{E \in \mathcal{Z}_i} \frac{\epsilon^H \mathcal{R} \epsilon}{(\mathcal{E}_i Q_i)^H \mathcal{E}_i Q_i} = \min_{E \in \mathcal{Z}_i} \left(\frac{\mathbf{e}_i^H \mathbf{H}_i^{-1} \mathbf{e}_i}{\mathbf{e}_i^H \mathbf{e}_i} \right) \geq \frac{1}{\lambda_{max}(\mathbf{H}_i)} \quad (4.70)$$

In the special case of synchronous CDMA,

$$\mathbf{H}_i = ((\mathbf{R}(0)^{-1})^{ii}) \mathbf{I} \eta_i \geq \min_{E \in \mathcal{Z}_i} \frac{\epsilon^H \mathcal{R} \epsilon}{(\mathcal{E}_i Q_i)^H \mathcal{E}_i Q_i} = \frac{1}{((\mathbf{R}(0)^{-1})^{ii})} \quad (4.71)$$

■

Since $\lambda_{max}(\mathbf{H}_i) \leq \lambda_{max}(\underline{\mathbf{R}}^{-1}) = \lambda_{min}^{-1}(\underline{\mathbf{R}}) = \lambda_{min}^{-1}(\mathcal{R})$, the lower bound of (4.63) is tighter than that of (4.52). For an infinite dimensional matrix \mathcal{R} , it is difficult to compute the exact value of $\lambda_{max}(\mathbf{H}_i)$. However, we can estimate the value by the following procedure.

Reorder the matrix \mathcal{R}_0^L as $\underline{\mathbf{R}}_L$,

$$\underline{\mathbf{R}}_L = \begin{bmatrix} \mathbf{A}_{i,L} & \mathbf{a}_{i,L} \\ \mathbf{a}_{i,L}^T & \mathbf{I}_L \end{bmatrix} \quad (4.72)$$

where $\mathbf{A}_{i,L}$ is obtained from \mathcal{R}_0^L by deleting all rows and columns related to the i -th user and $\mathbf{a}_{i,L}$ is comprised of the columns related to the i -th user with the entries of the i -th user removed, \mathbf{I}_L is an identity matrix of size $L \times L$. Let

$$\begin{bmatrix} \mathbf{A}_{i,L} & \mathbf{a}_{i,L} \\ \mathbf{a}_{i,L}^T & \mathbf{I}_L \end{bmatrix}^{-1} = \begin{bmatrix} \mathbf{G}_{i,L} & \mathbf{g}_{i,L} \\ \mathbf{g}_{i,L}^T & \mathbf{H}_{i,L} \end{bmatrix} \quad (4.73)$$

According to Lemma (4.3) $\lambda_{max}(\mathbf{H}_{i,L})$ forms a monotonically increasing convergent series as L increases. Thus the value of $\lambda_{max}(\mathbf{H}_{i,\infty})$ can be estimated by $\lambda_{max}(\mathbf{H}_{i,L})$ with a large value of L . This is further illustrated in the numerical section.

From propositions (4.3) and (4.4) it is shown that the squared minimum distance ratio between the system with \mathcal{R} and the system with a set of orthogonal spreading codes is lower and upper bounded, regardless of the kind of trellis code or linear filter \mathcal{D} used.

Proposition 4.5 *If binary channel signals $q_{i,1}, q_{i,2}$ are used, then $d_{min,i}^2 \geq d_{free,i} d_{min,i}^2$ for user i , where $d_{min,i}^2$ is the squared minimum Euclidean distance for a coded system and $d_{free,i}$ is the free distance.*

Proof: A multiuser error event comprises of error events (ie. $\mathbf{X}_i - \hat{\mathbf{X}}_i \neq 0$) or zero sequences ($\mathbf{X}_i - \hat{\mathbf{X}}_i = 0$) of individual users. For binary channel signals, $d_{free,i}$ is the

minimum number of positions for which $x_{p,i} \neq \hat{x}_{p,i}$. For synchronous CDMA systems with $\mathcal{D} = \mathbf{I}$,

$$d_{min,i}^2 = \min_{E \in \mathcal{Z}_i} (\mathbf{X} - \hat{\mathbf{X}})^T \mathcal{R}_m^{m+L} (\mathbf{X} - \hat{\mathbf{X}}) \quad (4.74)$$

$$= \min_{E \in \mathcal{Z}_i} \sum_{p=m}^{m+L} (\mathbf{x}_p - \hat{\mathbf{x}}_p)^T \mathbf{R}(0) (\mathbf{x}_p - \hat{\mathbf{x}}_p) \quad (4.75)$$

Let $\mathbf{x}_p - \hat{\mathbf{x}}_p = \mathbf{e}_p$. Since

$$d_{min,i}^2 = \min_{x_{p,i}, \hat{x}_{p,i}, x_{p,i} \neq \hat{x}_{p,i}} \mathbf{e}_p^T \mathbf{R}(0) \mathbf{e}_p \quad (4.76)$$

we obtain

$$d_{min,i}^2 = \min_{E \in \mathcal{Z}_i} \sum_{p=m}^{m+L} \mathbf{e}_p^T \mathbf{R}(0) \mathbf{e}_p \geq d_{free,i} d_{min,i}^2 \quad (4.78)$$

■

The above proposition indicates that if convolutional codes are used using binary signalling in synchronous multiuser systems, then the minimum distance of user i is no less than the product of $d_{free,i}$ and the corresponding minimum distance of the uncoded system. It also indicates that it may be better (in terms of maximising $d_{min,i}^2$) not to use the same error control code for all users.

4.5 Numerical Results

In this section we highlight numerically some of the propositions claimed. Firstly, we show the convergences of sequences (as $L \rightarrow \infty$): $\lambda_{max}(\mathbf{H}_{i,L})$, $\lambda_{min}(\mathcal{R}_m^{m+L})$ and $\lambda_{max}(\mathcal{R}_m^{m+L})$ in section (4.4.2). We generate 100 sets of \mathcal{R} for a 3-user asynchronous and synchronous systems with binary random spreading codes of length 5. Random spreading code sets have to be discarded due to singularities in the correlation matrix. A singular \mathbf{R} matrix occurs when the terms $\mathbf{F}^{i,i}(0) = 0$ for the k -th interval. In this case the whitening filter does not exist. If $\min(\mathbf{F}^{i,i}(0)) < 0.005$, $i = 1, \dots, K$, then the set is discarded. If the matrices generated were singular then the set was discarded and a new set of random waveforms generated. We present $\lambda_{max}(\mathbf{H}_{i,L})$, $\lambda_{min}(\mathcal{R}_m^{m+L})$ and $\lambda_{max}(\mathcal{R}_m^{m+L})$ as a

function of L for the best and worst cases. The worst cases each satisfy

$$\arg_L \max_{100sets\mathcal{R}} \left\{ \left| \frac{\lambda_{min}(\mathcal{R}_m^{m+L})}{\lambda_{min}(\mathcal{R}_m^{m+100})} - 1 \right| < 0.05 \right\}, \quad (4.79)$$

$$\arg_L \max_{100sets\mathcal{R}} \left\{ \left| \frac{\lambda_{max}(\mathcal{R}_m^{m+L})}{\lambda_{max}(\mathcal{R}_m^{m+100})} - 1 \right| < 0.05 \right\}, \quad (4.80)$$

$$\arg_L \max_{100sets\mathcal{R}} \left\{ \left| \frac{\lambda_{max}(\mathbf{H}_{i,L})}{\lambda_{max}(\mathbf{H}_{i,100})} - 1 \right| < 0.05 \right\} \quad (4.81)$$

and the best cases each satisfy

$$\arg_L \min_{100sets\mathcal{R}} \left\{ \left| \frac{\lambda_{min}(\mathcal{R}_m^{m+L})}{\lambda_{min}(\mathcal{R}_m^{m+100})} - 1 \right| < 0.05 \right\}, \quad (4.82)$$

$$\arg_L \min_{100sets\mathcal{R}} \left\{ \left| \frac{\lambda_{max}(\mathcal{R}_m^{m+L})}{\lambda_{max}(\mathcal{R}_m^{m+100})} - 1 \right| < 0.05 \right\}, \quad (4.83)$$

$$\arg_L \min_{100sets\mathcal{R}} \left\{ \left| \frac{\lambda_{max}(\mathbf{H}_{i,L})}{\lambda_{max}(\mathbf{H}_{i,100})} - 1 \right| < 0.05 \right\} \quad (4.84)$$

where the maximum value of L used is 100. From Figs. 4.7 and 4.8 it can be seen that we can approximate $\lambda_{max}(\mathbf{H}_{i,\infty})$, $\lambda_{min}(\mathcal{R}_m^{m+\infty})$ and $\lambda_{max}(\mathcal{R}_m^{m+\infty})$ by $\lambda_{max}(\mathbf{H}_{i,L})$, $\lambda_{min}(\mathcal{R}_m^{m+L})$ and $\lambda_{max}(\mathcal{R}_m^{m+L})$ with a sufficiently large value of L .

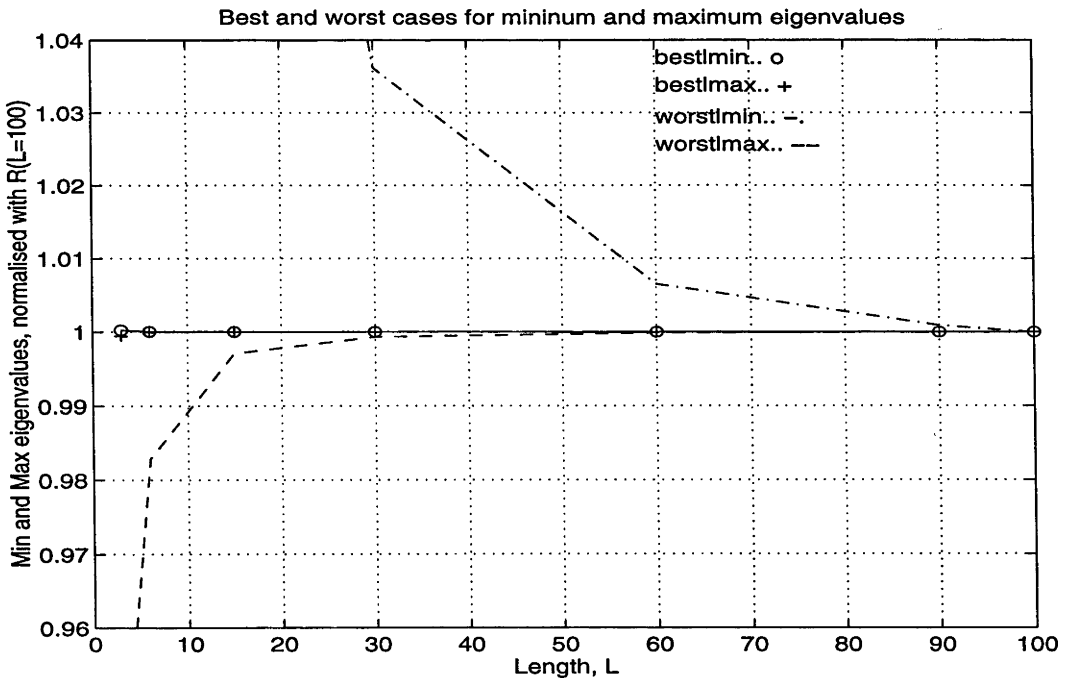


Figure 4.7: $\lambda_{min}(\mathcal{R}_m^{m+L})$ and $\lambda_{max}(\mathcal{R}_m^{m+L})$ as a function of L for the best and worst cases

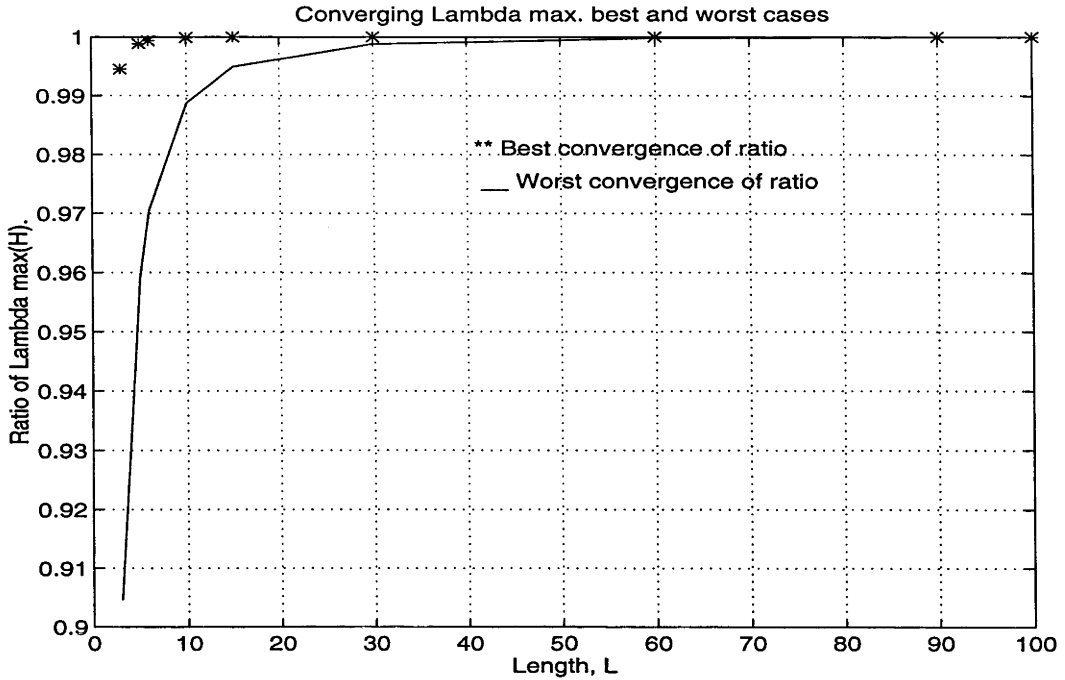


Figure 4.8: $\lambda_{max}(\mathbf{H}_{i,L})$ as a function of L for the best and worst cases

In Fig.4.9 we present the estimated bounds $L = 60$ and the exact value of $\min_{i=1,\dots,K} \eta_i$ where $\mathcal{D} = \mathbf{I}$ and $K = 3$. All users use a rate $1/2$, 4 state convolutional code (generator polynomial (5,7) in octal) to encode the binary data bits. The figure shows that for the 100 \mathcal{R} matrices investigated, the lower bound $\frac{1}{\lambda_{max}(\mathbf{H}_{i,L})}$ is always tighter than that of $\lambda_{min} \mathcal{R}_m^{m+60}$.

It is often an easy task to use the method described in chapter 3 to compute the minimum squared Euclidean distance for an uncoded system even for a large number of users, say 31. However, it has been found that this algorithm does not scale very well for the coded multiuser system. It grows exponential in complexity to compute d_{min}^2 . To illustrate the complexity, a tree search for a simple 2-user system, both users employing rate $2/3$ Ungerboeck 8PSK code requires more than 3 million paths to obtain $\min_{i=1,\dots,K} d_{min,i}^2$. This obstacle is due to the truncation threshold, T set at the minimum distance for the coded single user system (much larger than the corresponding distance of the uncoded system). Note that the tree collapses quickly as the paths have distances exceeding the threshold, T (see Fig. 4.10).

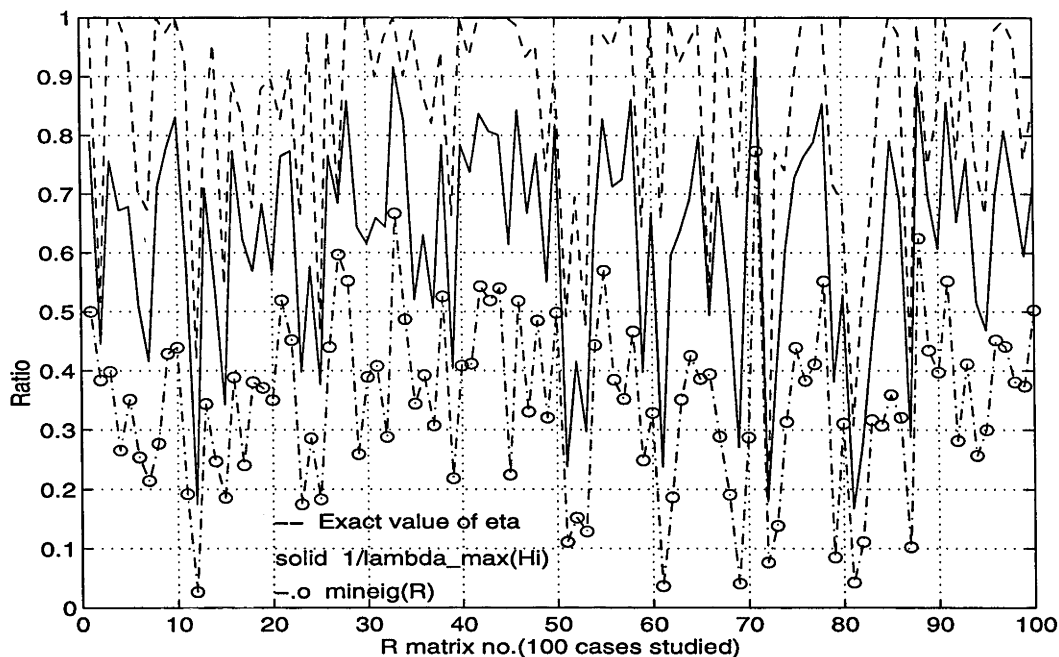


Figure 4.9: Lower bounds and exact values of η_i for 100 sets of \mathcal{R}

4.6 Summary

Several properties of the minimum squared Euclidean distance $d_{min,i}^2$ were presented for a coded multiuser system. Although intuitive, it has been proved that if all users use trellis codes with the same constraint length and the same number of input bits, but different signal mapping sets, then the upper bound of $d_{min,i}^2$ is identical to that of the upper bound of the single user case. This result indicates that a coded multiuser system may recover the minimum distance loss of an uncoded multiuser system due to non-orthogonal spreading (if there is indeed such a loss). We thus introduced a linear processing filter $\mathcal{D} = \mathcal{F}^{-1}$ before the spreading to negate the effects of non-orthogonal spreading. However, in a realistic situation this is not feasible, since the transmitter requires knowledge of the correlation matrix \mathcal{R} .

Motivated we then continued to study the effect of \mathcal{R} on d_{min}^2 . In particular, the ratio of d_{min}^2 between a system with $\mathcal{R} \neq \mathbf{I}$ and $\mathcal{R} = \mathbf{I}$ was investigated. Tight upper and lower bounds using matrix algebra for this ratio η_i were derived for a coded asynchronous system and their rates of convergences proved.

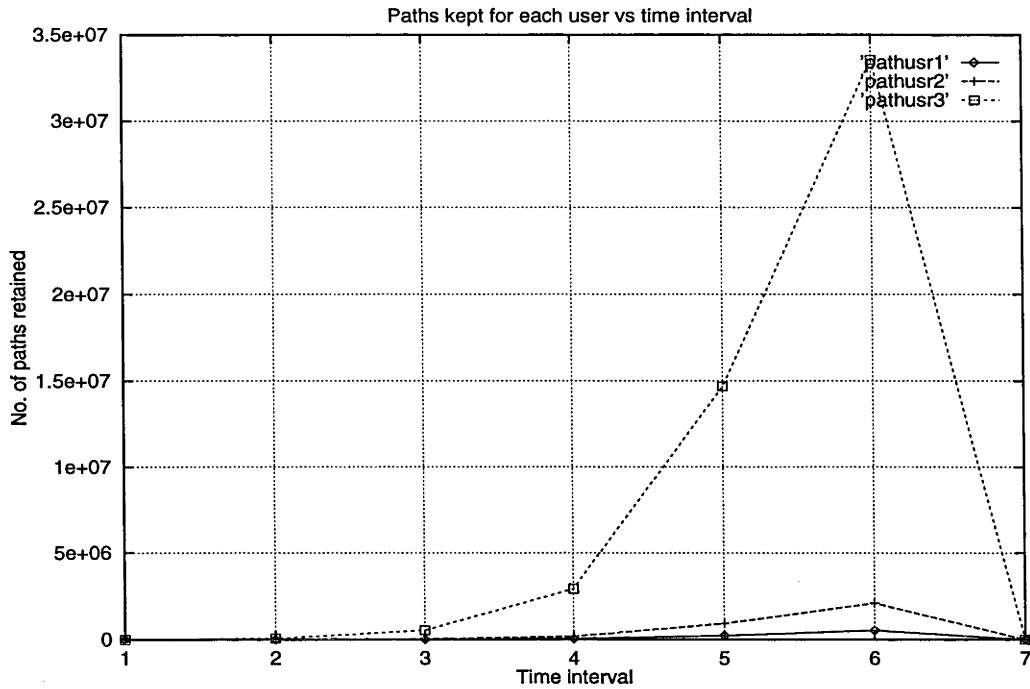


Figure 4.10: Number of paths kept vs time interval

Finally, numerical results were used to illustrate the convergence of the bounds. Approximations were made to estimate η_i for infinite dimensional \mathcal{R} matrices. A note on the computation complexity of minimum distance for a coded multiuser system was made. The algorithm developed in chapter 3 to compute the minimum squared Euclidean distance for an uncoded system has been found not to scale well for a coded system.

PART 2

Multuser Detection for the Time Varying Frequency Selective Channel

OVERVIEW: In the remainder of the thesis, we examine the design and performance of Maximum Likelihood Sequence Detectors (MLSDs) for linearly modulated or DS-CDMA signals sent over time varying, frequency selective Rayleigh fading channels, corrupted by Gaussian noise and multiple access interference. Two optimal multiuser detectors are investigated. One knows *a priori* the time varying channel impulse response, the other, more realistically, knows the channel autocovariance. The computational complexity of these centralised receivers grows exponentially with the number of users. To this end, we propose two additional single user receivers that are linear in complexity with respect to the number of users. The single user receivers take into account the structure of the multiple access interference when making decisions. An analysis of the MLSDs is also provided. We obtain tight bit error probability bounds using a truncated union bounding approach.

The Transmitter, Multipath Channel and Receiver

Overview: In this chapter, we characterize the transmitter, investigate a model for the wireless propagation environment and study the theories and practices of receiver design. We set the stage for the two subsequent chapters by providing a common signal model and an understanding of the need for more advanced receiver structures. The properties of time and frequency selective multipath channels are explained. An appreciation of the problems in mobile communications will be identified to allow the design of more sophisticated receiver architectures.

5.1 Introduction

The wireless channel in mobile communications is difficult to communicate over. When a radio signal is transmitted over a wireless channel, the wave propagates through a physical medium and interacts with physical objects such as buildings, trees, hills and moving vehicles. The propagation of radio waves through this medium is a complicated process that involves diffraction, refraction and multiple reflections. Any attempt to characterise the wireless communication channel must be a reasonably approximate model. In this chapter we capture the time varying dispersive nature of the multipath channel and represent some of its characteristics statistically. This model will then be used in subsequent chapters to design and evaluate the performance of multiuser receivers. Shown in Fig. 5.1 is a diagram of the multiuser communication system, where each user's transmitted signal is convolved with the time-varying channel impulse response $c_k(t, \tau)$.

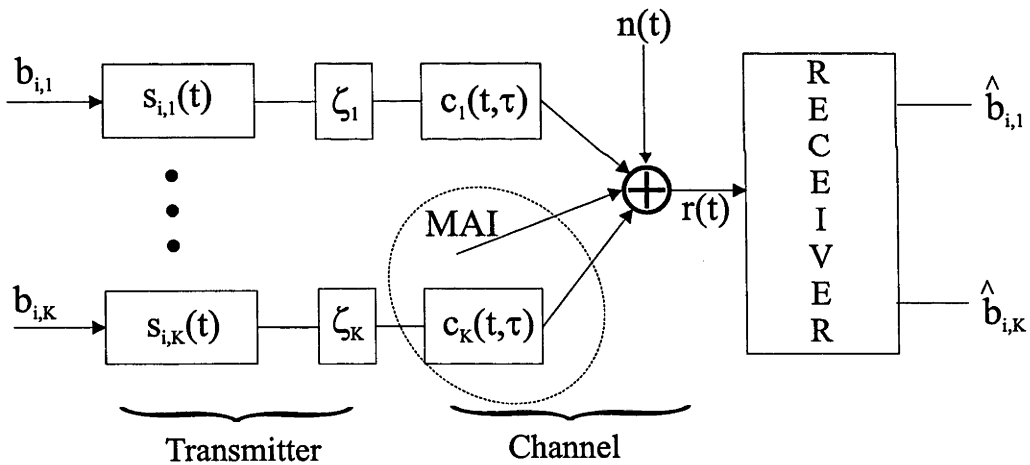


Figure 5.1: Multiuser CDMA communication system

5.2 The Transmitter

The spread spectrum generation process involves two fundamental steps: modulation and spreading. This modulated spread spectrum signal is then upconverted to the desired RF frequency. Each user is allocated the same RF carrier frequency and occupies the same RF bandwidth. In our discussion we assume that the complex baseband sig-

nal is transmitted and received (ie. we bypass upconversion and downconversion). The transmitter design is essentially the same as Part I, however, for the sake of completeness some notations must be reintroduced.

The transmitted signal $a_k(t)$ of the k th user is

$$a_k(t) = \sum_{i=0}^{I-1} b_{i,k} \sqrt{E_k} s_{i,k}(t - iT_s - \zeta_k) \quad (5.1)$$

where $b_{i,k}$ is the k th user's i th transmitted symbol; $\sqrt{E_k}$ is the k th user's transmitted bit energy (different due to power control); I is the data packet length (Note the change in notation from Ω in Part I to I in Part II); T_s is the symbol duration and ζ_k is the time delay of the k th user due to asynchronism. The data bits are combined into M -ary digits taken from an M -ary alphabet, then mapped either directly or with differential phase to the constellation points $b_{i,k}$. In CDMA signals, $b_{i,k}$ is usually taken from the binary constellation $\{+1, -1\}$. The data bits from all users are arranged in a $I \times K$ matrix \mathbf{B} such that $(\mathbf{B})_{i,k} = b_{i,k}$. $s_{i,k}(t)$ is either the k th user's unit energy signature waveform with DS-CDMA or every user's pulse shape with linear modulations (taking into account all transmitter filtering). In long code DS-CDMA signals (like IS-95) the signature sequence effectively changes every transmitted symbol. For linearly modulated or short code CDMA signals, $s_{i,k}(t) = s_k(t)$. We also introduce T_c as the duration of a chip, and N as the number of chips per symbol period (so $NT_c = T_s$ and $N = 1$ for linearly modulated signals).

Chip pulse shaping is important in asynchronous transmissions since it directly affects the amount of interchip or intersymbol interference in the received signal. In our investigations, each chip used a root raised cosine chip pulse shape truncated to 1.5 chip periods with 30% excess bandwidth. Bandwidth efficient pulses such as the raised cosine pulse,

$$h_p(t) = \frac{\sin \pi t / T_c \cos \chi \pi t / T_c}{\pi t / T_c \sqrt{1 - 4\chi^2 t^2 / T_c^2}} \quad (5.2)$$

and the square root raised cosine pulse,

$$h_p(t) = \frac{1-\chi}{T_c} \text{sinc}\left(\frac{(1-\chi)t}{T_c}\right) + \frac{\chi}{T_c} \text{sinc}\left(\frac{\chi t}{T_c} + \frac{1}{4}\right) \cos\left(\frac{\pi t}{T_c} + \frac{\pi}{4}\right) + \frac{\chi}{T_c} \text{sinc}\left(\frac{\chi t}{T_c} - \frac{1}{4}\right) \cos\left(\frac{\pi t}{T_c} - \frac{\pi}{4}\right) \quad (5.3)$$

are often used. χ is the excess bandwidth, $0 \leq \chi \leq 1$, so the one sided bandwidth of both pulses is $\frac{1+\chi}{2T_c}$. Shown in Figs. 5.2 and 5.3 are some typical pulse shapes in the time and frequency domains. The pulses were truncated to 50 chip periods.

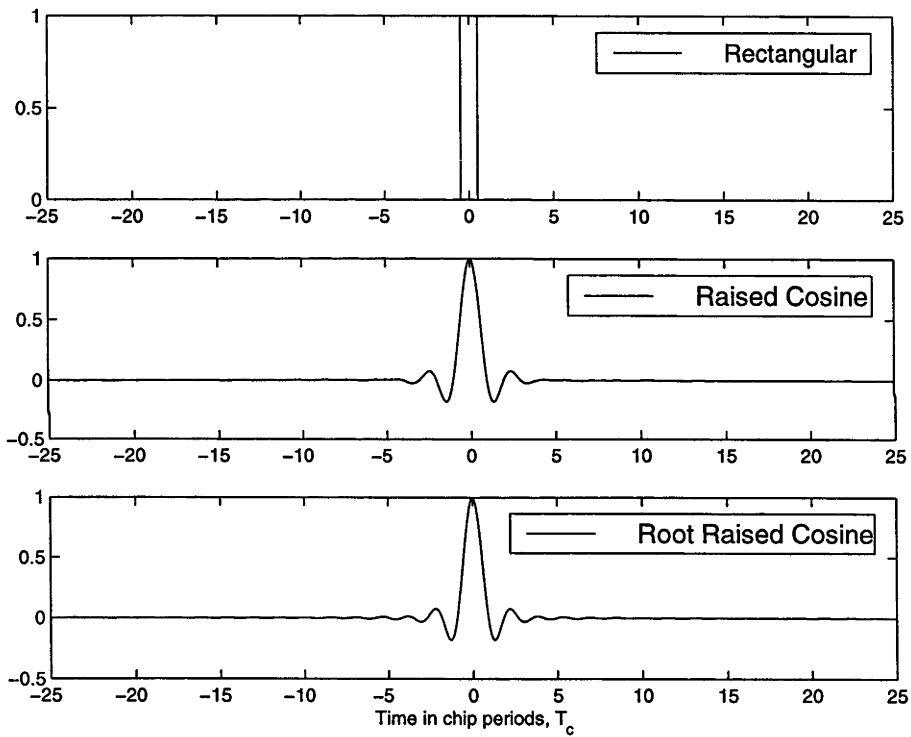


Figure 5.2: Chip waveforms in time domain, $\chi = 0.3$ for cosine and root raised cosine

5.3 Radio Propagation and Mother Nature

In this section we consider an asynchronous multiple access channel shared by multiple users whose signals are subject to a time varying frequency selective Rayleigh fading channel and additive white Gaussian noise. Fig. 5.4 shows a typical wireless communication environment. A typical model of land mobile radio consists of an elevated

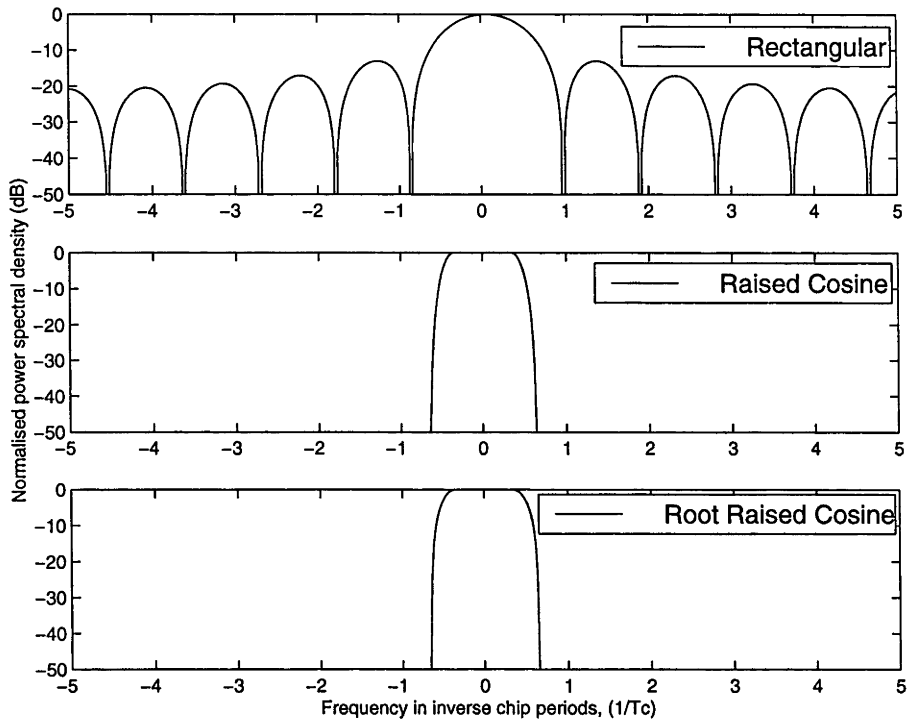


Figure 5.3: Chip waveforms in frequency domain

base-station antenna, a line of sight (LOS) propagation path, many non LOS propagation paths and a mobile antenna mounted on the vehicle or the portable unit. The situation of more than one propagation path is referred to as *multipath propagation*. Because of natural and man-made structures located between the mobile receiver and the base station, a direct LOS may not exist. The mechanisms which govern the propagation of the non LOS paths are complex and diverse, and that they can in general be attributed to three basic propagation mechanisms: reflection, diffraction and scattering. Reflection occurs when the electromagnetic wave impinges upon an obstruction with dimensions very large compared to the wavelength of the radio wave. Reflections are caused by the surface of the earth and from buildings. Diffraction occurs when the radio paths between the transmitter and receiver is completely obstructed by an impenetrable body. It explains how radio waves can travel without a LOS path and is often called “shadowing”. Scattering occurs when the radio channel contains objects with dimensions that are on the order of the wavelength or less of the propagating wave. Scattering causes energy from the transmitter to be reradiated in many different directions. For example if a mobile is at street level without a LOS path to the base station, diffraction and scattering are most

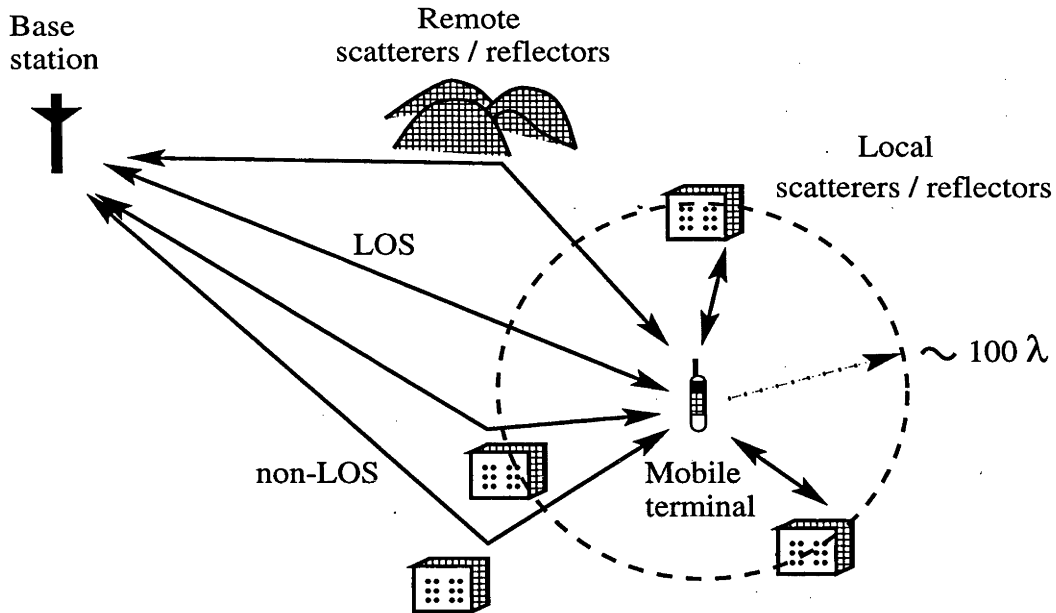


Figure 5.4: The Mobile communications environment

likely to dominate the propagation. As each propagating signal traverses a different path from its source to destination, not all signals arrive at the receiver exactly at the same time instant. When the difference is small with respect to the chip period, the only effect is a change in carrier phase. The complex gains of the multipaths may add constructively or destructively, leading to amplitude fading (Rayleigh or Rician). When the difference is comparable to the chip period the path time delays are described by the concept of *delay spread*. Since the carrier phase changes completely every carrier wavelength, the vector sum of the multiple paths' gains changes rapidly over short distances. Thus slight movements in either the receiver or its surroundings cause a time varying complex gain. The rate of variation of this is described as *Doppler spread*. In general, the multipath channel can be characterised as time varying and dispersive.

5.4 Channel - Linear Time Varying Filter

A time-varying multipath communication channel can be modelled as a linear time varying filter. Its applications in the characterising communication channels were studied in the late 1950's and 1960's by Bello [14]. His work, including dual theory [86] and the wide-sense stationary uncorrelated scattering (WSSUS) model, is part of the foundation

of today's channel measurement and modelling techniques. In the CDMA context, each user is characterised by its own channel $c_k(t, \tau)$. For convenience we examine just one user and thus drop the dependency on k .

A linear time varying filter can be represented by its impulse response $c(t, \tau)$. $c(t, \tau)$ is defined as the response measured at time t to a unit impulse applied at time $t - \tau$. For an input signal $x(t)$, the filter output $y(t)$ can be expressed by the convolution of $x(t)$ and $c(t, \tau)$, as

$$y(t) = \int_{-\infty}^{\infty} c(t, \tau) x(t - \tau) d\tau \quad (5.4)$$

This applies to all linear time varying linear channels, such as the telephone channel, the optical fibre channel and most importantly the mobile radio channel. Bello named $c(t, \tau)$ the Input Delay-Spread Function. The response of the time varying system can also be studied in the frequency domain. For the two time variables, there are two corresponding or dual frequency variables, namely

$$\tau \leftrightarrow f, \text{ and } t \leftrightarrow \nu,$$

where ν is the Doppler shift and f is the transfer function frequency. By performing Fourier transforms on each of the time domain variables we can obtain the dual functions. The time varying frequency response $C(t, f)$ is the Fourier transform in the τ domain of $c(t, \tau)$, as

$$C(t, f) = \int_{-\infty}^{\infty} c(t, \tau) \exp(-j2\pi f\tau) d\tau \quad (5.5)$$

The Doppler-delay spread function is defined by

$$S(\nu, \tau) = \int_{-\infty}^{\infty} c(t, \tau) \exp(-j2\pi\nu t) dt \quad (5.6)$$

The spread function has a clear physical meaning. It is the response of the network to a input $\exp(j2\pi\nu t)$ divided by $\exp(j2\pi\nu t)$. The impulse response can be obtained by the

inverse Fourier transform

$$c(t, \tau) = \int_{-\infty}^{\infty} S(\nu, \tau) \exp(j2\pi\nu t) d\nu \quad (5.7)$$

5.5 Channel - Random Time Varying Filter

Since $c(t, \tau)$ is difficult to estimate precisely and due to the complex scattering typical of the mobile communication channel, it is appropriate to model $c(t, \tau)$ by a random time-varying filter. Thus the behaviour of $c(t, \tau)$ is determined completely by its probability densities at all times t and for all impulse excitation delays τ_i . The ensemble mean of $c(t, \tau)$ is defined as

$$\mu_c(t, \tau) = E\{c(t, \tau)\} \approx \int_{-\infty}^{\infty} \int_{-\infty}^{\infty} c(t, \tau) p_{c(t, \tau)}(c(t, \tau)) dt d\tau \quad (5.8)$$

where $p_{c(t, \tau)}(c(t, \tau))$ is the probability density of $c(t, \tau)$ for any given τ and t . The auto-correlation function is defined as

$$\begin{aligned} R_c(t, t'; \tau, \tau') &= \frac{1}{2} E\{c(t, \tau) c^*(t', \tau')\} \\ &= \int_{-\infty}^{\infty} \int_{-\infty}^{\infty} \int_{-\infty}^{\infty} \int_{-\infty}^{\infty} c(t, \tau) c^*(t', \tau') p_{c(t, \tau) c^*(t', \tau')}(t, t', \tau, \tau') dt dt' d\tau d\tau' \end{aligned} \quad (5.9)$$

where $'^*$ denotes complex conjugation and $f_{c(t, \tau) c^*(t', \tau')}(t, t', \tau, \tau')$ denotes the joint probability density function for all pairs of $c(t, \tau)$ and $c^*(t', \tau')$.

5.6 Complex Gaussian Distributions

The envelope of a complex Gaussian random variable, z is $|z| = \sqrt{z_R^2 + z_I^2}$ and the phase is $\tan^{-1}(z_I/z_R)$. When the random variable z is zero-mean, the phase is uniformly distributed and the envelope is Rayleigh distributed.

$$p(z) = \frac{2z}{\sigma_z^2} \exp\left(-\frac{z^2}{\sigma_z^2}\right), z \geq 0 \quad (5.10)$$

where $\sigma_z^2 = E(z^2)$. If the channel has a non-zero mean, then the channel envelope has a Rician distribution.

Given a length n vector of samples, \mathbf{Z} from a complex Gaussian random process with mean $E(\mathbf{Z})$, the multivariate pdf equals

$$p(\mathbf{Z}) = \frac{1}{(2\pi)^n \det |\mathbf{R}_{\mathbf{Z}\mathbf{Z}}|} \exp\left(-\frac{1}{2}(\mathbf{Z} - E(\mathbf{Z}))^H \mathbf{R}_{\mathbf{Z}\mathbf{Z}}^{-1} (\mathbf{Z} - E(\mathbf{Z}))\right) \quad (5.11)$$

where the $n \times n$ autocovariance matrix is given by

$$\mathbf{R}_{\mathbf{Z}\mathbf{Z}} = \frac{1}{2} E \left((\mathbf{Z} - E(\mathbf{Z})) (\mathbf{Z} - E(\mathbf{Z}))^H \right) \quad (5.12)$$

This result (5.11) is a special case (ie. when the covariance matrix of the real and imaginary parts are equal) of a more general result. For the sake of completeness, we now state this general result [81]. Given a length n vector of samples $\mathbf{Z}' = \mathbf{X} + j\mathbf{Y} = [z_1, \dots, z_n]$, $z_i = x_i + jy_i$ from a complex Gaussian random process, the joint density is given by

$$p(\mathbf{Z}') = p(x_1, \dots, x_n, y_1, \dots, y_n) \quad (5.13)$$

$$p(\mathbf{Z}') = \frac{1}{\sqrt{(2\pi)^n \det |D|}} \exp\left\{-\frac{1}{2} \mathbf{Z}' D^{-1} \mathbf{Z}'^H\right\} \quad (5.14)$$

This function is an exponential in terms of the $2n$ by $2n$ matrix, D where

$$D = \begin{bmatrix} \mathbf{R}_{\mathbf{X}\mathbf{X}} & \mathbf{R}_{\mathbf{X}\mathbf{Y}} \\ \mathbf{R}_{\mathbf{Y}\mathbf{X}} & \mathbf{R}_{\mathbf{Y}\mathbf{Y}} \end{bmatrix} \quad (5.15)$$

consisting of the $2n + n^2$ real parameters $\mathbf{R}_{\mathbf{X}\mathbf{X}} = E\{\mathbf{x}_i \mathbf{x}_j\}$, $\mathbf{R}_{\mathbf{Y}\mathbf{Y}} = E\{\mathbf{y}_i \mathbf{y}_j\}$ and $\mathbf{R}_{\mathbf{X}\mathbf{Y}} = E\{\mathbf{x}_i \mathbf{y}_j\}$. The covariance matrix of the complex vector \mathbf{Z}' is an n by n Hermitian matrix

$$\mathbf{R}_{\mathbf{Z}\mathbf{Z}} = \mathbf{R}_{\mathbf{X}\mathbf{X}} + \mathbf{R}_{\mathbf{Y}\mathbf{Y}} - j(\mathbf{R}_{\mathbf{X}\mathbf{Y}} - \mathbf{R}_{\mathbf{Y}\mathbf{X}}) \quad (5.16)$$

If the vectors \mathbf{X} and \mathbf{Y} are such that $\mathbf{R}_{\mathbf{X}\mathbf{X}} = \mathbf{R}_{\mathbf{Y}\mathbf{Y}}$ and $\mathbf{R}_{\mathbf{X}\mathbf{Y}} = -\mathbf{R}_{\mathbf{Y}\mathbf{X}}$ then the joint density is given by (5.11).

5.7 Wide Sense Stationary Uncorrelated Scattering (WSSUS)

When the system is said to have the property of being wide-sense stationary (WSS), the mean $\mu_c(t, \tau)$ and the correlation function $R_c(t, t'; \tau, \tau')$ depend on time differences only, not absolute times, as

$$\mu_c(t, \tau) = \mu_c(\tau) \quad (5.17)$$

$$R_c(t, t'; \tau, \tau') = R_c(t - t'; \tau, \tau') \quad (5.18)$$

This is a good model for wireless communications as the channel is approximately WSS for long intervals (COST 207).

If the channel's responses at different delays τ are uncorrelated, the system is said to be uncorrelated scattered (US). Physically it means that rays at different delays traverse such different routes and are scattered by such different scatterers that the responses at different delays are uncorrelated.

$$R_c(t, t'; \tau, \tau') = R_c(t, t'; \tau) \delta(\tau - \tau') \quad (5.19)$$

Wide sense stationary uncorrelated scattering (WSSUS) is when both the WSS and US conditions are satisfied. This is the simplest statistical model that still has enough degrees of freedom to model practical channels accurately.

$$R_c(t, t'; \tau, \tau') = R(\Delta t, \tau) \delta(\tau - \tau') \quad (5.20)$$

where $R(\Delta t, \tau)$ is the autocorrelation in time of each tap τ .

5.8 Delay Spread and Doppler Spread

In a realistic multipath environment, there can be many paths and they can arrive at different, sometimes long, delays. These components form a delay power profile. The extent of the power delay profile is called the delay spread, τ .

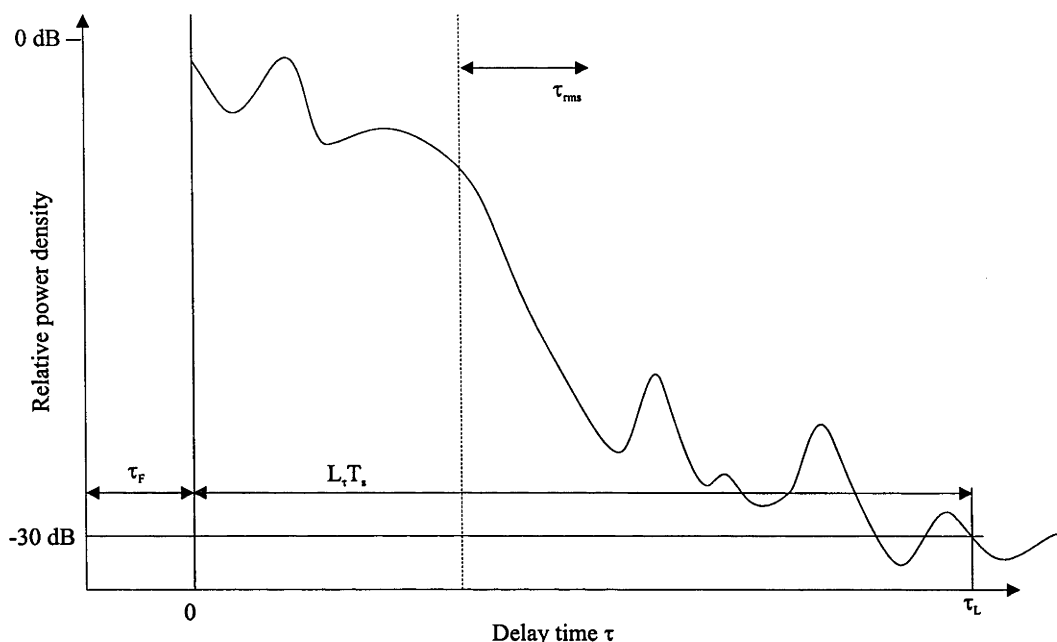


Figure 5.5: Typical delay power profile, τ_F = first arrival delay, τ_{rms} = rms delay, $L_\tau T_s = \tau_L - \tau_F$ maximum excess delay, τ_L = final arrival delay

The root-mean-square delay is normally used as a measure of delay spread, τ_{rms} . It is the delay standard deviation. The ratio τ_{rms}/T_c is an important measure of the channel's frequency selectivity. For $\tau_{rms}/T_c = 0$, the channel is frequency flat. The larger the delay spread the more severe the dispersion of the transmitted signal. In general, receiver complexity increases for increasing τ . Although τ_{rms} is a useful parameter to characterise the channel, the total delay spread, $L_\tau T_s$ is more important for MLSD receiver design. Note that τ_F may also be viewed as the asynchronism between users ζ_k .

The Fourier transform of the tap autocovariance $R(\Delta t, \tau)$ with respect to Δt is the Doppler spectrum,

$$S_{tt}(f, \tau) = \int_{-\infty}^{\infty} R(\Delta t, \tau) \exp(-j2\pi f \Delta t) d(\Delta t). \tag{5.21}$$

Doppler spread captures the rate of variation of the channel. Even the smallest movement causes time varying multipath, and thus randomly time varying signal reception. For example, if a carrier wave (an unmodulated sinusoidal tone) of frequency f_x is transmitted, then because of Doppler spread f_D , we receive a smeared signal spectrum with spectral

components between $f_x - f_D$ and $f_x + f_D$. The amount of “smearing” is characterised by a dimensionless quantity $f_D T_s$. When $f_D T_s = 0$, the channel is time-invariant. For higher values of $f_D T_s$, the fading is often labelled “fast” or “slow”. There are no precise definitions of these, and the most workable definition is that a channel is considered fast fading if a receiver designed for a slow fading channel is limited by the fading rate rather than the noise in its operating region. It is however, generally accepted for frequency flat channels that when $f_D T_s < 0.01$, the fading is considered slow (ie. the fading process remains relatively constant over a few symbol intervals), and when $f_D T_s > 0.1$, the fading process is known as fast fading.

5.9 Discrete Delay and Discrete Time Channel Modelling

Physically, (5.4) represents a transversal filter, where each value of τ indexes a tap with a time varying gain $c(t, \tau)$ and the outputs are summed together. The tap positions and gains are functions of time. For a discrete multipath channel with P paths, the complex baseband channel output is

$$y(t) = \sum_{i=0}^{P-1} c_i(t)x(t - \tau_i) \quad (5.22)$$

The channel impulse response is thus

$$c(t, \tau) = \sum_{i=0}^{P-1} c_i(t)\delta(\tau - \tau_i) \quad (5.23)$$

and is shown diagrammatically in Fig. 5.6. There are two types of limitations involved with a channel. One is associated with the physical limitation of the channel itself such as its delay spread and its rate of change reflected in the maximum delay L_τ and maximum Doppler shift f_D . The second type of limitation comes from the interaction of the channel with the signal, and is due to the latter’s bandwidth and duration. Limited bandwidth is precisely the condition required by the time sampling theorem. For example, if the complex baseband input signal $x(t)$ is bandlimited, that is

$$X(f) = 0, |f| > f_x \quad (5.24)$$

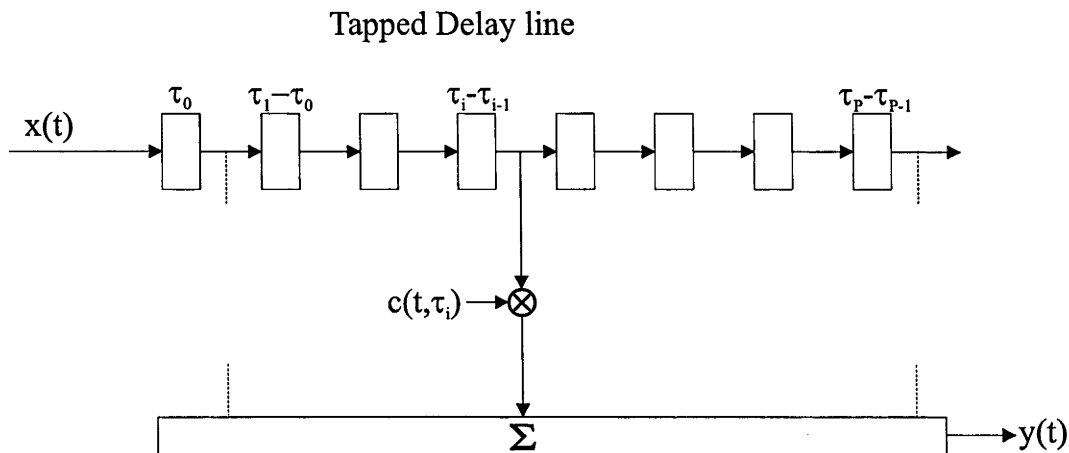


Figure 5.6: Channel impulse response represented as a tapped delay line

where $X(f)$ is the Fourier transform of $x(t)$, then the time sampling theorem states that

$$x(t) = \sum_{i=-\infty}^{\infty} x(iT_s) \text{sinc}(t/T_s - i) \tag{5.25}$$

if the sampling rate $f_s = 1/T_s$ satisfies

$$f_s \geq 2f_x \tag{5.26}$$

The frequency $2f_x$ is known as the Nyquist rate. In practice the transmitted signal $x(t)$ is bandlimited due to regulatory authorities imposing laws to reduce interference spill-over from adjacent frequency bands.

$$x(t) = \int_{-f_x}^{f_x} X(f) \exp(j2\pi ft) df \tag{5.27}$$

The Doppler spread is limited due to the finite speeds of the transmitters, receivers and scatterers. The channel tap processes are therefore bandlimited, and is restricted to $-f_D \cdots f_D$ Hz.

$$c(t, \tau) = \int_{-f_D}^{f_D} S(\nu, \tau) \exp(j2\pi \nu t) d\nu \tag{5.28}$$

Therefore, the received signal $y(t)$ is given by,

$$y(t) = \int x(t - \tau)c(t, \tau)d\tau \quad (5.29)$$

$$= \int_{-\infty}^{\infty} \int_{-f_x}^{f_x} \int_{-f_D}^{f_D} X(f) \exp(j2\pi f(t - \tau))df S(\nu, \tau) \exp(j2\pi\nu t)d\nu \quad (5.30)$$

$$= \int_{-f_x}^{f_x} \int_{-f_D}^{f_D} \exp(j2\pi(f + \nu)t) \int_{-\infty}^{\infty} X(f)S(\nu, \tau) \exp(-j2\pi f\tau)d\tau df d\nu \quad (5.31)$$

The inner integral in (5.31) is independent of time, so $y(t)$ is a weighted sum of complex exponentials with limited bandwidth due to the integral limits. $y(t)$ is thus bandlimited and is sampled at T_c/r sec, where the number of samples per chip, r , is made large enough to satisfy the signal's Nyquist rate. It can be readily seen from (5.31) that the received signal can now be represented completely if the sampling rate satisfies the following condition,

$$\frac{T_c}{r} < \frac{1}{2(f_x + f_D)} \quad (5.32)$$

5.10 Simulating the Channel

In our investigations, we adopt the simple P -path channel model,

$$c(t, \tau) = \sum_{i=0}^{P-1} c_i(t)\delta(\tau - \tau_i) \quad (5.33)$$

$$= \begin{cases} \sum_{i=0}^{P-1} c_i(t)\delta(\tau - \frac{i\tau}{P-1}), & P > 0 \\ c(t), & P = 0 \end{cases} \quad (5.34)$$

where the P paths have uniformly spaced delays and uniformly distributed mean powers, $E\{|c_i(t)|^2\} = \frac{1}{P}$ and the $c_i(t)$ are mutually independent, circularly symmetric correlated complex Gaussian (ie. Rayleigh fading) random processes. Therefore, the received

signal is given by

$$y(t) = \int_{-\infty}^{\infty} x(t - \tau)c(t, \tau)d\tau \quad (5.35)$$

$$= \begin{cases} \sum_{i=0}^{P-1} x(t - \frac{i\tau}{P-1})c_i(t), P \geq 2 \\ x(t)c_i(t), P = 1 \end{cases} \quad (5.36)$$

By convolving the delay with the transmitted pulse shape, the transmitter can generate P uniformly delayed versions of the transmitted signal at arbitrary delays without increasing the sampling rate. The individual tap processes, $c_i(t)$, are obtained by passing white Gaussian noise through a filter with impulse response [120],

$$g_l = \begin{cases} \frac{J_{\frac{1}{4}}(2\pi l f_D T_r)}{(|l|T_r)^{1/4}}, l \neq 0 \\ \frac{(\pi f_D)^{1/4}}{\Gamma(5/4)}, l = 0 \end{cases} \quad (5.37)$$

However, it is common in the literature to use $J_0(2\pi l f_D T_r)$ (Jake's model) where $J_0(\cdot)$ is a Bessel function of the first kind of order 0.

By windowing this infinite impulse response with a Hanning window, the filter's complexity can be restricted while ensuring that the fading process still evolves smoothly. An impulse response that does not taper to zero at its ends generates a fading process with an unpredictable fine structure [47]. Shown below are typical amplitude and phase variations of one tap of a fading process. Fig. 5.7 plots a sample fading process with time as a parameter. Any signal transmitted through the channel is dynamically distorted by this process. Hence, the signal strength drops substantially at certain times when the signal enters a deep fade. The smooth evolution of this process, a property of its bandlimit-edness, makes it easy to predict the channel. In Chapter 7, we depend on this property to design a multiuser receiver. The amplitude variation is shown in Fig. 5.8. Note that deep nulls occur frequently. In Fig. 5.9 the phase variation vs time is shown. Detection of a phase encoded signals becomes difficult in the vicinity of a deep fade, as rapid phase shifts occur. These large and abrupt changes can cause tracking and estimation errors. Finally, the power spectral density of a windowed and truncated fading process is shown.

The U-shaped Doppler spectrum is given as

$$S_{tt}(f) = \begin{cases} \frac{1}{\pi f_D \sqrt{1-(f/f_D)^2}} & |f| \leq f_D \\ 0 & \text{otherwise} \end{cases} \quad (5.38)$$

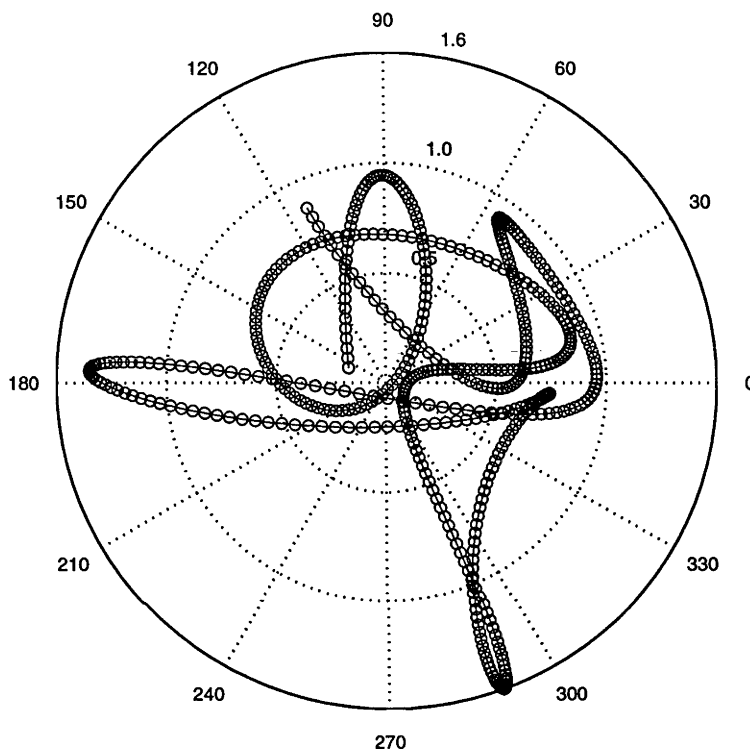


Figure 5.7: Polar plot of a fading process generated by filtering complex white noise by the truncated and windowed impulse response of (5.37). This process evolves smoothly.

5.11 The Time and Frequency Selective Channel

This channel is the most general of all linear channels. A sample of the transfer function (5.5) is plotted in Fig. 5.11. The channel distorts any transmitted signal in both time and frequency. The distortion has to be estimated by the receiver, for reliable detection of data. Essentially it means tracking the channel to see how it evolves with time and frequency/delay. The use of pilot tones or symbols are often sent together with the transmitted data to “probe” the channel.

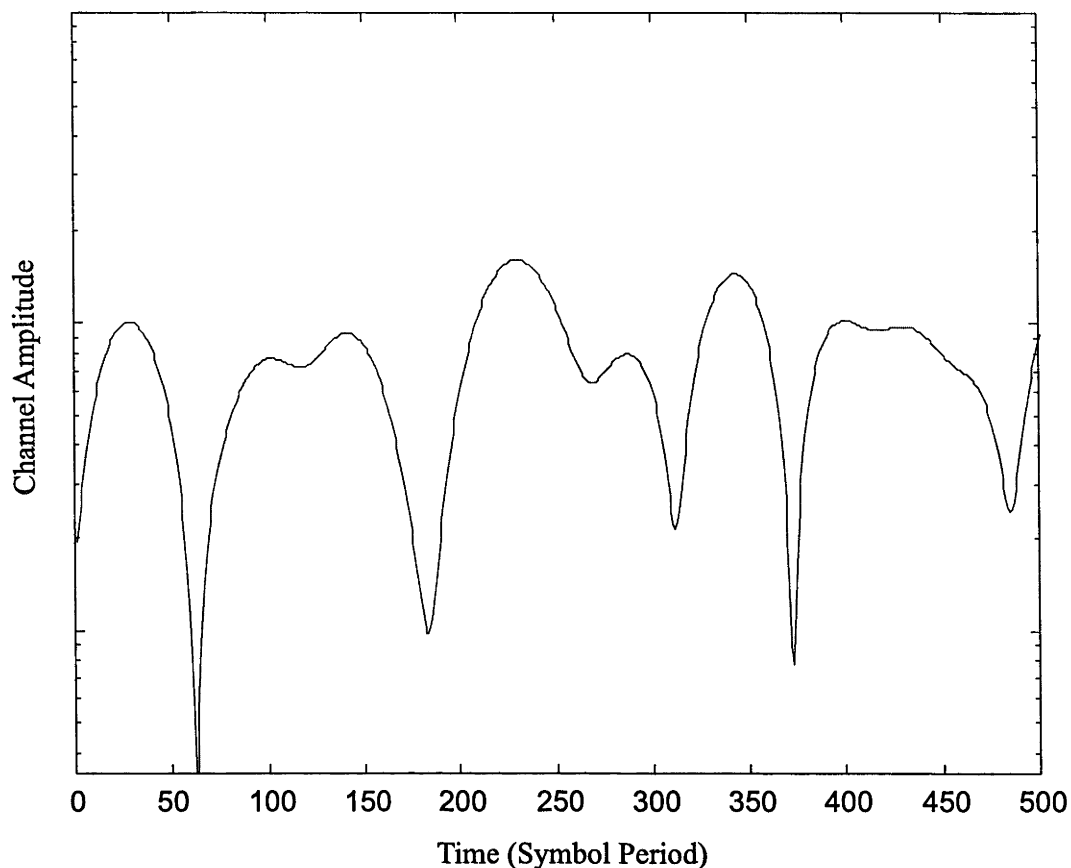


Figure 5.8: Logarithmic plot of fading amplitude vs time

5.12 The Time Selective Channel

This is a special case of the more general channel model, $c(t, \tau)$ where

$$c(t, \tau) = c(t)\delta(\tau) \quad (5.39)$$

The time selective channel (see Fig. 5.14) is fading in time but frequency flat. The transfer function $C(t, f)$ can be simplified to

$$C(t, f) = c(t) \quad (5.40)$$

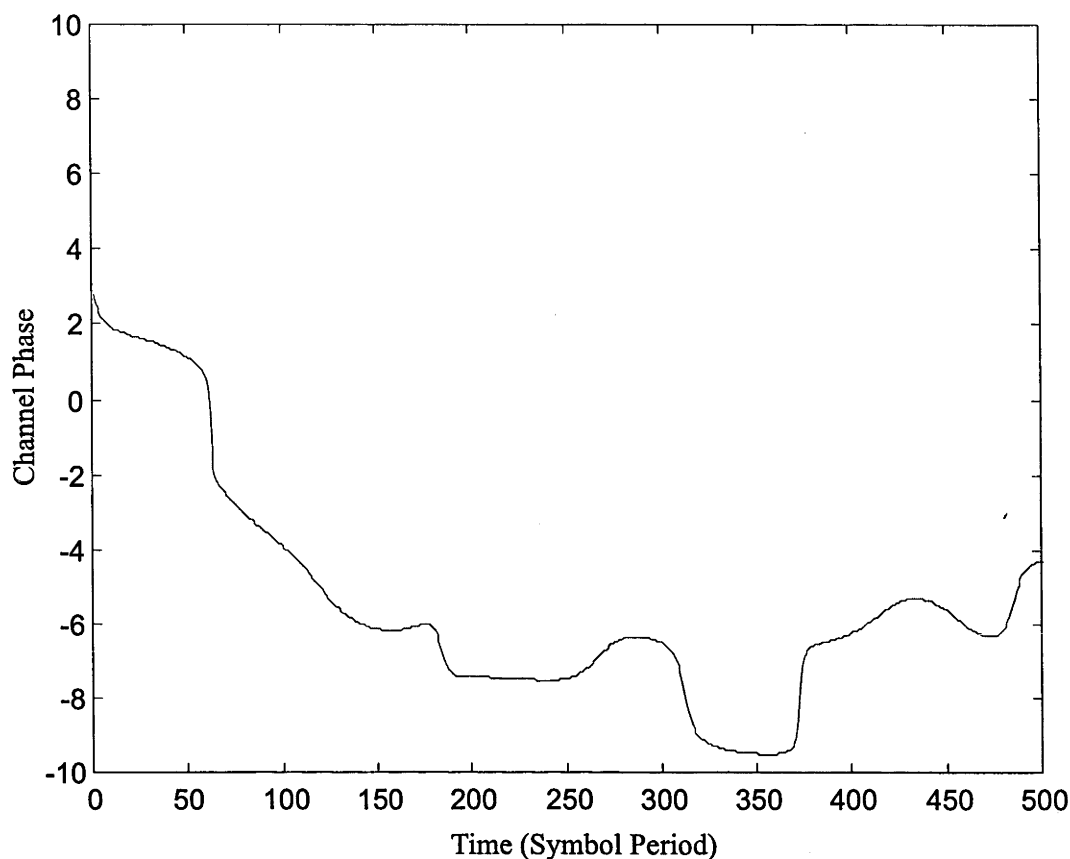


Figure 5.9: Plot of channel tap phase (radians) vs time. Large phase shifts occur during deep fades

The received signal is thus a scaling of the transmitted signal by a time varying random process, as

$$y(t) = x(t)c(t) \quad (5.41)$$

In this case the received signal appears to arrive at the receiver via a single fading path.

5.13 The Frequency Selective Channel

In high rate communications, the path length differences, d divided by the speed of light, c are comparable to the symbol period ($d/c \sim T_s$). If the scatterers and the mobile receiver are moving very slowly, the channel is said to be time invariant. Gathering these ideas

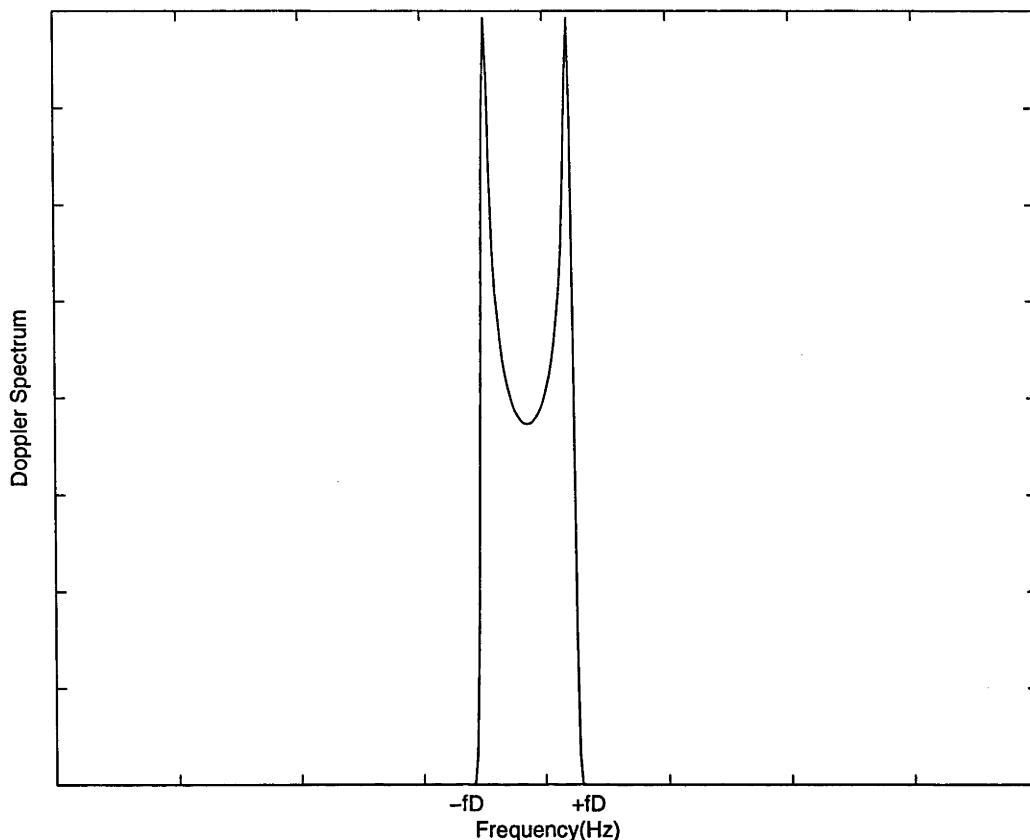


Figure 5.10: Power spectral density of a sample windowed and truncated fading process

together, we can say that the channel is fading in frequency but time invariant. The transfer function can be simplified to

$$C(t, f) = C(0, f) = \int_{-\infty}^{\infty} c(0, \tau) \exp(-j2\pi f\tau) d\tau \quad (5.42)$$

The received signal is thus the convolution of the transmitted signal and the channel's impulse response (now a linear time invariant filter). This is shown in Fig. 5.13.

5.14 The Receiver Front End

The transmitted signal distorted by the channel and corrupted by multiuser interference, additive white Gaussian noise finally arrives at the receiver. The receiver then has the job of deciding which data was originally transmitted based on all the information it

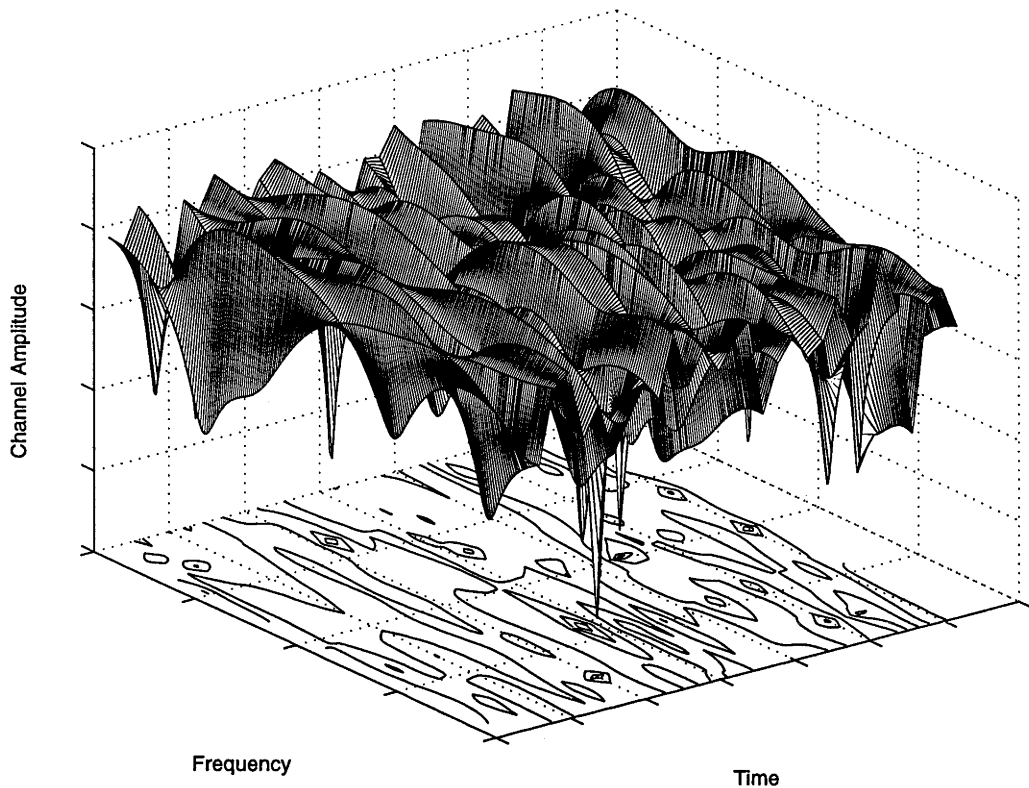


Figure 5.11: Plot of the amplitude of the time and frequency selective channel's amplitude transfer function as a function of time and frequency

has. First, however, it must perform carrier recovery, phase recovery, timing recovery and sample the signal without loss of information. For our purposes the first three are assumed to have been recovered perfectly, and we concentrate on the last. The receiver front end comprises a noise limiting filter followed by a sampler. Fig. 5.15 shows a typical receiver front end. The filter is designed such that the Doppler spread received signal is negligibly distorted. Samples are taken every $T_r = T_c/r$ such that there are $r \geq 1$ samples per chip period, where r is chosen large enough such that the filtered signal is negligibly aliased. With these constraints, negligible information is lost during filtering and sampling, and the received signal can be written in discrete form. The received samples are stored in the vector \mathbf{y} .

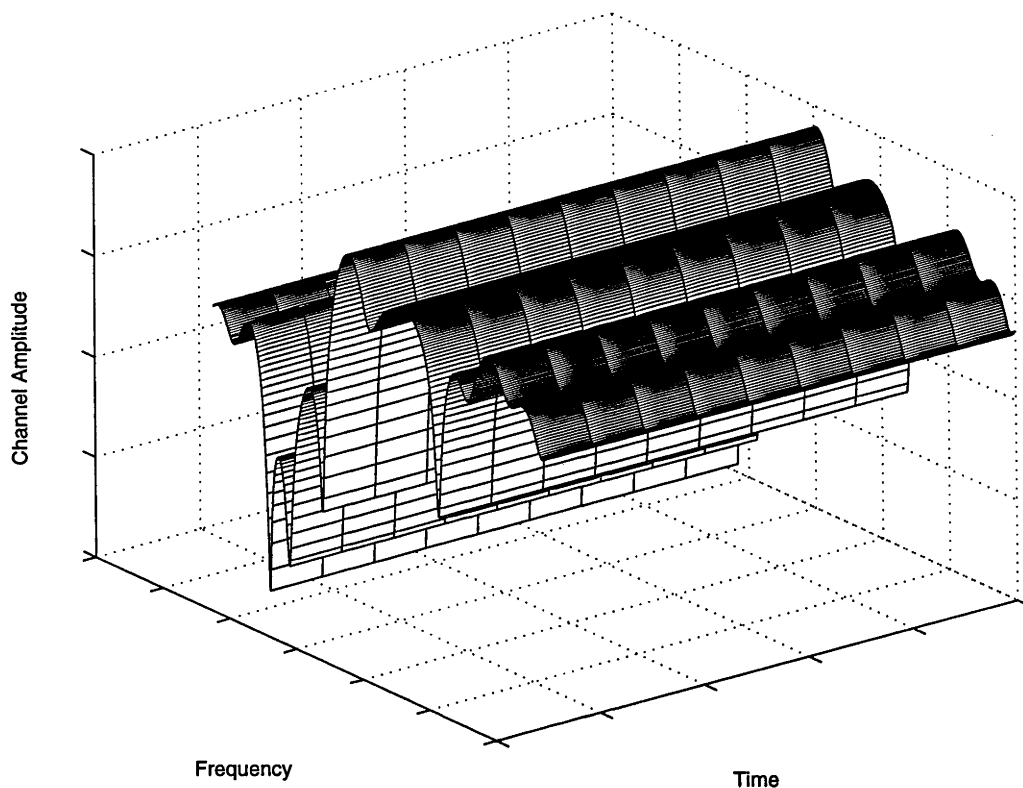


Figure 5.12: Plot of the amplitude of the time selective channel's transfer function as a function of time and frequency

5.15 Received Signal Model

Each sample is the cumulative signal of all users

$$y_m = \sum_{k=1}^K \int_{-\infty}^{\infty} a_k(mT_r - \tau) c_k(mT_r, \tau) d\tau + n_m \quad (5.43)$$

$$= \sum_{k=1}^K \sum_{i=0}^{I-1} b_{i,k} \sqrt{E_k} \int_{-\infty}^{\infty} s_{i,k}((m - irN)T_r - \zeta_k - \tau) c_k(mT_r, \tau) d\tau + n_m \quad (5.44)$$

where K is the number of users; n_m is a low pass sample of a zero mean additive white Gaussian bandpass noise process with two sided bandpass noise spectral density, $\frac{N_0}{2}$. $c_k(t, \tau)$ denotes the k th user's channel impulse response at time t to an impulse at time $t - \tau$. Alternatively, as in section 5.9, the channel can be visualised as a densely tapped transversal filter, where the taps are index by τ and $c_k(t, \tau)$ is the time varying random complex gain at that delay.

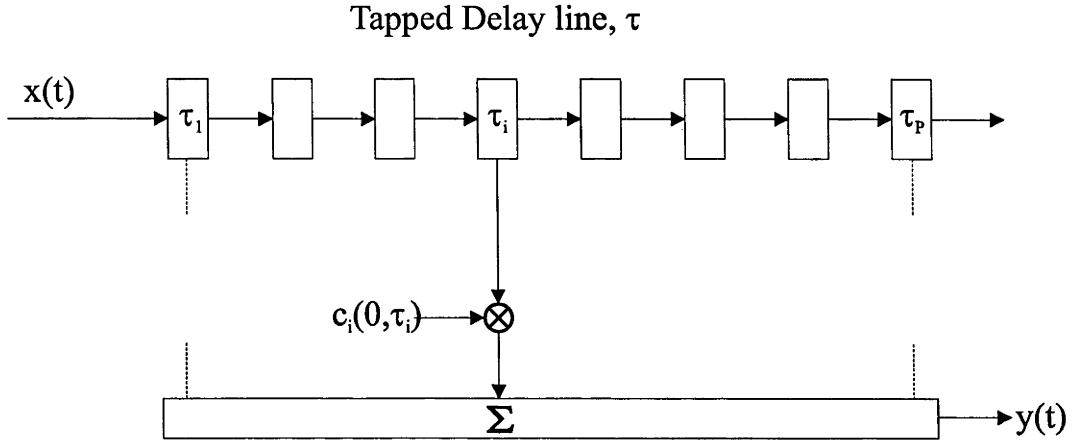


Figure 5.13: Tapped delay line model of frequency selective channel

Now define the k th user's i th time varying received pulse as

$$h_{i,k,m-irN} = \sqrt{E_k} \int_{-\infty}^{\infty} s_{i,k}((m - irN)T_r - iT_s - \zeta_k - \tau) c_k(mT_r, \tau) d\tau \quad (5.45)$$

In practice most of the transmitter pulse's energy is restricted to a finite duration. We also assume that the filtered signature waveform is time-limited to L_s (fractional) symbol periods, as $s_{i,k}(t) = 0$ for $t < 0$ and $t \geq L_s T_s$. The channel's maximum delay spread $L_r T_s$ is finite, as $c_k(t, \tau) = 0$ for $\tau < 0$ and $\tau > L_r T_s$. The asynchronism amongst users can also be characterised by $0 \leq \zeta_k \leq L_\zeta T_s$. Therefore the received pulse length equals $L_h = \lceil L_s + L_r + L_\zeta \rceil$ and the i th received pulse is fully located within the interval $irN \leq m \leq (L_h + i)rN - 1$. Using (5.45) the received signal of (5.44) may be more compactly written as

$$y_m = \sum_{k=1}^K \sum_{i=-L_h+1+\lceil m/rN \rceil}^{\lfloor m/rN \rfloor} b_{i,k} h_{i,k,m-irN} + n_m \quad (5.46)$$

This is the familiar notation for linear modulations, but now however, the received pulse shape is different between users and symbol period. The total number of data bearing received samples is $Y = (I + L_h - 1)rN$. The received samples are stored in the vector \mathbf{y} , $[y_0, \dots, y_{Y-1}]^T$. Define also \mathcal{Y}_{m-1} as the vector of received signal samples up to the $(m - 1)$ th sample ie. $[y_0, \dots, y_{m-1}]^T$. The channel vector \mathbf{h} is made up of all received

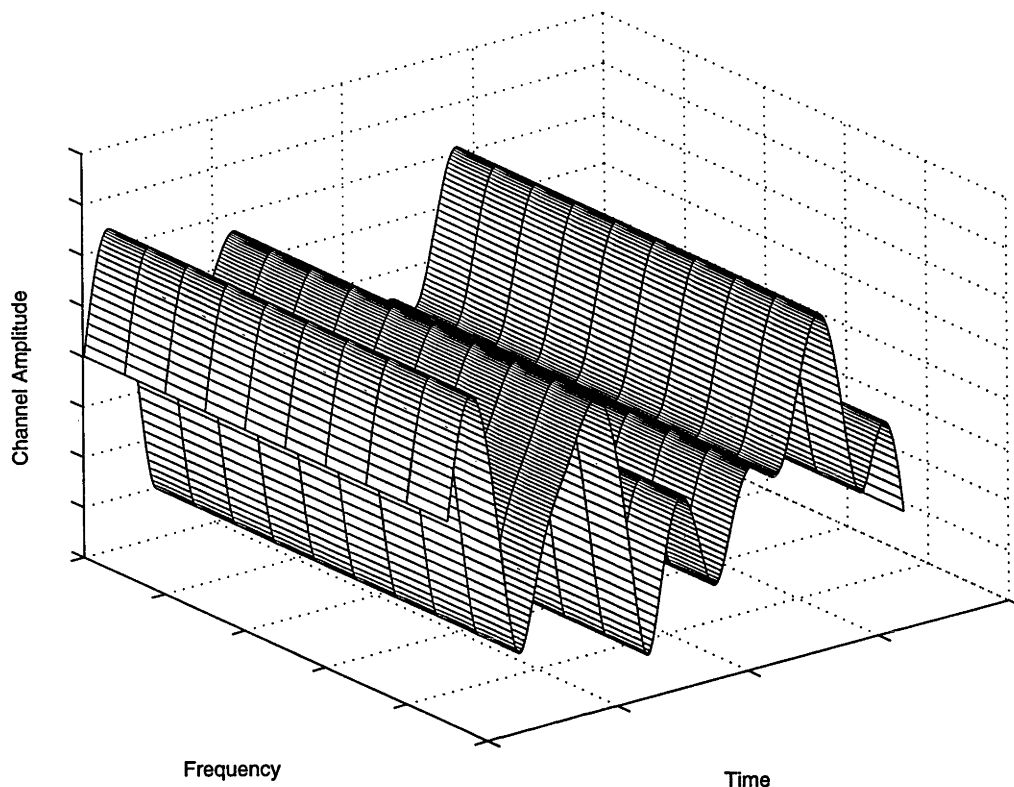


Figure 5.14: Plot of the amplitude of the frequency selective channel's transfer function as a function of time and frequency

pulse samples, as

$$\mathbf{h}_{i,k} = (h_{i,k,0}, \dots, h_{i,k,L_h \tau N-1}), \in \mathbb{C}^{1, L_h \tau N-1} \quad (5.47)$$

$$\mathbf{h}_i = (\mathbf{h}_{i,1}, \dots, \mathbf{h}_{i,K}) \in \mathbb{C}^{1, KL_h \tau N-1} \quad (5.48)$$

$$\mathbf{h} = (\mathbf{h}_0, \dots, \mathbf{h}_{Y-1}) \in \mathbb{C}^{1, IY L_h \tau N-1} \quad (5.49)$$

Define $\mathbf{n} = [n_0, \dots, n_{Y-1}]^T$ as the vector of the sampled noise process. The noise autocovariance is $\mathbf{R}_{nn} = \frac{1}{2} E\{\mathbf{nn}^H\}$. When the noise-limiting filter is designed such that the sampled noise remains white (eg. it has the transfer function $\text{rect}(fT_r)$), the noise autocovariance equals $\mathbf{R}_{nn} = N_0/T_r \mathbf{I}$, where \mathbf{I} is the identity matrix. Define the received

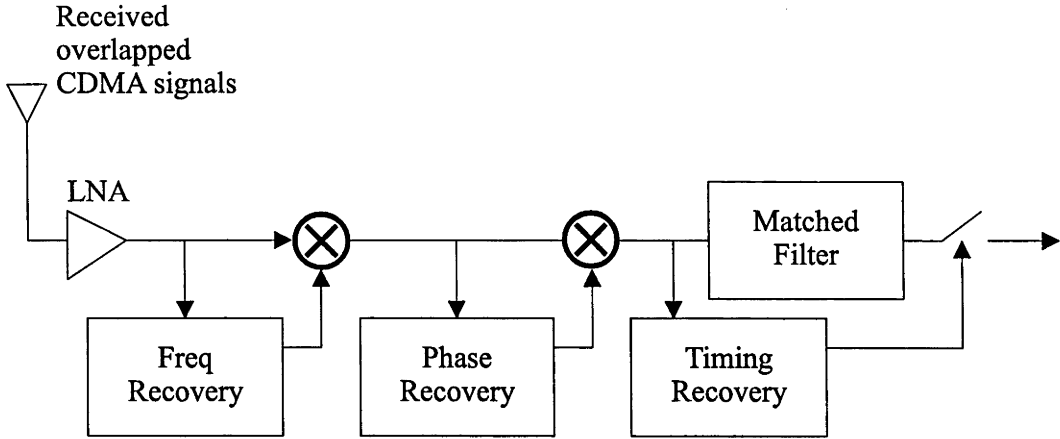


Figure 5.15: A basic receiver front end

sample autocovariance as $\mathbf{R}_{yy} = \frac{1}{2}E\{\mathbf{y}\mathbf{y}^H | \mathbf{B}\}$, with entries given by

$$\frac{1}{2}E\{y_m y_{m'}^* | \mathbf{B}\} = \sum_{k=1}^K \sum_{k'=1}^K \sum_{i=-L_h+1+\lceil m/rN \rceil}^{\lfloor m/rN \rfloor} \sum_{i'=-L_h+1+\lceil m'/rN \rceil}^{\lfloor m'/rN \rfloor} b_{i,k} b_{i',k'}^* \frac{1}{2}E\{h_{i,k,m-irN} h_{i',k',m'-i'rN}^*\} + \frac{1}{2}E\{n_m n_{m'}^*\} \quad (5.50)$$

where the pulse autocovariance is

$$\frac{1}{2}E\{h_{i,k,m-irN} h_{i',k',m'-i'rN}^*\} = \sqrt{E_k E_{k'}} \int_{-\infty}^{\infty} \int_{-\infty}^{\infty} s_{i,k}((m-irN)T_r - \zeta_k - \tau_1) \times s_{i',k'}^*((m'-i'rN)T_r - \zeta_{k'} - \tau_2) \frac{1}{2}E\{c_k(\tau_1, mT_r) c_{k'}^*(\tau_2, m'T_r)^*\} d\tau_1 d\tau_2 \quad (5.51)$$

5.16 Detection Criteria

In this section we are concerned with the general design methodology for an optimum receiver. There are basically four criteria of optimality that can be applied to signal detection and estimation; they are

1. Maximum likelihood sequence detection (MLSD),

$$\hat{\mathbf{B}} = \arg \max_{\tilde{\mathbf{B}}} p(\mathbf{y} | \tilde{\mathbf{B}})$$

2. ML symbol detection

$$\hat{b}_{i,k} = \arg \max_{\tilde{b}_{i,k}} p(\mathbf{y} | \tilde{b}_{i,k})$$

3. Maximum *a posteriori* sequence detection (MAPSD)

$$\hat{\mathbf{B}} = \arg \max_{\tilde{\mathbf{B}}} p(\tilde{\mathbf{B}} | \mathbf{y})$$

4. MAP symbol detection

$$\hat{b}_{i,k} = \arg \max_{\tilde{b}_{i,k}} p(\tilde{b}_{i,k} | \mathbf{y})$$

The data symbols from all users are arranged in a $I \times K$ matrix $\mathbf{B}_{i,k}$ such that $(\mathbf{B})_{i,k} = b_{i,k}$. The MLSD (ie. the Viterbi algorithm, add-compare-select) and the MAP symbol by symbol (ie. forward backward algorithm, soft input soft output algorithm for decoding of Turbo codes [18]) detection the two most important criteria. Let the data symbol matrix \mathbf{B} be transmitted and \mathbf{y} be received. Then the *a posteriori* sequence probability is the probability that the sequence \mathbf{B} was transmitted, given that \mathbf{y} was received, and may be written as

$$p(\mathbf{B} | \mathbf{y}) \tag{5.52}$$

The MAP decision is therefore the value of \mathbf{B} that maximizes the *a posteriori* probability density function,

$$p(\mathbf{B} | \mathbf{y}) = \frac{p(\mathbf{y} | \mathbf{B})p(\mathbf{B})}{p(\mathbf{y})} \tag{5.53}$$

where $p(\mathbf{B})$ is the *a priori* probability density function of \mathbf{B} . The maximum likelihood (ML) estimate of \mathbf{B} is the value that maximises $p(\mathbf{y} | \mathbf{B})$. Note that if there is no prior knowledge of \mathbf{B} , it is usually assumed that $p(\mathbf{B})$ is uniform over the range of values of \mathbf{B} . In such a case the value of \mathbf{B} that maximises $p(\mathbf{B} | \mathbf{y})$ is identical to the value of \mathbf{B} that maximises $p(\mathbf{y} | \mathbf{B})$. Thus the MAP and ML criteria are identical for sequence detection (and for equiprobable symbol detection also). In this thesis we only adopt MLSD criterion for detection due to its straightforward implementation (add-compare-select).

The conditional probabilities can be computed in a recursive fashion. The MLSD receiver as written, has to compute the likelihood $p(\mathbf{y} \mid \tilde{\mathbf{B}})$ for each hypothesis, $\tilde{\mathbf{B}}$. In general the number of metric computations grows exponentially with the transmission duration. Moreover, the computation of the log-likelihoods is impossible in a realistic environment involving unknown and random processes, since it becomes mathematically difficult to construct the joint pdf. To this end, the MLSD receiver is infeasible.

However, there are a few exceptions. If the transmission interval is small (ie. small tree search) or if the branch metric computation depends only on the finite past, the optimisation problem can be solved recursively. Assume for now that the channel impulse response is known completely. If the intersymbol interference only lasts L symbols, then the branch metric only depends on a finite number, KL , of past symbols and therefore there are M^{KL} hypothesis vectors (ie. all the immediate L past symbols are important since the energy spreads across their L neighbouring symbols due to the channel or deliberate design). A trellis of $M^{K(L-1)}$ states and M^{KL} branches is used to find the most likely transmitted sequence. In essence, the multiuser joint trellis is just a super trellis constructed by combining each user's individual trellis. The joint trellis state at a particular symbol i is given by the past $K(L-1)$ symbols. A branch is represented by the most recent KL symbols.

The Viterbi Algorithm (VA), originally proposed for decoding convolutional codes in 1967 by Viterbi [129], is an effective implementation of the solution to the MLSD problem. The sequence metrics can be written as the recursive accumulation of branch metrics $\lambda_i(\sigma_{i-1}, \sigma_i)$ by keeping a running total, the path metric $\Gamma_i(\mathbf{B}_i)$. It equals the path metric at the $(i-1)$ th symbol period plus the branch metric for the i th symbol period, $\lambda_i(\sigma_{i-1}, \sigma_i)$, as

$$\Gamma_i(\mathbf{B}_i) = \Gamma_{i-1}(\mathbf{B}_{i-1}) + \lambda_i(\sigma_{i-1}, \sigma_i) \quad (5.54)$$

$$\text{where} \quad (5.55)$$

$$\sigma_i = \begin{pmatrix} \tilde{b}_{i-L+2,1} & \cdots & \tilde{b}_{i-L+2,K} \\ \vdots & & \vdots \\ \tilde{b}_{i,1} & & \tilde{b}_{i,K} \end{pmatrix} \quad (5.56)$$

denotes a particular state in the trellis at time i . At any time i there are $M^{K(L-1)}$ paths that need to be retained and extended for the next time interval. The branch retained is referred to as the survivor. The sequence of survivors from the current time back to the start of processing is known as the survivor sequence. There are $M^{K(L-1)}$ survivors at any point, and when their sequences are followed back for some period they merge with high probability. When these paths merge, a decision can be made regarding the most likely transmitted symbol for that time interval. For the VA to be practically implementable, it is important to limit this decision delay to some fixed value. It is generally accepted that this delay should be about seven times the memory length of the error control code or L in our case.

5.17 Multiuser Detection in Multipath Fading Channels

Multipath fading presents a major limitation on the performance of wireless CDMA systems. To date most of the research has been conducted for slow or time-invariant fading channels. In this section we only highlight contributions in this latter area (ie. for the slow fading channel).

The conventional receiver, in the case of a multipath fading channel with delay spread, consists of a bank of RAKE receivers, one for each active user at the base station and one for the desired user in a mobile. A RAKE receiver can be interpreted as a combiner of correlator outputs. The correlations performed at each tap of the RAKE receiver are simply cross correlations of the received signal with the locally generated signature waveform. Thus the spreading waveforms are used to resolve the multipath introduced by the channel. In a frequency selective channel, the receiver observes P faded replicas of the same transmitted signal. Hence a receiver that processes the received signal in an optimum manner will achieve a performance equivalent to a P th order diversity system. The RAKE receiver ignores the MAI, and this results in an error probability floor. This error floor directly determines the maximum number of users in a CDMA system. These disadvantages of conventional reception techniques can be found in [60].

The optimal MLSD receiver for multipath fading CDMA channel consists of the same front-end, a bank of RAKE filters, followed by the Viterbi algorithm. This receiver has the same error probability in the single user case at the expense of high complexity [153].

Motivated by the high complexity of the optimum MLSD receiver, many low complexity multiuser detectors for frequency selective Rayleigh channels have been proposed whose performance is independent of the interfering signal energy [154][155]. For wide-band signals, the total number of resolvable paths is given by

$$P = \lceil \tau_{max}/T_c \rceil + 1 \quad (5.57)$$

where τ_{max} is the maximum multipath delay spread of the channel. Zvonar [154] looks at passing the PK signal replicas through a decorrelator to eliminate MAI. The output of the decorrelator is then fed into a maximum ratio combiner. In coherent detection knowledge of the individual fading paths' phase plus the carrier phase is required for coherent combining. For the case where the channel coefficients cannot be estimated differentially coherent detection using Differential Phase Shift Keying (DPSK) signalling has also been studied in [154]. The difference in performance between differentially coherent and coherent detection is of the order of the single user case. It has been shown that both these multiuser detectors alleviate the near-far problem and remove the error probability floor.

5.18 MLSE Receiver Analysis

In this section we briefly outline the theory involved in analysing the bit error rate performance of a receiver. The exact BER is difficult to compute since it involves computing the joint pdf of all hypothesised sequences' path metrics for a particular transmitted sequence and integrating it over an irregular region, corresponding to the ML sequence. The average BER is this quantity averaged across all transmitted sequences. Since the number of path metrics increase exponentially with the transmission length, the joint pdf gets extremely complicated.

However, a tight upper and lower bound on the BER is still possible using Forney's or Verdu's technique [35][125]. When the ML sequence is detected instead of the transmitted sequence, there are a number of bit errors. The probability that the ML sequence is not the transmitted sequence can be upper bounded by the probability that any error sequence has a larger path metric than the transmitted sequence. Thus a joint pdf is not needed, only the pdf of the path metric difference, for all possible transmitted and error

sequences.

The upper bound on the BER can be deduced from a union bound over all error events. The union bound of the error events can be written as

$$BER \leq \sum_{\mathbf{B}} \sum_{\tilde{\mathbf{B}}} \frac{P(\mathbf{B})P(\mathbf{B} \rightarrow \tilde{\mathbf{B}})w(\mathbf{B} \rightarrow \tilde{\mathbf{B}})}{K \log_2 M} \quad (5.58)$$

where $P(\mathbf{B})$ is the transmission probability, $P(\mathbf{B} \rightarrow \tilde{\mathbf{B}})$ is the pairwise probability of error and $w(\mathbf{B} \rightarrow \tilde{\mathbf{B}})$ indicates the number of bit errors in the error event. This is an infinite sum and must be truncated. If at least the dominant error events are considered, the truncated bound can still reasonably be considered an approximate upper bound. The pairwise error probability computation will be detailed in the next few chapters.

5.19 Summary

In this chapter, we revisited the transmitter, channel and receiver. In particular, a time varying frequency selective multipath channel was modelled and described in detail to serve as a grounding for subsequent chapters. Simplifications of the general channel model resulted in the purely time selective or frequency selective channel. We reviewed optimal receiver detection strategies and proposed a typical receiver front end. The performance analysis of such receivers is studied using union bounds.

Optimum Multiuser Detection for Known Time Varying, Frequency Selective Rayleigh Channels

Overview: This chapter develops a multiuser maximum likelihood sequence detector for the time varying, frequency selective, multipath fading channel corrupted by additive Gaussian noise. To ensure optimality, the receiver assumes perfect knowledge of the channel's time varying channel impulse response. It is proposed as a benchmark for comparing other more practical detectors, such as multiuser detectors whose complexity is linear in the number of users. An analysis of the multiuser receiver is also provided. Bit error probability bounds are obtained using a truncated union bound approach.

6.1 Introduction

This chapter develops a multiuser maximum likelihood sequence detector (MLSD) for linearly modulated or DS-CDMA signals sent over time varying, frequency selective Rayleigh fading channels. The receiver assumes perfect knowledge of the channel impulse response (CIR). Accordingly, it shall be known as the multiuser known channel impulse response receiver (MUKCIR).

Two of the most significant factors limiting the performance of existing mobile wireless systems are multipath fading and multiple access interference. Multipath fading is due to the presence of multiple scatterers, and the mobility of the transmitter, scatterers and receiver. It results in a received signal comprising the sum of delayed and dynamically distorted replicas of the original signal, modelled as a time varying and frequency selective channel. Multiple access interference, on the other hand, is caused by the multiple users transmitting on the same channel simultaneously. Diversity (including channel coding) can help to combat the detrimental effects of the channel's Rayleigh fading, but only proper equaliser design can minimise the consequences of the channel's amplitude and frequency distortion as a function of time and frequency. As discussed in previous chapters, MAI is inherent in DS-CDMA systems, but it also arises in TDMA systems as inter-cellular cochannel interference.

Research into equaliser design has followed three main threads. First, there is single user equalisation of DS-CDMA signals for frequency selective multipath channels. The RAKE receiver is used in practice to combat fading [86][91]. Fast fading encountered in many mobile communication scenarios significantly degrades the performance of the RAKE receiver due to less reliable channel estimation. In fact existing systems exhibit a limiting bit error probability floor that cannot be improved by increasing the transmitted power [106].

Second, there is multiuser equalisation for DS-CDMA signals in AWGN and slowly time varying multipath channels [121][114][33]. Previous work in the area of multiuser detection in fading channels by Zvonar et al. looked at detectors for synchronous transmissions over Rician channels [118] and the optimum detector for the asynchronous CDMA frequency selective Rayleigh fading channel which incorporates multipath di-

versity reception [155]. Multiuser RAKE receivers have been proposed to combat MAI in fading channels; however, such schemes are applicable only in slow fading scenarios in which the channel characteristics change slowly over time [154]. Multiuser MAP based receivers have been studied by Davis and Collings [26][27] in fast fading channels.

Recently several single user receiver structures have been developed to combat the fast fading that caused the limiting error floor in the RAKE receivers [48][65][152]. Recently, a novel multiuser receiver was proposed that exploits both the Doppler spread and the delay spread [96][97]. At the heart of the approach is a time-frequency channel decomposition of a WSSUS channel model. This leads to a time-frequency formulation of the RAKE receiver that exploits joint multipath-Doppler diversity. This is shown in Fig. 6.1. Multiuser detectors based on this idea show improved performance compared to exist-

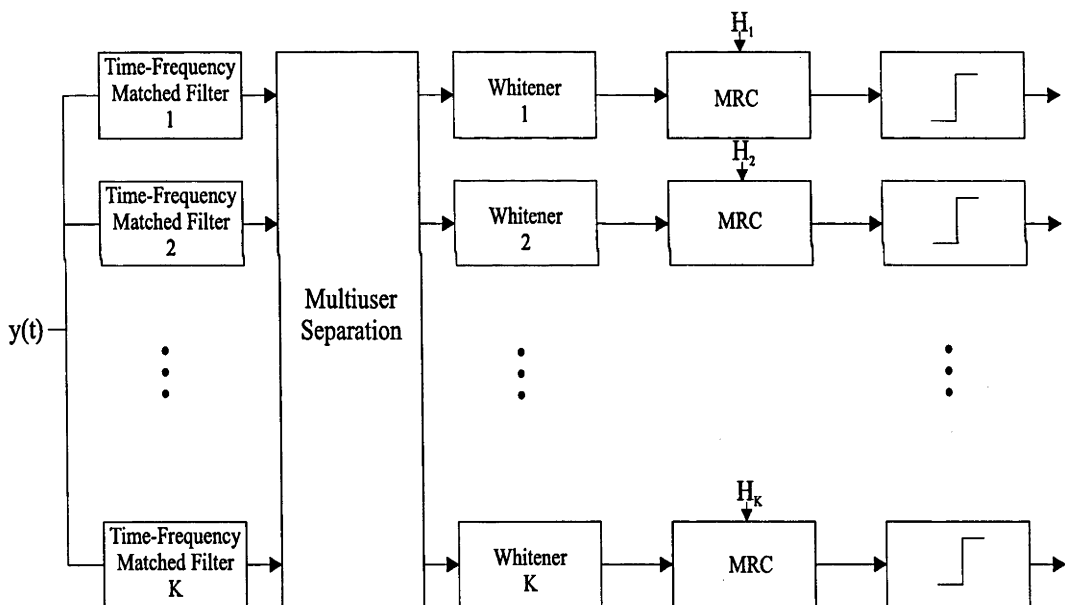


Figure 6.1: Time-frequency RAKE receiver

ing systems by achieving an inherently higher level of diversity. We put this in context by deriving and analysing the performance of the optimum receiver for this case. Both are fundamentally performing the same function: exploiting joint multipath-Doppler diversity in a multiuser CDMA framework, but one relies on the idea of using a RAKE structure with a time-frequency representation of the signal, and the other is based on the generalisation of Ungerboeck's matched filter MLSD [113][48].

In this chapter we leverage these new approaches to propose a new multiuser detector to combat MAI in fast fading multipath channels. The MUKCIR receiver relies on the provision of high quality channel information. This can be estimated in a real time system from a comb of pilot tones and/or pilot symbols. The comb of pilot tones/symbols is multiplexed in frequency/time with the transmitted signal and is thus distorted in a similar manner. A pilot tone characterises the time varying transfer function, $C(t, f)$, at some frequency for all time. A pilot symbol characterises $C(t, f)$ at some time for the frequency range of the transmitted signal. Interestingly in a channel that changes very slowly, it can be tracked accurately by applying past channel information to predict the future, an idea that will be pursued in the next chapter to design a new multiuser receiver. For a fast fading channel, the channel transfer function earlier than $t - T_s$ can vary considerably from the transfer function at t . Neither pilot tones nor pilot symbols can deal with fast fading and a large delay spread.

In this chapter the MUKCIR receiver is derived for all linear channel models as long as the transmitted chip waveform, the signature waveforms of all users and the exact CIR is available. We propose this receiver as a theoretical structure. Though it cannot be implemented, it is the optimal receiver and provides a benchmark for rating other suboptimum receivers. Towards the end of the chapter we analyse the receiver's BER performance and highlight some interesting numerical results.

6.2 MUKCIR Receiver Derivation

The MLSD searches all allowed transmitted sequences and chooses the one with maximum likelihood, as

$$\hat{\mathbf{B}} = \arg \max_{\tilde{\mathbf{B}}} p(\mathbf{y} | \tilde{\mathbf{B}}, \mathbf{h}) = \arg \max_{\tilde{\mathbf{B}}} \ln p(\mathbf{y} | \tilde{\mathbf{B}}, \mathbf{h}) = \arg \max_{\tilde{\mathbf{B}}} \Gamma(\tilde{\mathbf{B}}) \quad (6.1)$$

where $\ln p()$ is the log likelihood, $\Gamma(\tilde{\mathbf{B}})$ is labelled the sequence metric and the channel vector \mathbf{h} is given by

$$\mathbf{h}_{i,k} = (h_{i,k,0}, \dots, h_{i,k,L_h r N-1}), \in \mathbb{C}^{1, L_h r N-1} \quad (6.2)$$

$$\mathbf{h}_i = (\mathbf{h}_{i,1}, \dots, \mathbf{h}_{i,K}) \in \mathbb{C}^{1, K L_h r N-1} \quad (6.3)$$

$$\mathbf{h} = (\mathbf{h}_0, \dots, \mathbf{h}_{Y-1}) \in \mathbb{C}^{1, IY L_h r N-1} \quad (6.4)$$

Since $\mathbf{y} - E\{\mathbf{y} \mid \tilde{\mathbf{B}}, \mathbf{h}\} = \mathbf{n}$ (conditioned on $\tilde{\mathbf{B}}$ being transmitted), the desired log-likelihood in (6.1) matches the log likelihood of the Gaussian noise vector \mathbf{n} , as

$$-\ln p(\mathbf{y} \mid \tilde{\mathbf{B}}, \mathbf{h}) = -\ln p_n(\mathbf{n}) \quad (6.5)$$

Using the multivariate Gaussian density function, the log-likelihood $\ln p_n(\mathbf{n})$ equals (up to a constant independent of the hypothesised sequence $\tilde{\mathbf{B}}$),

$$\begin{aligned} \ln p_n(\mathbf{n}) &\sim - \sum_{m=0}^{Y-1} \sum_{m'=0}^{Y-1} \left\{ y_m^* - \sum_{k=1}^K \sum_{i=0}^{I-1} \tilde{b}_{i,k}^* h_{i,k,m-irN}^* \right\} (\mathbf{R}_{nn}^{-1})_{m,m'} \times \\ &\quad \left\{ y_{m'} - \sum_{k'=1}^K \sum_{i'=0}^{I-1} \tilde{b}_{i',k'} h_{i',k',m'-i'rN} \right\} \quad (6.6) \\ &= - \sum_{m=0}^{Y-1} \sum_{m'=0}^{Y-1} \left[y_m^* (\mathbf{R}_{nn}^{-1})_{m,m'} y_{m'} - y_m^* (\mathbf{R}_{nn}^{-1})_{m,m'} \sum_{k'=1}^K \sum_{i'=0}^{I-1} \tilde{b}_{i',k'} h_{i',k',m'-i'rN} - \right. \\ &\quad \left. y_{m'} (\mathbf{R}_{nn}^{-1})_{m,m'} y_{m'} \sum_{k=1}^K \sum_{i=0}^{I-1} \tilde{b}_{i,k}^* h_{i,k,m-irN}^* + \right. \\ &\quad \left. \sum_{k=1}^K \sum_{i=0}^{I-1} \sum_{k'=1}^K \sum_{i'=0}^{I-1} \tilde{b}_{i,k}^* h_{i,k,m-irN}^* \tilde{b}_{i',k'} h_{i',k',m'-i'rN} \right] \end{aligned}$$

This log-likelihood can now be represented as a sequence metric, $\Gamma(\tilde{\mathbf{B}})$, by interchanging the order of summations and neglecting the term $-\sum_{m=0}^{Y-1} \sum_{m'=0}^{Y-1} y_m^* (\mathbf{R}_{nn}^{-1})_{m,m'} y_{m'}$, since it is independent of the hypothesised sequence. The sequence metric can now be written as

$$\Gamma(\tilde{\mathbf{B}}) = \sum_{i=0}^{I-1} \sum_{k=1}^K 2\text{Re} \left\{ \tilde{b}_{i,k}^* m_{i,k} \right\} - \sum_{i=0}^{I-1} \sum_{i'=0}^{I-1} \sum_{k=1}^K \sum_{k'=1}^K \tilde{b}_{i,k}^* f_{i,i',k,k'} \tilde{b}_{i',k'} \quad (6.7)$$

where $\text{Re}(\cdot)$ denotes the real part of (\cdot) and the matched filter term $m_{i,k}$ and the ISI term $f_{i,i',k,k'}$ are defined as

$$m_{i,k} = \sum_{m=0}^{Y-1} \sum_{m'=0}^{Y-1} y_{m'} (\mathbf{R}_{nn}^{-1})_{m,m'} h_{i,k,m-irN}^* \quad (6.8)$$

$$f_{i,i',k,k'} = \sum_{m=0}^{Y-1} \sum_{m'=0}^{Y-1} h_{i,k,m-irN}^* (\mathbf{R}_{nn}^{-1})_{m,m'} h_{i',k',m'-i'rN} \quad (6.9)$$

Equation (6.8) can be viewed as an equivalent despreading and MF operation for time varying channels in coloured noise. By exploiting the conjugate symmetry of $f_{i,i',k,k'}$, as $f_{i,i',k,k'} = f_{i,i',k,k'}^*$, the sequence metric can be simplified as

$$\Gamma(\tilde{\mathbf{B}}) = \sum_{i=0}^{I-1} 2\text{Re} \left\{ \sum_{k=1}^K \tilde{b}_{i,k}^* m_{i,k} - \sum_{k=1}^K \sum_{k'=1}^K \sum_{i'=0}^{i-1} \tilde{b}_{i,k}^* f_{i,i',k,k'} \tilde{b}_{i',k'} \right\} - \sum_{k=1}^K |\tilde{b}_{i,k}|^2 f_{i,i,k,k} \quad (6.10)$$

Note that the effects of fast fading are incorporated implicitly in the above formulation by the channel vector \mathbf{h} . The first term is similar to the time-frequency RAKE receiver in [96], and the second term eliminates the MAI and ISI. Exhaustive comparison is needed to find the maximum metric and thus the maximum likelihood sequence. If the ISI term has a finite memory, say L , then $f_{i,i',k,k'} = 0$ for $|i' - i| \geq L$ and the sequence metric simplifies to

$$\Gamma(\tilde{\mathbf{B}}) = \sum_{i=0}^{I-1} 2\text{Re} \left\{ \sum_{k=1}^K \tilde{b}_{i,k}^* m_{i,k} - \sum_{k=1}^K \sum_{k'=1}^K \sum_{i'=i-L+1}^{i-1} \tilde{b}_{i,k}^* f_{i,i',k,k'} \tilde{b}_{i',k'} \right\} - \sum_{k=1}^K |\tilde{b}_{i,k}|^2 f_{i,i,k,k}$$

Past symbols and the state matrix are defined as

$$\tilde{\mathbf{B}}_{i-1} = \begin{pmatrix} \tilde{b}_{0,1} & \tilde{b}_{0,K} \\ \vdots & \vdots \\ \tilde{b}_{i-1,1} & \tilde{b}_{i-1,K} \end{pmatrix} \quad \sigma_i = \begin{pmatrix} \tilde{b}_{i-L+2,1} & \cdots & \tilde{b}_{i-L+2,K} \\ \vdots & & \vdots \\ \tilde{b}_{i,1} & & \tilde{b}_{i,K} \end{pmatrix} \quad (6.11)$$

The sequence metrics can be written as the recursive accumulation of branch metrics $\lambda_i(\sigma_{i-1}, \sigma_i)$ by keeping a running total, the path metric $\Gamma_i(\mathbf{B}_i)$. It equals the path metric

at the $(i - 1)$ th symbol period plus the branch metric $\lambda_i(\sigma_{i-1}, \sigma_i)$ as

$$\Gamma_i(\tilde{\mathbf{B}}_i) = \Gamma_{i-1}(\tilde{\mathbf{B}}_{i-1}) + \lambda_i(\sigma_{i-1}, \sigma_i) \quad (6.12)$$

where

$$\Gamma_{i-1}(\tilde{\mathbf{B}}_{i-1}) = \sum_{l=0}^{i-1} 2\text{Re} \left\{ \sum_{k=1}^K \tilde{b}_{l,k}^* m_{l,k} - \sum_{k=1}^K \sum_{k'=1}^K \sum_{l'=l-L+1}^{l-1} \tilde{b}_{l,k}^* f_{l,l',k,k'} \tilde{b}_{l',k'} \right\} - \sum_{k=1}^K |\tilde{b}_{l,k}|^2 f_{l,l,k,k} \quad (6.13)$$

$$\lambda_i(\sigma_{i-1}, \sigma_i) = 2\text{Re} \left\{ \sum_{k=1}^K \tilde{b}_{i,k}^* m_{i,k} - \sum_{k=1}^K \sum_{k'=1}^K \sum_{i'=i-L+1}^{i-1} \tilde{b}_{i,k}^* f_{i,i',k,k'} \tilde{b}_{i',k'} \right\} - \sum_{k=1}^K |\tilde{b}_{i,k}|^2 f_{i,i,k,k} \quad (6.14)$$

The path metric is a function of the previous hypothesised sequences, $\tilde{\mathbf{B}}_{i-1}$, which contains symbols up to the the start of transmission. The branch metric, however, depends only on the L previous symbols and thus the evolution of the path metrics may be described by a trellis. Since the ISI lasts L symbols only, there are only $M^{K(L-1)}$ combinations of σ_i or states in the trellis and each state has M^K branches. The Viterbi algorithm automates the calculation of these path metrics and the minimisation procedure of (6.1). This has exponential computational complexity in the number of users. For $L = 2$, as is often the case in CDMA, the trellis is fully connected. To reduce the complexity of this receiver we propose a linear complexity receiver in chapter 7. We delay this proposition since the techniques introduced in chapter 7 will greatly facilitate the derivation of the Single User Known Channel Impulse Response receiver (SUKCIR).

6.2.1 White Noise

In the case of white noise the noise autocovariance matrix equals of $\mathbf{R}_{nn} = \frac{1}{2} E\{\mathbf{nn}^H\} = N_o/T_r \mathbf{I}$. By substituting $\mathbf{R}_{nn}^{-1} = (N_o/T_r)^{-1} \mathbf{I}$ into (6.8) and (6.9), and neglecting the common data independent factor of $(N_o/T_r)^{-1}$, the receiver structure is particularly simple

since

$$m_{i,k} = \sum_{m=irN}^{(L_h+i)rN-1} y_m h_{i,k,m-irN}^* = y_m * h_{i,k,-m}^* |_{m=irN}, \quad (6.15)$$

$$= \sum_{k=1}^K \sum_{i=-L_h+1+\lfloor m/rN \rfloor}^{\lfloor m/rN \rfloor} b_{i,k} f_{i,i',k,k'} + \sum_{m=irN}^{(L_h+i)rN-1} n_m h_{i,k,m-irN}^* \quad (6.16)$$

$$f_{i,i',k,k'} = \sum_{m=irN}^{(L_h+i)rN-1} h_{i,k,m-irN} h_{i',k',m-i'rN}^* \quad (6.17)$$

and it is clear that $L = L_h$ in this instance.

An alternate Euclidean distance sequence metric that merits mention is obtained directly obtained by substituting $\mathbf{R}_{nn}^{-1} = (N_o/T_r)^{-1} \mathbf{I}$ into (6.6),

$$\Gamma(\tilde{\mathbf{B}}) = \sum_{m=0}^{Y-1} \left| y_m - \sum_{k=1}^K \sum_{i=0}^{I-1} b_{i,k} h_{i,k,m-irN} \right|^2 \quad (6.18)$$

The same sequence, path and branch metric of (6.7), (6.13) and (6.14) are still correct.

Now that the noise covariance is not present, it is easier to see that the quantity $m_{i,k}$ can be interpreted as a time-frequency matched filter for the k th user's i th symbol. In time varying channels, the matched filter has a different response, $h_{i,k,m}^*$ in m for each symbol and user. The k th matched filter's irN th output sample is a sufficient statistic for the k th user's i th transmitted symbol. The quantity $f_{i,i',k,k'}$ can be viewed as the ISI introduced by the k' th user's i' th symbol on the k th user's i th symbol.

6.2.2 The Time Invariant Frequency Selective Channel

When short codes are transmitted, $s_{i,k}(t) = s_k(t)$. In time invariant channels, $c_k(t, \tau) = c_k(0, \tau)$ and the received pulse is time invariant,

$$\begin{aligned} h_{i,k,m-irN} &= \sqrt{E_k} \int_{-\infty}^{\infty} s_k(m-irN)T_r - \tau) c_k(0, \tau) d\tau \\ &= h_{0,k,m-irN} \end{aligned} \quad (6.19)$$

Hence the MF and the ISI values reduce to

$$m_{i,k} = \sum_{m=irN}^{(L_h+i)rN-1} y_m h_{0,k,m-irN}^* \quad (6.20)$$

$$f_{i,i',k,k'} = \sum_{m=irN}^{(L_h+i)rN-1} h_{0,k,m-irN} h_{0,k',m-i'rN}^* \quad (6.21)$$

It is clear from (6.21) that the ISI terms are due to interference within users (self interference) and between users (multiuser interference). This is a generalisation of the result proved by Ungerboeck in [113]. Note that if long codes are employed, $h_{i,k,m-irN} \neq h_{0,k,m-irN}$ since the signature sequences change every symbol period, i (ie. $s_{i,k}(t) \neq s_{0,k}(t)$). In this special case the MF and ISI terms and hence the received pulse change every symbol even if the channel is time invariant.

6.2.3 The Time Selective Frequency Flat Channel

In time selective, frequency flat channels ($c(t, \tau) = c(t)\delta(\tau)$), the received pulse is given by

$$h_{i,k,m-irN} = \sqrt{E_k} s_{i,k}(m-irN)T_r - \zeta_k c_k(mT_r) \quad (6.22)$$

In the white noise environment, the k th matched filter output is computed as

$$\begin{aligned} m_{i,k} &= \sqrt{E_k} \sum_{m=0}^{Y-1} y(m) s_{i,k}^*((m-irN)T_r - \zeta_k) c_k^*(mT_r) \\ &= (y(m) c_k^*(mT_r)) * s_{i,k}^*(-mT_r - \zeta_k) \end{aligned} \quad (6.23)$$

It can be readily seen that the optimum receiver obtains its sufficient statistics by multiplying the received signal with the conjugated fading process, then filtering this signal by the time reversed signature waveform (ie. a matched filter). This has an intuitive explanation. As the transmitted pulse is distorted in time by the fading process, the receiver must compensate for this scaling by weighting the received pulse according to the depth of the fade (ie. matching to the channel), followed by the conventional matched filtering

operation used in the AWGN channel.

The ISI term is time varying over L_h symbol periods and K users.

$$f_{i,i',k,k'} = \sum_{m=irN}^{(L_h+i)rN-1} s_{i,k}^* ((m - irN)T_r - \zeta_k) s_{i',k'} ((m - i'rN)T_r - \zeta_{k'}) c_k^*(mT_r) c_{k'}(mT_r)$$

6.2.4 The Time Invariant Frequency Flat Channel

This special case has been widely explored by many researchers and is the subject of Part I of this thesis. Essentially, the receiver only needs to know the constant complex gains of the channels (c_m), so the received pulse is given by

$$h_{i,k,m-irN} = \sqrt{E_k} c_m s_{i,k} ((m - irN)T_r - \zeta_k) \quad (6.24)$$

The k th matched filter output is

$$m_{i,k} = \sqrt{E_k} \sum_{m=irN}^{(L_h+i)rN-1} y_m s_{i,k} ((m - irN)T_r - \zeta_k) c_m \quad (6.25)$$

$$= (y_m c_m^*) * s_{i,k}^* (-mT_r - \zeta_k) \quad (6.26)$$

The received signal is thus filtered with the time reversed complex conjugated signature waveform. Note the ISI is no longer time varying since it is completely determined by the cross-correlation of the users' signatures as

$$f_{i,i',k,k'} = \sum_{m=irN}^{(L_h+i)rN-1} s_{i,k}^* ((m - irN)T_r - \zeta_k) s_{i',k'} ((m - i'rN)T_r - \zeta_{k'}) |c_m|^2 \quad (6.27)$$

For orthogonal spreading sequences, the correlation between user's signatures is zero, however, the signatures still exhibit self interference, since each user is still correlated with itself.

6.3 Receiver Operation

The operation of the receiver is shown in Fig. 6.2. In a practical receiver, the CIR is unavailable. An estimate of this must be obtained to allow the computation of $m_{i,k}$ and $f_{i,i',k,k'}$ according to (6.8) and (6.9) respectively. However, the MUKCIR receiver assumes ideal CIR provided as side information (ie. genie aided).

For each symbol period, M^{KL} branch metrics are computed according to (6.14) for all possible hypothesised sequences and applied to a Viterbi processor.

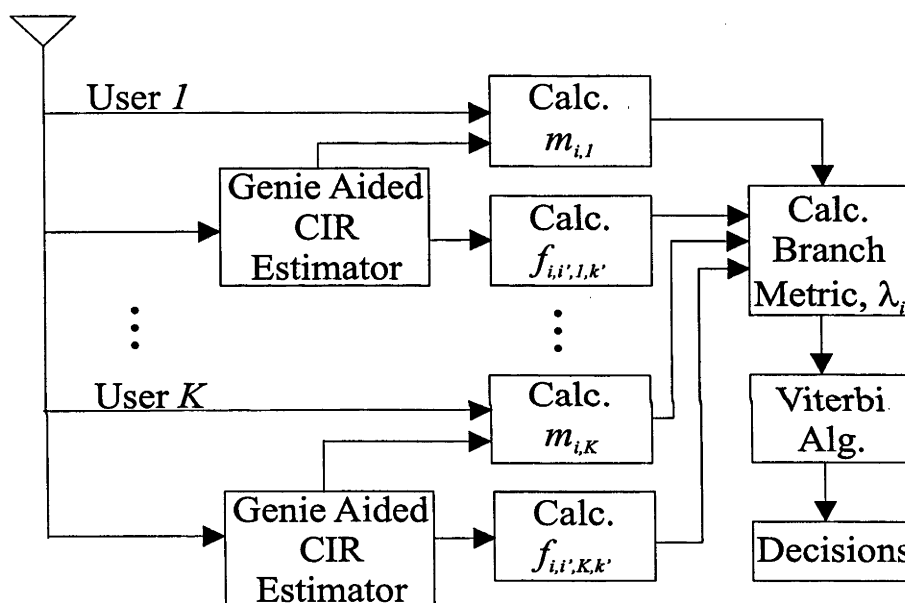


Figure 6.2: MUKCIR receiver block diagram

6.4 Receiver Analysis

In this section the MUKCIR receiver's BER is analysed for a *fast*, frequency selective Rayleigh fading channel in white noise. The conventional methods (ie. distance spectrum and transfer function bounds) of analysing the BER described in Part I do not apply. They require the fading to be sufficiently slow such that it is approximately constant over the error event, hence, the BER maybe computed as a function of the fading amplitude. The average BER is then obtained by weighting the BER according to the fading amplitude pdf [86].

The technique presented here does not require any approximation about slow or flat fading and therefore applies to the time varying frequency selective channels in question. Since the channel is known, coherent detection is possible. Let \mathbf{B} be the matrix of transmitted symbols and $\tilde{\mathbf{B}}$ be the matrix of detected symbols. Define $\mathbf{E} = \tilde{\mathbf{B}} - \mathbf{B}$ as the difference between the transmitted and detected sequence. The receiver's performance is characterised via the application of the union bound. An error event occurs when an erroneous detected sequences has a greater likelihood than the transmitted sequence. An error event of length ee starts at symbol t_e and stops at $t_e + ee$.

The BER can be upper bounded by (5.58), as

$$BER \leq \sum_{\mathbf{B}} \sum_{\tilde{\mathbf{B}}} \frac{P(\mathbf{B})P(\mathbf{B} \rightarrow \tilde{\mathbf{B}})w(\mathbf{B} \rightarrow \tilde{\mathbf{B}})}{K \log_2 M} \quad (6.28)$$

The pairwise probability of error for a particular sequence can be written as

$$\begin{aligned} P(\mathbf{B} \rightarrow \tilde{\mathbf{B}}) &= P(\Gamma(\tilde{\mathbf{B}}) > \Gamma(\mathbf{B})) \\ &= P \left[\sum_{i=0}^{I-1} 2\text{Re} \left\{ \sum_{k=1}^K \tilde{b}_{i,k}^* m_{i,k} - \sum_{k=1}^K \sum_{k'=1}^K \sum_{i'=i-L+1}^{i-1} \tilde{b}_{i,k}^* f_{i,i',k,k'} \tilde{b}_{i',k'} \right\} - \sum_{k=1}^K | \tilde{b}_{i,k} |^2 f_{i,i,k,k} \right. \\ &\quad \left. \sum_{i=0}^{I-1} 2\text{Re} \left\{ \sum_{k=1}^K b_{i,k}^* m_{i,k} - \sum_{k=1}^K \sum_{k'=1}^K \sum_{i'=i-L+1}^{i-1} b_{i,k}^* f_{i,i',k,k'} b_{i',k'} \right\} - \sum_{k=1}^K | b_{i,k} |^2 f_{i,i,k,k} > 0 \right] \\ &= P \left[\text{Re} \left\{ \sum_{i=t_e}^{t_e+ee-1} \sum_{k=1}^K \left[2e_{i,k}^* m_{i,k} - 2 \sum_{k'=1}^K \sum_{i'=i-L+1}^{i-1} e_{i,k}^* f_{i,i',k,k'} e_{i',k'} - \right. \right. \right. \\ &\quad \left. \left. \sum_{k=1}^K \sum_{i'=\max\{0,i-L+1\}}^{\min\{ee-1,i+L-1\}} e_{i,k}^* f_{i,i',k,k'} e_{i',k'} \right] \right\} > 0 \right] \quad (6.29) \end{aligned}$$

Substituting (6.8) and (6.9) into (6.29), this pairwise probability of error equals

$$\begin{aligned} &= P \left[\text{Re} \left\{ \sum_{i=t_e}^{t_e+ee-1} \sum_{k=1}^K \left[\sum_{l=irN}^{(L+i)rN-1} 2e_{i,k}^* n_l h_{i,k,l-irN}^* - \right. \right. \right. \\ &\quad \left. \left. \sum_{i'=\max\{0,i-L+1\}}^{\min\{ee-1,i+L-1\}} \sum_{k'=1}^K \sum_{l=\max\{i,i'\}rN}^{(L+\min\{i,i'\})rN-1} e_{i,k}^* e_{i',k'} h_{i,k,l-irN}^* h_{i',k',l-i'rN} \right] \right\} > 0 \right] \quad (6.30) \end{aligned}$$

The left hand side of the inequality is a Gaussian quadratic form in the received pulse

and noise samples, so the desired probability can be calculated easily via its characteristic function. The Gaussian quadratic form only depends explicitly on the error sequence \mathbf{E} , but as this may only take on certain values, it still depends implicitly on the transmitted sequence, \mathbf{B} . The computation of the BER bound is still prohibitive since all possible combinations of the transmitted sequences have to be accounted for. Error events can begin in any symbol interval, during which $K \log_2 M$ bits are sent. In a fast fading scenario, long error events are very unlikely since most errors occur in deep fades. Hence, it is important to note that the upper bound is not the union of *all* error events, instead only error events of short lengths. As we shall soon see, this truncated bound is easily calculated and still asymptotically correct at high SNRs. From this discussion, the union bound may be rewritten as a function of a limited set of error events \mathbf{E} , as

$$BER \leq \sum_{\mathbf{E}} \frac{P(\mathbf{E})w(\mathbf{E})}{K \log_2 M} \quad (6.31)$$

It has been noted in [48] that the union bound over all error events is a difficult task computationally. Although a rigorous proof of the upper bound convergence cannot be established, it is seen that if the fading is fast and the SNR high, the dominant error events are short. Thus there is a balance between incorporating sufficient error events so that some reasonable claim of "upper bound" can be supported, yet disregarding ones that evidently contribute little to the bound and thus reduce the computation involved.

Define \mathbf{g} as a column vector $\mathbf{g} = [\mathbf{h}_e \ \mathbf{n}_e]^T$ where \mathbf{h}_e is a column vector of length $ee \times K \times LrN$ of the received pulse samples and \mathbf{n}_e is a column vector of length $(L + ee) \times rN$ of the additive noise samples. This \mathbf{g} contains the relevant Gaussian random variables during the error event. Define $\kappa = \mathbf{g}^H \mathbf{G} \mathbf{g}$ as the left hand side of the inequality in (6.30) where the kernel \mathbf{G} is a Hermitian symmetric matrix defined implicitly. The autocovariance matrix of \mathbf{g} , \mathbf{R}_{gg} is given by

$$\mathbf{R}_{gg} = \frac{1}{2} E\{\mathbf{g}\mathbf{g}^H\} = \begin{pmatrix} \mathbf{R}_{hh} & 0 \\ 0 & \mathbf{R}_{nn} \end{pmatrix} \quad (6.32)$$

where the noise and channel are assumed independent and $\mathbf{R}_{hh} = \frac{1}{2} E\{\mathbf{h}_e \mathbf{h}_e^H\}$ and its entries are calculated from (5.51). With these definitions, \mathbf{R}_{gg} is completely described.

The pairwise probability of error for each error sequence (ie. the probability that one sequence's metric exceeds the transmitted sequence's metric) can be written as a Gaussian quadratic function (GQF). In complex Gaussian fading channels both metrics are GQFs and so too is their difference. The pairwise error probability is evaluated by integrating the pdf of the metric difference over the positive axis. Thus the pdf of a GQF is required. A real GQF, κ is given by

$$\kappa = \mathbf{g}^H \mathbf{G} \mathbf{g} \quad (6.33)$$

where \mathbf{g} is a vector of zero mean, i.i.d complex Gaussian random variables. The GQF's pdf is calculated from the characteristic function. Given a pdf, $p_\kappa(\kappa)$, its characteristic function, $C_\xi(\xi)$ is given by

$$C_\xi(\xi) = \int_{-\infty}^{\infty} p_\kappa(\kappa) \exp(j\xi\kappa) d\kappa \quad (6.34)$$

The pdf can similarly be computed from the inverse transform of the characteristic function,

$$p_\kappa(\kappa) = \frac{1}{2\pi} \int_{-\infty}^{\infty} C_\xi(\xi) \exp(-j\xi\kappa) d\xi \quad (6.35)$$

The characteristic function of a GQF can be written as [103][111]

$$C_\xi(\xi) = \det(\mathbf{I} - j2\xi \mathbf{R}_{gg} \mathbf{G})^{-1} \quad (6.36)$$

$$= \prod_{i=1}^I \frac{1}{(1 - \xi/p_i)} \quad (6.37)$$

where the poles, p_i are zeros of the determinant as,

$$p_i = \frac{1}{2j \operatorname{eig}_i\{\mathbf{R}_{gg} \mathbf{G}\}} \quad (6.38)$$

where $\operatorname{eig}_i(\cdot)$ denotes the i th eigenvalue of (\cdot) . The pairwise probability of error is the

probability that $\kappa > \kappa_{min}$

$$\int_{\kappa_{min}}^{\infty} p_{\kappa}(\kappa) d\kappa = \int_{\kappa_{min}}^{\infty} \frac{1}{2\pi} \int_{-\infty}^{\infty} C_{\xi}(\xi) \exp(-j\xi\kappa) d\xi d\kappa \quad (6.39)$$

$$= \frac{1}{2} + \int_{-\infty}^{\infty} \frac{C_{\xi}(\xi) \exp(-j\xi\kappa_{min})}{j2\pi\xi} d\xi \quad (6.40)$$

This is a line integral along the real axis. For $\kappa_{min} \leq 0$, the pairwise probability of error equals [48]

$$\int_{\kappa_{min}}^{\infty} p_{\kappa}(\kappa) d\kappa = 1 + \sum_{i, \Im\{p_i\} < 0} \text{Res}_i \left\{ \frac{C_{\xi}(\xi) \exp(-j\xi\kappa_{min})}{\xi} \right\} \quad (6.41)$$

and for $\kappa_{min} \geq 0$

$$\int_{\kappa_{min}}^{\infty} p_{\kappa}(\kappa) d\kappa = - \sum_{i, \Im\{p_i\} < 0} \text{Res}_i \left\{ \frac{C_{\xi}(\xi) \exp(-j\xi\kappa_{min})}{\xi} \right\} \quad (6.42)$$

where $\text{Res}_i(\cdot)$ is the residue at the i -th pole defined by,

$$\text{Res}_i\{X(\xi)\} = \lim_{\xi \rightarrow p_i} \frac{1}{(n_i - 1) d\xi^{(n_i-1)}} ((\xi - p_i)_i^{n_i} X(\xi)) \quad (6.43)$$

The pairwise probability of error can now be calculated as

$$P(\mathbf{B} \rightarrow \tilde{\mathbf{B}}) = \sum_{i, \Im\{p_i\} < 0} \prod_{k \neq i} \frac{1}{(1 - p_i/p_k)} \quad (6.44)$$

where p_i is the i th pole of (6.37).

6.5 Numerical Results

The following section provides an overview of the MUKCIR receiver's performance for a variety of transmitter, channel and receiver parameters. It is not possible to explore all combinations of such parameters; instead we highlight the influence of a particular parameter by keeping all others fixed. The chosen baseline signal model is as follows.

The DS-CDMA transmitter uses a root raised cosine chip pulse shaping truncated to 1.5 chip periods with 30% excess bandwidth, with a random signature sequence comprising 5 chips. The channel has $P = 2$ paths with equal mean power. A relatively large delay spread is used, $L_\tau = 0.5T_s$ and so the received pulse is restricted to $L = 2$ symbol periods. Due to the exponential growth in complexity, it is feasible to simulate and analyse a maximum of 5 users. The Doppler spectra of the simulated fading processes closely approximate Jakes model with $f_D T = 0.1$ (ie. very fast fading). It is assumed that $r = 2$ samples per chip period satisfies the Nyquist criterion.

Shown in Fig. 6.3 are the analytic performance graphs for the baseline model for 1 user. The BER is asymptotically correct at high SNRs. It becomes increasingly difficult to compute the upper bound for longer error events and beyond two symbol errors. However, the two symbol error events bound converge quickly on the one symbol curve. Thus it can be clearly seen that the dominant error events are the one symbol error events in fast fading and high SNR.

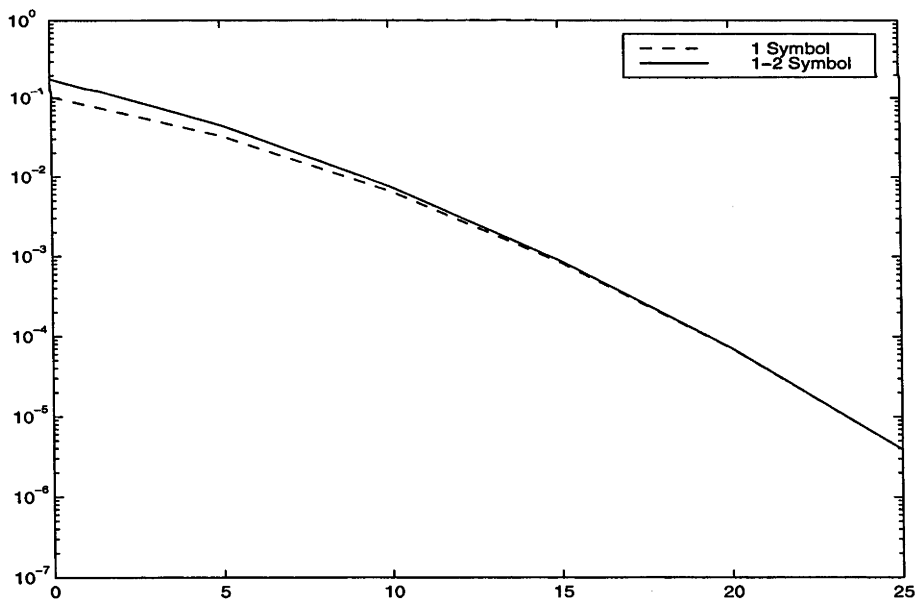


Figure 6.3: BER-SNR curves for different union bounds: all one symbol error events; and all one and two symbol error events

Figure 6.4 shows the dependence of the BER on the chip pulse's excess bandwidth. As χ is increased from 0.1 to 0.9 there is only a slight change in the BER at high SNRs.

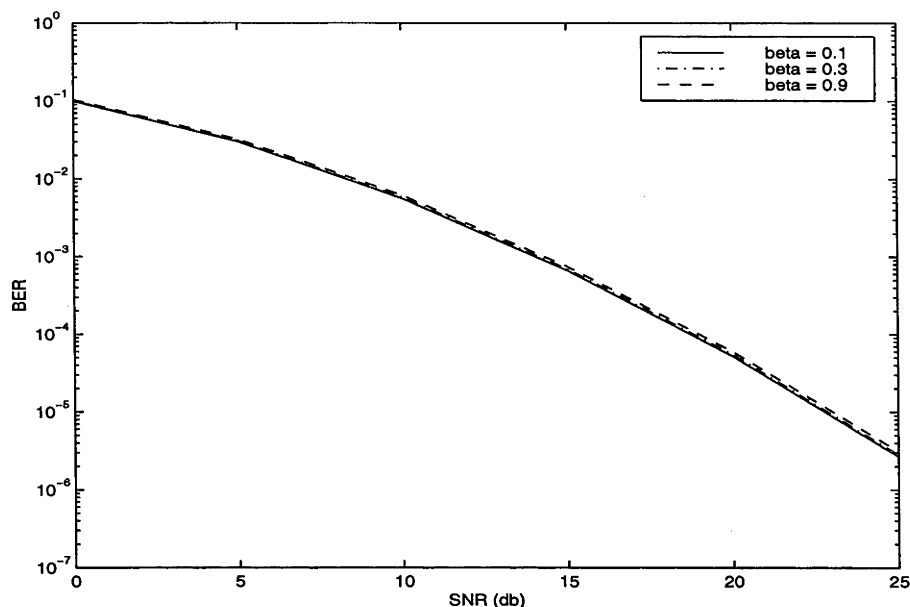


Figure 6.4: BER-SNR curves for root raised cosine chip pulse shaping with varying excess bandwidth, χ for 1 user

Figure 6.5 shows the dependence of the BER on the severity of the chip pulse's truncation. Once again, as the chip pulse's duration varies from 1.5 chips to 3.5 chips, there is minimal change in the BER. Note that elongating the chip pulse only slightly increases the overall spread-bit duration: it is still less than 2 symbol periods. For pulses longer than 2 symbol periods the analysis' complexity becomes substantially higher.

Figure 6.5 shows the graceful BER degradation of the MUKCIR and as the number of users increases. The analytic bounds agree well with the simulations.

Figure 6.7 highlights a benefit of wideband CDMA. In frequency selective channels, spreading the signal further captures more of the implicitly delay diversity, hence, the MUKCIR receiver's performance improves. However, there must be multiple paths for the benefits to be realised.

Joint multipath-Doppler diversity gains in a multiuser environment were also reported in [96]. Time selective signalling and reception in a single user environment was also looked at by Bhasyam et al. [20]. By introducing overlaps between successive symbol waveforms, significant gains were observed. Clearly, the overlap between symbols introduces ISI, however, for signature waveforms with good autocorrelation properties the

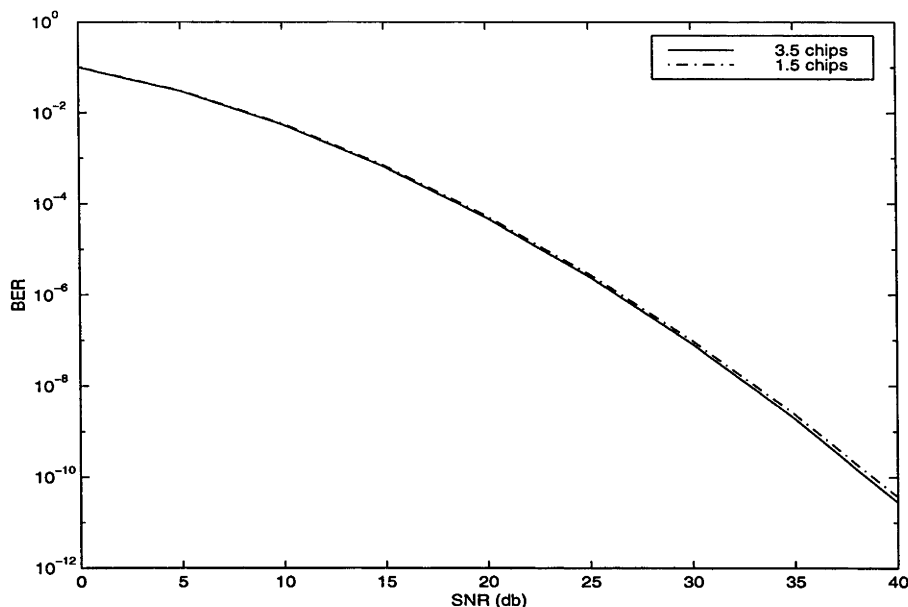


Figure 6.5: BER-SNR curves for root raised cosine chip pulse shaping truncated to different lengths

ISI is negligible.

Fig. 6.8 shows the MUKCIR receiver's ability to exploit the channel's implicit diversity, both in delay and Doppler. The faster fading and longer delay spread steepen the BER curve's gradient. A slight degradation in the BER with respect to the users can be seen especially at low SNRs. This difference is minimal at high SNRs. The other aspect is the variation in the Doppler spread. Fixing the delay spread at the small value of 0.005, and increasing the Doppler spread from 0.005 to 0.5 steepens the BER.

In the common situation where all of the signals arriving at the receiver are of different strengths, the strong signals tend to overwhelm the weak signals, even with good signature sequences. This problem is referred to as the *near - far* problem. The near-far resistance of this receiver has not been explicitly simulated. However, this optimal receiver must be near-far resistant since we assume perfect knowledge of the user signatures, channel impulse responses and timing/synchronisation parameters, thus ensuring that the optimal solution is obtained for all users regardless of the fluctuating users' energies.

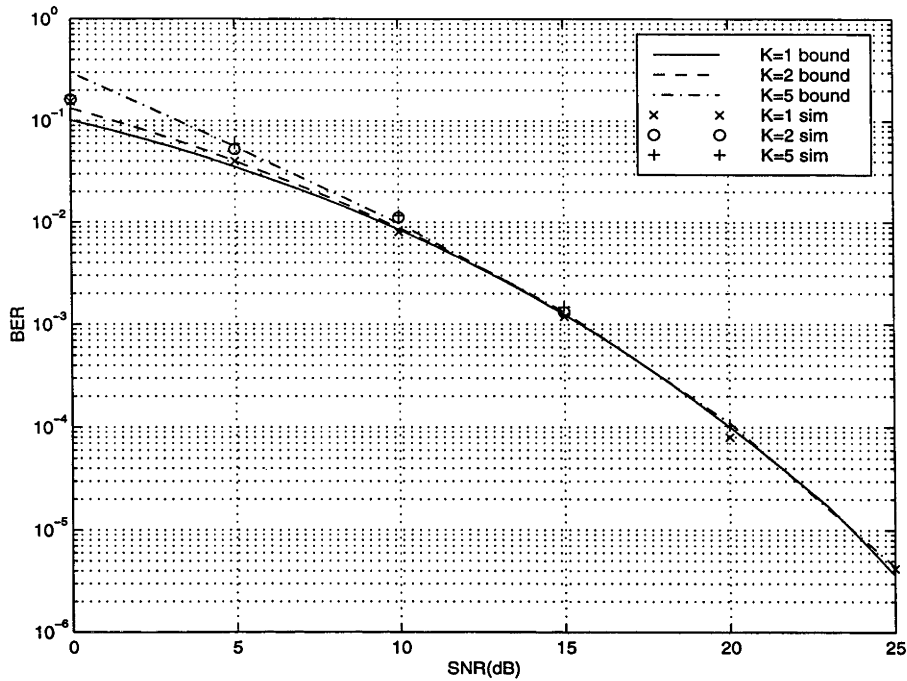


Figure 6.6: BER-SNR curves of the MUKCIR receiver for a fast time varying frequency selective channel where $f_D T_s = 0.1$, $L_r T_s = 0.5 T_s$, $r = 2$, $N = 5$, $P = 2$

6.6 Summary

In this chapter the MLSD receiver for a multiuser CDMA system operating over a time varying, frequency selective Rayleigh channel was derived and its BER upper bounded. This receiver is exponential in complexity with respect to the number of users. The BER has been bounded assuming ideal knowledge of the time varying channel impulse response. We evaluated the performance of the receiver under varying transmitter, channel and receiver parameters. Relatively small Doppler and delay spreads encountered in practice can be leveraged into significant diversity gains. This near far resistant receiver has the ability to achieve an inherently higher level of diversity due to joint multipath-Doppler processing.

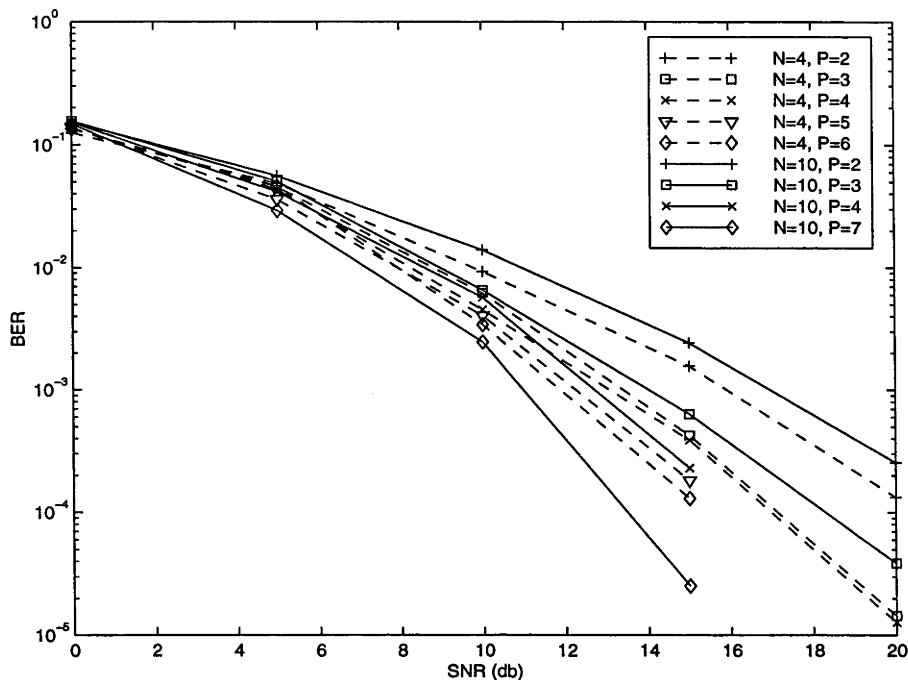


Figure 6.7: Effect on the MUKCIR receiver's BER of varying the number of independent paths, P , $K = 1, L_{\tau}T_s = 0.5T_s, f_D T_s = 0.01$

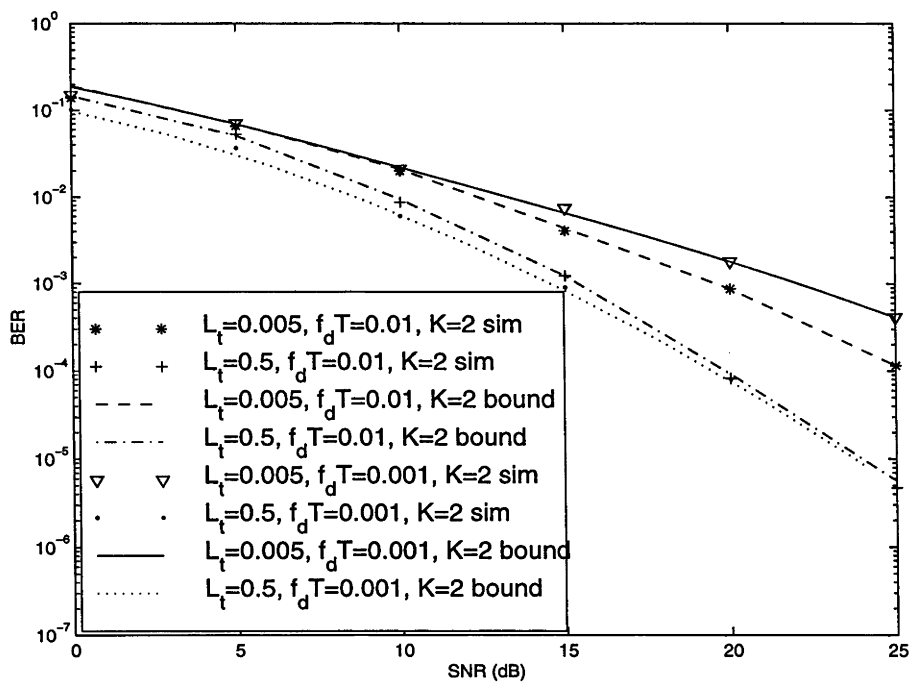


Figure 6.8: Effect on the MUKCIR receiver's BER of varying the Doppler and delay spreads, $r=2, N=4, P=2$

Predictor Based Multiuser Detection for Time Varying, Frequency Selective Rayleigh Channels

Overview: Multiuser detection is considered for linearly modulated signals (eg. asynchronous Code Division Multiple Access (CDMA) signals) sent over time varying, frequency selective Rayleigh fading channels. The multiuser maximum likelihood sequence detector (MLSD) using linear predictors is derived assuming knowledge of the channel second order statistics only, hence, the name Multiuser Known Channel Autocovariance (MUKCA) receiver. This receiver is appropriate when there is no pilot information and the channel's time varying impulse response cannot be accurately estimated. The receiver uses predictors to estimate the received signal and form a weighted Euclidean distance between the predicted and received samples. The computational complexity of this receiver grows exponentially with the number of users. To this end, we propose an additional single user receiver, SUKCA, that is constrained to track and lock to the signal of the desired user. Unlike the conventional single user receiver, it is optimised to take into account the structure of the multiple access interference (MAI). As an extension, we use similar techniques and propose a single user receiver, (SUKCIR) for the optimal receiver derived in chapter 6. An analysis of the multiuser receiver is also provided. We obtain tight bit error probability bounds using a truncated union bound approach.

7.1 Introduction

An optimal multiuser MLSD receiver, the MUKCIR receiver structure, was derived assuming perfect knowledge of the channel impulse response in chapter 6. In this chapter, we approach the same problem from a more practical perspective. We assume knowledge of the channel's second order statistics only (ie. the CIR is unavailable) and thus derive another MLSD receiver structure. Accordingly, the MLSD receiver will be known as the Multiuser Known Channel Autocovariance (MUKCA) receiver. However, due to its exponential computational complexity in the number of users, lower complexity suboptimal receivers are often sought in practice. Hence, we discuss an approach for designing a single user receiver that is computationally feasible yet can take into account properties of the multiple access interference (MAI) when making decisions. This receiver will be known as the Single User Known Channel Autocovariance (SUKCA) receiver.

Research in the design of such receivers can be classified into three main areas (see Fig. 7.1), namely 1) known CIR, 2) estimated CIR and 3) averaged CIR. A known CIR detector was discussed in chapter 6 where the channel was assumed completely known through the aid of a "genie". The decision rule can be written as

$$\hat{\mathbf{B}} = \arg \max_{\tilde{\mathbf{B}}} p(\mathbf{y} | \tilde{\mathbf{B}}, \mathbf{h}) \quad (7.1)$$

Detectors which attempt to estimate the CIR may use training symbols prior to transmission or no training symbols at all in which case they are classified as "blind". Blind receivers assume no *a priori* knowledge of the channel or any of its second order statistics. For detectors which estimate the CIR, the decision criterion is

$$\hat{\mathbf{B}} = \arg \max_{\tilde{\mathbf{B}}} p(\mathbf{y} | \tilde{\mathbf{B}}, \hat{\mathbf{h}}) \quad (7.2)$$

where $\hat{\mathbf{h}}$ is the estimated CIR vector (ie. the estimated parameter is used as if it were exact). Finally, detectors which average over the "nuisance" CIR make their decisions as

$$\hat{\mathbf{B}} = \arg \max_{\tilde{\mathbf{B}}} \int p(\mathbf{y} | \tilde{\mathbf{B}}, \mathbf{h}) p(\mathbf{h}) d\mathbf{h} \quad (7.3)$$

$$= \arg \max_{\tilde{\mathbf{B}}} p(\mathbf{y} | \tilde{\mathbf{B}}) \quad (7.4)$$

In the case of complex Gaussian channels, this averaging requires the channel autocovariance and noise variance. As before, these may be known (the MUKCA receiver) estimated or averaged over. This leads to a tree where at each level of the tree there is a known parameter, an estimated parameter and a parameter to be averaged over. Each node of the infinite tree is a possible realisation of a new receiver structure.

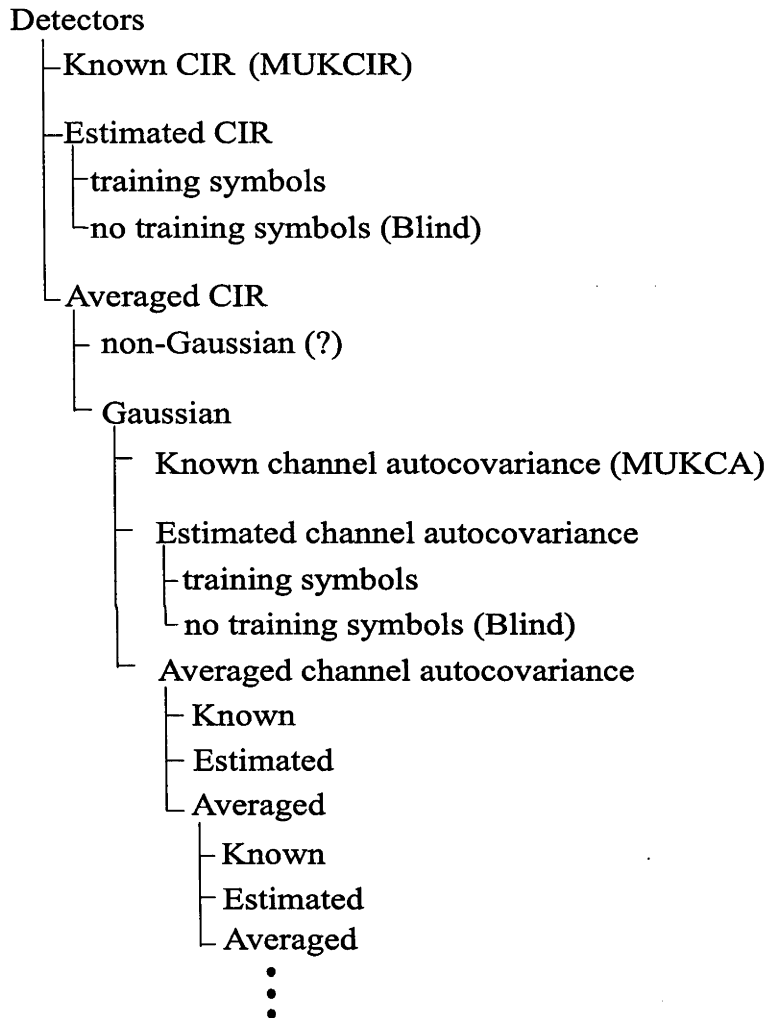


Figure 7.1: Different detector realisations

Our development of the receivers is based on a generalisation of Yu and Pasupathy [152] and of Hart and Taylor [49]. In time varying channels it is generally impossible to estimate the channel impulse response (CIR) exactly. The channel and noise autocovariances are generally more stationary than the CIR, so they can be accurately estimated from prior transmissions. Hence such receivers can actually be closely obtained.

Nonetheless, we do not explore how the Rayleigh channel's second order statistics can be estimated in a realistic situation. This is more clearly explained in [49]. The most practical method is via a long training sequence.

Yu and Pasupathy describe a receiver structure for the case of Rayleigh fading, independent diversity and ideal synchronisation. Hart and Taylor have extended this by relaxing the requirements for ideal carrier acquisition, symbol timing and Rayleigh fading. However, for our purposes it is important to note that at the heart of both their approaches, linear prediction is used to estimate the received signal. The receiver then forms a weighted Euclidean distance between the predicted and received samples, and this is used as a measure in the Viterbi Algorithm (VA) to reliably detect the (single) user's data.

Our formulation still results in an optimal receiver provided that only the received pulse and noise second order statistics are known. We propose it as a benchmark for other receivers operating in the same environment.

7.2 MUKCA Receiver Derivation

We consider the problem of detecting the K users' maximum likelihood transmitted sequences. Under the assumption that all the possible transmissions by each user over the interval under consideration are equally likely, the MLSD rule is one important criterion of optimality as discussed in section (5.16). MAP symbol detection is another. Thus the MLSD searches all allowed transmitted sequences and chooses the one with maximum likelihood, as

$$\hat{\mathbf{B}} = \arg \max_{\tilde{\mathbf{B}}} p(\mathbf{y} | \tilde{\mathbf{B}}) \quad (7.5)$$

$$= \arg \min_{\tilde{\mathbf{B}}} -\ln p(\mathbf{y} | \tilde{\mathbf{B}}) \quad (7.6)$$

That is the MLSD receiver requires as a metric the probability of observing the sequence of received samples \mathbf{y} , conditioned on the hypothesised symbols. Since the received signal samples, y_m , conditioned on \mathbf{B} , are complex Gaussian (because they are a linear combination of only the complex Gaussian random variables, $h_{i,k,m-irN}$ and n_m), we can

write

$$p(\mathbf{y} | \tilde{\mathbf{B}}) = \frac{1}{\det(2\pi\mathbf{R}_{yy})} \exp\left(-\frac{1}{2}\mathbf{y}^H \mathbf{R}_{yy}^{-1}(\tilde{\mathbf{B}})\mathbf{y}\right) \quad (7.7)$$

Hence the log-likelihood can be written as

$$-\ln p(\mathbf{y} | \tilde{\mathbf{B}}) = -\sum_{m=0}^{Y-1} \ln p(y_m | \tilde{\mathbf{B}}, \mathcal{Y}_{m-1}) \quad (7.8)$$

$$= \frac{1}{2}\mathbf{y}^H \mathbf{R}_{yy}^{-1}(\tilde{\mathbf{B}})\mathbf{y} + \ln(\det(2\pi\mathbf{R}_{yy}(\tilde{\mathbf{B}}))) \quad (7.9)$$

where $\mathbf{R}_{yy} = \frac{1}{2}E\{\mathbf{y}\mathbf{y}^H | \tilde{\mathbf{B}}\}$ as described in (5.51). \mathbf{R}_{yy} is positive definite if the noise is non-zero and so its inverse can be Cholesky decomposed as [152],

$$\mathbf{R}_{yy}^{-1}(\tilde{\mathbf{B}}) = \mathbf{A}^H(\tilde{\mathbf{B}})\mathbf{D}^{-1}(\tilde{\mathbf{B}})\mathbf{A}(\tilde{\mathbf{B}}) \quad (7.10)$$

where $\mathbf{A}(\tilde{\mathbf{B}})$ is a lower triangular forward prediction matrix with unity main diagonal entries,

$$\mathbf{A}(\tilde{\mathbf{B}}) = \begin{pmatrix} 1 & 0 & 0 & \cdots & 0 \\ -w'_{2,1}(\tilde{\mathbf{B}}) & 1 & 0 & \cdots & 0 \\ -w'_{3,2}(\tilde{\mathbf{B}}) & -w'_{3,1}(\tilde{\mathbf{B}}) & 1 & \cdots & 0 \\ \vdots & & & & \vdots \\ -w'_{I-1,I-1}(\tilde{\mathbf{B}}) & -w'_{I-1,I-2}(\tilde{\mathbf{B}}) & \cdots & & 1 \end{pmatrix} \quad (7.11)$$

and $2\mathbf{D}$ is a diagonal matrix, written as $2\mathbf{D} = \text{diag}(2\sigma_0^2, \dots, 2\sigma_{Y-1}^2)$.

Therefore (7.9) can be rewritten as

$$-\ln p(\mathbf{y} | \tilde{\mathbf{B}}) = \sum_{m=0}^{Y-1} \frac{|y_m - \sum_{l=1}^{m-1} w_{m,l}(\tilde{\mathbf{B}})y_{m-l}|^2}{2\sigma_m^2(\tilde{\mathbf{B}})} + \ln 2\pi\sigma_m^2(\tilde{\mathbf{B}}) \quad (7.12)$$

In a parallel derivation, we can expand the desired pdf of (7.6) by using the definition of

conditional probability repeatedly to obtain

$$p(\mathbf{y} | \tilde{\mathbf{B}}) = \prod_{m=0}^{Y-1} p(y_m | \tilde{\mathbf{B}}, \mathcal{Y}_{m-1}) \quad (7.13)$$

where $\mathcal{Y}_{m-1} = [y_0, \dots, y_{m-1}]^T$. Relying on the received samples' Gaussianity, this equals

$$-\ln p(\mathbf{y} | \tilde{\mathbf{B}}) = \sum_{m=0}^{Y-1} \left\{ \frac{|y_m - E\{y_m | \tilde{\mathbf{B}}, \mathcal{Y}_{m-1}\}|^2}{2\sigma_m^2(\tilde{\mathbf{B}})} + \ln 2\pi\sigma_m^2(\tilde{\mathbf{B}}) \right\} \quad (7.14)$$

Matching (7.12) up with (7.14), we identify that $E\{y_m | \tilde{\mathbf{B}}, \mathcal{Y}_{m-1}\}$ is calculated as the linear combination of past samples as

$$E\{y_m | \tilde{\mathbf{B}}, \mathcal{Y}_{m-1}\} = \sum_{l=1}^{m-1} w_{m,l}(\tilde{\mathbf{B}})y_{m-l} \quad (7.15)$$

where $w_{m,l}(\tilde{\mathbf{B}})$ is the l th tap for the ML predictor of y_m , given the hypothesised sequence and $2\sigma_m^2(\tilde{\mathbf{B}})$ is the variance of the error. It now remains to be shown that the conditional expectation $E\{y_m | \tilde{\mathbf{B}}, \mathcal{Y}_{m-1}\}$ is in fact the output of the best linear predictor, where y_m are samples of a random zero mean process that is complex Gaussian. First, the prediction error must satisfy the Orthogonality Principle (ie. the prediction error is orthogonal to past samples of the random process $y_{m-m'}$), as

$$\begin{aligned} \frac{1}{2}E\left\{ \left(y_m - \sum_{l=1}^W w_{m,l}(\tilde{\mathbf{B}})y_{m-l} \right) y_{m-m'}^* \right\} &= \\ \frac{1}{2}E(y_m y_{m-m'}^*) - \sum_{l=1}^W w_{m,l}(\tilde{\mathbf{B}}) \frac{1}{2}E(y_{m-l} y_{m-m'}^*) &= 0, \end{aligned} \quad (7.16)$$

Second, by comparison, the MMSE taps are designed to satisfy

$$w_{m,l}(\tilde{\mathbf{B}}) = \arg \min_{w_{m,l}(\tilde{\mathbf{B}})} \frac{1}{2} \left| y_m - \sum_{l=1}^W w_{m,l}(\tilde{\mathbf{B}})y_{m-l} \right|^2 \quad (7.17)$$

Differentiating (7.17) with respect to $w_{m,l}(\tilde{\mathbf{B}})$, and setting the result to zero we obtain a

system of W linear equations that identify the MMSE taps $w_{m,l}(\tilde{\mathbf{B}})$, as

$$\frac{1}{2}E\{y_m y_{m-l}^* + \sum_{m'} w_{m,m'}(\tilde{\mathbf{B}}) y_{m-l} y_{m-m'}^*\} = 0 \quad (7.18)$$

which is an identical system of equations to (7.15) Thus the conditional expectation is the output of a linear MMSE predictor, as (7.15).

$$\frac{y_m - E\{y_m | \tilde{\mathbf{B}}, \mathcal{Y}_{m-1}\}}{2\sigma_m^2(\tilde{\mathbf{B}})} \quad (7.19)$$

is the Innovations process. “Innovations” is used since the sequence comprises the unpredictable part of the random process. The expectation is computed by a predictor which takes a linear combination of the past samples.

Since rN samples are received every symbol interval, the log-likelihood can also be written in recursive form as

$$\Gamma_i(\tilde{\mathbf{B}}_i) = \Gamma_{i-1}(\tilde{\mathbf{B}}_{i-1}) + \lambda_i(\sigma_{i-1}, \sigma_i) \quad (7.20)$$

where

$$\Gamma_{i-1}(\tilde{\mathbf{B}}_{i-1}) = \sum_{m=0}^{irN-1} \left\{ \frac{|y_m - E\{y_m | \tilde{\mathbf{B}}, \mathcal{Y}_{m-1}\}|^2}{2\sigma_m^2(\tilde{\mathbf{B}})} + \ln 2\pi\sigma_m^2(\tilde{\mathbf{B}}) \right\} \quad (7.21)$$

$$\lambda_i(\sigma_{i-1}, \sigma_i) = \sum_{m=irN}^{(i+1)rN-1} \left\{ \frac{|y_m - E\{y_m | \tilde{\mathbf{B}}, \mathcal{Y}_{m-1}\}|^2}{2\sigma_m^2(\tilde{\mathbf{B}})} + \ln 2\pi\sigma_m^2(\tilde{\mathbf{B}}) \right\} \quad (7.22)$$

It can be clearly seen from (7.15) that the predictor tap weights $w_{m,l}(\tilde{\mathbf{B}})$ depend on its infinite past history of transmitted symbols. This is not very practical since the receiver then has a complexity which increases exponentially with time. In order to fix the complexity of the receiver it is necessary to make $w_{m,l}(\tilde{\mathbf{B}})$ depend only on its finite past history. This is achieved by providing the predictors with a fixed number of finite past samples, W . Accordingly, we can now approximate $E\{y_m | \tilde{\mathbf{B}}, \mathcal{Y}_{m-1}\}$ by $E\{y_m | \tilde{\mathbf{B}}, \hat{\mathcal{Y}}_{m-1}\}$ where $\hat{\mathcal{Y}}_{m-1} = [y_{m-W}, \dots, y_{m-1}]^T$ and W is the order of the truncated predictor [152].

The quantity $2\sigma_m^2(\tilde{\mathbf{B}})$ is reinterpreted as the variance of this suboptimal prediction error. The prediction, predictor tap weights and the prediction error variances are computed according to

$$E \left\{ y_m \mid \tilde{\mathbf{B}}, \hat{\mathbf{y}}_{m-1} \right\} = \mathbf{w}_m^T(\tilde{\mathbf{B}}) \hat{\mathbf{y}}_m \quad (7.23)$$

$$\mathbf{R}_{yy,m}(\tilde{\mathbf{B}}) \mathbf{w}_m^H(\tilde{\mathbf{B}}) = \mathbf{r}_{yy,m}(\tilde{\mathbf{B}}) \quad (7.24)$$

$$\sigma_m^2(\tilde{\mathbf{B}}) = (\mathbf{R}_{yy}(\tilde{\mathbf{B}}))_{m,m} - \mathbf{w}_m^H(\tilde{\mathbf{B}}) \mathbf{r}_{yy,m}(\tilde{\mathbf{B}}) \quad (7.25)$$

where

$$\mathbf{R}_{yy,m}(\tilde{\mathbf{B}}) = \frac{1}{2} E \left\{ \hat{\mathbf{y}}_m \hat{\mathbf{y}}_m^H \mid \tilde{\mathbf{B}} \right\} \quad (7.26)$$

$$\mathbf{r}_{yy,m}(\tilde{\mathbf{B}}) = \frac{1}{2} E \left\{ \hat{\mathbf{y}}_m y_m^* \mid \tilde{\mathbf{B}} \right\} \quad (7.27)$$

$$\mathbf{w}_m = [w_{m,1}, \dots, w_{m,W}]^H \quad (7.28)$$

Therefore $E \left\{ y_m \mid \tilde{\mathbf{B}}, \mathcal{Y}_{m-1} \right\}$ is now approximated by the truncated prediction,

$$E \left\{ y_m \mid \tilde{\mathbf{B}}, \hat{\mathbf{y}}_{m-1} \right\} = \sum_{l=1}^W w_{m,l}(\tilde{\mathbf{B}}) y_{m-l} \quad (7.29)$$

having the prediction error

$$\sigma_m^2(\tilde{\mathbf{B}}) = E \left(y_m^2 \mid \tilde{\mathbf{B}}, \hat{\mathbf{y}}_{m-1} \right) - \sum_{l=1}^W w_{m,l}^*(\tilde{\mathbf{B}}) E \left(y_m y_{m-l}^* \mid \tilde{\mathbf{B}} \right) \quad (7.30)$$

The log-likelihood metric can now be approximated by the finite complexity predictor

$$\Gamma_i(\tilde{\mathbf{B}}_i) = \Gamma_{i-1}(\tilde{\mathbf{B}}_{i-1}) + \lambda_i(\sigma_{i-1}, \sigma_i) \quad (7.31)$$

where

$$\Gamma_{i-1}(\tilde{\mathbf{B}}_{i-1}) = \sum_{m=0}^{irN-1} \left\{ \frac{|y_m - E\{y_m | \tilde{\mathbf{B}}, \hat{\mathbf{y}}_{m-1}\}|^2}{2\sigma_m^2(\tilde{\mathbf{B}})} + \ln 2\pi\sigma_m^2(\tilde{\mathbf{B}}) \right\} \quad (7.32)$$

$$\lambda_i(\sigma_{i-1}, \sigma_i) = \sum_{m=irN}^{(i+1)rN-1} \left\{ \frac{|y_m - E\{y_m | \tilde{\mathbf{B}}, \hat{\mathbf{y}}_{m-1}\}|^2}{2\sigma_m^2(\tilde{\mathbf{B}})} + \ln 2\pi\sigma_m^2(\tilde{\mathbf{B}}) \right\} \quad (7.33)$$

Past symbols and the state matrix are defined as

$$\tilde{\mathbf{B}}_{i-1} = \begin{pmatrix} \tilde{b}_{0,1} & \tilde{b}_{0,K} \\ \vdots & \vdots \\ \tilde{b}_{i-1,1} & \tilde{b}_{i-1,K} \end{pmatrix} \quad \sigma_i = \begin{pmatrix} \tilde{b}_{i-L+2,1} & \cdots & \tilde{b}_{i-L+2,K} \\ \vdots & & \vdots \\ \tilde{b}_{i,1} & & \tilde{b}_{i,K} \end{pmatrix} \quad (7.34)$$

The branch metric $\lambda_i(\sigma_{i-1}, \sigma_i)$ is a function of L hypothesised sequences where $L = \lceil W/rN \rceil + L_h$. The number of states in a multiuser trellis is $M^{K(L-1)}$ and the number of branches M^{KL} . These are fixed and finite due to restricting the predictor and ISI lengths to L symbol periods. This trellis search is done most efficiently by the Viterbi algorithm.

The path metric for the i th symbol is computed based only on the path metric's current state σ_{i-1} and the next state σ_i . Note that the predictions are being computed on-line; the predictor coefficients are however, precomputed. Note however, that for long codes, \mathbf{R}_{yy} in (7.27) change every symbol period, even if the data sequence does not. Therefore, different prediction coefficients are needed every sample and it is infeasible to precompute them. A better, but still infeasible, strategy is to compute them on the fly.

7.3 SUKCA Receiver Derivation

Due to the prohibitive complexity of the MUKCA receiver, we investigate a simplified version of MUKCA, whose complexity is linear with respect to the number of users. A single user approach is studied whereby the receiver is constrained to track and lock to the signal of the desired user. Unlike the conventional single user receiver, it is optimised to take into account the colouration of the MAI. The received signal is given by (5.46). The contributions from the interfering users ($k = 2, \dots, K$) are grouped with the additive

noise as

$$y_m = \sum_{i=-L_h+1+\lfloor m/rN \rfloor}^{\lfloor m/rN \rfloor} b_{i,1} h_{i,1,m-irN} + \sum_{k=2}^K \sum_{i=-L_h+1+\lfloor m/rN \rfloor}^{\lfloor m/rN \rfloor} b_{i,k} h_{i,k,m-irN} + n_m \quad (7.35)$$

The simplification comes when we assume that the latter two terms comprise coloured Gaussian noise without further structure. The MAI plus Gaussian noise equals

$$v_m = \sum_{i=-L_h+1+\lfloor m/rN \rfloor}^{\lfloor m/rN \rfloor} \sum_{k=2}^K b_{i,k} h_{i,k,m-irN} + n_m \quad (7.36)$$

with autocovariance equal to

$$\begin{aligned} (\mathbf{R}_{vv})_{m,m'} &= \frac{1}{2} E\{v_m v_{m'}^*\} \\ &= \sum_{i=-L+1+\lfloor m/rN \rfloor}^{\lfloor m/rN \rfloor} \sum_{k=2}^K \sum_{i'=-L+1+\lfloor m'/rN \rfloor}^{\lfloor m'/rN \rfloor} \sum_{k'=2}^K \\ &\quad E\{b_{i,k} b_{i',k'}^*\} \frac{1}{2} E\{h_{i,k,m-irN} h_{i',k',m'-i'rN}^*\} + \frac{1}{2} E\{n_m n_{m'}^*\} \\ &= \sum_{i=-L+1+\lfloor m/rN \rfloor}^{\lfloor m/rN \rfloor} \sum_{k=2}^K \frac{1}{2} E\{h_{i,k,m-irN} h_{i,k,m'-i'rN}^*\} + \frac{1}{2} E\{n_m n_{m'}^*\} \quad (7.37) \end{aligned}$$

since the crosscorrelation of the interfering users' bits is unity if they match in time i and user k otherwise zero. Define the vector $\tilde{\mathbf{B}}_{SU} = (\mathbf{B})_{i,1}$ as the first column in $\tilde{\mathbf{B}}$ so that it only contains only the desired user's transmitted symbols. Assuming that the MAI is Gaussian, the MLSD decision rule for $\tilde{\mathbf{B}}_{SU}$ can be written as

$$\tilde{\mathbf{B}}_{SU} = \arg \min_{\tilde{\mathbf{B}}_{SU}} \frac{1}{2} \mathbf{y}^H \mathbf{R}_{yy}^{-1}(\tilde{\mathbf{B}}_{SU}) \mathbf{y} + \ln(\det(2\pi \mathbf{R}_{yy}(\tilde{\mathbf{B}}_{SU}))) \quad (7.38)$$

where the received signal autocorrelation $\mathbf{R}_{yy}(\tilde{\mathbf{B}}_{SU})_{m,m'}$ is given by

$$\begin{aligned} \frac{1}{2} E\{y_m y_{m'}^* | \tilde{\mathbf{B}}_{SU}\} &= \sum_{i=-L_h+1+\lfloor m/rN \rfloor}^{\lfloor m/rN \rfloor} \sum_{i'=-L_h+1+\lfloor m'/rN \rfloor}^{\lfloor m'/rN \rfloor} \\ &\quad b_{i,1} b_{i',1}^* \frac{1}{2} E\{h_{i,1,m-irN} h_{i',1,m'-i'rN}^*\} + (\mathbf{R}_{vv})_{m,m'} \quad (7.39) \end{aligned}$$

As with (7.22) this may be Cholesky factorised, and the sequence metric of (7.38) converted to a recursive path plus branch metric, processed by the VA with a considerably reduced number of states, namely M^{L-1} , where $L = L_h + \lceil W/rN \rceil$. For example, a full state MUKCA receiver with 10 users and a memory length of 3, where $L_h = 2$ and $W = rN$) has 2^{20} states and 2^{30} branches. For a single user receiver, there are 4 states and 8 branches in all. Moreover, in practice a viable reduced complexity receiver can retain fewer survivor sequences during the trellis search. Of course, this reduction in complexity comes at a cost of an increased BER.

7.3.1 The SUKCIR Receiver Derivation

The ideas presented in section 7.3 can also be applied to the MUKCIR receiver to derive a single user receiver with substantially reduced complexity, the single user known channel impulse response (SUKCIR) receiver. However, the MUKCIR receiver omits the noise whitening operation in white noise and so, applying the ideas of section 7.3 will appear to be more complex. The received signal may be written as

$$y_m = \sum_{i=-L_h+1+\lfloor m/rN \rfloor}^{\lfloor m/rN \rfloor} b_{i,1} h_{i,1,m-irN} + v_m \quad (7.40)$$

Using the same steps as in 7.2, the sequence metric may be derived as

$$\begin{aligned} \Gamma(\tilde{\mathbf{B}}) &= \sum_{l=0}^{Y-1} \sum_{m=0}^{Y-1} \left(y_m^* - \sum_{i=-L+1+\lfloor m/rN \rfloor}^{\lfloor m/rN \rfloor} \tilde{b}_{i,1}^* h_{i,1,m-irN}^* \right) \times \\ &\quad (\mathbf{R}_{vv}^{-1})_{l,m} \left(y_l - \sum_{i'=-L+1+\lfloor l/rN \rfloor}^{\lfloor l/rN \rfloor} \tilde{b}_{i',1} h_{i',1,l-i'rN} \right) \\ &= \sum_{i=-L+1+\lfloor m/rN \rfloor}^{\lfloor m/rN \rfloor} 2\text{Re}\{\tilde{b}_{i,1} m_{i,1}\} - \sum_{i=-L+1+\lfloor m/rN \rfloor}^{\lfloor m/rN \rfloor} \sum_{i'=-L+1+\lfloor l/rN \rfloor}^{\lfloor l/rN \rfloor} \tilde{b}_{i,1}^* f_{i,i',1,1} \tilde{b}_{i,1} \end{aligned}$$

where

$$m_{i,1} = \sum_{l=0}^{Y-1} \sum_{m=0}^{Y-1} y_l (\mathbf{R}_{vv}^{-1})_{l,m} h_{i,1,m-irN}^* \quad (7.41)$$

$$f_{i,i',1,1} = \sum_{l=0}^{Y-1} \sum_{m=0}^{Y-1} h_{i,1,m-irN}^* (\mathbf{R}_{vv}^{-1})_{l,m} h_{i',1,l-i'rN} \quad (7.42)$$

It is important to note that the computation of \mathbf{R}_{vv}^{-1} in the previous equation is prohibitively difficult, since it does not have finite span in general. Accordingly to contain the complexity, we must employ the same technique as in section 7.2. \mathbf{R}_{vv}^{-1} is Cholesky factored, interpreted as a MMSE predictor with an increasing number of taps, then reinterpreted as a MMSE predictor using a fixed number of past samples, W . By restricting L to $L_h + \lceil W/rN \rceil$ we may proceed as per section 7.2 to compute the log-likelihood metric. However, we do not pursue this any further since our motivation for studying the MUK-CIR receiver was to devise an absolute benchmark, not for obtaining an implementable receiver.

7.4 Receiver Operation

The predictions of (7.29) are being computed during detection and are therefore evolving with the channel. However, for stationary channels and short codes the *predictor tap weights* are invariant and may be precomputed. The calculation of the branch metric is shown more clearly in Figure 7.2. For each symbol interval, rN received samples are admitted into the receive buffer one by one. Each sample, y_m , is estimated via the prediction $E \{ y_m \mid \tilde{\mathbf{B}}, \hat{\mathbf{y}}_{m-1} \}$ using the precalculated predictor coefficients. These are used in computing a scaled, squared Euclidean distance plus a bias term which is then summed over all rN samples of the symbol period. This forms the branch metric of each state.

7.5 Receiver Analysis

In this section the MUKCA receiver's BER is analysed for a *fast*, time varying frequency selective Rayleigh fading channel in white noise. Once again as in chapter 6, let \mathbf{B} be the matrix of transmitted symbols and $\tilde{\mathbf{B}}$ be the matrix of detected symbols. An error event

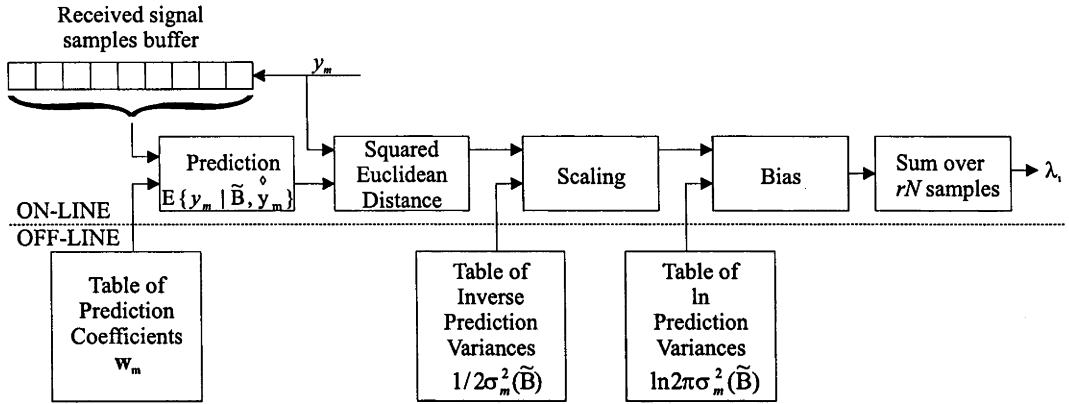


Figure 7.2: Branch metric computation

occurs when an erroneous detected sequence has a greater likelihood than the transmitted sequence. An error event of length ee starts at symbol t_e and stops at $t_e + ee$. Only the dominant short error events are considered. In a fast fading situation the dominant error events are short, and hence the truncated bound can neglect longer error events. On the other hand, for a very slow fading channel, it is not valid to neglect the longer error events since most errors occur in deep fades and persist for hundreds of symbols at reasonable SNRs. The BER can be upper bounded by

$$BER \leq \sum_{\mathbf{B}} \sum_{\tilde{\mathbf{B}}} \frac{P(\mathbf{B})P(\mathbf{B} \rightarrow \tilde{\mathbf{B}})w(\mathbf{B} \rightarrow \tilde{\mathbf{B}})}{K \log_2 M} \tag{7.43}$$

where $P(\mathbf{B})$ is the transmission probability, $P(\mathbf{B} \rightarrow \tilde{\mathbf{B}})$ is the probability that the erroneous sequence is detected above the the transmitted sequence and $w(\mathbf{B} \rightarrow \tilde{\mathbf{B}})$ indicates the number of bit errors in the error event.

Define the normalised predictor tap weights as

$$\tilde{e}_{m,l} = \begin{cases} \frac{1}{\sqrt{2\sigma_m(\tilde{\mathbf{B}})}}, l = 0 \\ \frac{-w_{m,l}(\tilde{\mathbf{B}})}{\sqrt{2\sigma_m(\tilde{\mathbf{B}})}}, l = 1..W \end{cases} \tag{7.44}$$

and

$$e_{m,l} = \begin{cases} \frac{1}{\sqrt{2\sigma_m(\mathbf{B})}}, l = 0 \\ \frac{-w_{m,l}(\mathbf{B})}{\sqrt{2\sigma_m(\mathbf{B})}}, l = 1..W \end{cases} \quad (7.45)$$

Define the ratio of the bias terms as

$$\kappa_{min} = \sum_{m=0}^{Y-1} \ln \left(\frac{\sigma_m^2(\tilde{\mathbf{B}})}{\sigma_m^2(\mathbf{B})} \right) \quad (7.46)$$

Then the pairwise probability of error is given by

$$\begin{aligned} P(\mathbf{B} \rightarrow \tilde{\mathbf{B}}) &= \\ &P \left(\sum_{m=0}^{Y-1} \frac{|y_m - E\{y_m | \mathbf{B}, \mathcal{Y}_m\}|^2}{2\sigma_m^2(\mathbf{B})} + \ln(2\pi\sigma_m^2(\mathbf{B})) > \right. \\ &\quad \left. \sum_{m=0}^{Y-1} \frac{|y_m - E\{y_m | \tilde{\mathbf{B}}, \mathcal{Y}_m\}|^2}{2\sigma_m^2(\tilde{\mathbf{B}})} + \ln(2\pi\sigma_m^2(\tilde{\mathbf{B}})) \right) \\ &= P \left(\sum_{m=0}^{Y-1} \frac{|y_m - \sum_{m'=1}^W w_{m,m'}(\mathbf{B})y_{m-m'}|^2}{2\sigma_m^2(\mathbf{B})} + \ln(2\pi\sigma_m^2(\mathbf{B})) > \right. \\ &\quad \left. \sum_{m=0}^{Y-1} \frac{|y_m - \sum_{m'=1}^W w_{m,m'}(\tilde{\mathbf{B}})y_{m-m'}|^2}{2\sigma_m^2(\tilde{\mathbf{B}})} + \ln(2\pi\sigma_m^2(\tilde{\mathbf{B}})) \right) \\ &= P \left(\sum_{m=0}^{Y-1} \left| \sum_{m'=0}^W e_{m,m'} y_{m-m'} \right|^2 - \left| \sum_{m'=0}^W \tilde{e}_{m,m'} y_{m-m'} \right|^2 > \kappa_{min} \right) \\ &= P \left(\sum_{m=0}^{Y-1} \sum_{m_1=0}^W \sum_{m_2=0}^W [\tilde{e}_{m,m_1} \tilde{e}_{m,m_2}^* - e_{m,m_1} e_{m,m_2}^*] y_{m-m_1} y_{m-m_2}^* > \kappa_{min} \right) \quad (7.47) \end{aligned}$$

We define κ as the left hand side of the inequality in (7.47). It is a Gaussian quadratic

function in y_m with a Hermitian symmetric matrix kernel, \mathbf{Y} defined implicitly by (7.47).

$$\kappa = \mathbf{y}_e^H \mathbf{Y} \mathbf{y}_e \quad (7.48)$$

$$\mathbf{y}_e = [y_{-W}, \dots, y_{(L+ee-1)rN-1+W}] \quad (7.49)$$

The entries in the autocovariance matrix \mathbf{R}_{yy} are given by (5.51) and the characteristic function of κ is thus given by

$$C(\xi) = \det(\mathbf{I} - j2\xi \mathbf{R}_{yy} \mathbf{Y})^{-1} \quad (7.50)$$

From standard residue calculus, the pairwise probability of error equals [49]

$$P(\mathbf{B} \rightarrow \tilde{\mathbf{B}}) = 1 - \sum_{i, \Im\{p_i\} > 0} \exp(-jp_i \kappa_{min}) \prod_{k=1, k \neq i} \frac{1}{(1 - p_i/p_k)} \quad (7.51)$$

for $\kappa_{min} \leq 0$ and

$$P(\mathbf{B} \rightarrow \tilde{\mathbf{B}}) = 1 + \sum_{i, \Im\{p_i\} > 0} \exp(-jp_i \kappa_{min}) \prod_{k=1, k \neq i} \frac{1}{(1 - p_i/p_k)} \quad (7.52)$$

for $\kappa_{min} \geq 0$ where p_i is the i th pole of (7.50).

The single user receivers may be analysed following a similar approach. In this special case, the normalised predictor tap weights $e_{m,l}$, and the variance of the prediction error $\sigma_m^2(\tilde{\mathbf{B}})$ in (7.47), defined explicitly in terms of $w_{m,l}(\tilde{\mathbf{B}})$ in (7.44) and (7.30), are replaced by the single user quantities $w_{m,l}$ and $e_{m,l}$ obtained from (7.39).

7.6 Numerical Results

This section provides an overview of the two proposed receivers' performances for a variety of transmitter, channel and receiver parameters. It is not possible to explore all combinations of such parameters; instead we highlight the influence of a particular parameter by keeping all others fixed. The baseline signal model is chosen as follows. The DS-CDMA transmitter uses a root raised cosine chip pulse shape truncated to 1.5 chip

periods with 30% excess bandwidth, with a random signature sequence comprising of 5 chips. Two users are transmitting (to keep complexity low). The channel comprises $P = 2$ equally spaced paths with equal mean power. The delay spread is $L_\tau = 0.5$. The Doppler spectra of the simulated fading processes closely approximate Jakes model (the $J_0(2\pi f_D \Delta t)$ model) with $f_D T = 0.1$ (ie. fast fading). The receiver takes $r = 2$ samples per chip period and uses $W = 10$ taps for the predictor. Note that the simulations have been done using fixed but randomly selected codes. Codes with better crosscorrelation properties will normally be used and accordingly, the graphs shown represent “moderate” performance.

Fig. 7.3 shows the graceful BER degradation of the MUKCA receiver as the number of users increases. The analytic bounds agree well with the simulations. To make the simulation/analysis complexity manageable a maximum of 3 users were simultaneously active.

Fig. 7.4 shows that the effect of increasing the number of multipaths. If the channel impulse response were known ideally the receiver’s performance would improve with each additional path due to the additional implicit delay diversity available. However, for the MUKCA receiver this improvement in BER is not significant for the SNRs shown, although it appears that there may be at higher SNRs (for predictor receivers, a steepening in the BER curve is usually headed by an initial flattening).

In Fig. 7.5 it is the delay spread that is varied. The performance degrades slightly with the addition of new users. For the larger delay spreads of half a symbol period, the receiver performs remarkably well at high SNR, with an implicit diversity gain of 5dB.

Fig. 7.6 show similar results, and as before, it is interesting to note that the MUKCA adapts well to a slower fading rate. For the more extreme channel, the implicit diversity is lost, since accurate prediction is difficult. The slowly fading channel is predicted more easily and the delay spread offers significant gains. When there is considerable Doppler and delay diversity together, it becomes difficult to distinguish the data from the highly distorted received signal and performance degrades (for the value of W chosen).

Fig. 7.7 shows the effect on the BER performance of increasing the number of active users. Both the KCA receivers show graceful degradations in the BER as the number

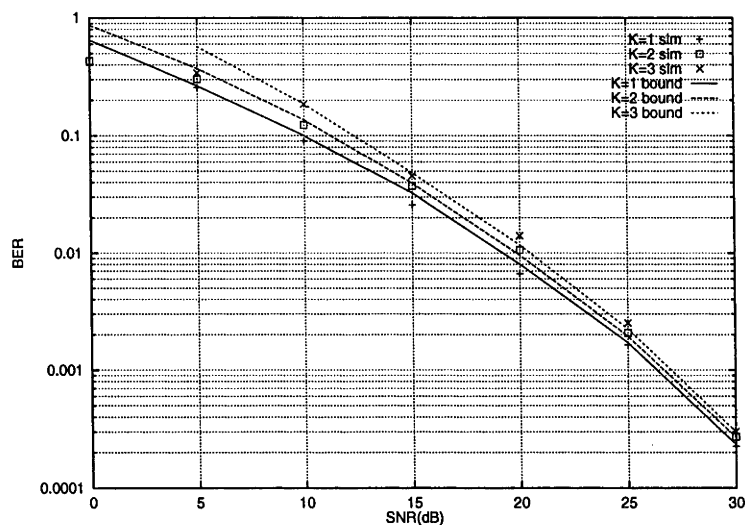


Figure 7.3: BER-SNR curves of the MUKCA receiver for a fast time varying frequency selective channel where $f_D T_s = 0.1$, $L_r T_s = 0.5 T_s$, $r = 2$, $N = 5$, $P = 2$

of users increase. The dramatic reduction in the SUKCA's computational complexity outweighs its slight BER degradation.

Fig. 7.8 studies the effect of truncating the predictor taps to contain the complexity of the receiver designs. For very short predictors the receiver's performance reaches a high BER floor. As the number of predictor taps increase, the BER floor diminishes. For $K = 2$ users, $r = 2$ samples per T_c , $N = 5$ chips and at moderate to high SNRs $W \geq 7$ is sufficient. Proper choice of W will depend from case to case and in general as the number of users increase, W will also grow.

7.7 Summary

This chapter proposed two receivers for linearly modulated or DS-CDMA signals sent over a time varying frequency selective channel. The complexity of the multiuser known channel autocovariance (MUKCA) receiver grows exponentially with the number of users. As a result, we propose a linear complexity receiver which is able to exploit the structure of the MAI when making decisions. Both receivers provide useful tradeoff between *a priori* information, performance and complexity. An analysis of the optimal receiver is also provided which shows good agreement with simulation.

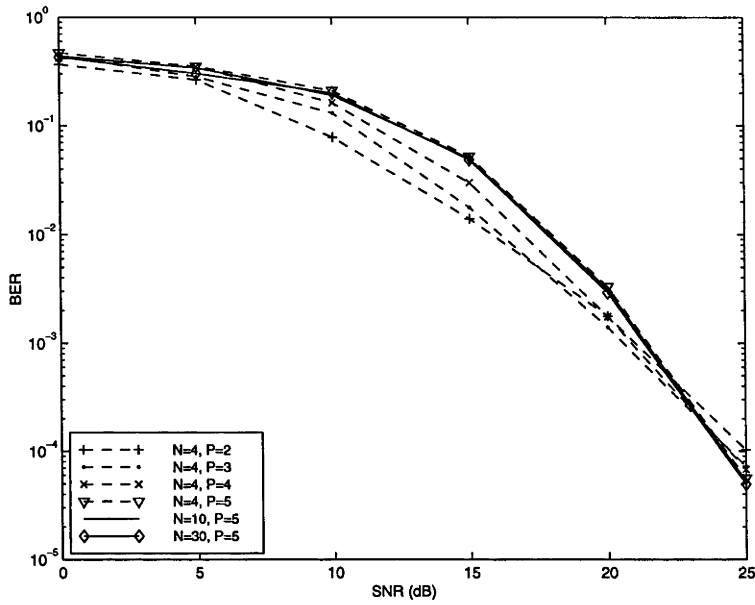


Figure 7.4: Effect on the MUKCA receiver's BER of varying the number of independent paths, P , where $r = 2, N = 4, L_{\tau}T_s = 0.5T_s, f_D T_s = 0.01$

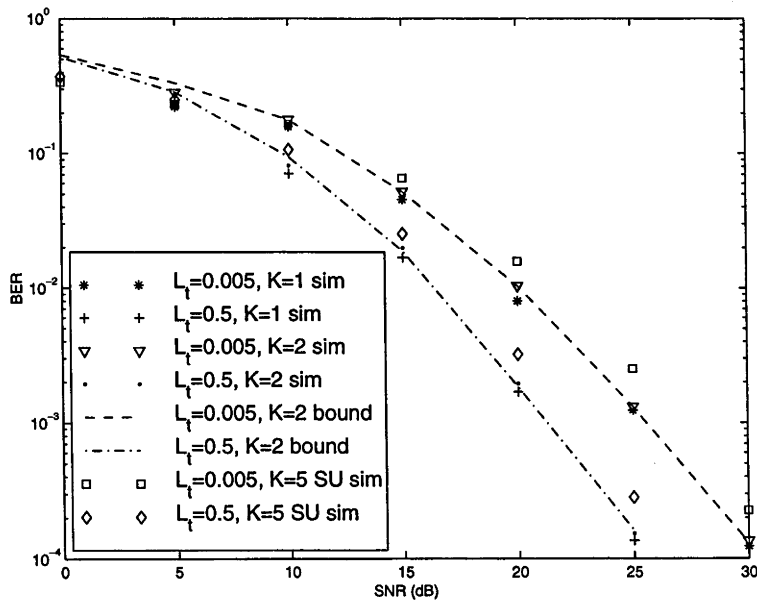


Figure 7.5: Effect on the MUKCA receiver's BER for varying delay spreads, where $f_D T_s = 0.01$ and $P = 2$

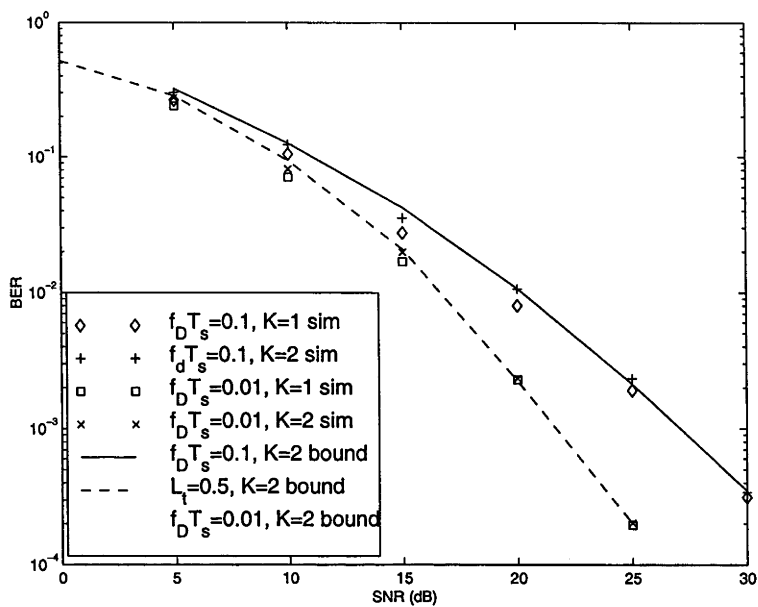


Figure 7.6: Effect on the MUKCA receiver's BER for varying Doppler spreads, where $L_\tau T_s = 0.5T_s, P = 2$

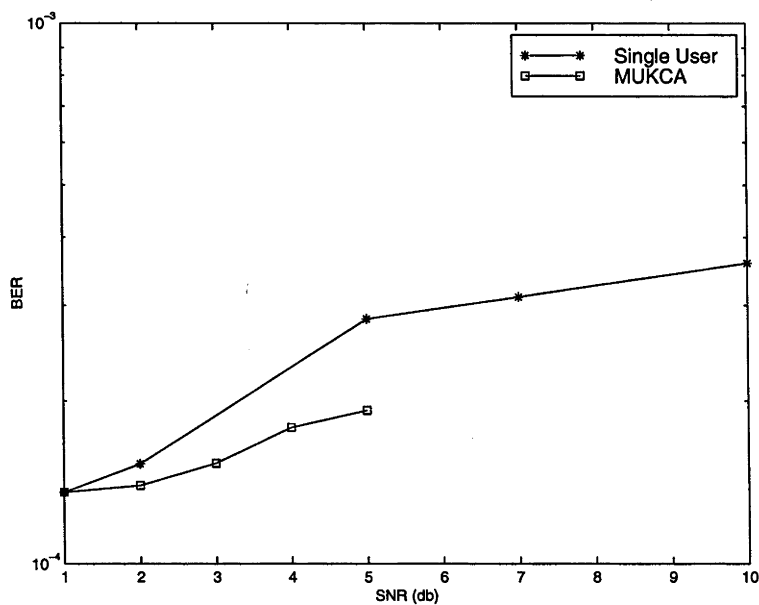


Figure 7.7: Effect of the single user and MUKCA receiver's BER for varying the number of users, where $L_\tau T_s = 0.5T_s, f_D T_s = 0.01, SNR = 25dB$

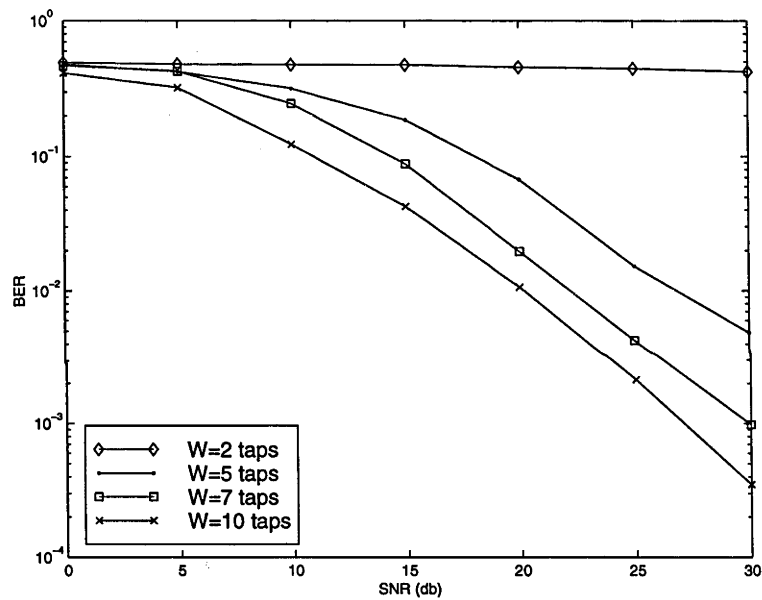


Figure 7.8: Effect of the MUKCA receiver's BER for different predictor lengths, W , where $K = 2$

Conclusion

8.1 Achievements

The performance evaluation of CDMA for a range of channel models and receiver complexities is an important research topic for mobile communications systems. The author has contributed to the area directly.

To date the effectiveness of a multiuser CDMA system has always been ascertained by comparing its performance to that of a single user system. Driven by the need to find a more accurate benchmark, an efficient method is proposed in chapter 3 to compute tight bit error rate performance bounds. Applying the well known union bounding technique, upper and lower bounds were obtained for both synchronous and asynchronous systems in Gaussian noise channels. It was observed that as the number of users exceeded the processing gain there is a graceful degradation in the BER for optimum multiuser detection. This method is finally applied to obtain a lower bound for the slow frequency flat Rayleigh fading channel. The technique was found to be relatively fast and simple to use. However, it is important to note that the method relies on perfect knowledge of the channel parameters and signature sequences of all users.

Our understanding of the value of applying error control coding to the CDMA channel has been limited to date. The author investigates several important properties of the minimum squared Euclidean distance for a coded multiuser system in chapter 4. The minimum distance is (a) indicative of the error correcting capability of the system and (b) it determines the performance of the system at asymptotically high signal to noise ratios. It was proved that the upper bound on the minimum squared Euclidean distance for a multiuser system is the same as that of a single user system provided all users use

trellis codes with the same constraint length, number of input bits and mapping sets. This has implications which warrant further research into the design of error control code and signature sequences in a joint fashion. The impact of non orthogonal signature sequences on d_{min}^2 was investigated next. More specifically, we studied the ratio of the squared minimum distance between a non orthogonal system and an interference free system. This resulted in the computation of tight asymptotic efficiency bounds for both synchronous and asynchronous coded systems. Finally it was shown that the minimum Euclidean distance for a convolutional coded synchronous multiuser system is no less than the product of the free distance and the minimum distance of the corresponding uncoded synchronous multiuser system. This provides a quick way of computing d_{min}^2 .

While Part I investigated techniques to evaluate the performance of both uncoded and coded multiuser systems for Gaussian channels, Part II of the thesis was devoted to the design of receiver structures for the more general time varying frequency selective Rayleigh fading channel. A brief introduction to the modelling of such a channel was discussed in chapter 5. Two novel receiver structures have been designed, simulated and analysed. The first, the MUKCIR receiver, is the multiuser MLSD receiver structure with perfect knowledge of the channel and signature sequence of all users and involves matched filtering. The second, the MUKCA receiver, assumes, more realistically, knowledge of the channel's second order statistics, and makes use of linear prediction.

The MUKCIR receiver is the optimal receiver structure for the time varying, frequency selective Rayleigh channel. Accordingly, its performance is a benchmark for other receivers. However, it is exponential in the complexity with respect to the number of users. The main advantage of this receiver is its ability to jointly exploit relatively small Doppler and delay spreads and transform them into substantial dB gains. The receiver's BER is also bounded for the fast Rayleigh fading frequency selective channel. Under fast fading environments, it was found that the error events which contributed most to the union bound were relatively short.

The MUKCA receiver is also an optimal multiuser receiver in the absence of *a priori* knowledge about the channel impulse response. Similarly it acts as a benchmark for other receiver structures. This receiver predicts the received signal and forms a weighted Euclidean distance between these predicted and received samples. Once again the computational complexity grows exponentially with the number of users. The receiver's BER

is bounded and the analysis shows good agreement with simulations. A comprehensive set of BER results shows that the receiver is capable of exploiting the implicit Doppler and delay diversity in fast fading. As a means to reduce complexity a single user linear complexity receiver, the SUKCA receiver, was proposed. It takes into account the structure of the multiple access interference when making decisions, unlike the conventional single user detector.

Finally, a suboptimal multiuser detector that used a sequential decoding algorithm was presented. The traditional metric function (Fano's metric) was modified using a Gaussian approximation method to enable the computation of the metric efficiently for a synchronous CDMA system with a large number of users. The improved receiver's performance was obtained using computer simulations. It was found that this detector achieved results comparable to the optimal receiver with much reduced complexity.

8.2 Future Research

This thesis can be extended in many directions. A number of future research directions are listed as follows.

- Equation (4.4.3) computes the minimum Euclidean distance for a convolutionally coded, synchronous multiuser system. It remains to be seen if it can be generalised to trellis coded synchronous multiuser systems with a higher dimensional signalling constellation.
- In general the technique developed in chapter 3 for computing d_{min}^2 for uncoded multiuser systems could be applied to the case of a large number of users. However, as seen in the numerical results section of chapter 4, it was only possible to compute $d_{min,i}^2$ for a maximum of 3 users using error control coding. This can be attributed to the cut-off threshold T being much larger for coded systems. Improved algorithms need to be devised to accommodate more users in a realistic situation. In all our studies we have assumed that the receiver has perfect knowledge of timing, channel information and correlation between spreading waveforms. Relaxing some of these assumptions would make it difficult if not impossible to compute the partial distance spectrum. Further research is required in this direction to find

appropriate methods to compute tight upper bounds.

- Chapter 6 and 7 have not addressed the issue of error control coding. This can significantly enhance the receivers' BER. Furthermore, this thesis has ignored the presence of multiple antennae (in particular directional antennae) as an added means of diversity. The benefits of multiple antennae in a single user context are considerable [48]; however, at the expense of additional complexity.
- Two single user receivers were proposed in chapter 7 each with an attractive complexity relative to their corresponding multiuser receivers. The analysis of these receivers is a direct extension of the techniques provided for multiuser receivers.
- We have not investigated any "blind" receiver structures for the fast fading, frequency selective channel. Sub-space based or CMA algorithms have shown promise in the design of blind linear complexity multiuser receivers. This has generally been applied to slow fading channels. Research on the applicability of these algorithms to the fast fading frequency selective channel merits further investigation.
- Last but not least the author has worked on change detection algorithms for a very general teletraffic model (see Appendix B). Presently, CDMA systems overcome multiple access interference by taking advantage of knowledge of the cross correlations between the desired user's code and all other users' codes with a multiuser detector. This implies that the detector knows which users are active. However, knowing which users are active is difficult when users are constantly entering and leaving the system. The author is currently investigating techniques developed in Appendix B to detect a new user and estimate that user's parameters so that they can be incorporated into a multiuser detector.

A Suboptimal Multiuser CDMA Receiver Using Sequential Decoding

Overview: This chapter considers the application of sequential decoding to the detection of data transmitted over the additive white Gaussian noise channel by K synchronous transmitters using direct sequence spread spectrum multiple access (DS-SSMA). A modification of Fano's sequential decoding metric is derived using a Gaussian approximation (GA) method. The performance of such a decoder which uses the improved metric for a multiuser system is compared using computer simulations. It is found that the decoder achieves results comparable to the optimal receiver with much reduced complexity.

A.1 Introduction

The work of Verdú has shown that optimum near-far resistance and a significant performance improvement over the conventional detector can be obtained by an optimum maximum likelihood multiuser detector, [121]. The substantial improvements, however, are obtained at the expense of a dramatic increase in computational complexity. The complexity grows exponentially with the number of users. Thus, when the number of users is large the optimum detector becomes infeasible. For this reason, several low complexity multiuser detectors have been proposed, including tree-type maximum likelihood sequence detectors. The Fano metric is closely related to the likelihood function and it is developed so that paths of different lengths can be compared [71]. In the literature two types of sequential metric functions have been proposed by Xie et al. in [148] and by Xiong and Shwedyk in [149]. Xie applied sequential decoding to the matched filter outputs directly, however, his results show good performance only for very low cross

correlations between users. Wei et al. have also investigated other suboptimal detectors for Gaussian and fading channels, mainly employing the M and T algorithm [140][137]. The complexity of the sequential detector with the conventional Fano metric becomes much higher than the M- and T- algorithms. The fundamental feature of a sequential decoder is that it searches for the most likely path based upon some appropriate metric, rather than evaluating all candidates for the best path as does the Viterbi algorithm. The key ingredient in a sequential decoder is the metric function, whose properties determine the speed of the tree search and ultimately the bit-error probability of the decoder. In this chapter we use the whitened matched filter outputs (see chapter 3) fed to a sequential decoder and obtain asymptotically optimal performance for high cross correlations between users and a large number of users.

A.2 Metric Functions for Sequential Detection

The system model is the same as Fig. 3.6. \mathbf{r}' is a vector of matched filtered output signals given by

$$\mathbf{r}' = \mathcal{R}\mathcal{W}\mathbf{b} + \mathbf{z}, \quad (\text{A.1})$$

where \mathcal{R} is cross-correlation of the signature sequences. It is also assumed that \mathcal{R} is positive definite. If a whitening filter is applied to the sampled output of the MF and stored in vector \mathbf{y} ,

$$\mathbf{y} = \mathcal{F}\mathcal{W}\mathbf{b} + \mathbf{n} \quad (\text{A.2})$$

The fundamental feature of a sequential decoder is that it searches for the most likely path based upon local metric values, rather than evaluating all candidates for the best path, as does the Viterbi algorithm. As a result, the decoding effort is only linearly dependent on the number of users in the system, a significant improvement over the exponential dependence of the optimal receiver. We now focus on the metric function of the sequential decoder, the properties of which determine the speed and bit error probability of the decoder. The optimum multiuser detector selects the hypothesis $\hat{\mathbf{b}}$ which, given

the receiver observations, maximises

$$\hat{\mathbf{b}} \in \arg \max_{\mathbf{b} \in \{-1,1\}^K} \left[2\mathbf{r}'^T \mathcal{W}\mathbf{b} - \mathbf{b}^T \mathbf{H}\mathbf{b} \right] \quad (\text{A.3})$$

where $\mathbf{H} = \mathcal{W}^T \mathcal{R}\mathcal{W}$ and

$$m_i^{<MF>} = -b_i \left[2r'_i \sqrt{E_b} - b_i E_b - 2 \sum_{j=1}^{i-1} b_j H_{ji} \right] \quad (\text{A.4})$$

is a metric function based on the matched filter outputs. The metric function given in equation (3.14) of [148] is based on the matched filter output. We can rewrite this expression for user i of a synchronous CDMA system as

$$m_i^{<MF>} = -b_i \left(2r'_i - b_i E_b - 2 \sum_{j=1}^{i-1} b_j H_{ji} - 2 \sum_{j=i+1}^K \text{sgn}[r_j] H_{ji} \right) - N_0 \log(2) \quad (\text{A.5})$$

The well known Fano metric for sequential decoding was shown to have certain optimal properties by Massey [71]. This approach was taken by Xiong in [149] equation (10), for intersymbol interference channels. Since a synchronous CDMA system can be treated as a time varying ISI channel a similar metric can be obtained for the whitened matched filter. The branch metric function corresponding to a branch in the multiuser tree, $\{-1, 1\}^K$ for user i driven by a whitened matched filter output y_i , can then be written as

$$m_i^{<WMF>} = \left(\ln \left(\frac{p_n(y_i - \hat{y}_i)}{p_o(y_i)} \right) - \ln(2) \right) \quad (\text{A.6})$$

In the sequential search process, \hat{y}_i is calculated based on tentative estimates of the previous $i - 1$ users' consecutive input symbols and the present guess of the input bit for user i , $\hat{y}_i = \sum_{j=1}^i \mathbf{F}^{i,j}(0)b_j$ Since the cascade of the whitened matched filter with the channel results in a noise sequence which is white the noise probability density is given by

$$p_n(y_i - \hat{y}_i) = \frac{1}{\sqrt{\pi N_0}} \exp \left(-\frac{(y_i - \hat{y}_i)^2}{N_0} \right) \quad (\text{A.7})$$

Using \hat{y}_i and (A.7) one can simplify (A.6) to

$$m_i^{<WMF>} = \frac{(y_i - \hat{y}_i)^2}{N_0} - \ln(2) - \ln(p_o(y_i)) + 0.5 \ln(\pi N_0) \quad (\text{A.8})$$

To compute the metric in (A.6) one must determine $p_o(y_i)$. This is the heart of the problem in multiuser communications using sequential decoding. Proceeding in a similar fashion

as [149] we have for equiprobable input, $p_o(y_i)$ is given as

$$p_o(y_i) = \frac{1}{2^i} \sum_{j=1}^{2^i} \frac{1}{\sqrt{\pi N_0}} \exp\left(-\frac{(y_i - \hat{y}_j)^2}{N_0}\right) \quad (\text{A.9})$$

This shows that the unconditional probability density function $p_o(y_i)$, of the noisy sufficient statistic r_i is the ensemble average over all the conditional density functions $p_n(y_i - \hat{y}_i)$. Note that $p_o(y_i)$ is not independent of the number of users. For small values of K and for fixed signature sequences, this task is manageable, although demanding. For a sufficiently large number of users, the straightforward evaluation of (A.9) becomes impractical. To deal with this situation numerical estimation methods can be used. In this section we investigate one such procedure namely the Gaussian Approximation method. Taking a closer look at equations (A.5) and (A.6), it is seen that the matched filter metric has five terms, the first three of which are similar to the maximum likelihood metric derived by Verdú in [121]. The bias term, $N_0 \log(2)$, takes into account the paths explored at different depths in the tree search. The fourth term, $\sum_{j=i+1}^K \text{sgn}[r_j] H_{ji}$ shows the dependence on the future section of the path that has not been searched yet. Assuming that the decoder has successfully decoded the first $i - 1$ users, i.e., $\{\hat{b}_j = b_j \text{ for } j = 1, 2, \dots, i - 1\}$, then on simplification

$$m_i^{<MF>} = -\hat{b}_i \left(2 \sum_{j=i+1}^K \{b_j - \text{sgn}[r_j] |H_{ji}|\} + 2b_i E_b - \hat{b}_i E_{\hat{b}_i} + 2z_i \right) - N_0 \log(2) \quad (\text{A.10})$$

and

$$m_i^{<WMF>} = -\frac{(\mathbf{F}^{i,i}(0)(b_i - \hat{b}_i) + n_i)^2}{N_0} - \ln(2) - \ln(p_o(y_i)) + 0.5 \ln(\pi N_0) \quad (\text{A.11})$$

The metric in (A.10) clearly shows that a particular decision suffers from MAI (the first term in (A.10)). However, for (A.11), there is no MAI term. It is easy to verify that the average behaviour of this metric along the correct path is positive, which tends to favour the desired choice and opposes by making the incremental metric negative if a wrong path is followed along its course of journey.

We can now rewrite (A.9) by grouping the multiuser interference terms together and use

a Gaussian Approximation method to evaluate the modified unconditional probability density function to be used later for metric calculations in the sequential decoding algorithm [86].

$$y_i = \mathbf{F}^{i,i}(0)b_i + \sum_{j=1}^{i-1} \mathbf{F}^{i,j}(0)b_j \quad (\text{A.12})$$

$$= \mathbf{F}^{i,i}(0)b_i + \nu \quad (\text{A.13})$$

Since the user in consideration can be either +1 or -1

$$p_o(y_i) = \frac{1}{2} \int_{-\infty}^{\infty} \left(\frac{1}{\sqrt{2\pi}\sigma_E} \exp\left(\frac{-(y_i - \mathbf{F}^{i,i}(0) - \nu)^2}{2\sigma_E^2}\right) + \frac{1}{\sqrt{2\pi}\sigma_E} \exp\left(\frac{-(y_i + \mathbf{F}^{i,i}(0) - \nu)^2}{2\sigma_E^2}\right) \right) p(\nu) d\nu$$

where $p(\nu) = \frac{1}{\sqrt{2\pi}\sigma_\nu} \exp\left(\frac{-\nu^2}{2\sigma_\nu^2}\right)$ (A.14)

In the appendix of this chapter we show how the integral of (A.14) can be simplified. The second term in (A.14) can be also be simplified in a similar fashion. Hence the Gaussian approximated unconditional probability density function may now be written as

$$p_o(y_i) = K \exp\left(\frac{B^2}{4} - C\right) + K \exp\left(\frac{B_1^2}{4} - C_1\right), \quad (\text{A.15})$$

where B, B_1 and C, C_1 are due to the two possible hypotheses respectively for the user in consideration. In Fig. A.1 the distribution for 10 users are plotted against the domain of received values y_i . In Fig. A.2 the absolute deviation, i.e., absolute difference between the exact pdf and the Gaussian Approximated pdf is plotted as a function of the number of users and received values. It clearly shows that as the number of users increase, by modelling the multiple access interference as a Gaussian process the approximation error diminishes and hence serves as a good tool for calculating (A.9) for a large number of users. Although the GA metric is very attractive for practical implementation, exact analytical results seem difficult to obtain. We will illustrate the performance of this new decoder by computer simulations.

A.3 Numerical Results

This decoder (whitened matched filter output followed by the sequential decoding algorithm) accommodated 10 users. We assume that the buffer size for the stack was infinite, thus there are no anticipated problems with erasure or buffer overflow. The SNR range was 0-8 dB, which represents low to moderate signal to noise ratios. The channel input was a random binary sequence with frames of 1024 bits. Simulations were done for the synchronous CDMA channel. The correlation matrix, \mathcal{R} was generated for 10 users with a spreading length of 31. As a comparison to the method used in [148] we have also simulated the performance for the same channel matrix with the matched filtered outputs being used in the algorithm. In Fig.A.3 the bit error rate graph is plotted against signal to noise ratio. It is clearly seen that the Gaussian approximated metric degrades only slightly as compared to the accurate metric. The matched filter output being fed to the sequential decoding algorithm produced an interference limited performance.

A.4 Conclusion

In this chapter we have applied sequential decoding to synchronous multiuser detection. The modification of the Fano metric by using the Gaussian Approximation method to group multiuser interference terms proved to be very useful in making reliable decisions for large number of users. It was shown that the approximation error reduced as the number of users in the system increased. Finally we showed by simulations that the GA method suffers only slight degradation in the bit error rate when compared to optimal detection, hence making this method attractive for practical implementation.

A.5 Appendix

$$p_o(y_i) = \int_{-\infty}^{\infty} \frac{1}{\sqrt{2\pi}\sigma_E} \exp\left(\frac{-(y_i - \mathbf{F}^{i,i}(0) - \nu)^2}{2\sigma_E^2}\right) p(\nu) d\nu \quad (\text{A.16})$$

Replacing $A = y_i - F_{ii}$, $p_o^1(y_i) =$

$$\begin{aligned}
 &= \int_{-\infty}^{\infty} \frac{1}{2\pi\sigma_E\sigma_\nu} \exp\left(-\frac{\nu^2(\sigma_\nu^2 + \sigma_E^2) + A^2\sigma_\nu^2 - 2A\nu\sigma_\nu^2}{2\sigma_E^2\sigma_\nu^2}\right) d\nu \\
 &= \int_{-\infty}^{\infty} \frac{1}{2\pi\sigma_E\sigma_\nu} \exp\left(-\frac{\nu^2 - \frac{2A\nu\sigma_\nu^2}{\sigma_\nu^2 + \sigma_E^2} + \frac{A^2\sigma_\nu^2}{\sigma_\nu^2 + \sigma_E^2}}{\frac{2\sigma_E^2\sigma_\nu^2}{\sigma_\nu^2 + \sigma_E^2}}\right) d\nu \\
 &= \int_{-\infty}^{\infty} \frac{1}{2\pi\sigma_E\sigma_\nu} \exp\left(-\frac{(\nu - \frac{B}{2})^2 - \frac{B^2}{4} + C}{2\sigma_x^2}\right) d\nu
 \end{aligned}$$

where

$$B = \frac{2A\sigma_\nu^2}{\sigma_\nu^2 + \sigma_E^2} \tag{A.17}$$

$$C = \frac{A^2\sigma_\nu^2}{\sigma_\nu^2 + \sigma_E^2} \tag{A.18}$$

$$\sigma_x^2 = \frac{\sigma_E^2\sigma_\nu^2}{\sigma_E^2 + \sigma_\nu^2} \tag{A.19}$$

$$p_o^1(y_i) = K \exp\left(\frac{\frac{B^2}{4} - C}{2\sigma_x^2}\right) \int_{-\infty}^{\infty} \frac{1}{\sqrt{2\pi}\sigma_x} \exp\left(-\frac{(\nu - \frac{B}{2})^2}{2\sigma_x^2}\right) d\nu$$

Since the integral of a probability density function is 1, $p_o^1(y_i)$ can be approximated as

$$p_o^1(y_i) = K \exp\left(\frac{\frac{B^2}{4} - C}{2\sigma_x^2}\right), K = \frac{\sigma_x}{\sqrt{2\pi}\sigma_E\sigma_\nu} \tag{A.20}$$

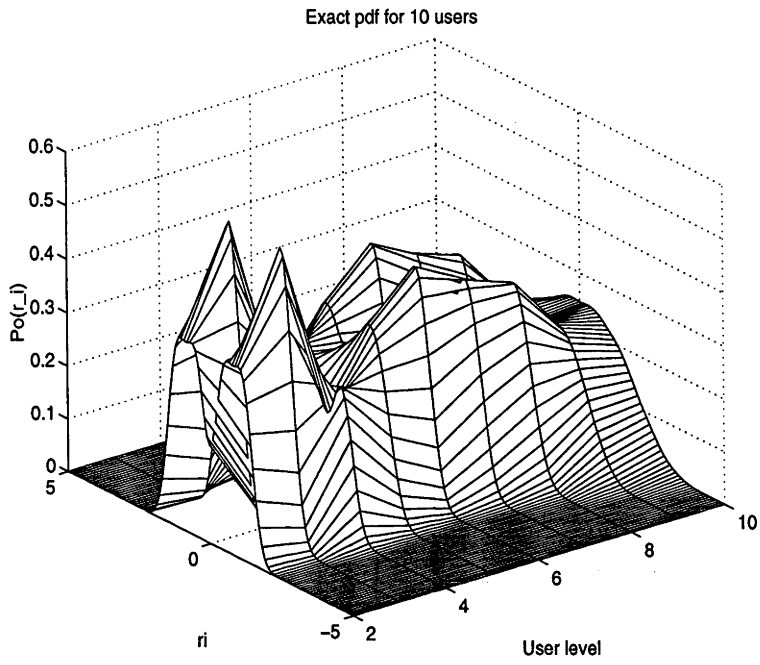


Figure A.1: Exact pdf of $p_0(y_i)$ for 10 users

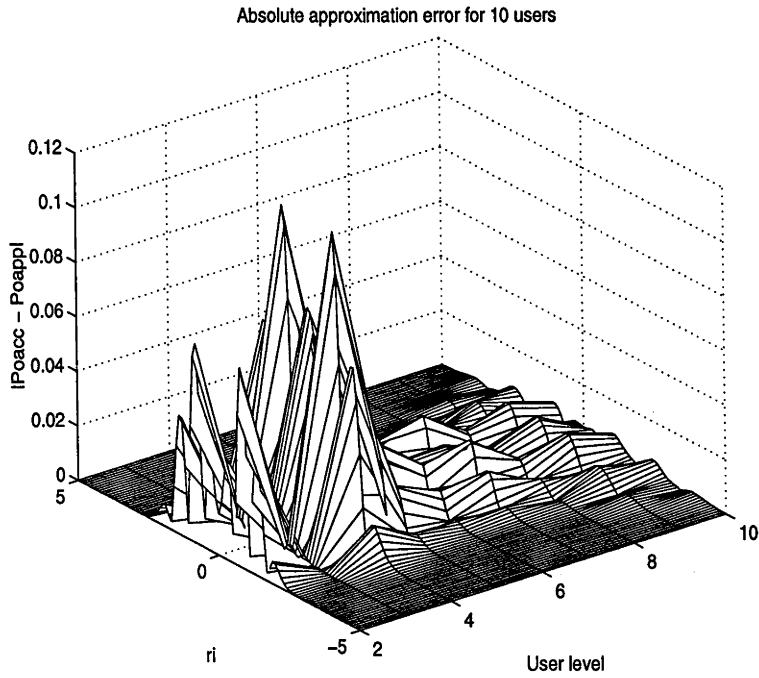


Figure A.2: Pdf of the approximation error for 10 users

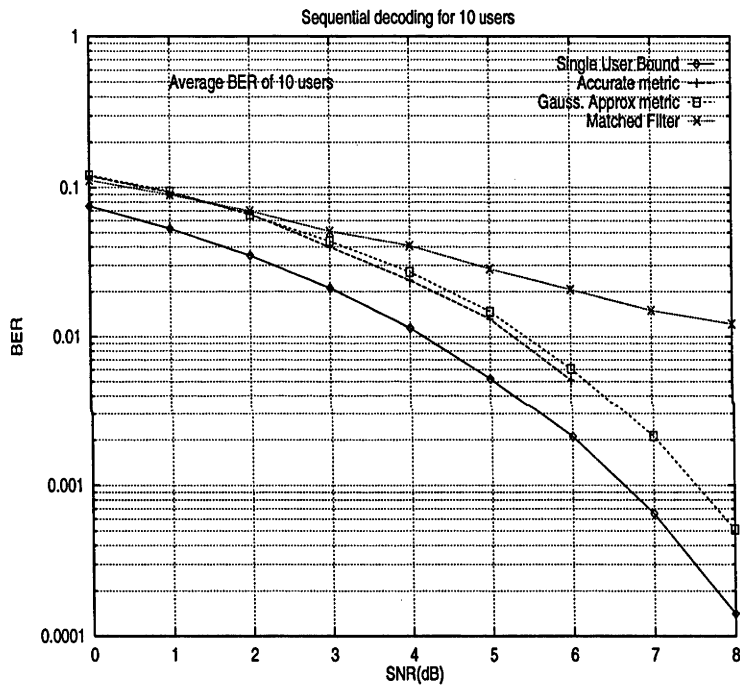


Figure A.3: BER-SNR curves for 10 users

Change Detection in Teletraffic Models

B.1 Abstract

In this chapter we propose a likelihood based ratio test to detect distributional changes in common teletraffic models. These include traditional models like Markov Modulated Poisson Process and processes exhibiting long range dependency, in particular Gaussian fractional ARIMA processes. A practical approach is also developed for the case where the parameter after the change is unknown. It is noticed that the algorithm is robust enough to detect slight perturbations in the parameter space after change. A comprehensive set of numerical results including results for the mean detection delay is provided¹.

B.2 Introduction

Change detection algorithms have been studied extensively for the past 50 years [80] [13]. Adaptive identification algorithms can track only slow fluctuations of the characteristic parameters and are not suited for detection of abrupt changes in general. Detection of abrupt changes however, is necessary in many applications like fault detection in navigational systems, onset detection in seismic signal processing, and segmentation of speech signals. We are interested in the problem of on-line detection of an abrupt change, with the minimum delay in detection with a constraint on the mean time between false alarms. Most of the signals treated in [13] are time-series models (linear or nonlinear). Follow-

¹This work was done in collaboration with Dr. Subhrakanti Dey, Dept. of Systems Engineering, The Australian National University

ing techniques similar to [23], an on-line change detection algorithm was developed in [28] for Markov-modulated time-series models based on the CUSUM (Cumulative Sum)-like test derived from Page's test and the Sequential Probability Ratio Test (SPRT) [105]. In this chapter, we develop on-line change detection algorithms based on a CUSUM-like procedure for teletraffic models, ranging from traditional models like Markov-modulated Poisson Process (MMPP) to a class of current self-similar models proposed for internet traffic, specifically long memory time series models.

It is known that the CUSUM test is optimal in the sense that it optimizes the worst mean delay in detection when the mean time between false alarms goes to infinity [13]. The CUSUM algorithm also gives the infimum of the worst mean delay for a class of stopping times with pre-assigned rate of false alarms [13]. Simulations in [92] illustrated via a comparative study of five algorithms, (for a change in the mean of a Gaussian distribution), that the CUSUM algorithm is more robust and efficient than the others. Optimal properties for the CUSUM algorithm are discussed in detail in [13]. Since the idea of the test is based on calculating the logarithm of the ratio of the conditional likelihood functions before and after the change, one can extend the CUSUM algorithm to the case of dependent observations (although initially it was designed for independent observations) where calculations of such likelihood functions are possible (e.g., hidden Markov models [23] and Markov-modulated time-series [28]).

In this chapter, we develop on-line change detection algorithms based on the CUSUM-like test for teletraffic models. The first model we treat is a traditional model for modelling traffic data in communication networks also known as the Markov modulated Poisson Process (MMPP). It has been extensively used for modelling processes like overflow from a finite trunk group, superposition of packetized voice processes and packet data (see [34] and references therein). Although this model can account for time-varying arrival rates and captures some of the important correlations between interarrival times, it cannot model long-range dependence (or long memory with hyperbolically decaying autocorrelation functions arising as a striking feature of the so-called "self-similarity"). Starting with the seminal paper [64], it was shown in many other works that self-similarity existed in ATM traffic, compressed digital video streams and web traffic between browsers and servers (e.g., see [93]). While self-similarity is measured by the so-called Hurst parameter (taking values between 0.5 and 1.0), it has been shown that high degrees of self-

similarity (Hurst parameter > 0.7) have a detrimental effect on network performance, including packet loss and queueing delay (see [93] and references therein). Also, increasing load on the Ethernet increases the degree of self-similarity. In the context of multimedia traffic such as video and voice with their diverse Quality of Service (QoS) requirements, it is important therefore that the effect of self-similarity on interconnected issues like queueing delay, packet loss and buffer sizes is well understood. Hence, the issue of detecting changes in the degree of self-similarity is quite important in such applications. In this chapter, we address this issue by developing on-line change detection algorithms for a class of long-range dependent processes namely, Gaussian Fractional ARIMA (FARIMA) processes.

It is to be remembered however, that these algorithms are optimal when the parameters before and after the change are exactly known. In most realistic situations, that is not the case (e.g, network traffic). While one can extend such methods to Generalized Likelihood Ratio (GLR) tests (assuming that the parameters before the change are known but not so after the change), one can also develop more sub-optimal methods by substituting the parameters before the change by their estimated values and running a bank of change detection algorithms with different assumed values for the parameters after the change. While the closest value will result in a better performance, such algorithms are obviously computationally quite expensive, particularly when the number of parameters is high. Analytical or even approximate computations of the mean delay in detection and mean time between false alarms are quite difficult in the case when the sequence of the test statistic is not independent and will not be considered in this chapter for our algorithms except for some simulation results.

B.3 Signal Models

B.3.1 Markov Modulated Poisson Process (MMPP)

A MMPP is a doubly stochastic Poisson process where the rate of the Poisson process is modulated by the state of a Markov chain. Let $s_t \in S = \{1, 2, \dots, N\}$, $t \in \mathbb{N}^+$ denote a finite state, discrete-time, homogeneous Markov chain with a transition probability matrix $A = (a_{ij})$ where $a_{ij} = P(s_{t+1} = i | s_t = j)$ and initial probability distribution given

by π such that $P(s_0 = i) = \pi(i)$. The number of arrivals (e.g., of data packets) in the t -th time slot is modelled by a Poisson process and is denoted by n_t . The rate of arrival during the t -th time slot is given by μ_t where essentially μ_t is modulated by s_t . Let $\mu_t \in \mu \triangleq \{\mu(1), \mu(2), \dots, \mu(N)\}$ where $\mu_t = \mu(i)$ if $s_t = i$.

Define $B(n_t) = \text{diag}\{b_1(n_t), b_2(n_t), \dots, b_N(n_t)\}$, where $b_i(n) = P(n_t = n | s_t = i)$. Due to the Poisson nature of the process n_t , we obviously have $P(n_t = n | s_t = i) = \frac{\mu(i)^n}{n!} \exp(-\mu(i))$. The complete parameter space for the MMPP is then characterised by $\lambda = (A, \pi, \mu)$. The problem at hand is to detect change from one parameter space λ_H , to another, λ_K .

B.3.2 Long Memory Processes

By generalising the well known ARIMA(p, d, q) models of Box-Jenkins [21], it is possible to relax the degree of differencing d to any real value to model long-term persistence. In what follows, we consider stationary fractional ARIMA processes with $0 < d < 1/2$ and Gaussian innovations.

B.3.2.1 Fractional ARIMA

We formally define a FARIMA($0, d, 0$) process to be discrete-time stochastic process $\{x_t\}$ represented as

$$\Delta^d x_t = \epsilon_t \tag{B.1}$$

where the operator Δ^d is defined by

$$\Delta^d = (1 - B)^d = 1 - dB - \frac{1}{2}d(1 - d)B^2 - \frac{1}{6}d(1 - d)(2 - d)B^3 - \dots \tag{B.2}$$

where B is the backward shift operator defined by $Bx_t = x_{t-1}$. $\{\epsilon_t\}$ is a sequence of independent identically distributed *i.i.d.* random variables. In this chapter, we assume ϵ_t is Gaussian distributed with mean 0 and variance unity.

The covariance function of $\{x_t\}$ is

$$\gamma_k^x = E\{x_t x_{t-k}\} = \frac{(-1)^k \Gamma(1-2d)}{\Gamma(k-d+1)\Gamma(1-k-d)} \quad (\text{B.3})$$

and the correlation function

$$\rho_k^x = \frac{\Gamma(1-d)\Gamma(k+d)}{\Gamma(d)\Gamma(k+1-d)} \quad (\text{B.4})$$

When $d = 0$, the FARIMA(0, 0, 0) process is a white noise with a constant spectral density. For $0 < d < 1/2$, the FARIMA(0, d , 0) process is stationary with long memory. The correlations are all positive and decay monotonically and hyperbolically to zero as the lag increases. For the purpose of this work, we assume $d < 1/2$, since for $d \geq 1/2$ the process is not stationary. When $-1/2 < d < 0$, the FARIMA(0, d , 0) process has short memory.

A more general model of the ARIMA family, namely FARIMA(p , d , q) can be defined by a stochastic process $\{y_t\}$ represented as

$$\phi(B)\Delta^d y_t = \theta(B)\epsilon_t \quad (\text{B.5})$$

where Δ^d is the fractional differencing operator, $\phi(B) = 1 - \phi_1 B - \dots - \phi_p B^p$ and $\theta(B) = 1 - \theta_1 B - \dots - \theta_q B^q$, and ϵ_t is a white noise process. The effect of the d parameter on distant observations decay hyperbolically as the lag increases, while the effects of ϕ and θ parameters decay exponentially. Thus d may be chosen to describe correlation in a time series between distant observations whereas ϕ and θ describe the short term correlation.

In practice, it is expected that the FARIMA(p , d , q) processes are likely to be of most interest when p and q are small [53]. We will consider the simplest of such processes, namely, FARIMA(1, d , 0) and FARIMA(0, d , 1). These two time-series are given by the following equations:

$$(1 - \phi B)\Delta^d y_t = \epsilon_t \quad (\text{B.6})$$

$$\Delta^d y_t = (1 - \theta B)\epsilon_t \quad (\text{B.7})$$

To ensure stationarity and invertibility of $\{y_t\}$, we assume $|d| < \frac{1}{2}$, $|\phi| < 1$, $|\theta| < 1$. The covariance functions of the FARIMA(1, d , 0) and FARIMA(0, d , 0) processes can be found in [53].

B.4 On-Line Change Detection

Consider a sequence of independent and identically distributed random variables y_t with a probability density $f(\cdot)$ depending on a parameter space characterised by λ . Before the unknown change time t_{opt} , the parameter space is given by $\lambda = \lambda_H$ and after the change it is $\lambda = \lambda_K$. Assuming that the parameter space λ_H and λ_K are completely known a priori, the problem is then to detect and estimate this change in parameter. A cumulative sum (CUSUM) algorithm that uses the logarithm of likelihood ratios to detect such a change was devised by Page [80] in 1954. The key statistical properties of this ratio can be summarised as follows. A change in the parameter space λ is reflected as a change in the sign of the mean of the log-likelihood ratio. Let $S_t = \sum_{i=1}^t s_i$, $s_t(y) = \ln \frac{f_{\lambda_K}(y_t)}{f_{\lambda_H}(y_t)}$. The typical behaviour of the log-likelihood ratio S_t shows a negative drift before change and a positive drift after change. Although this test was designed for an independent sequence $\{y_t\}$, a similar CUSUM like test can be designed for dependent sequences of $\{y_t\}$ also [13]. This is based on measuring the ratio of the conditional likelihood functions before and after the change. Note from [13] that such a sequential CUSUM-like procedure in a manner similar to Page's recursive test can be written as a recursion in the test statistic S_t in the following manner:

$$S_t = \max\{0, S_{t-1} + g(t)\} \quad (\text{B.8})$$

where

$$g(t) = \log \left(\frac{f_{\lambda_K}(y_t|y_{t-1}, \dots, y_0)}{f_{\lambda_H}(y_t|y_{t-1}, \dots, y_0)} \right) \quad (\text{B.9})$$

As far as the change is concerned, the relevant information lies in $g(t)$, the difference between the log-likelihood functions according to the parameter spaces λ_H and λ_K . The key property that allows detectability in a CUSUM-like procedure is $E(g(t)|\lambda_H) < 0$, $E(g(t)|\lambda_K) >$

0. To detect a change from λ_H to λ_K , usually a threshold h is set such that a change is detected when $S_t > h$. There are two quantities associated with the detection: the mean time between false alarms and the mean delay in detection. The general nature of these quantities are that the mean time between false alarms increases approximately exponentially with increasing values of the threshold, mean delay in detection increases approximately linearly with increasing values of the threshold. These two properties make the CUSUM test quite useful. Computation of the exact conditional log-likelihood functions is possible (as shown in the next section) for the MMPP process but not for long memory processes. So, we resort to approximate computations for long memory processes.

B.4.1 MMPP

Consider an MMPP defined in Section II A. Note that here we replace $\{y_t\}$ by the observation sequence $\{n_t\}$. Define the following forward variable $\alpha_t^l \triangleq (\alpha_t^l(1), \dots, \alpha_t^l(N))'$ where obviously $\alpha_t^l \in \mathbb{R}^N$, such that the following recursion in α_t^l holds:

$$\alpha_t^l = B(n_t)^l P^l \frac{\alpha_{t-1}^l}{\sum_i \alpha_{t-1}^l(i)}, \quad \alpha_0^l = B(n_0)^l \pi^l \quad (\text{B.10})$$

Note that in the right hand side of the first equation in (B.10), α_{t-1}^l is normalized to avoid numerical problems.

It is easy to show that according to the above recursion, $\alpha_t^l(j)$ is equal to the quantity $\frac{f_l(n_t, n_{t-1}, \dots, n_0, s_t=j | \lambda_l)}{f_l(n_{t-1}, \dots, n_0 | \lambda_l)}$. Then it easily follows that $f_l(n_t | n_{t-1}, \dots, n_0)$, $l = K, H$ is given by $f_l(n_t | n_{t-1}, \dots, n_0) = \sum_j \alpha_t^l(j)$. It is clear that one can now perform computations of the test statistic as given by (B.8), (B.9).

B.4.2 Gaussian FARIMA

In this section, we show how one can extend the on-line change detection algorithm for long memory time-series, specifically Gaussian FARIMA(0, d , 0), FARIMA(1, d , 0) and FARIMA(0, d , 1).

B.4.2.1 Gaussian FARIMA(0, d , 0)

Let $X = \{x_0, \dots, x_{T-1}\}$ be a T -length sequence of observations from a Gaussian FARIMA(0, d , 0) process with $0 < d < \frac{1}{2}$ satisfying (B.1). For the FARIMA(0, d , 0), the parameter subject to change is d . For FARIMA(1, d , 0), the parameters concerned are d, ϕ and for FARIMA(0, d , 1), they are d, θ . We assume that the parameters before and after the change are completely known. In the next section, where we present simulation results, we consider a practical sub-optimal scheme for the case where the parameter (d in that particular case) is unknown after change. Next, we describe how one can go about performing a CUSUM-like test for long memory time series like those given by (B.1), (B.7).

It is well known [17] that an exact likelihood computation of a long memory time series, e.g., FARIMA(0, d , 0) is computationally prohibitive due to the covariance matrix being high-dimensional (for long time series) and often numerically unstable for certain values of d such that inverting the matrix might be a problem. There are several ways to compute an approximate likelihood function like ("Whittle's approximate MLE", see [142]). We take an alternative approach as given in Section 5.6 of [17]. Consider (B.1). Assuming that the long memory time series has a causal linear representation one could write x_t as

$$x_t = \sum_{l=1}^{\infty} b(l)x_{t-l} + \tilde{\epsilon}_t \quad (\text{B.11})$$

where asymptotic properties of the AR coefficients $b(\cdot)$ can be found in [17]. If we knew the infinite past of x_t given by $x_s, s < t$, we could reconstruct the sequence of *i.i.d.* innovations $\tilde{\epsilon}_s, s \leq t$. Instead of the infinite past, if only a finite number of past values is observed, the innovations can be estimated by $\hat{\tilde{\epsilon}}_t = x_t - \sum_{l=1}^{t-1} b(l)x_{t-l}$. Here, we would further truncate the memory such that we only consider M past samples. This is to prevent growing computational needs with increasing length of the time-series. In that case, we represent x_t by

$$x_t = \sum_{l=1}^M \beta_{Ml} x_{t-l} + e_t(d) \quad (\text{B.12})$$

where $\sum_{l=1}^M \beta_{Ml} x_{t-l}$ is the best linear prediction of x_t given the past M samples. For a

FARIMA(0, d , 0) series the predictor taps β_{Ml} are given by

$$\beta_{Ml} = - \binom{M}{l} \frac{\Gamma(l-d)\Gamma(M-d-l+1)}{\Gamma(-d)\Gamma(M-d+1)} \quad (\text{B.13})$$

$e_t(d)$ denotes the prediction error at time t where the dependence on d is explicitly shown. An approximate log-likelihood function $L_t(X_t, d)$ can be calculated by (where $X_t = (x_t, x_{t-1}, \dots, x_1)$) [150] [17]

$$L_t(X_t, d) = -\frac{t}{2} \log(2\pi) - \frac{t}{2} \log \left(\frac{\sum_{i=1}^t \sigma_i^2(d)}{2t} \right) - \frac{1}{2} \sum_{i=1}^t \frac{e_i^2(d)}{\sigma_i^2(d)} \quad (\text{B.14})$$

where the mean squared prediction error $\sigma_i^2(d) \triangleq E[e_i^2(d)]$ is given by [150]

$$\sigma_i^2(d) = \Gamma(t)\Gamma(t-2d) / (\Gamma(t-d)^2) \quad (\text{B.15})$$

An approximate CUSUM-like test can now be devised (we call it approximate because of the approximate log-likelihood function) by computing $g(t)$ in (B.9) by the logarithm of the ratio of $f_{d_K}(x_t|x_{t-1}, \dots, x_1)$ and $f_{d_H}(x_t|x_{t-1}, \dots, x_1)$ where d_H, d_K are the respective d values before and after the change. It is not hard to see that this is given by (due to Bayes' Theorem)

$$g(t) = (L_t(X_t, d_K) - L_{t-1}(X_{t-1}, d_K)) - (L_t(X_t, d_H) - L_{t-1}(X_{t-1}, d_H)) \quad (\text{B.16})$$

B.4.2.2 Gaussian FARIMA(1, d , 0) and FARIMA(0, d , 1)

The on-line change detection algorithm is essentially based on the computation of the approximate log-likelihood function for both FARIMA(1, d , 0) and FARIMA(0, d , 1). These approximations are based on the best linear prediction of the time-series given finite number of past samples. Hence one can repeat the same procedure (as done in the previous subsection for Gaussian FARIMA(0, d , 0)) for obtaining the predictor taps, the prediction error covariance, and finally equations similar to (B.14) and (B.16). One will need to use the covariance formulae for FARIMA(1, d , 0) and FARIMA(0, d , 1) (see [53]) and to

compute the predictor taps recursively, one can use the Levinson-Durbin algorithm. For space limitations, we do not go into the details of the calculations.

One can potentially consider a case where the long memory processes like Gaussian FARIMA(p, d, q) for nonzero p or q can have Markov modulated AR or MA parameters. This is an analytically hard problem and will be considered elsewhere.

B.5 Simulation

In our simulations, the Markov-modulated Poisson Process has an underlying Markov chain that takes values in a 4-dimensional state space. We assume that the process changes from a parameter space λ_H to λ_K after the first 1000 points and then changes back to λ_H after another 1000 points. Different transition probability matrices A_H and A_K were used, along with two different sets of rate of arrivals of packets μ_H and μ_K (details are omitted for space limitations).

Fig. 1 shows the plot of the test statistic clearly showing the changes at $t = 1000$ and $t = 2000$. Fig. 2 shows the corresponding mean delay in detection versus the detection threshold, h . As the threshold is increased, the time required to detect a discernible change increases approximately linearly.

Figures 3,4 show the change detection for long memory processes. The data for the FARIMA(0, d , 0) process was generated using a statistical software package SPW, and FARIMA(1, d , 0) was generated by passing a FARIMA(0, d , 0) process through an appropriate filter. Each process was subdivided into three equal sections. The first change can be seen at $t = 1000$ and the next change at $t = 2000$. Figure 6 shows the delay in detection for the FARIMA(0, d , 0) process of Figure 3 and as expected, the delay is seen to be approximately linear in the detection threshold.

Next, we show some results where the parameter after the change, d_K is assumed to be unknown. A practical on-line approach would be to run several change detection algorithms in parallel with guessed values for d_K . If d_H , the parameter before the change is not known, one can substitute d_H by some estimated value. Here we only concentrate on the case where d_K is unknown. The following figures (Figures 7-11) show the plots

of the test statistic for various “guesses” for d_K for such an algorithm. We investigate the proposed detection algorithm using a filter bank with the FARIMA(0, d , 0) process. The process was 3000 samples long and was divided into three equal sections, namely ($t = 0..999, t = 1000..1999, t = 2000..2999$). The data sequence was generated using $d_H = 0.1$ for the first 1000 samples, $d_K = 0.3$ for the next 1000 and back to $d_H = 0.1$ in the final section. Thus the first change can be seen at $t = 1000$ and the next at $t = 2000$.

It is readily seen that for slight changes in assumed d_K the test statistic is more “jittery” and have no clean transition boundaries at the time of change. More importantly, the average rate of change in the test statistic decreases for a branch assuming an incorrect d_K that is farther away from the true d_K . Figure 9 shows the change for the correctly assumed d_K value (i.e. $d_K = 0.3$). Note that for the other branches, S_n plateaus at a lesser value. So, a higher slope of increase in the values of the test-statistic and cleaner transitions with less jitter are indicative of a better guess. However, these are only empirical guidelines and the complexity of this algorithm obviously increases exponentially with the number of parameters.

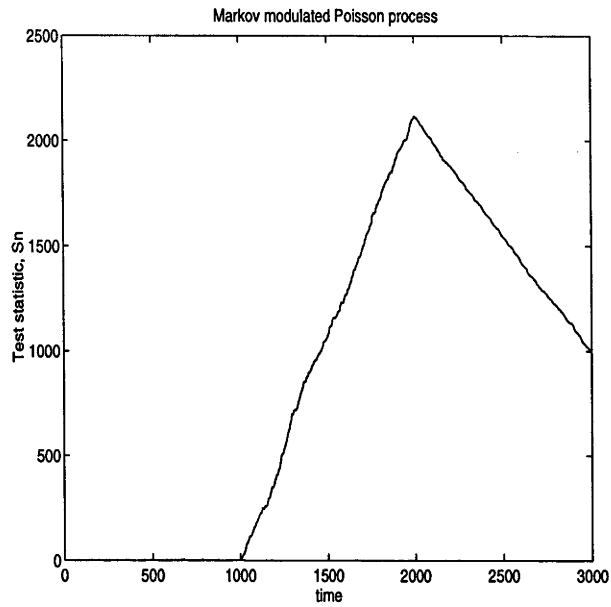


Figure B.1: Change detection for a MMPP process

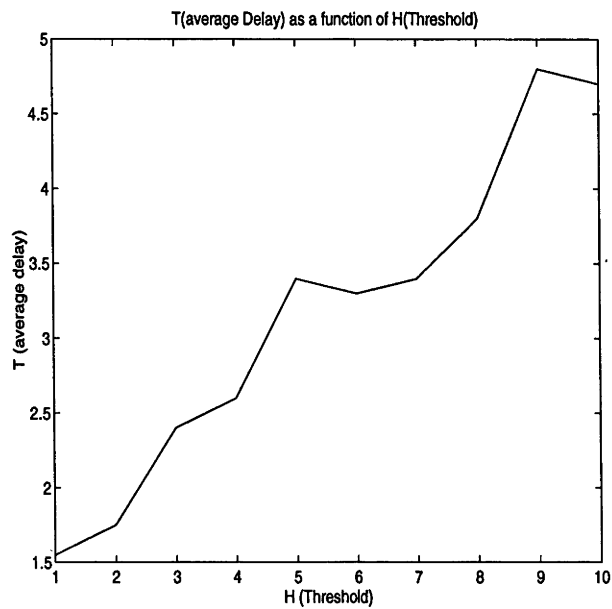


Figure B.2: Delay in detection for a MMPP process, Plot of Average delay-Threshold

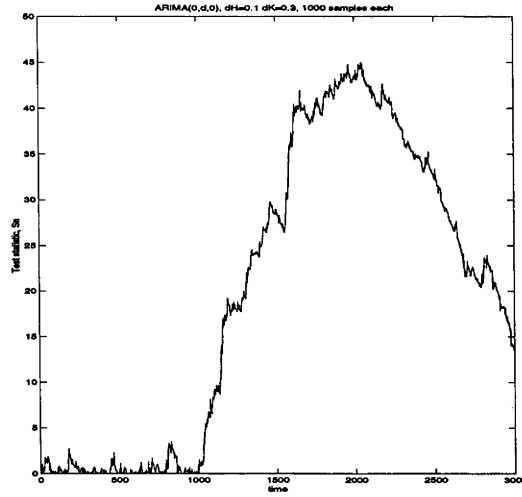


Figure B.3: Change detection for ARIMA(0, d , 0) process, $d_H = 0.1$ ($t = 0..999$), $d_K = 0.3$ ($t = 1000..1999$) and $d_H = 0.1$ ($t = 2000..2999$)

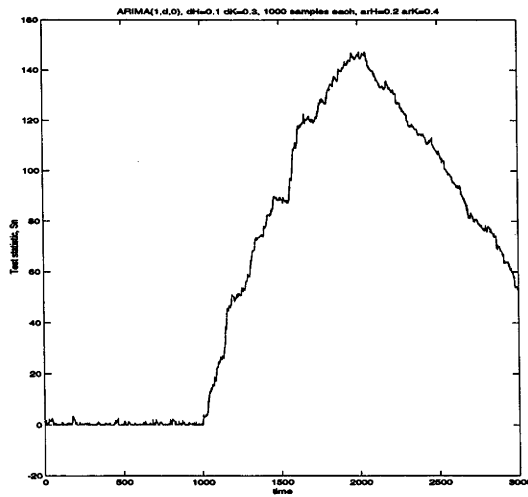


Figure B.4: Change detection for ARIMA(1, d , 0) process, $d_H = 0.1$, $\phi = 0.2$ ($t = 0..999$); $d_K = 0.3$, $\phi = 0.4$ ($t = 1000..1999$); $d_H = 0.1$, $\phi = 0.2$ ($t = 2000..2999$)

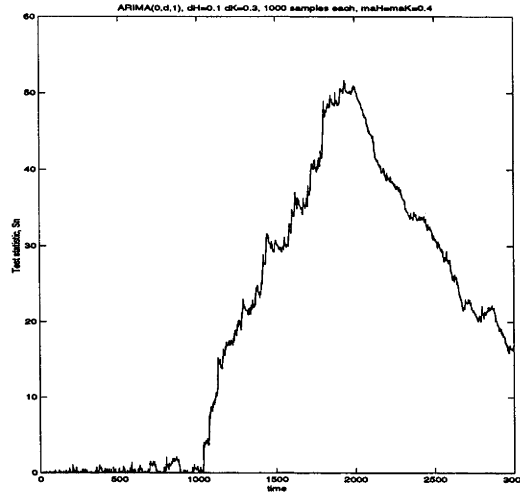


Figure B.5: Change detection for ARIMA(0, d , 1) process, $d_H = 0.1$, $\theta = 0.2$ ($t = 0..999$); $d_K = 0.3$, $\theta = 0.4$ ($t = 1000..1999$); $d_H = 0.1$, $\theta = 0.2$ ($t = 2000..2999$)

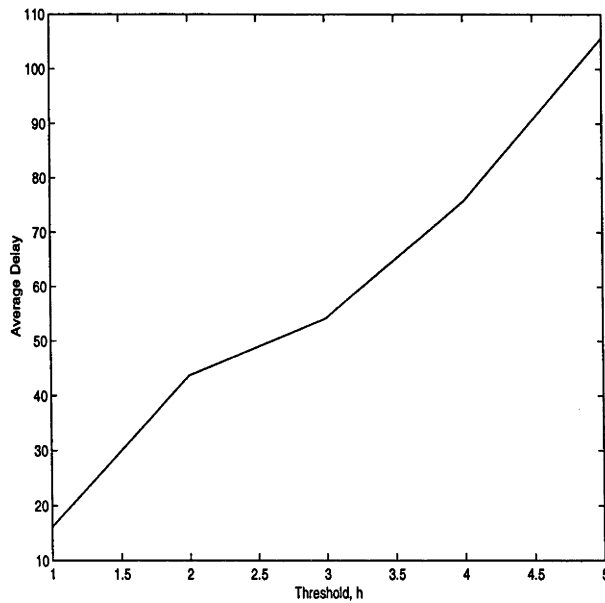


Figure B.6: Delay in detection for ARIMA(0, d , 0) process, $d_H = 0.1$, ($t = 0..999$); $d_K = 0.3$, $\theta = 0.4$ ($t = 1000..1999$); $d_H = 0.1$, $\theta = 0.2$ ($t = 2000..2999$)

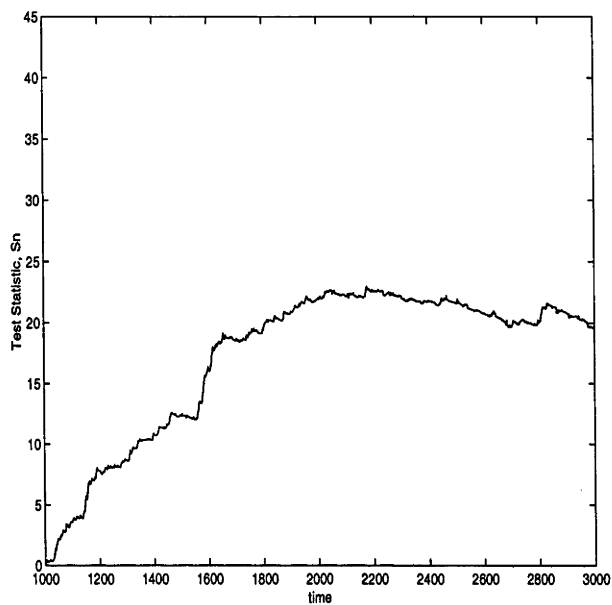


Figure B.7: Change detection for ARIMA(0, d , 0) process, Tested $dK = 0.20$, Actual $dK = 0.3$

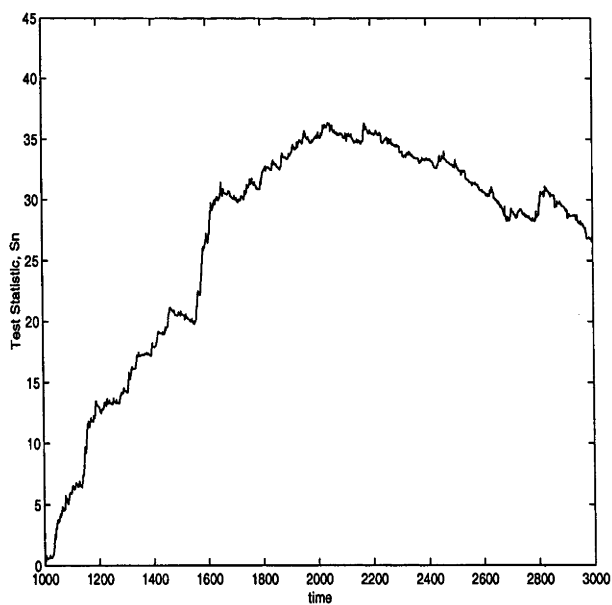


Figure B.8: Change detection for ARIMA(0, d , 0) process, Tested $dK = 0.25$, Actual $dK = 0.3$

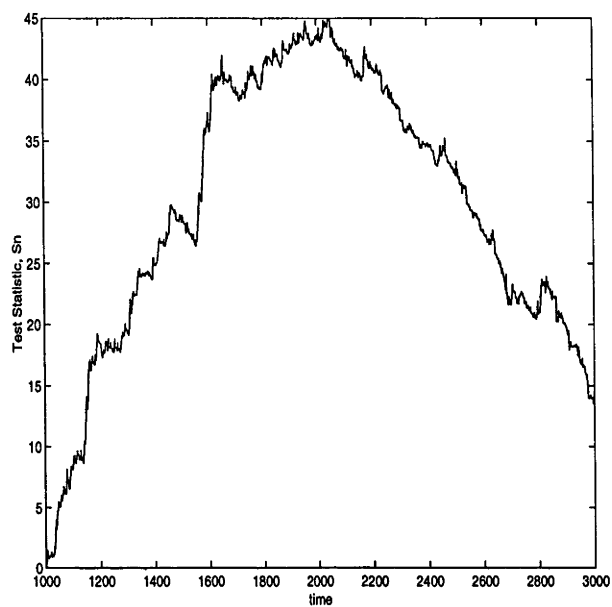


Figure B.9: Change detection for ARIMA(0, d , 0) process, Tested $dK = 0.3$, Actual $dK = 0.3$

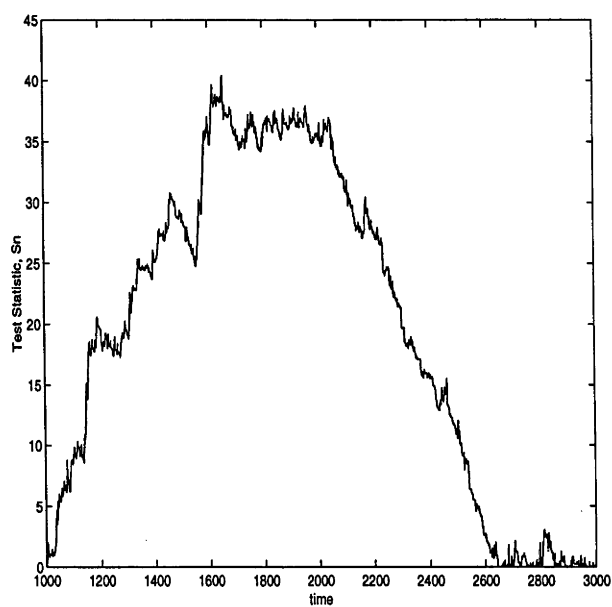


Figure B.10: Change detection for ARIMA(0, d , 0) process, Tested $dK = 0.35$, Actual $dK = 0.3$

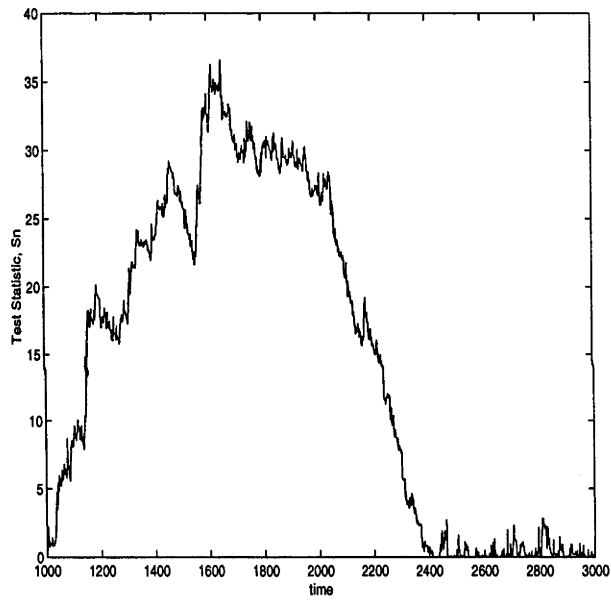


Figure B.11: Change detection for ARIMA(0, d , 0) process, Tested $dK = 0.40$, Actual $dK = 0.3$

Bibliography

1. B. Aazhang, B. P. Paris and G. C. Orsak, "Neural networks for multi-user detection in code-division-multiple-access communications," *IEEE Trans. on Commun.*, vol. 40, pp. 1212–1222, July 1992.
2. B. G. Agee, "Solving the near-far problem: Exploitation of spatial and spectral diversity in wireless personal communications networks," *Virginia Tech's Third Symposium on Wireless Personal Communications*, pp. 15–1, June 9–11, 1993.
3. P. D. Alexander and L. K. Rasmussen, "An efficient technique for deriving receiver filters in multiuser asynchronous DS/SSMA," in *The Fifth International Symposium on Personal, Indoor and Mobile Radio Communications*, vol. 2, (The Hague, The Netherlands), pp. 519–523, Sept. 1994.
4. P. D. Alexander, A. J. Grant, M. J. Miller, L. K. Rasmussen, and P. Whiting, "Multiuser mobile communications," in *International Symposium on Information Theory and its Applications*, (Sydney, Australia), Nov. 1994. Keynote Address by M. Miller.
5. P. D. Alexander, L. K. Rasmussen, and C. B. Schlegel, "A linear receiver for coded multiuser CDMA," *IEEE Trans. Commun.*, 1997. To Appear.
6. P. D. Alexander and P. Jung, "A unified approach to multiuser receivers and their geometrical interpretations," in *The Sixth International Symposium on Personal, Indoor, and Mobile Radio Communications*, vol. 3, (Toronto, Canada), pp. 970–974, Sept. 1995.
7. P. D. Alexander, L. K. Rasmussen, and C. B. Schlegel, "A linear receiver for the coded asynchronous multiuser CDMA channel," in *33rd Annual Allerton Conference on Communication, Control, and Computing*, (Urbana, Illinois), pp. 29–38, Oct. 1995. Invited Paper.
8. P. D. Alexander and L. K. Rasmussen, "Sub-optimal MAP metrics for single user decoding in multiuser CDMA," in *Int. Symp. Info. Theory and Apps.*, vol. 2, (Victoria, Canada), pp. 657–660, Sept. 1996.
9. J. B. Anderson and S. Mohan, "Sequential coding algorithms: A survey and cost analysis," *IEEE Trans. Commun.*, vol. 32, pp. 169–176, Feb. 1984.
10. V. Aue and J. H. Reed, "An interference robust CDMA demodulator that uses spectral correlation properties," in *IEEE Vehicular Tech. Conf.*, pp. 563–567, 1994.
11. L. R. Bahl, J. Cocke, F. Jelinek, and J. Raviv, "Optimal decoding of linear codes for minimising symbol error rate," *IEEE Trans. Inform. Theory*, vol. 20, pp. 284–287, 1974.

-
12. P. W. Baier, "CDMA or TDMA? CDMA for GSM?," in *5th International Symposium on Personal, Indoor and Mobile Radio Communications*, vol. 3, (The Hague, the Netherlands), pp. 1280–1284, Sept. 1994.
 13. M. Basseville and L. V. Nikiforov, *Detection of abrupt changes*. Prentice Hall, 1993.
 14. P. A. Bello, "Characterisation of randomly time-variant linear channels," *IEEE Trans. Commun.*, vol. 11, pp. 360–393, Dec. 1962.
 15. S. E. Bensley and B. Aazhang, "Subspace-based estimation of multipath channel parameters for CDMA communications systems," in *Globecom Miniconference*, pp. 154–158, 1994.
 16. S. E. Bensley and B. Aazhang, "Subspace-based channel estimation for code division multiple access communication systems," *IEEE Trans. Commun.*, vol. 44, pp. 1009–1020, Aug. 1996.
 17. J. Beran, *Statistics for Long-Memory Processes*. New York: Chapman & Hall, 1994.
 18. C. Berrou, A. Glavieux, and P. Thitimajshima, "Near Shannon limit error-correcting coding and decoding: turbo-codes," in *IEEE Int. Conf. on Communications*, (Geneva, Switzerland), pp. 1064–1070, May 1993.
 19. V. K. Bhargava, D. Haccoun, R. Matyas, and P. Nuspl, *Digital Communications by Satellite*. Wiley-Interscience, New York, 1981.
 20. S. Bhasyam, A. M. Sayeed, B. Aazhang, "Time selective signalling and reception for communication over multipath fading channels," *submitted to IEEE Trans. Commun.*, 1998.
 21. G.E.P.Box and G.M.Jenkins, *Time series analysis forecasting and control*. San Francisco: Holden-Day, 2nd ed., 1970.
 22. A. R. Calderbank, J. E. Mazo and H. M. Shapiro, "Upper bounds on the minimum distance of trellis codes," in *Bell System Technical Journal*, vol. 62, pp. 2617–2645, No.8, Oct. 1983.
 23. B. Chen and P. Willett, "Quickest detection of hidden markov models," in *Proceedings of the 36th IEEE CDC*, (San Diego, U.S.A), pp. 3984–3989, 1997.
 24. D. C. Cox, "Wireless network access for personal communications," *IEEE Commun. Mag.*, pp.96–115, Dec. 1992.
 25. Q. Dai, E. Shwedyk, "Detection of bandlimited signals over frequency-selective Rayleigh fading channels," *IEEE Trans. Commun.*, vol. 42, pp. 941–950, No. 2–4, 1994.
 26. L. Davis and I. Collings, "Joint MAP detection and channel estimation for CDMA over frequency selective fading channels," in *Proc. of ISPACS*, Melbourne, pp. 432–436, Nov. 1998.

-
27. L. Davis and I. Collings, "Multi-user MAP decoding for flat fading CDMA channels," in *Proc. DSPCS'98*, Perth, pp. 79–86, Feb. 1999.
 28. S. Dey and S. I. Marcus, "Change detection in markov-modulated time series," in *Proceedings of Information Decision and Control*, (Adelaide, Australia), pp. 21–24, February 1999.
 29. A. Duel-Hallen, "Decorrelating decision-feedback multiuser detector for synchronous code-division multiple-access channel," *IEEE Trans. Commun.*, vol. 41, pp. 285–290, Feb. 1993.
 30. A. Duel-Hallen, "Performance of multiuser zero-forcing and MMSE decision-feedback detectors for CDMA channels," in *Globecom*, vol. 4, (Houston, Texas), Nov. 1993.
 31. A. Duel-Hallen, "A family of multiuser decision-feedback detectors for asynchronous code-division multiple-access channels," *IEEE Trans. Commun.*, vol. 43, pp. 421–434, Feb. 1995.
 32. A. Duel-Hallen, J. Holtzman, and Z. Zvonar, "Multiuser detection for CDMA systems," *IEEE Personal Communications Magazine*, pp. 46–58, April 1995.
 33. U. Fawer and B. Aazhang, "A multiuser receiver for code division multiple access communications over multipath channels," *IEEE Trans. Commun.*, vol. 43, pp. 1556–1565, Feb./Mar./Apr. 1995.
 34. W. Fischer and K. Meier-Hellstern, "The Markov-modulated Poisson Process," *Performance Evaluation*, vol. 18, pp. 149–171, 1992.
 35. G. D. Forney, "Maximum likelihood sequence estimation of digital sequences in the presence of intersymbol interference," *IEEE Trans. Inform. Theory*, vol. IT-18, pp. 363–378, May, 1972.
 36. T. R. Giallorenzi and S. G. Wilson, "Decision feedback multiuser receivers for asynchronous CDMA," in *Globecom*, (Houston, Texas), pp. 1677–1681, Dec. 1993.
 37. T. R. Giallorenzi and S. G. Wilson, "Trellis based multiuser receivers for convolutionally coded CDMA systems," in *31st Allerton Conference on Communications*, Oct. 1993.
 38. K. S. Gilhousen, I. M. Jacobs, R. Padovani, A. Viterbi, L. A. Weaver, C. Wheatly, "On the capacity of a cellular CDMA system," *IEEE Trans. on Vehicular Tech.*, vol. VT-40(2), pp. 300–312, May 1991.
 39. R. Gold, "Optimum binary sequences for spread spectrum multiplexing," *IEEE Trans. Inform. Theory*, vol. 13, pp. 619–621, Oct. 1967.
 40. G. H. Golub and C. F. V. Loan, *Matrix Computations*. The John Hopkins University Press, 2nd ed., 1989.

-
41. A. J. Grant and L. K. Rasmussen, "A new coding method for the asynchronous multiple access channel," in *33rd Annual Allerton Conference on Communication, Control, and Computing*, (Urbana, Illinois), pp. 21–28, Oct. 1995. Invited Paper.
 42. A. Grant, B. Rimoldi, R. Urbanke, and P. Whiting, "Single user coding for the discrete memoryless multiple access channel," in *Proc. IEEE Int. Symp. on Information Theory*, (Whistler, Canada), p. 448, Sept. 1995.
 43. A. J. Grant, P. D. Alexander, and P. A. Whiting, "Why design spreading codes for multiuser CDMA channels?," in *The Sixth International Symposium on Personal, Indoor, and Mobile Radio Communications*, vol. 3, (Toronto, Canada), pp. 1331–1334, Sept. 1995.
 44. A. J. Grant and P. D. Alexander, "Randomly selected spreading sequences for coded CDMA," in *IEEE Int. Symp. on Spread Spectrum Techniques and Applications*, vol. 1, (Mainz, Germany), pp. 54–57, Sept. 1996.
 45. A. J. Grant and P. D. Alexander, "On random sequence multisets for synchronous code-division multiple-access channels." Submitted to *IEEE Transactions on Information Theory*, Dec. 1995.
 46. *ETSI/TC GSM Recommendation 05.05: Transmission and Reception*, 1988.
 47. B. D. Hart, *MLSE Diversity Receiver Structures*, PhD thesis, University of Canterbury, New Zealand, 1996.
 48. B. D. Hart and D. P. Taylor, "Extended MLSE Diversity receiver for the Time and Frequency-Selective Channel," *IEEE Trans. on Commun.*, vol. COM-45:3, pp.322-333, Mar. 1997.
 49. B. D. Hart and D. P. Taylor, "Maximum likelihood synchronisation, equalisation and sequence estimation for unknown time-varying, frequency-selective Rician channels" *IEEE Trans. on Commun.* , vol. 46, no. 2, pp.211-221, Feb. 1998.
 50. P. Hoeher, "On channel coding and multiuser detection for DS-CDMA," in *Proc. 2nd Int. Symp. on Universal Personal Communications*, (Ottawa, Canada), pp. 641-646, Oct. 1993.
 51. J. M. Holtzman, "DS/CDMA successive interference cancellation," in *IEEE Int. Symp. on Spread Spectrum Techniques and Applications*, (Oulu, Finland), pp. 69–78, July 1994.
 52. M. Honig, U. Madhow, and S. Verdú, "Blind adaptive multiuser detection," *IEEE Trans. Inform. Theory*, vol. 41, pp. 944–960, July 1995.
 53. J.R.M.Hosking, "Fractional differencing," *Biometrika*, vol. 68, pp. 165–176, 1981.
 54. P. Jung, P. W. Baier, and A. Steil, "Advantages of CDMA and spread spectrum techniques over FDMA and TDMA in cellular mobile radio applications," *IEEE Trans. Veh. Technol.*, vol. 42, pp. 357–364, Aug. 1993.

-
55. P. Jung, M. Naßhan, and J. Blanz, "Application of turbo-codes to a CDMA mobile radio system using joint detection and antenna diversity," in *IEEE 44th Vehicular Technology Conference*, (Stockholm, Sweden), pp. 770–774, June 1994.
 56. P. Jung, M. Naßhan, and J. Blanz, "Application of turbo-codes to a CDMA mobile radio system using joint detection and antenna diversity," *IEEE Trans. Veh. Technol.*, 1996. to appear.
 57. P. Jung and B. Steiner, "A joint detection CDMA mobile radio system concept developed within COST 231," in *IEEE 45th Vehicular Technology Conference*, (Chicago, Illinois), July 1995.
 58. P. Jung and P. D. Alexander, "A unified approach to multiuser detectors for CDMA and their geometrical interpretations," *IEEE J. Selected Areas Commun.*, vol. 14, pp. 1595–1601, Oct. 1996.
 59. R. E. Kamel and Y. Bar-Ness, "Anchored blind equalisation using the constant modulus algorithm," *IEEE Trans. on Circuits and Systems-II*, vol. 44, no 5, pp. 397–403, May 1997.
 60. C. Kchao and G. Stuber, "Performance analysis of a single cell direct sequence mobile radio system," *IEEE Trans. on Commun.*, vol. 41, no 10, pp. 1507–1516, Oct. 1993.
 61. J. D. Laster and J. H. Reed, "Interference rejection in digital wireless communications," *IEEE Signal Proc. Magazine*, vol. 14, no. 3, pp. 37–62, May, 19917
 62. W. C. Y. Lee, *Mobile Cellular Telecommunications Systems*, McGraw–Hill, 1989.
 63. W. C. Y. Lee, "Overview of cellular CDMA," *IEEE Trans. Veh. Technol.*, vol. 40, no. 2, pp. 291–301, 1991.
 64. W. E. Leland *et al.*, "On the self-similar nature of ethernet traffic," *IEEE Transactions on Networking*, vol. 2, pp. 1–15, February 1994.
 65. J. H. Lodge and M. L. Moher, "Maximum Likelihood Sequence Estimation of CPM Signals Over Rayleigh Flat-Fading Channels," *IEEE Trans. on Commun.*, vol. COM-38, no. 6, pp.787-794, June 1990.
 66. R. Lupas and S. Verdú, "Linear multiuser detectors for synchronous code-division multiple-access channels," *IEEE Trans. Inform. Theory*, vol. 35, pp. 123–136, Jan. 1989.
 67. R. Lupas and S. Verdú, "Near-far resistance of multiuser detectors in asynchronous channels," *IEEE Trans. Commun.*, vol. 38, pp. 496–508, April 1990.
 68. U. Madhow and M. L. Honig, "MMSE detection of direct-sequence CDMA signals: Analysis for random signature sequences," in *Proc. IEEE Int. Symp. on Information Theory*, (San Antonio, Texas), pp. 49, Jan. 1993.
 69. U. Madhow and M. L. Honig, "MMSE interference suppression for direct-sequence spread-spectrum CDMA," *IEEE Trans. Commun.*, vol. 42, pp. 3178–3188, Dec. 1994.

-
70. U. Madhow, "Blind adaptive interference suppression for direct-sequence CDMA," *Proceedings of the IEEE*, vol. 86, no 10, pp. 2049–2069, Oct. 1998.
 71. J.L.Massey "Variable length codes and the Fano metric" *IEEE Trans. Info. Theory*, vol. IT-18, pp. 196–198, Jan. 1972.
 72. J. Miguez and L. Castedo, "Linearly constrained constant modulus approach to blind adaptive multiuser interference suppression," *IEEE Commun. Letters*, vol. 2, no 8, pp. 217-219, Aug. 1998.
 73. U. Mitra and H. V. Poor, "Neural network techniques for adaptive multiuser demodulation," *IEEE Journal of Selected areas in Commun*, vol. 12, pp. 1460-1470, Dec. 1994.
 74. S. Moshavi, "Multiuser detection for DS-CDMA systems," *IEEE Communications magazine*, vol. 34, no. 10, pp. 124–136, Oct. 1996.
 75. R. S. Mowbray and P. M. Grant, "Wideband coding for uncoordinated multiple access communication," *Electronics and Communication Engineering Journal*, pp. 351–361, Dec. 1992.
 76. M. Nasiri-Kernari and C. K. Rushforth, "An efficient soft-decision algorithm for synchronous CDMA communications with error-control coding," in *Proc. IEEE Int. Symp. on Information Theory*, (Trondheim, Norway), p. 227, June 1994.
 77. I. Opperman, P. Rapajic, and B. S. Vucetic, "Pseudo random sequences with good cross-correlation properties," in *International Symposium on Information Theory and Its Applications*, vol. 2, (Sydney, Australia), pp. 1001–1006, Nov. 1994.
 78. G. Orsak and B. Aazhang, "On the theory of importance sampling applied to the analysis of detection systems," *IEEE Trans. on Commun.*, vol. COM-35, no. 6, pp.332-339, April 1989.
 79. G. Orsak and B. Aazhang, "Efficient importance sampling techniques for simulation of multiuser communication systems," *IEEE Trans. on Commun.*, vol. COM-40, no. 6, pp.332-339, June 1992.
 80. E.S.Page, "Continuous inspection schemes," *Biometrika*, vol. 41, pp. 100–115, 1954.
 81. A. Papoulis, "Probability, random variables and stochastic processes," *McGraw-Hill*, 3rd Edition, 1991.
 82. S. Parkvall and E. G. Ström, "Parameter estimation and detection of DS-CDMA signals subject to multipath propagation," in *IEEE/IEE Workshop on Signal Processing in Multipath Environments*, (Glasgow, Scotland), Feb. 1995.
 83. S. Parkvall, E. Ström, and B. Ottersten, "The impact of timing errors on the performance of linear DS-CDMA receivers," *IEEE J. Selected Areas Commun.*, 1997. To appear.

-
84. P. Patel, "Performance comparison of a DS/CDMA system using a successive interference cancellation (IC) and a parallel IC scheme under fading," in *Proc. of ICC*, New Orleans, pp. 510–515, May 1994.
 85. R. Prasad, *CDMA for wireless personal communications*, Artech House, Boston, 1996.
 86. J. G. Proakis, *Digital Communications*. McGraw–Hill, 2 ed., 1989.
 87. Qualcomm, "An overview of the application of code division multiple access (CDMA) to digital cellular systems and personal cellular networks." An updated version of the report submitted to the TIA TR45.5 subcommittee on March 28, 1992., May 1992.
 88. TIA/EIA/IS–95, "Mobile station - base station compatibility standard for dual mode wideband spread spectrum cellular system," in *Telecommunications industry association (TIA)*, July 1993.
 89. P. B. Rapajic and B. S. Vucetic, "Adaptive receiver structures for asynchronous CDMA systems," *IEEE J. Selected Areas Commun.*, vol. 12, pp. 685–697, May 1994.
 90. P. B. Rapajic and B. S. Vucetic, "Linear adaptive transmitter-receiver structures for asynchronous CDMA systems," *European Transactions on Telecommunications*, vol. 6, no. 1, pp. 21–27, Jan-Feb. 1995.
 91. S. Rappaport, "Wireless communications," Prentice Hall, 1996
 92. S. W. Roberts, "A comparison of some control chart procedures," *Technometrics*, vol. 8, pp. 411–430, 1966.
 93. Z. Sahinoglu and S. Tekinay, "On multimedia networks: Self-similar traffic and network performance," *IEEE Communications Magazine*, vol. 37, pp. 48–52, January 1999.
 94. A. Saifuddin, R. Kohno, and H. Imai, "Cascaded combination of cancelling co-channel interference and decoding of error-correcting codes for CDMA," in *IEEE Int. Symp. on Spread Spectrum Techniques and Applications*, (Oulu, Finland), pp. 171–175, 1994.
 95. D. V. Sarwate, "Optimum PN sequences for CDMA systems," in *IEEE Int. Symp. on Spread Spectrum Techniques and Applications*, vol. 1, (Oulu, Finland), pp. 27–35, July 1994.
 96. A. M. Sayeed and B. Aazhang, "Exploiting Doppler Diversity in Mobile Wireless Communications," in *Proceedings of the 1997 Conference on Information Sciences and Systems(CISS)*, Baltimore, MD, March 1997.
 97. A. M. Sayeed and B. Aazhang, "Joint multipath-Doppler diversity in mobile wireless communications," to appear in *IEEE Trans. Commun'* 1998.
 98. D. L. Schilling, G. R. Lomp and J. Garodnick, "Broadband-CDMA overlay," in *IEEE Vehicular Technology Conference*, pp. 452–455, 1993.

-
99. C. Schlegel and Z. Xiang, "Multiuser projection receivers," in *Proc. IEEE Int. Symp. on Information Theory*, (Whistler, Canada), p. 318, Sept. 1995.
 100. C. Schlegel, S. Roy, P. Alexander, and Z. Xiang, "Multi-user projection receivers," *IEEE J. Selected Areas Commun.*, vol. 14, pp. 1610–1618, Oct. 1996.
 101. C. Schlegel, "Trellis Coding", *Prentice Hall*, 1996.
 102. C. Schlegel and L. Wei, "A simple way to compute the minimum distance in multiuser CDMA systems," *IEEE Trans. Commun.*, vol. 45, pp. 532–536, May. 1997.
 103. M. Schwartz, W.R. Bennett and S. Stein, "Communication Systems and Techniques," *McGraw-Hill*, 1966.
 104. K. S. Shanmugan and P. Balaban, "A modified Monte-Carlo simulation technique for the evaluation of error rate in digital communication systems," *IEEE Trans. Commun.*, vol. 28, pp. 1916–1924, Nov 1980.
 105. D. Siegmund, *Sequential Analysis - Tests and Confidence Intervals*. New York: Springer-Verlag, 1995.
 106. B. Sklar, "Rayleigh fading channels in mobile digital communication systems Part II: Mitigation" *IEEE Communications Magazine*, pp. 103–109, July, 1997.
 107. E. G. Ström and S. Parkvall, "Joint parameter estimation and detection of DS-CDMA signals in fading channels," in *Globecom*, (Singapore), Nov. 1995.
 108. E. G. Ström, S. Parkvall, S. Miller, and B. E. Ottersten, "Propagation delay estimation in asynchronous direct-sequence code-division multiple access systems," *IEEE Trans. Commun.*, 1996. To appear.
 109. H. Suzuki, "A statistical model for urban radio propagation," *IEEE Trans. Commun.*, vol. 25, pp. 673–680, July 1977.
 110. J. K. Tugnait, "On blind MIMO channel estimation and blind signal separation in unknown additive noise," in *Proc. of the IEEE Signal processing workshop on Signal Processing Advances in Wireless Communication (SPAWC)*, pp. 53–60, 1997.
 111. G. L. Turin, "The characteristic function of Hermitian quadratic forms in complex normal variables," *Biometrika*, pp. 199–201, 1960.
 112. G. L. Turin, "Introduction to spread spectrum antimultipath techniques and their application to urban digital radio," *Proceedings of the IEEE*, pp. 328–354, 1980.
 113. G. Ungerboeck, "Adaptive maximum-likelihood receiver for carrier-modulated data-transmission systems," *IEEE Trans. Commun.*, vol. 22, pp. 624–636, May 1974.
 114. M. K. Varanasi and B. Aazhang, "Multistage detection in asynchronous code-division multiple-access communications," *IEEE Trans. Commun.*, vol. 38, pp. 509–519, April 1990.

-
115. M. K. Varanasi and B. Aazhang, "Near-optimum detection in synchronous code-division multiple-access systems," *IEEE Trans. Commun.*, vol. 39, pp. 725-736, May 1991.
 116. M. K. Varanasi, "Noncoherent detection in asynchronous multiuser channels," *IEEE Trans. Inform. Theory*, vol. 39, pp. 157-176, Jan. 1993.
 117. M. K. Varanasi, "Group detection for synchronous Gaussian code-division multiple-access channels," *IEEE Trans. Inform. Theory*, vol. 41, pp. 1083-1096, July 1995.
 118. S. Vasudevan and M. K. Varanasi, "Multiuser detectors for Rician fading CDMA channels," in *Proc. of the twenty ninth Allerton conference on communications, Control and computing*, pp. 390-399, Oct. 1991.
 119. S. Vembu and A. J. Viterbi, "Two different philosophies in CDMA - A Comparison," in *Proc. of IEEE Vehicular Tech. Conf.*, Apr 1996, pp. 869-873.
 120. D. Verdin and T. C. Tozer, "Generating a fading process for the simulation of land-mobile radio communications," *Electronics Letters*, vol. 29, pp. 2011-2012, Nov. 1993.
 121. S. Verdú, "Minimum probability of error for asynchronous Gaussian multiple-access channels," *IEEE Trans. Inform. Theory*, vol. 32, pp. 85-96, Jan. 1986.
 122. S. Verdú, "Optimum multiuser asymptotic efficiency," *IEEE Trans. Commun.*, vol. 34, pp. 85-96, Sept. 1986.
 123. S. Verdú, "Recent progress in multiuser detection," N. Abramson, Ed.,) *Multiple access communications: Foundations for emerging technologies*, IEEE Press N.Y., 1993.
 124. S. Verdú, "Computational complexity of optimum multiuser detection," *Algorithmica*, vol.4, 1989.
 125. S. Verdú, "Maximum likelihood sequence detection for intersymbol interference channels: A new upper bound on error probability," *IEEE Trans. Inform. Theory*, vol. IT-33, no. 1, pp. 62-68, Jan. 1987.
 126. S. Verdú, "Adaptive multiuser detection," in *IEEE Int. Symp. on Spread Spectrum Techniques and Applications*, (Oulu, Finland), pp. 43-50, July 1994.
 127. S. Verdú, "Multiuser detection", *Cambridge University Press*, Cambridge, UK, 1998.
 128. G. Vietta and D. P. Taylor, "Maximum likelihood sequence detection of uncoded and coded PSK signals transmitted over Rayleigh frequency flat channels," in *Supercomm, ICC*, New Orleans, pp. 1-7, 1997.
 129. A. J. Viterbi, "Error bounds for convolutional codes and an asymptotically optimum decoding algorithm," *IEEE Trans. Inform. Theory*, vol. IT-13, pp. 260-269, Apr. 1967.
 130. A. J. Viterbi and J. K. Omura, *Principles of Digital Communication and Coding*. McGraw-Hill, 1979.

-
131. A. J. Viterbi, "Very low rate convolutional codes for maximum theoretical performance of spread-spectrum multiple-access channels," *IEEE Trans. Veh. Technol.*, vol. 8, pp. 641–649, May 1990.
 132. A. J. Viterbi, "Wireless Digital Communication: A view based on three lessons learned," *IEEE Communications Magazine*, pp. 33–36, Sept. 1991.
 133. A. M. Viterbi, A. J. Viterbi, "Erlang capacity of a power controlled CDMA system," *IEEE J. Selected Areas Commun.*, vol. 11, pp. 892–900, Aug. 1993.
 134. A. J. Viterbi, "The orthogonal-random waveform dichotomy for digital mobile personal communications" *IEEE Personal Communications*, 1st Quarter, pp. 18–24, 1994.
 135. A. J. Viterbi, *CDMA - Principles of spread spectrum communications*. Addison Wesley, 1995.
 136. X. Wang and H.V. Poor, "Blind multiuser detection: A sub-space approach," *IEEE Trans. Inform. Theory*, vol. 44, pp. 677–690, Mar. 1998.
 137. L. Wei, L. K. Rasmussen and R. Wyrwas, "Bit-Synchronous CDMA system with tree search algorithms over Flat Rayleigh fading channel", in *proceedings of the IEEE ISITA, pp.91-95, November 1994, Australia*
 138. L. Wei and C. Schlegel, "Synchronous DS-SSMA with improved decorrelating decision-feedback multiuser detection," *IEEE Trans. Veh. Technol.*, vol. 43, pp. 767–772, Aug. 1994. Special Issue on Future PCS Technologies.
 139. L. Wei, "Estimated bit error probability of DS-SSMA/MPSK with coherent detector on satellite mobile channel," *IEEE J. Selected Areas Commun.*, vol. 13, pp. 250–263, Feb. 1995.
 140. L. Wei and L. K. Rasmussen, "A near ideal noise whitening filter for an asynchronous time-varying CDMA system," *IEEE Trans. Commun.*, vol. 44, pp. 1355–1361, Oct. 1996.
 141. L. R. Welch, "Lower bounds on the maximum cross correlation of signals," *IEEE Trans. Inform. Theory*, vol. IT-20, pp. 397–399, May 1974.
 142. P. Whittle, "Estimation and information in stationary time series," *Ark. Mat.*, vol. 2, pp. 423–434, 1953.
 143. S. B. Wicker, *Error Control Systems for Digital Communication and Storage*. Prentice Hall, 1995.
 144. S. S. H. Wijayasuriya, J. P. McGeehan, and G. H. Norton, "rake decorrelating receiver for DS-CDMA mobile radio networks," *IEE Electron. Lett.*, vol. 29, pp. 395–396, Feb. 1993.
 145. Z. Xie, C. K. Rushforth, and R. T. Short, "Multiuser signal detection using sequential decoding," *IEEE Trans. Commun.*, vol. 38, pp. 578–583, May 1990.

-
146. Z. Xie, R. T. Short, and C. K. Rushforth, "A family of suboptimum detectors for coherent multiuser communications," *IEEE J. Selected Areas Commun.*, vol. 8, pp. 683–690, May 1990.
 147. Z. Xie, C. K. Rushforth, R. T. Short, and T. K. Moon, "Joint signal detection and parameter estimation in multiuser communications," *IEEE Trans. Commun.*, vol. 41, pp. 1208–1216, Aug. 1993.
 148. Z. Xie, C.K.Rushforth, R.T.Short "Mutiuser signal detection using sequential decoding" *IEEE Trans. Comm.*, vol. COM-38, pp.578–583
 149. F.Xiong and E.Shywedyk "Sequential Sequence Estimation for Multiple Channel Systems with Intersymbol Interference" *IEEE Trans. Comm.*, vol. COM-41, pp.322–331, Feb. 1993.
 150. Y.Yajima, "On estimation of long memory time series models," *Austral. J. Statistics*, vol. 27, pp. 303–320, 1985.
 151. D. C. Youla and N. N. Kazanjian, "Bauer-type factorisation of positive matrices and the theory of matrix polynomials orthogonal on the unit circle," *IEEE Transactions on Circuits and Systems*, vol. 25, pp. 57–69, Feb. 1978.
 152. X. Yu and S. Pasupathy, "Innovations-Based MLSE for Rayleigh Fading Channels," *IEEE Trans. on Communications*, vol. COM-43, no2/3/4, pp.1534-1544, Feb./Mar./Apr. 1995.
 153. Z. Zvonar and D. Brady, "Optimum detection in asynchronous multiple access multipath Rayleigh fading," in *Proc. of the twenty sixth annual conference on Information Sciences and Systems*, Princeton University, pp. 826-831, March 1992.
 154. Z. Zvonar and D. Brady, "Coherent and differentially coherent multiuser detectors for asynchronous CDMA frequency selective channels," in *Milcom*, San Diego, California, pp. 442–446, Oct. 1992.
 155. Z. Zvonar and D. Brady, "Linear multipath-decorrelating receiver for CDMA frequency selective fading channels," in *IEEE Trans. Commun.*, vol. 44, pp. 650–653, June 1996.